Valorization of MSWI Fly Ash for Use in Cement-Based Materials

Ebert, Benjamin Alexander Regaard

Publication date:
2021

Document Version
Publisher's PDF, also known as Version of record

PhD Thesis R-465
Department of Civil Engineering

Benjamin Alexander Regaard Ebert

Valorization of MSWI Fly Ash for Use in Cement-Based Materials

Valorization of MSWI Fly Ash for Use in Cement-Based Materials

This thesis was prepared by:

Benjamin A. R. Ebert
Section for Materials & Durability
Department of Civil Engineering
Technical University of Denmark

Supervisor:

Gunvor M. Kirkelund
Section for Materials & Durability
Department of Civil Engineering
Technical University of Denmark

Co-Supervisors:

Mette R. Geiker
Norwegian University of Science and Technology

Britt-Marie Steenari
Chalmers University of Technology

Department of Civil Engineering

Technical University of Denmark
Brovej, Building 118
2800 Kgs. Lyngby
Denmark
Phone: +45 45 25 17 00
Mail: byg@byg.dtu.dk

Preface

This doctoral thesis was submitted to the Technical University of Denmark (DTU) in Kgs. Lyngby for the degree of Philosophiae Doctor (PhD).

The thesis is the product of a PhD project funded by the Technical University of Denmark as part of an alliance project with Chalmers University of Technology (Chalmers) and the Norwegian University of Science and Technology (NTNU). The project started in December 2017 and ended in May 2021, after a six months extension.

The majority of the research was carried out at the Department of Civil Engineering at DTU Kgs. Lyngby. Part of the research was done at Chalmers during an extended sojourn to Sweden. The majority of the ECTS point required to complete the PhD were acquired at NTNU.

The academic supervisor's part of the project was main supervisor associate professor Gunvor M. Kirkelund (DTU), co-supervisor professor Mette R. Geiker (NTNU) and co-supervisor Britt-Marie Steenari (Chalmers).

Benjamin A. R. Ebert

Signature

31-05-2021

Date

Acknowledgements

I would first and foremost like to express my gratitude to my supervisor Gunvor Marie Kirkelund for accepting my application to this PhD project and the countless meetings we have held discussing the scope and work of the project. Thank you for your help in understanding some of the many new skills required and problems encountered as a new researcher. With my time here at DTU, I have not only learned how to become a researcher, I have also grown as a person. I would also like to thank my co-supervisors, Mette Rica Geiker and Britt-Marie Steenari, for their help during the project, their recommendations and their comments on the scientific papers. Ensuring a high level of research during my pursuit of knowledge. I also want to thank Wolfgang Kunther for collaborating on one of my papers.

I want to thank the lab technicians Ebba, Malene, Sabrina, Natasha and Anisa for their help in performing laboratory measurements. Your help and high spirits have assisted tremendously in what would otherwise have been a strenuous and lengthy process. I would also like to thank Klaus Bræmer for his assistance. Additionally, I would like to thank my colleagues for contributing to the wonderful years I had at DTU. I want to thank my office mates Nina, Anne Mette, Ida and Louise for enduring PhD life with me and especially Nina for her collaborations through the years.

Last but not least, I would like to thank my family. They supported me through the years and these trying times. They always showed interest and asked how my work progressed, although at times tediously. Thank you for everything.

Abstract

The production of cement emits large amounts of CO_2 to the atmosphere. It is estimated that cement production accounts for 8% of the global yearly anthropogenic CO_2 emissions. One way to reduce these emissions is to replace part of the cement used for concrete manufacturing with secondary cementitious materials (SCMs). However, limited availability and supplies call for the identification of new cement replacements. Fly ash residues originating from municipal solid waste incineration (MSWI) could potentially be used as a new secondary cementitious material. However, treating the residues may be required before they can be used as a cement replacement, as MSWI fly ash residues are considered hazardous and pose an environmental problem. If the treatment also extracts the valuable metals from the MSWI fly ash residues, it could be beneficial. Therefore, this PhD project aimed to develop a treatment process that could extract valuable metals from the MSWI residues and enable their use as a partial cement replacement.

Five MSWI fly ash residues (four fly ashes and one air pollution control (APC) residue) were acquired from three waste incinerators for this PhD project. The five residues were characterised based on their chemical composition and particle size distribution and subsequently screened for use in cement-based materials. The residues were very different from the commonly used fly ash from coal incineration, and that they were not suitable for use as a cement replacement. Multivariate data analysis showed that one of the residues, the MSWI APC residue, had an average chemical composition for MSWI fly ash residues. Three residues had less common compositions. The fifth, a sulphur-rich MSWI fly ash residue, was an outlier in the analysis compared to a range of samples from the literature. The MSWI APC residue, one of the three MSWI fly ashes and the sulphur-rich MSWI fly ash were chosen for further study, as this would provide a broad interpretation of how MSWI fly ash residues perform.

Electrodialytic remediation was chosen to treat the three residues, as this method can potentially extract the valuable metals from the residues and improve the residues performance in cement-based materials. Although the treatment improved the characteristics of the residues, the treated residues were still very different from the traditionally used SCMs, and that they may be characterised as high Ca mineral additions. Furthermore, the electrodialytic remediation treatment did not recover a large amount of the valuable metals from the residues compared to acid leaching. Acid leaching had a combined average removal of Cd, Cr, Cu, Pb and Zn of 50-65% at lab-scale, while remediation removed between 32-37% at lab-scale and 18% at bench-

scale. Therefore, electrodialytic remediation may be an inefficient treatment for recovering the valuable metals from MSWI fly ash residues.

Remediation did improve the residues performance in blended binders with 10% cement replaced with one of the residues. It reduced the setting time delay and expansion caused by the residues. For the MSWI fly ash and sulphur-rich fly ash, it improved the compressive strength and resulted in a higher strength than 10% cement replacement with inert quartz. The treated residues were not pozzolanic. Therefore, the contribution to the compressive strength may be hydraulic and due to the formation of additional ettringite and monocarbonate, binding more water. The untreated APC residue resulted in as high compressive strength as a control without any cement replacement.

Heavy metals leaching from the blended binders with MSWI fly ash was a concern for their potential use since external environmental factors such as chlorides and sulphates may increase leaching. It was determined that the monolithic heavy metal leaching was below regulatory limits, even with external environmental factors. Cr was the only metal leaching from crushed binder material in higher concentrations than the regulatory limits permit. However, the control specimen with only cement leached as high a Cr concentration as the specimens with MSWI residues, indicating that the residues were not an issue but that the cement itself may be.

During the experiments, it was observed that the untreated APC residue could function as an accelerator and that the treated sulphur-rich residue may replace the gypsum in cement. Additional experiments then showed that the APC residue could indeed function as an accelerator, although not as efficiently as a commonly used accelerator, and that the treated sulphur-rich residue can replace gypsum.

In summary, it was concluded that the EDR process shows potential as a treatment for using MSWI fly ash residues in cement-based material but may require additional research to optimise the process and results, especially to increase metal extraction.

Resume

Cementproduktion udleder store mængder CO_2 til atmosfæren. Det er estimeret at produktionen af cement står for 8% af de menneskeskabte CO_2 udledninger om året. Én måde at reducere emissionerne på, er ved at benytte mineralske tilsætninger til at lave beton med. Grundet lave forsyninger er der brug for nye mineralske tilsætninger. Flyveaske fra affaldsforbrænding kan potentielt benyttes som en ny mineralsk tilsætning. Dette kræver dog at flyveasken forbehandles først da denne anses for at være skadelig for mennesker of udgør et miljøproblem. Hvis man med forbehandlingen også er i stand til at udtage de værdifulde metaller i affaldsflyveasken, vil det være fordelagtigt. Derfor er formålet med dette ph.d.-projekt at udvikle en forbehandlingsmetode, som kan udtage de værdifulde metaller i affaldsflyveasken og gøre at asken kan benyttes som et mineralsk tilsætningsmiddel.

Fem affaldsflyveasker (fire flyve asker og en luftforureningskontrol rest) blev anskaffet til ph.d.-projektet fra tre forskellige affaldsforbrændingsværker. Affaldsflyveaskerne blev karakteriseret på baggrund af deres kemiske sammensætning og partikelstørrelse og derefter screenet baseret på brug i cementbaserede materialer. Burgen af multivariat dataanalyse viste at en af affaldsflyveaskerne, luftforureningskontrol resten, havde en gennemsnitlig sammensætning for affaldsflyveaske rester. Tre af affaldsflyveaskerne havde mindre gennemsnitlig sammensætninger. Den sidste, en svovlrig affaldsflyveaske, var en udstikker i dataanalysen sammenlignet med affaldsflyveaske fra litteraturen. Luftforureningskontrol resten, en af de tre affaldsflyveasker og den svovlrige affaldsflyveaske blev valgt til det videre studie, da disse tre kunne bidrage med en bred forståelse for hvordan affaldsflyveaske kan benyttes.

Elektrodialytisk rensning blev valgt til at forbehandle de tre affaldsflyveasker, da denne metode potentielt kan udtage de værdifulde metaller og forbedre affaldsflyveaskernes egenskaber i cement baserede materialer. Selvom den valgte forbehandlings metode forbedrede affaldsflyveaskernes egenskaber var de behandlede affaldsflyveasker stadig meget forskellige fra de traditionelt benyttede mineralske tilsætninger og ville kunne betegnes som mineralske tilsætninger med meget Ca. Foruden dette, kunne elektrodialytisk rensning ikke udtage store mængder af de værdifulde metaller fra affaldsflyveaskerne sammenlignet med syre udludning. Syre udludning havde en kombineret gennemsnitlig fjernelse af Cd, Cr, Cu, Pb og Zn på 50-65% mens den elektrodialytiske rensning kun fjernede 18-37%. Derfor er det muligt at elektrodialytisk rensing ikke er en velegnet metode til at udtage værdifulde metaller fra affaldsflyveaske.

Forbehandlingsmetoden forbedrede dog affaldsflyveaskernes effekt i blandede bindemidler, hvor 10% af cementen var erstattet med en af de forbehandlede affaldsflyveasker. Forbehandlingen reducerede afbindingstiden og den volumen udvidelse affaldsflyveaskerne forårsagede. Tilsætningen med en af de mindre gennemsnitlige affaldsflyveasker og den svovlrige affaldsflyveaske forbedrede det trykstyrken og resulterede i en trykstyrke højere end en referenceprøve indeholdende 10% inert kvarts. De forbedrede affaldsflyveasker var dog ikke pozzolanske. Den forbedrede tryk styrke kunne skyldes en hydraulisk effekt og en øget udfældning af ettringit og monokarbonat, hvilket binder mere vand. Den ubehandlede luftforureningskontrol rest resulterede i en tilsvarende høj trykstyrke som en referenceprøve uden noget cement udskiftning.

Udludning af tungmetaller fra de cement baserede materialer indholdene affaldsflyveaske var et muligt problem, da de cement baserede materialer kunne udsættes fra eksterne miljømæssige faktorer så som Cl^- og SO_4^{2-}, der ville kunne øge udludningen. Resultaterne viste dog, at tungmetalsudludningen fra hele cement hærdede prøver var under de lovgivningsmæssige grænser selv med de udvendige miljømæssige faktorer. Cr udludning fra knuste cement hærdede prøver var dog højere end de lovgivningsmæssige grænser tilladte. Prøven uden noget cement erstatning udludede Cr i lige så store mængder som prøverne med cement erstatning, hvilket indikerede, at den høje udludning ikke skyldtes affaldsflyveaskerne.

Under forsøgene blev det observeret, at den ubehandlede luftforureningskontrol rest kunne benyttes som en accelerator, og at den svovlrige affaldsflyveaske ville kunne udskifte den gips, der benyttes i cement. Yderligere eksperimenter viste at luftforureningskontrol resten ville kunne benyttes som en accelerator, dog ikke lige så effektivt som en af de traditionelt benyttede acceleratorer, og at den svovlrige affaldsflyveaske kan udskifte gipsen i cement.

Sammenfattende blev det konkluderet, at elektrodialytisk rensning har potentiale som behandlingsmetode for affaldsflyveaske, så den behandlede affaldsflyveaske kan benyttes i cement baserede materialer. Yderligere forskning skal dog forbedre metoden optimeres så flere af de værdifulde metaller kan udtages.

Structure of Thesis

The thesis is organised into four parts, followed by the appendix:

Part I – Introduction & Framework. The first part of the thesis provides a general introduction to the topic and the background of the thesis by exploring the theory and knowledge gaps concerning the project and defining the project's limitations and objectives.

Part II – Experimental Approach & Methods. The second part of the thesis gives a brief overview of the research methodology and methods used as part of the PhD study. The methods are more thoroughly described in the appended papers.

Part III – Results, Discussion & Conclusion. Part three of the thesis presents the main findings of the appended papers and the additional note, providing a combined discussion and conclusion of the work.

Part IV – Appended Papers. The fourth part of the thesis contains the collection of appended papers and abstracts that serves as the basis for the thesis.

List of Appended Papers

This thesis includes four journal papers, a conference paper, a conference abstract, and an additional note. One of the four journal papers has been published. The remainder is, as of the writing of this thesis, under review.

1) **Screening of untreated municipal solid waste incineration fly ash for use in cement-based materials**, Journal paper, Published.

2) **Electrodialytic Remediation and Combined Acid Leaching and Solvent Extraction – Potential Methods for Recovery of Metals from MSWI Fly Ash**, Journal paper, Under review.

3) **Effects of Chloride and Sulphates on Leaching from Mortar with Raw and Electrodialytically Treated MSWI Fly ash**, Journal paper, Under review.

4) **Impact of Electrodialytic Remediation of MSWI Fly Ash on Hydration and Mechanical Properties of Blended Binders**, Journal paper, Under review.

5) **The Effect of MSWI Fly Ash on Mortar Workability**, Conference paper, Published.

6) **Valorisation of MSWI Fly Ash for Use in Cement Based Materials**, Conference abstract, Published.

7) **Alternative Strategies for Using MSWI Fly Ash in Cement-Based Materials**, Additional note, Unpublished.

Table of Contents

Appendix

List of Symbols and Abbreviations

Cement chemistry shorthand notations employed in this thesis:

C = CaO	S = SiO_2	A = Al_2O_3	F = Fe_2O_3
M = MgO	H = H_2O	= CO_2	= SO_3

Shorthand notation of anhydrous components and hydrates in cement systems:

Name	Shorthand	Formula
Alite	C_3S	$3CaO{\cdot}SiO_2$
Belite	C_2S	$2CaO{\cdot}SiO_2$
Tricalcium Aluminate	C_3A	$3CaO{\cdot}Al_2O_3$
Tricalcium Aluminoferrite	C_4AF	$4CaO{\cdot}Al_2O_3{\cdot}Fe_2O_3$
Gypsum	$C\bar{S}H_2$	$CaSO_4{\cdot}2H_2O$
Calcite	$C\bar{C}$	$CaCO_3$
Calcium Silicate Hydrate	C-S-H	Variable composition
Calcium Aluminate Hydrate	C-A-H	Variable composition
Calcium Aluminate Silicate Hydrate	C-A-S-H	Variable composition
Portlandite	CH	$Ca(OH)_2$
Monosulphate	$C_4A\bar{S}H_{12}$ (Ms)	$4CaO{\cdot}Al_2O_3{\cdot}SO_3{\cdot}12H_2O$
Ettringite	$C_6A\bar{S}_3H_{32}$ (Et)	$6CaO{\cdot}Al_2O_3{\cdot}3SO_3{\cdot}32H_2O$
Monocarbonate	$C_4A\bar{C}H_{11}$ (Mc)	$4CaO{\cdot}Al_2O_3{\cdot}CO_3{\cdot}11H_2O$
Hemicarbonate	$C_4A\bar{C}_{0.5}H_{12}$ (Hc)	$4CaO{\cdot}Al_2O_3{\cdot}0.5CO_3{\cdot}12H_2O$

Other abbreviations:

AMA : MSWI fly ash residue sampled from Amager Bakke.

AMA-X : Additional MSWI fly ash residue sampled from Amager Bakke.

NUU : MSWI fly ash residue sampled from the incinerator in Nuuk.

NUU-X : Additional MSWI fly ash residue sampled from the incinerator in Nuuk.

RYA : MSWI fly ash residue sampled from Ryaverket.

AFm : Monosulphate, Monocarbonate, Hemicarbonate

AFt	: Ettringite
APC:	: Air Pollution Control
CHP	: Combined Heat and Power
CFA	: Coal Fly Ash
EDR	: Electrodialytic Remediation
ESP	: Electrostatic Precipitator
GGBFS	: Ground Granulated Blast Furnace Slag
ICP-OES	: Inductively Coupled Plasma – Optical Emission Spectroscopy
L/S	: Liquid to Solid ratio
MSWI	: Municipal Solid Waste Incineration
OPC	: Ordinary Portland Cement
PCA	: Principal Component Analysis
SCM	: Supplementary Cementitious Materials
SDG	: Sustainable Development Goals
XRD	: X-Ray Diffraction
XRF	: X-Ray Fluorescence

Part I
Introduction & Framework

1. Transitioning to a Sustainable Society

As a consequence of human activities, the global climate has begun to change [1]. There has been an increase in global anthropogenic greenhouse gas emissions, resulting in increasing global temperatures and increased environmental instability, leading to the contamination or destruction of the environment. To prevent future adverse environmental effects from occurring, focus on sustainable development and the environment has increased.

The United Nations Framework Convention on Climate Change is the global environmental agreement from 1992 that addresses climate change and seeks to stabilise the concentration of greenhouse gases in the atmosphere and mitigate the consequences of climate change [2]. Furthermore, In 2015 the United Nations proposed 17 new goals to ensure socially, economically and environmentally sustainable development and increase peace, safety, and international collaboration [3]. See Fig. 1. One part of the sustainable development goals (SDG) concerns responsible development and resource use and reducing the amount of waste generated and released into the environment (SDG 12). Part of the goals also concerns the sustainable development of the environment and combating climate change and its consequences (SDG 13). Therefore, climate change mitigation or "green conversion" has become an essential goal of which the implementation of clean energy is crucial. As CO_2 accounts for 72% of the greenhouse gasses, 88% of which come from coal, oil and natural gas combustion [4], it is understandable. However, the need for commitment and action is required by all levels of society. To that end, several alterations may be implemented to the construction and building materials field.

Figure 1: The 17 sustainable development goals of the United Nations. Modified from [5].

A potential alteration to the current materials used for construction that may help climate change mitigation and assist in achieving SDG 12 and 13 may be found by combining concrete manufacturing and municipal solid waste incineration (MSWI).

Concrete is a durable, robust and versatile material that can be moulded into any shape while relatively inexpensive and easy to produce due to ample access to the required raw materials, making it the most widely used material on earth, after water. Concrete is not an environmentally harmful material in terms of CO_2 release. Compared to other building materials, concrete manufacturing results in less CO_2 emissions [6]. However, due to the amount of concrete used for construction, large quantities of CO_2 have been emitted annually [6]. The majority of the CO_2 release originates from ordinary Portland cement (OPC) production, the key component in concrete manufacturing. Cement clinker production accounts for 4% of the global anthropogenic CO_2 emissions, 8% if fuel combustion emissions are included [4,7]. Cement producers and concrete manufacturers can do a lot to reduce the CO_2 footprint of concrete. The raw materials used for cement production may be replaced with raw materials containing less CO_2 [8]. The OPC may be replaced with low-emission cement types such as belite rich clinkers [8]. The concrete could be made with recycled aggregates or local aggregates susceptible to alkali-silica reaction, avoiding long transport of non-reactive aggregates. Using less cement is also a possibility and may be an ecologically and economically beneficial solution [6]. Leaner concrete with less cement per m^3 can be produced using plasticisers, or slimmer structures may be produced with high strength concrete using more cement per m^3 but using less m^3 [6,8]. Concrete manufacturing's contribution to the global anthropogenic CO_2 emissions may also be reduced by substituting cement with supplementary cementitious materials (SCMs). Cement substitution with SCMs, such as ground granulated blast furnace slag (GGBFS) or coal fly ash (CFA), has already been done to significant effect, replacing high amounts of cement without compromising the end concrete product, and in some cases, improving the quality. However, SCM use is highly reliant on availability and rising demand. Limited supplies of the most commonly used SCMs can limit the potential for further CO_2 reduction through cement substitution [8].

Introducing new materials that can partially replace cement can help continue to reduce CO_2 emissions from concrete manufacturing. This is where municipal solid waste incineration may be introduced, as fly ash residues from municipal solid waste incineration may be used for concrete manufacturing [9]. However, this is not a clear-cut process as MSWI fly ash residues differ in chemical composition compared to CFA and are considered hazardous due to their high content of toxic metals, soluble salts and organic contaminants. Therefore, the MSWI fly ash residues

would require a pre-treatment before being utilised as an SCM. A standard disposal strategy for MSWI fly ash residues is landfilling in landfills designed to accommodate hazardous waste. Landfilling the MSWI fly ash residues results in the loss of a potential new SCM and valuable metals seen as toxic hazardous in landfills, but if extracted, may be considered a resource. Therefore, the implemented pre-treatment should enable MSWI fly ash residues to replace cement partially and extract the valuable metals to be used for other projects, making MSWI fly ash residues a resource and creating synergy between waste disposal and construction, see Fig 2. A potential treatment that may extract valuable metals, remove the soluble salts and improve the MSWI fly ash residue for use with cement is electrodialytic remediation (EDR) [10–12]. However, the treatment and the treated residue requires further studying before this can become a possibility.

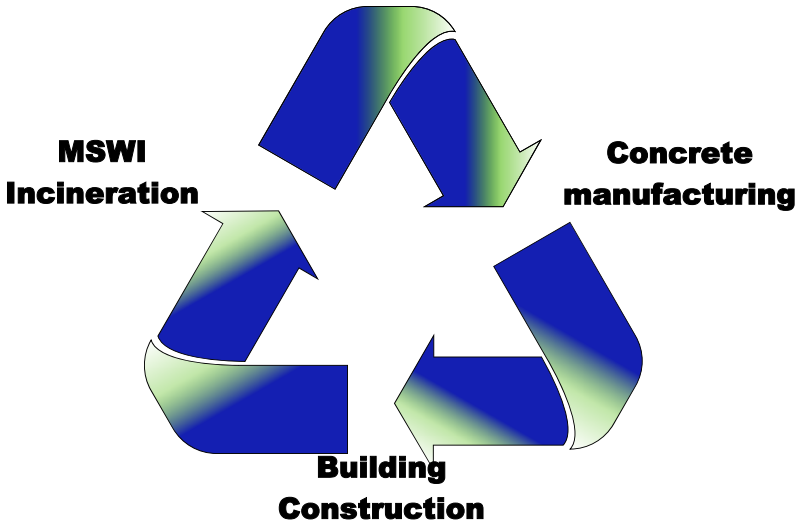

Figure 2: Synergy between waste disposal and construction

2. Background

2.1 Ordinary Portland Cement

Ordinary Portland cement is produced from a variety of raw materials that are finely ground. The primary raw material limestone is burned in rotary kilns at temperatures above 1300 ˚C, together with secondary raw materials such as Chalk, Marl, Clay and Sand [13]. The reactions occurring during the thermal process can be summarised as [13]:

$CaCO_3$	➔ $CaO + CO_2$	~ 800 ˚C -
$2CaO + SiO_2$	➔ $2CaO{\cdot}SiO_2$	800 ˚C -
$3CaO + Al_2O_3$	➔ $3CaO{\cdot}Al_2O_3$	900 ˚C -
$4CaO + Al_2O_3 + Fe_2O_3$	➔ $4CaO{\cdot}Al_2O_3{\cdot}Fe_2O_3$	900 ˚C -
$CaO + (CaO)_2{\cdot}SiO_2$	➔ $3CaO{\cdot}SiO_2$	> 1300 ˚C

Due to the CO_2 released from the incineration of $CaCO_3$, cement clinker production accounts for 4 % of the global yearly anthropogenic CO_2 emissions [4,7]. The clinker, obtained after burning, is rapidly cooled, blended with gypsum and ground to a fine powder.

The principal oxides in ordinary Portland Cement clinker are CaO, SiO_2, Al_2O_3 and Fe_2O_3. Other oxides present are alkalis (K_2O and Na_2O), Free lime (CaO) and magnesia or periclase (MgO) [13]. The principal oxides constitute the primary mineral phases of Portland cement clinker, which are [13]:

Alite	55 - 65 %
Belite	15 - 25 %
Tricalcium Aluminate	8 - 14 %
Tricalcium Alminoferrite	8 - 12 %

Alite and belite react with water to form C-S-H gel (varying Ca/Si ratio) and portlandite according to the following reactions [13]:

$3CaO{\cdot}SiO_2 + xH_2O$ ➔ $yCaO{\cdot}SiO_2{\cdot}(x+y-3)H_2O + (3-y)Ca(OH)_2$
$2CaO{\cdot}SiO_2 + xH_2O$ ➔ $yCaO{\cdot}SiO_2{\cdot}(x+y-2)H_2O + (2-y)Ca(OH)_2$

Alite reacts faster than belite and is the principal contributor to hydrated cement paste's strength development during the first 28 days of hydration. Belite reacts slowly, and part of it can remain unreacted after one year of hydration. Tricalcium Aluminate reacts rapidly with water to form (in the absence of portlandite) a gel-like material that transforms into $2CaO{\cdot}Al_2O_3{\cdot}8H_2O$ and $4CaO{\cdot}4Al_2O_3{\cdot}19H_2O$ that later convert into thermodynamically stable $3CaO{\cdot}Al_2O_3{\cdot}6H_2O$ [13]. The rapid reaction of tricalcium aluminate is reduced by blending the clinker with gypsum. In the

presence of gypsum, tricalcium aluminate reacts to form ettringite that, after all of the gypsum has reacted, reacts with the remaining tricalcium aluminate to form monosulphate, according to the following reactions [13]:

$3CaO{\cdot}Al_2O_3 + 3CaSO_4{\cdot}2H_2O + 26H_2O \rightarrow 6CaO{\cdot}Al_2O_3{\cdot}3SO_4{\cdot}32H_2O$

$6CaO{\cdot}Al_2O_3{\cdot}3SO_4{\cdot}32H_2O + 2(3CaO{\cdot}Al_2O_3) \rightarrow 3(4CaO{\cdot}Al_2O_3{\cdot}SO_4{\cdot}12H_2O)$

The tricalcium aluminoferrite phase reacts similarly to tricalcium aluminate with similar reaction products, as the Al in ettringite and monosulphate can be replaced with Fe. However, the reaction of tricalcium aluminoferrite occurs at a much slower reaction rate [13]. In the presence of limestone, the remaining tricalcium aluminate reacts with the limestone forming a combination of mono- and hemicarbonate according to the following reactions [14]:

$3CaO{\cdot}Al_2O_3 + CaCO_3 + 11H_2O \rightarrow 4CaO{\cdot}Al_2O_3{\cdot}CO_3{\cdot}11H_2O$

$3CaO{\cdot}Al_2O_3 + 0.5CaCO_3\ 0.5Ca(OH) + 11.5\ H_2O \rightarrow 4CaO{\cdot}Al_2O_3{\cdot}0.5CO_3{\cdot}12H_2O$

Mono- and hemicarbonate formation stabilises ettringite that no longer decomposes to form monosulphate. After seven days of hydration, a relatively large peak for hemicarbonate can be observed with X-ray diffraction, decreasing over time as monocarbonate forms instead. It may be attributed to the limited solubility/slow dissolution of limestone [14].

2.2 Supplementary Cementitious Materials

Supplementary cementitious materials or supplementary cementing materials is the umbrella term for a broad category of materials used in concrete manufacturing, which may be defined as materials that contribute to the properties of hardened concrete [15]. SCMs are commonly divided into two categories, pozzolanic SCMs and latent hydraulic SCMs [16]. Pozzolanic SCMs are defined as SiO_2-Al_2O_3-Fe_2O_3 materials that independently do not react with and harden in water. However, when finely ground and mixed with water, they may react with portlandite and form similar compounds as hydrating cement [17]. Pozzolanic SCMs are naturally or industrially formed compounds that may be further subdivided, based on their major oxides, into silicas (e.g. silica fume, nano-silica, rice husk ash, hydrothermal silica and diatomaceous earth), aluminosilicates (e.g. siliceous coal fly ash, calcined clays, burnt shale, trass and scoria) and alumina (e.g. nano-alumina) [16]. Latent hydraulic SCMs are defined as inorganic materials that can react with water and form cementitious products independently. However, their reaction is considerably slower than ordinary Portland cement, requiring a chemical activator of alkaline or sulphate origin, which OPC provides [16,18]. Commonly used latent hydraulic SCMs are ground granulated blast furnace slag, synthetic calcium aluminate glasses, and to some extent, high

calcium CFA [16,18]. A third category of SCMs may be defined, referred to as carbonates [16]. Carbonates have long been considered inert filler in ordinary Portland cement, only contributing as nucleation sites accelerating cement setting [16]. However, they may react with aluminate hydrates, as shown in Section 2.1, and have recently been shown to increase strength in ternary blends with CFA due to increased alumina from the CFA [16]. SCMs may have a physical and chemical effect in blended binders [16]. The physical effects include pore refinement, connectivity of pores and particle packing. Often SMCs have a lower density, lower particle size and higher surface area, where partially replacing the cement increases the binder volume relative to the aggregates. This leads to a considerable void size refinement at the start and reduced permeability during setting, limiting the transport of aggressive species into the concrete [16].

The different SCMs react in various ways forming C-S-H gel (silica), C-A-H gel (alumina) and C-A-S-H gel (aluminosilicates) [16,18]:

$Ca(OH)_2 + SiO_2 + H_2O$ ➔ C-S-H
$Ca(OH)_2 + Al_2O_3 + H_2O$ ➔ C-A-H
$Ca(OH)_2$ + Aluminosilicates + H_2O ➔ C-S-H + C-A-H + C-A-S-H

A representative for Calcium aluminate hydrate may be C_3AH_6, while C_2AH_6 may represent the mixed C-A-S-H product [16]. The C-S-H gel formed from the pozzolanic reaction differs from the gel formed during cement hydration. The pozzolanic reaction formed gel has a lower C/S ratio and longer linear polysilicate anions [16]. In addition to increasing the compressive strength, the additional gel also makes the blended binder more durable.

2.3 Municipal Solid Waste Incineration

Municipal solid waste incineration is the act of thermally treating solid waste, preventing large volumes of waste from being landfilled. Solid waste is commonly incinerated at combined heat and power (CHP) plants. The purpose of incinerating waste is to reduce the total organic matter content, destroy organic contaminants, concentrate inorganic contaminants, preserve raw materials and resources and recover the innate energy content of the waste [19]. Furthermore, incineration reduces the volume of waste by approximately 90% and mass by approximately 75% [19]. After incineration, the remaining solid residues, fly ash, air pollution control (APC) residues, and bottom ash require further processing.

The incinerated waste consists of household, industrial waste and waste from commercial sites. Hazardous waste is treated at special hazardous waste incineration facilities. The quality and quantity of incinerated waste can be influenced by waste prevention and recycling, waste

processing, and sorting and separate collection. The residue after incineration is dependent on the waste input, separate collection of small electrical appliances could, as an example, reduce the Cu in part of the residue by up to 80% [19].

Municipal solid waste incinerators can be divided into two categories based on the incinerated waste. Waste can be burned in the state that it is received as, in mass burn systems or pre-processed, e.g. shredded to reduce its size, in refuse-derived fuel systems [19]. Although the two systems differ in how the waste is processed, incinerators consist of four operational stages: waste handling, storage and pre-processing, waste combustion, heat recovery and air pollution control [19]. Fig. 3 depicts a general schematic design of a modern grate fired mass-burn incinerator.

Mass burn systems are the most common type of incinerator in use and can be divided into two sub-categories. European-design mass burn systems, where waste is generally fed onto furnace grates using gravity and transported through the furnace by the reciprocating or tumbling action of the grates. These incinerators can burn 100 - 1000 tonnes of waste per day while maintaining furnace temperatures above 1000˚C [19]. Two-stage mass burn systems consist of a primary and secondary combustion chamber. Hydraulic rams transport waste down an oxygen-starved primary chamber (approximately 800˚C), mixing the waste inefficiently. The process then generates fuel-rich flue gasses, which are passed into the highly oxidative conditions of the burn systems, limited in capacity to 100 tonnes of waste per day [19].

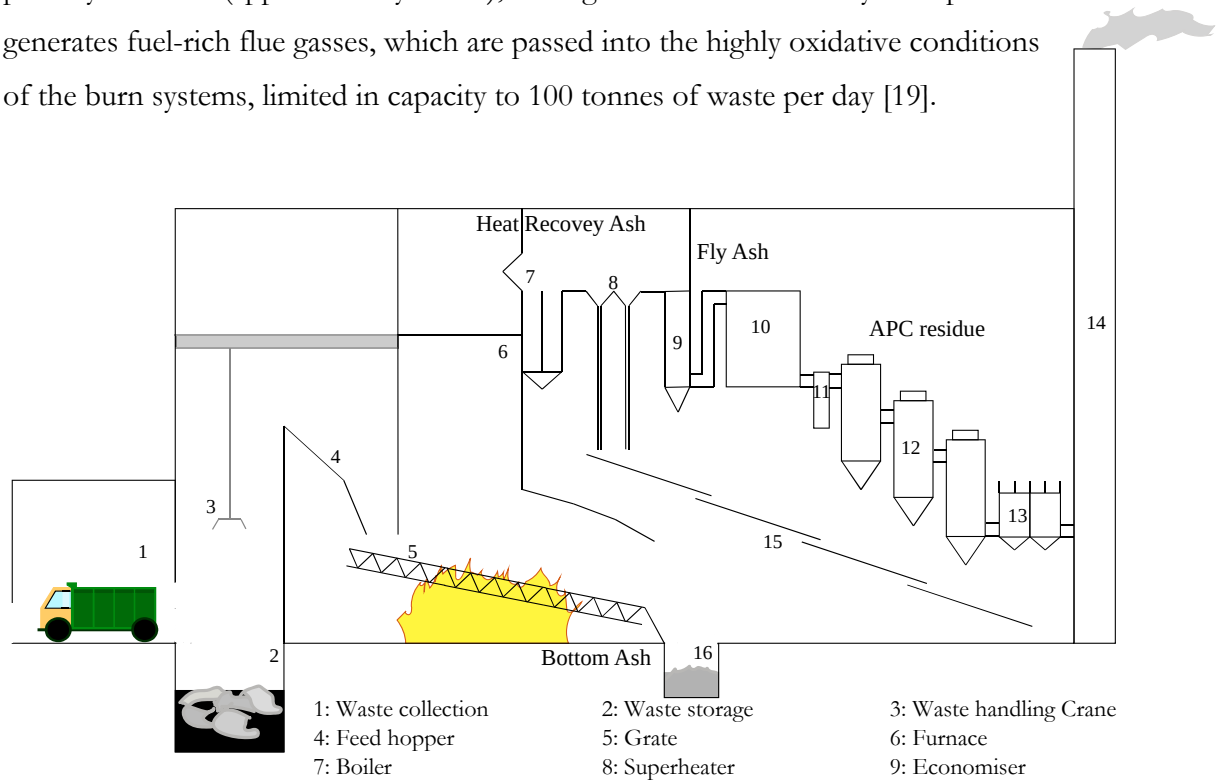

1: Waste collection
2: Waste storage
3: Waste handling Crane
4: Feed hopper
5: Grate
6: Furnace
7: Boiler
8: Superheater
9: Economiser
10: ESP
11: Catalysator
12: Scrubber System
13: Fabric filter
14: Stack
15: Fly ash conveyor
16: Ash bunker

Figure 3: General schematic design of a modern grate fired mass-burn incinerator. Drawn based on information from [19,20].

Refuse-derived fuel systems can be divided into three sub-categories, semi-suspension units, spreader stoker units and fluidised bed incinerators. In a semi-suspension unit, shredded waste is injected into the furnace high above a grate, where it burns as it falls down the furnace to the grate. Semi-suspension units incinerate more than 400 tonnes of waste per day at temperatures close to or above 1000°C [19]. Spreader stoker units are similar to semi-suspension units, injecting the fuel across the burning grates of the furnace instead of high above. Spreader stoker units can be smaller than semi suspension units but maintain similar temperatures [19]. Fluidised bed incinerator systems consist of a furnace with a bed of inert material, typically sand, where combustion air is injected into the bed to fluidise the inert material. Shredded waste is then fed separately into the bed. The inert materials heat retention and the abrasion of the waste with the inert material ensures efficient combustion conditions at low temperatures (approximately 850°C). The incineration capacity of fluidised bed incinerators is approximately 200 tonnes of waste per day [19].

In combined heat and power plants, regardless of incinerator type, the released heat is recovered in the heat recovery system, producing steam. The heat recovery system typically consists of a radiant and convective heat recovery section, an economiser and a superheater section. The temperature of the heat recovery section ranges from approximately 900°C to 180°C at the exit of the economiser section. Most incinerator units contain air pollution control systems (Catalysator, Dry-scrubber and Wet-Scrubber) to limit the release of pollutants into the atmosphere. The flue gas leaving the heat recovery system contains gaseous combustion products such as water vapour, CO_2, HCl, SO_2 and NO_x, vaporous forms of metals and organic species, and solid particulate matter.

There are two primary types of APC systems. The dry/semi-dry scrubber systems and the wet scrubber systems.

In a dry and semi-dry APC system, the release of pollutants is controlled by cooling and chemical conditioning. Cooling is facilitated by adiabatic evaporation of a water spray without the formation of a liquid effluent stream. Acid gas neutralisation is achieved by injecting an acid gas sorbent, either in the form of powdered lime in the dry scrubber system or a lime slurry in the semi-dry scrubber system. The injected sorbents neutralise the gas and increase the surface area available to absorb the flue gas condensation products. The dry and semi-dry scrubber system then requires particle removal from the flue gas downstream of the scrubbers [19].

A wet scrubber APC system uses a water spray to cool the flue gas adiabatically and generate a fine mist, acting as condensation nuclei for the contaminants. Furthermore, a liquid effluent

stream is generated by adding excess water. Wet scrubber systems can be either one or two-stage systems. The first stage is run under strongly acidic conditions, and the second stage is run under neutral conditions by adding either NaOH, lime or other alkaline reagents to remove SO_2 better. Wet scrubber systems generate a wastewater discharge stream that contains high amounts of various salts and a solid stream in the form of a sludge or filter cake [19].

The incineration converts organic matter into CO_2 and H_2O while leaving behind various inorganic materials as residue. The leftover residue is generally classified into two categories, bottom ash and fly ash. Bottom ash is the material discharged from the bottom of the furnace, including any material injected into the flue gas [19]. Bottom ash can be subdivided into grate ash, the heterogeneous material discharged from the burning grates, and grate siftings, the material that falls through the grate and is collected at the bottom of the furnace [19]. Fly ash is the residue carried from the furnace by the flue gas. It can be subdivided into heat recovery ash, the particulate matter collected from the heat recovery system, fly ash, the particulate matter removed after the heat recovery system before any flue gas injections and APC residues, the particulate matter collected after the flue gas treatment [19]. The inorganic portion of the waste can be divided into lithophilic and volatile elements, see Table 1. Lithophilic elements are elements where their main elemental compounds have boiling points higher than 1500˚C and are more concentrated in the bottom ash [19]. Volatile elements are when the main elemental compounds have high vapour pressures under waste combustion conditions and are transferred to the vapour phase during combustion Volatile elements are when the main elemental compounds have high vapour pressures under waste combustion conditions and are transferred to the vapour phase during combustion [19]. These elements are then split between the bottom ash and fly ash streams. Lithophilic elements can be found in fly ash due to entrainment and carry over from solid particles in the furnace. Halogens and sulphur initially present in the incinerated waste are mainly found in the flue gas as acid gas, where it then condenses during heat recovery [19].

Table 1: Distribution of elements during incineration [19].

	Lithophilic	Volatile
Alkali Metals	Be, Mg, Ca, Sr, Ba, Ra	Na, K, Rb
Heavy Metals	Ti, Cr, Mn, Fe, Ni, Cu	Hg, Cd, Sn, Se, Ti, Te, Zn, Pb
Halogens		Cl, Br, I
Other	Al	S

During incineration, toxic organic compounds such as polychlorinated dibenzo-P-dioxins (PCDDs) and polychlorinated dibenzofurans (PCDFs) can form that persist through the flue gas stream [19]. However, data indicate that PCDDs/PCDFs mainly occur in older or improperly managed facilities, while significant net destruction of the compounds occurs in modern well-operated facilities [19].

Bottom ash has a high content of alkali/ alkali earth elements and metal oxides, resulting in a pH between 9.5 and 11.5. The major elements (>10.000 mg/kg) are Al, C, Ca, Fe, K, O and Si, while the minor elements (1000-10000 mg/kg) are Ba, Cl, Cr, Cu, Mg, Ti, Pb and Zn. The trace elements in bottom ash (<1000 mg/kg) are Ag, As, B, Br, Ce, Co, F, Hg, I, Mo, Ni, Sb, Se, Sn and Sr [19].

Fly ash from MSWI has an alkaline pH as well, and the major elements (>10.000 mg/kg) are Al, Ca, Cl, Fe, K, Na, S and Si, commonly present as oxides. Substantial amounts of Mg, Pb and Zn are also present. The minor elements (1000-10000 mg/kg) are Ba, Cu, Mn, Sn and Ti, while the trace elements are Ag, As, Cd, Co, Cr, Mo, Ni, S, Sb and Sr (<1000 mg/kg) [19]. The major elemental constituents of dry and semi-dry APC residues are Al, Ca, Cl, Fe, K, Mg, Na, O, S, Si and Zn. Only Ca, Cl and SO_4 are present in dry and semi-dry APC residues in higher amounts than non-APC fly ash residues [19]. However, the concentration of the various elements and pH of the different residues are dependent and varies from incinerator to incinerator

Incineration is not a final solution for waste disposal as the generated residues require further management and disposal [19]. MSWI bottom ash has found use as an aggregate substitute for engineering work, while MSWI fly ash residues are disposed of in landfills. However, due to their content of organic contaminants, toxic metals and salts, MSWI fly ash residues are considered hazardous and are commonly treated before disposal.

2.4 MSWI Fly Ash Treatment

The different methods of treating MSWI fly ash developed and investigated can be classified into three categories, solidification/stabilisation, thermal treatments and separation/extraction, as reviewed by Zhang et al. [21].

Solidification/stabilisation consists of cement solidification, chemical stabilisation, hydrothermal stabilisation and mechanochemical treatments [21]. Cement solidification is regarded as an essential treatment method that plays a critical role in the disposal of hazardous waste at a relatively low disposal cost [21]. The fundamental principle of cement solidification is only briefly summarised here, while the method is further discussed as part of section 2.5. During the

reaction between cement and water, the heavy metals and dioxins from the MSWI fly ash may be encapsulated in the C-S-H gel, preventing leaching from the solidified product and resulting in long-term physical, chemical and biological stability [21]. Chemical stabilisation is stabilisation by chemical reactions between the heavy metals in MSWI fly ash and a reagent forming insoluble compounds, reducing leaching [21]. Both inorganic and organic reagents are used to varying degrees of effectiveness. Inorganic reagents used are among other phosphates, sulphides and iron oxides, while organic chemicals used include, among others, Thiourea, thiodiglycolic acid and dithiocarbamates [21]. The hydrothermal treatment utilises aluminosilicate mineral synthesis at 150-200°C under alkaline conditions to stabilise the heavy metals and decompose the dioxins in the MSWI fly ash [21]. Mechanochemical treatments use collision, compression, shear or friction, and additives to change the physical and chemical properties of MSWI fly ash [21], stabilising the heavy metals and reducing the dioxin content in MSWI fly ash. To achieve this, ball milling has been used, while the additives include, among others, CaO and iron powders.

Thermally treating MSWI fly ash is the process of converting the inorganic matter into a stable glassy slag by exposing it to a high temperature while the organic matter is decomposed, burned and vaporised [21]. Thermal treatment methods may be divided into two categories, sintering and melting/vitrification [21]. Sintering consists of heating the MSWI fly ash to 900-1200°C so that the chemical phases are reorganised, and particle bonding occurs, ensuring that the heavy metals are difficult to leach and the dioxins are destroyed [21]. Melting/ vitrification is a three-step process involving dehydration, polymorphic transition and fusion into a molten slag liquid [21]. Higher temperatures than sintering are required during the melting process. The process decomposes organic matter and transforms the inorganic matter into a glass slag via crystal phase transformation. Vitrification differs from melting, as it requires glass-forming additives to form a homogeneous liquid phase. Melting/vitrification is further divided into fuel burning and electric methods [21].

Separation/extraction treatments are a series of separation methods that may separate the salts and heavy metals from MSWI fly ash, resulting in leachate rich in salts and heavy metals [21]. Water-washing MSWI fly ash may remove the readily soluble chlorides in the form of soluble chlorides such as NaCl, $MgCl_2$ and $CaCl_2$, while also removing soluble sulphates [21]. The liquid to solid ratio and the washing time affect the Cl removal rate. The best washing conditions vary and are closely related to the washed fly ash residues characteristics [21]. A short term washing process does not result in the dissolution of heavy metals. However, as the process is prolonged, heavy metals may be dissolved partially [21]. Research has also shown that washing may change the heavy metals form, promoting solidification [21]. Water-washing is commonly used before

other treatment methods, such as thermal treatment, where the Cl in the MSWI fly ash hinders heavy metal fixation in the melting product [21]. Chemical and biological reagents are used to separate heavy metals by promoting leaching, resulting in a leachate solution enriched with heavy metals and MSWI fly ash with a low heavy metal content [21]. Acids, bases, salts and organic chelating agents are commonly used to leach heavy metals from MSWI fly ash. However, the highest heavy metal removal occurs under acidic conditions [21]. Inorganic acids (e.g. HNO_3, HCl and H_2SO_4) and organic acids (e.g. formic acid, acetic acid and lactic acid) have been used to leach heavy metals from MSWI fly ash. Generally, organic acids are not as effective as inorganic acids, while the different inorganic acid effectiveness depends on the heavy metal leached [21]. The biological leaching reagents used are organic acid-producing bacteria, such as the thiobacillus and Aspergillus niger strains. The biological reagents have been shown to have good potential for organic acid production and metal leaching. However, the treatment time is prolonged compared to chemical reagent leaching [21]. Leaching with chemical or biological reagents produce solutions rich in salts and heavy metals that may be extracted [21]. The water in the leachates may be evaporated to produce salts rich in a variety of heavy metals. The salts would then require further treatment before disposal [21]. Therefore, other methods of extracting heavy metals are of interest, with several potential methods developed or otherwise researched.

Two prospective extraction treatments that may recover the potentially valuable heavy metals from MSWI fly ash residues are electrodialytic remediation and combined acid leaching and solvent extraction.

2.4.1 Electrodialytic Remediation

Most heavy metals are leachable at low pH, which is why the previously discussed treatments use acidic chemical solutions or the acidic scrubber water from the flue gas treatment to extract heavy metals from MSWI fly ash. However, using chemicals may leave unwanted residuals on the ash, hindering further reuse of the ash. To avoid adding new chemical compounds or elements to the ash, electrodialytic remediation (EDR) may be used instead to extract the heavy metals. The basis for EDR is the combination of electrokinetic remediation and electrodialysis [22]. The process removes ions by applying a direct current to particulate materials in a liquid solution between two electrodes in separate electrolyte solutions [22]. The ions are then removed by electromigration, where anions migrate towards the anode and the cations towards the cathode [22].

The exchange of ions occurs in a series of compartments combined in a configuration referred to as a cell. Fig. 4 depicts the configuration of a three-compartment cell.

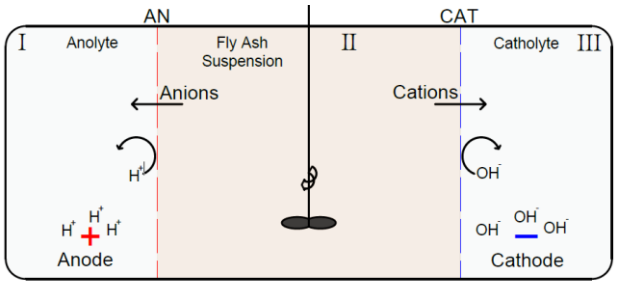

Figure 4: Principle sketch of a three-compartment cell. From journal paper II [23].

Ion exchange membranes split the different compartments of the stack, separating the particle solution (compartment II) from the electrolyte solutions (compartment I and III) circulated by pumps. The cathode is separated by a cation penetrating membrane and the anode an anion penetrating membrane. The ion exchange membranes ensure current efficiency by allowing ions from the suspension to migrate to the electrolytes while preventing the migration of oppositely charged ions [24].

At the anode, oxidation occurs, producing oxygen and protons, while a reduction occurs at the cathode resulting in hydrogen gas and hydroxide:

$$2H_2O \rightarrow O_2 + 4H^+ + 4e^-$$

$$2H_2O + 2e^- \rightarrow H_2 + 2OH^-$$

Only the free ions in the suspension migrate along the electric field. Any precipitated or adsorbed metals must become mobile before they can be removed. As the different heavy metals become mobile at an acidic pH, the suspension must be acidified. However, the electrodialytic remediation process does acidify the suspension, enhancing ion mobilisation. The ion exchange membranes may not be 100% efficient, thus transporting protons from the anolyte to the suspension [24]. Water splitting at the anion exchange membrane may also cause suspension acidification [25].

The treatment process was initially developed to treat contaminated soil [22]. but has been further developed to remediate other materials, such as wood waste [26], mine tailings [27], sewage sludge ash [28] and MSWI residues [24]. The material may be pre-treated with water washing [29] or sieving [30] before the EDR process.

At first, the EDR process consisted of a static system, treating the materials in a saturated state without stirring. Suspending ash residues in water or other solutions using a stirrer was more stable than a static system due to the high dissolution of ash, causing operational problems [29].

Several lab-scale EDR cells have been developed, other than the three-compartment. A two-compartment cell has been developed where the anode/cathode is placed directly in the suspension chamber. See Fig. 5 for a principal sketch of the cell. Furthermore, a five-compartment cell has been developed, consisting of two electrode compartments, two electrolyte compartments and the suspension chamber. In the five-compartment cell, the electrodes are separated from the electrolyte solution, preventing ions such as Cl^- from reaching the anode and forming chlorine gas or metal ions from precipitating on the cathode. Recently the effect of intermittently switching the anode and cathode has been tested for the two and three-compartment cells [11].

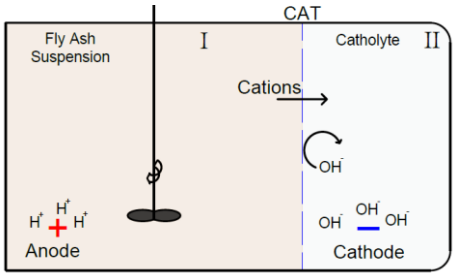

Figure 5: Principal sketch of the two-compartment cell. From journal paper II [23].

Previous lab-scale EDR experiments have found that up to 70% Cd, 28% Cr, 90% Cu, 40% Pb, and 73 % Zn can be removed from MSWI fly ash residues using the different EDR cells and changing the set-up. However, the concentration of removed metals has been found to depend on the pH in the suspension chamber, and the heavy metal speciation in the MSWI fly ash residues. Table 2 provides an overview of the different studies performed and their main findings. An effort has been made in up-scaling the treatment process to treat MSWI fly ash residues in bench-scale and pilot-scale. However, these studies and the previous lab-scale experiments aimed at removing the easily mobile part of the metals in the residues instead of achieving as high a removal percentage as possible. This was done to reduce the metal leaching from the residues.

Table 2: Selected studies EDR treating MSWI fly ash residues.

Reference	Setup	Major Findings
[31]	Three-compartment cell	Cu and Pb removal were highly pH-dependent. Up to 90 and 40% could be removed, respectively, at a pH of 3.9. However, the Pb concentration in the residue was increased, despite the removal. Up to 98% Cl could be removed.
[32]	Three-compartment cell	At an L/S ratio of 10 and a pH of 4.1 up to 60% Cd, 45% Zn and 20% Ni, Ba could be removed in 14 days. Regardless of remediation time and L/S ratio, the fraction of soluble Ba, Cr and Pb was decreased due to EDR.
[33]	Three-compartment cell	Approximately 70% Cd and between 2.5-8% Pb and 24-73% Zn could be removed from MSWI fly ash residues. The difference in removal % may be related to variations in the final pH and the heavy metal speciation in the ash.
[24]	Three-compartment cell	Up to 86% Cd, 44% Cr, 81% Cu, 20% Pb and 62% Zn could be removed from an MSWI fly ash residue when using ammonium citrate as an assisting agent.
[34]	Three-compartment cell Various types of membranes	The remediation decreased, in general, leaching from the residues. The choice of the membrane was shown to affect the subsequent leaching after the EDR treatment with statistical significance.
[35]	Five-compartment cell	The best assisting agent for Cd removal was NH3, potentially due to the formation of stable tetraammine complexes, while the best agent for Pb removal was Na-citrate. A combination of NH3 and NA-citrate showed potential for Cd, Cr, Cr, Pb and Zn removal.
[36]	Two-compartment cell Three-compartment cell	The EDR treatment reduced Cd, Cu, Pb and Zn leaching compared to the untreated residue, but Cr leaching was increased.
[37]	Two-compartment cell Three-compartment cell	The suspension chamber acidification occurs faster with the two-compartment cell than the three-compartment cell. The EDR treatment reduced Cd, Cu, Pb and Zn leaching unless the pH was reduced below 8. Cr leaching was increased.
[11]	Two-compartment cell Three-compartment cell Changing EDR cell set-up	By combining different EDR cell set-ups and changing the redox conditions up to 27.5% Cr could be extracted.
[38]	Two-compartment cell Three-compartment cell Multivariate analysis	At a pH between 6-10 1-10%, the cumulative metal removal % of As, Ca, Cd, Cr, Cu, Pb and Zn was less than 50%. For chloride rich materials, up to 40% of the metal remained in the two-compartment cell as anionic/uncharged metal species. Multivariate analysis showed that the choice of cell set-up should depend on the metals targeted and the material characteristics.

Table 2 continued: Selected studies EDR treating MSWI fly ash residues.

Reference	Setup	Major Findings
[10]	ED Stack	Metal removal was dependent on the initial concentration in the MSWI fly ash residue. The EDR treatment significantly reduced Cd, Cr, Cu, Pb and Zn leaching from the MSWI fly ash residue.
[39]	Continues-flow bench-scale reactor	The results indicated that Cd, Cu, Pb and Zn was successfully removed with the reactor and reduced leaching one size order of magnitude.
[40]	Pilot-scale experimental set-up	A significant reduction in Pb, Zn and Cl leaching occurred after the EDR treatment. The final leaching was dependent on the initial metal concentration in the MSWI fly ash residue. Cr and SO4 leaching increased during the EDR treatment.
[41]	Pilot-scale experimental set-up	Depending on the MSWI fly ash residue type, the mercury in the ash was either enriched or decreased
[42]	Pilot-scale experimental set-up	Heavy metal and salts leaching were significantly reduced after an MSWI fly ash residue had undergone EDR treatment with the Pilot-scale set-up. However, it was estimated that the set-up needs to be optimised.
[43]	Pilot-scale experimental set-up	The pilot-scale EDR treatment was found to increase the PCDD/PCDF (dioxin) levels in MSWI fly ash residues. This was estimated to be due to an accumulation of the dioxins in the residues.

2.4.2 Combined Acid Leaching & Solvent Extraction

Solvent extraction is a separation/extraction method that takes advantage of the immiscibility of liquids to selectively separate different species from one liquid to another liquid, commonly from an aqueous phase to an organic phase [44,45]. Kerosene has previously been used as an organic solvent [44,45]. Organic ligand molecules (extractants) designed to form soluble lipophilic complexes with the targeted species selectively aid the extraction process [44,45]. For heavy metal extraction, the targeted species are the metal ions of the targeted metal. The extractant is dissolved in the organic phase and mixed rapidly with the metal-containing aqueous phase, binding the targeted metal ions to the extractant and transferring the metal to the organic phase [45]. When the mixing ends, the immiscibility separates the phases again. Many extractants have been developed for solvent extraction, as the method is used industrially as part of hydrometallurgical processes for obtaining metals from mined ore. Solvent extraction was first used commercially in 1969 by Ranchers Bluebird for Cu production, and its industrial use has only grown since [46]. The process has been developed further to extract metals from various wastes, such as wastewater [47] and MSWI fly ash residues [44,45,48].

The first step in the solvent extraction process is leaching the metals from the metal-bearing material with an aqueous solution. Previous studies have shown that strong mineral acids and special complex-forming agents can leach heavy metals from MSWI fly ash to significant effect, especially Cd, Cu, Pb and Zn [49,50]. Organic acids are, in general, not as effective at leaching metals as mineral acids and complex-forming agents [49]. Fedje et al. [49] found that using 3 M

HNO_3 or 3 M HCl acid at L/S 5 100 % Cu, >95 Pb and >70% Zn could be leached from MSWI fly ash after 24 hours. Fedje et al. [49] also found that using 3M NH_4NO_3 or 0.1M EDTA with pH adjustments at L/S 5 could leach 100 % Cu after 24 hours. However, the NH_4NO_3 solution only leached 1% Pb and 29% Zn, while EDTA leached 94% Pb and 40% Zn. H_2SO_4 was also investigated as part of the study, leaching 100% Cu and Zn after 24 hours. However, only 1% Pb was leached due to $PbSO_4$ precipitation [49]. Tang et al. [50] sought to optimise the leaching yield by investigating the effect of a mineral acid at different L/S ratios, pH, temperature, and varying leaching time. They found that HCl acid could leach more Cd, Cu, Pb and Zn from MSWI fly ash than HNO_3 at the same L/S and pH. Furthermore, they found that although more metals leached initially at L/S 50, the same amount could be leached at L/S 5 the longer the leaching time. However, Pb leaching appeared to depend on the L/S ratio as the more Pb could be leached, the lower the L/S ratio [50]. The temperature was found to have little influence on Zn leaching. Leaching at 60˚C instead of 20˚C did increase Fe leaching [50]. The study by Lassesson et al. [51] investigated the influence of metal speciation on Cu leaching and found that the occurrence of Cu as phosphates or silicates hinders leaching, while as sulphates and Chlorides leaching is unhindered.

Following the leaching step is the extraction step, where the targeted metal is extracted from the leachate (aqueous phase) to the organic phase. Some of the basic parameters used in solvent extraction are the distribution ratio D_m, the separation Factor SF, the phase ratio θ, the extraction factor P and the extraction percentage E% [44,45,52].

The distribution ratio is the ratio between the total concentration of the targeted metal in the organic ($[M]_{org}$) and aqueous ($[M]_{aq}$) phases.

$$D_m = \frac{[M]_{org}}{[M]_{aq}}$$

The separation factor is the ratio between the distribution ratio of two metals (m_1 and m_2) and is defined as always being larger than 1.

$$SF_{\frac{m_1}{m_2}} = \frac{D_{m_1}}{D_{m_2}}$$

The phase ratio also referred to as the phase volume ratio, is the ratio between the organic phase volume (V_{org}) and the aqueous phase volume (V_{aq}).

$$\theta = \frac{V_{org}}{V_{aq}}$$

The extraction factor is the product of the phase ratio and the distribution ratio.

$$P = \theta \cdot D_m$$

The extraction percentage is calculated based on the distribution ratio.

$$E\% = \frac{D_m}{D_m+1} \cdot 100$$

Several criteria should be considered when assessing if an extractant is suitable for industrial applications [53,54]. The extractant should be highly selective and result in a high distribution ratio. The extractant and diluent organic phase should be chemically and temperature stable, nontoxic, noncorrosive, and inexpensive. The extractant should release the targeted metal again for further recovery, regenerating the extractant for additional use.

Several extractants have previously been investigated for recovering Cu and Zn from MSWI fly ash leachate [44,45,48,52]. These include aldoxime, ketoxime and β-ketone acid chelating extractants [44,45], phosphorus-based acidic extractants [45,48,52] and phosphorus-based chelating extractants [44,52]. Such experiments have shown great promise as between 50-95% Cu [44,45] and 75-91% Zn [44,45] can be extracted at lab-scale. Depending on the extractant used, the extraction process may be reliant on the pH of the aqueous phase [44]. The yield of the extraction was shown to be heavily dependent on the initial metal leaching. Tang et al. demonstrated that the extraction of Cu with an aldoxime might be selective. In contrast, the extraction of Zn with a phosphorus-based extractant may co-extract Fe and Pb, among other metals [44].

After the targeted metal has been transferred to the organic phase, it can be transferred to a new aqueous phase in a stripping stage, regenerating the extractant. To accomplish this, an acid such as H_2SO_4 can be used to strip Cu from a Cu-loaded organic phase to the new aqueous phase. Tang et al. found that 85-95% Cu can be transferred using 1.5M H_2SO_4 while co-stripping only a small fraction of Fe [44]. After the stripping stage, the metals may be recovered with electrowinning.

The solvent extraction process can be up-scaled to pilot-scale by using a multistage countercurrent mixer settler system. Laboratory pilot-scale experiments have found that more than 90% Cu may be extracted with a two-stage system using LIX860N-I and that more than 99% Zn may be extracted with a three-stage system using Cyanex 923 [55].

2.5 MSWI Fly Ash Residues in Binders

2.5.1 Solidification

MSWI fly ash has been characterised as having a cement-like composition, making it suitable for immobilisation in cement-based materials [56]. The effect cement solidification has on MSWI fly ash and vice versa has been studied in great detail. Cement-based materials may be the best material for solidifying hazardous waste due to relatively low costs and application ease [57]. Cement solidification can effectively reduce the environmental pollution from MSWI fly ash by reducing the leaching of heavy metals [58] and dioxins [21]. Heavy metals may be immobilised by sorption, chemical interaction or micro/macro encapsulation [59]. However, the addition of MSWI fly ash has a negative impact on cement hydration [21]. Research has shown that mortar's compressive strength and flexural strengths reduced while the setting is delayed [58]. Low dosages of MSWI fly ash may strongly delay the setting [60]. A major concern of solidification is the interaction of waste contaminants on cement properties [61]. MSWI fly ash's effect on the setting depends on the cement used, as CSA and CAC blends have a shorter setting time than OPC [62]. According to the findings of Guo-Xia et al., OPC dosage should be 35 wt%, CAC 25 wt% and CSA wt% in the solidified product to fulfil landfill standards [62].

Heavy metals may inhibit C_3S hydration based on their effect on the setting time, strength development, portlandite precipitation and heat evolution [59]. Zn^{2+} has been reported to retard early C_3S hydration, potentially due to calcium zincate coating the C_3S grains and preventing material transport necessary for hydration [59]. It has also been reported that Cu^{2+}, Cr^{3+} and Pb^{2+} may accelerate hydration due to either H^+ attack resulting from the hydrolyses of heavy metal ions or the formation of double hydroxides that consumes calcium ions, thus facilitating C_3S decomposition [59]. Polettini et al. found that Zn, Cl^- and SO_4^{2-} greatly influenced the strength and acid neutralisation capacity of cementitious products, occasionally combined with other contaminants [61].

Organics may adsorb onto cement particles or cement hydration products due to the electrostatic force, hydrophobic force, chemical bonding, hydrogen-bonding interaction, altering the surface properties of the cement particles. This may decrease unconfined compressive and impart short or long-term durability [59]. The potentially accelerating or retarding effect of organics is poorly understood [59].

Solidification may be combined with water washing to maximise the MSWI fly ash in the solidified product [63,64]. High levels of soluble chlorides may negatively affect the solidification

process and can be removed with a washing pre-treatment [64]. Alternative methods of cement solidification have also been studied. Xue et al. combined 2% trimercapto-s-triazine and 20 %cement and found that MSWI fly ash solidified blocks could meet their pollution control standards [65]. Yang et al. combined cement and a chelating agent to immobilise the hazardous elements. Magnesium potassium phosphate cement has also been studied as a potential solidification agent [66].

MSWI fly ash solidification may be improved using SCMs such as silica fume to form additional cement hydrates, reducing heavy metal leachability [67]. The addition of green stabilisers may also improve solidification by forming heavy metal precipitates or generating additional cement hydrates by internal curing [67].

2.5.1 Secondary Cementitious Material

Table 3 shows the main findings of several previous studies that investigated using untreated or treated MSWI fly ash in cement-based materials. Included in the table are the treatment method used. Several studies have investigated the possibility of using untreated or milled/sieved MSWI fly ash residues as a partial cement replacement, estimating it to be feasible. However, doing so may reduce or increase the mechanical properties, delay the hydration, increase the flow time, lead to volume expansion, and form Friedel's salt and thernadite [68–73]. Washing the MSWI fly ash residues has been reported as a feasible pre-treatment for partial cement replacement, showing promising results. However, a slight reduction in compressive strength should still be expected to occur [74–77]. Thermal treatments have shown the most promise, with increased compressive strength beyond the control reported due to the pozzolanic reaction [78–83]. Furthermore, it was reported that heavy metal leaching was not an issue when the MSWI fly ash residues were incorporated into cement-based materials and that the measured yields were within the regulatory limits. However, these treatments have not focused on recovering the potentially valuable metals in the residues. In contrast, the EDR treatment also focuses on recovering the metals and has also shown potential for use in cement-based materials [12].

Table 3: Selected studies using untreated or treated MSWI fly ash residues in cement-based materials.

Reference	Treatment	Major Findings
[68]	Ball-milling	The mechanical properties of blended binders decreased with increasing MSWI fly ash content. MSWI fly ash does exhibit cementitious activity, but the reactivity is relatively low. MSWI fly ash addition may lead to hydration retardation. Including commonly used SCMs in the blend improves the mechanical properties and reinforces heavy metal stabilisation.
[71]	Ball-milling	The hydration process of blended cement with MSWI fly ash can be divided into five periods and shows similarities to cement hydration. However, the induction period was 102 minutes longer, while the second heat evolution peak occurred earlier. The Ca(OH)2 content of the blended cement was increased before 14 days, followed by a decrease with curing time.
[69]	None	The activity ratio of MSWI fly ash is 43.58%. MSWI fly ash results in decreased mortar compressive strength. MSWI fly ash delayed cement hydration. Leaching from cement paste mixed with MSWI fly ash was below regulations
[70]	Sieved	MSWI fly ash contains a considerable amount of metallic aluminium, leading to hydrogen gas evolution and cracks and air voids. Cement paste containing MSWI fly ash had a similar or higher strength than a control specimen. The setting of paste with MSWI fly ash was accelerated.
[72]	Sieved	Cement paste with MSWI fly ash forms Friedel's salt, ettringite and thernardie. The C-S-H structure is close to that of pure cement pastes. MSWI fly ash increases the setting time of mortar and may be due to the ashes Pb and Zn content. Incorporating up to 15% MSWI fly ash in mortar increases the compressive strength. A strength reduction occurs after extended hydration (> 565 days)
[84]	-	Modelling results show that MSWI fly ash affects the aluminate phases hydration in cement paste, forming Friedel's salt and leading to a high sulphate concentration in the interstitial solution, slowing down monosulphate formation. A simplified macroscopic leaching model was developed.
[74]	Washing/milling	MSWI fly ash leached As, Cd, Cr and Sb in acidic mediums. Using MSWI fly ash in mortar decreases the compressive strength. Washing and/ or grinding the residue could enable it to be used as a partial cement replacement.
[75]	Washing	Reduced workability was observed for fresh concrete made with MSWI fly ash residues. The concrete with MSWI fly ash had slightly lower compressive strength than the control, showing some hydraulic behaviour of the MSWI fly ash.
[76]	Washing	The compressive strength of washed MSWI fly ash composites gradually decreased with increasing washed MSWI fly ash additions. The cementitious potential of the wasted MSWI fly ash is less than portland cement. To ensure sufficient strength, a maximum substitution of 40% should be used. Washed MSWI fly ash may enhance the initial and final setting time. A TCLP leaching test showed that the composites leaching yield was below regulations.
[77]	Washing/chelate addition	The washed MSWI fly ash was similar to class C CFA. 10 and 20 % cement replacement with washed MSWI fly ash showed acceptable mortar compressive strength. The washed MSWI fly ash resulted in a slight increase in heavy metal leachability with TCLP and monolithic leaching tests. The addition of chelate reduced the leaching.
[85]	Washing/acid treated sieving	Water washed MSWI fly ash performed better than acid-treated MSWI fly ash. Mortar with washed MSWI fly ash had a moderately reduced compressive strength, while it had improved resistance to freezing action. Washing the MSWI fly ash reduced its negative influence on setting kinetics.
[86]	Mechanical activation	Wet ball milling promotes the dissolution of Ca, Cl, K and Na effectively and reduces the volume expansion observed in blended binders. The result is a blended binder with flexural and compressive strength similar to a control specimen. MSWI fly ash from grate fired incinerators results in blended binders with poor performance. Circulating fluidised bed MSWI fly ash showed greater potential and better properties for utilisation than grate fly ash.
[87]	Wet sieving/washing	The treated MSWI fly ash had a chemically inert behaviour. However, it exhibited a physical effect, where the high specific surface of the treated MSWI fly ash lead to a good activity coefficient and enhanced portlandite formation. The treated MSWI fly ash was not pozzolanic reactive. It did not affect the durability of mortar as well. Ca, Cr, Pb and Zn leaching were below regulations.

Table 3 continued. Selected studies using untreated or treated MSWI fly ash residues in cement-based materials.

[88]	None	The compressive strength decreases with increasing MSWI fly ash in an MSWI fly ash/OPC blend but increases in an MSWI fly ash/ GGBFS blend until 55% MSWI fly ash. GGBFS may be activated by the chloride and sulphate in MSWI fly ash and forms ettringite and Friedel's salt. The maximum volume of ettringite and Friedel's salt is obtained close to 55% MSWI fly ash. The MSWI fly ash /GGBFS blend showed good heavy metal solidification
[12]	EDR	Heavy metal leaching from mortars with the treated MSWI fly ash was similar to a control. The compressive strength of the mortar was less than the control. The setting of the mortar was delayed by up to 16 hours and the mortars workability was decreased.
[89]	Thermal	The compressive strength of mortar with treated MSWI fly ash was higher than the control at all ages. The mortar showed could workability and had a shorter setting time than the control. The heavy metal leaching yield was far below the regulatory limits. The results showed that the treated MSWI fly ash was pozzolanic.
[78]	Thermal	Mortar with the treated MSWI fly ash exhibited similar fluidity to a control and had a similar compressive strength as the control after three days and higher strength after seven days. Tests showed that the treated MSWI fly ash was pozzolanic. Heavy metal leaching was below regulatory limits.
[79]	Thermal	Mortar with the treated MSWI fly ash had an inferior early age compressive strength compared to the but had similar to higher strength after 90 days. Modifying the basicity with CaCO3 improved the compressive strength. The improvements were due to enhanced hydration, densification and the pozzolanic reaction
[90]	Thermal	Heavy metal leaching from the treated MSWI fly ash was below regulatory limits. Mortar with the treated MSWI fly ash had a higher compressive strength than the control after 28 days. The treated MSWI fly ash had little impact on the slump, setting time, and eleastic modulus while increasing corrosion resistance.
[82]	Thermal	The treated MSWI fly ash reduced the fluidity of prolonged the mortar setting slightly compared to a control. The treated MSWI fly ash resulted in reduced early age strength but increased strength after 60-90 days due to the pozzolanic and a decrease in pores.
[91]	Thermal	The Taguchi method showed that the optimal substitution % with the treated MSWI fly ash was 27%. After 90 days of hydration, compressive strengths 139% that of the control could be obtained. Leaching from the mortar with the treated MSWI fly ash was barely detectable.
[83]	Thermal	Mortar made with the treated MSWI fly ash leached heavy metals within the regulatory limits. The mortar had a slightly lower fluidity and longer setting time. The mortar's compressive strength with the treated MSWI fly ash was lower than the control until after 28 days of hydration. The increased strength was attributed to the pozzolanic reaction.
[92]	Thermal	The compressive strength of mortar with 10% treated MSWI fly ash was lower than a control until after 60 days, where it was similar to the control. A 40% substitution resulted in a meagre strength compared to the control. The positive effect of the treated MSWI fly ash is an increase in the finest pore size. A strong correlation was found between the compressive strength and porosity.
[81]	Thermal	Higher compressive strength than a could be achieved with mortar containing treated MSWI fly ash after 14 days. This was attributed to the pozzolanic reaction and a reduction in the total pore volume. The treated MSWI fly ash reduced the fluidity and shortened the initial and final setting time. Heavy metal leaching from the treated MSWI fly ash/ cement binder was less than the regulatory limit.
[93]	Thermal	Heavy metal leaching was below regulatory limits. The treated MSWI fly ash increases the initial and final setting time. The early age compressive strength of specimens with the treated MSWI fly ash develops slowly. A more significant decree of reaction was observed at later ages. The degree of hydration of cement paste with the treated MSWI fly ash behaved similarly to the control. Variations in the cement used may affect early age strength gains but have no significant effect on the degree of hydration at later ages.

Table 3 continued. Selected studies using untreated or treated MSWI fly ash residues in cement-based materials.

[94]	Thermal	The leaching tests showed that the treated MSWI fly ash is non-hazardous. Cement may be substituted with up to 20% of the treated MSWI fly ash without sacrificing quality. The compressive strength increases while the setting time lengthens and fluidity increases.
[80]	Thermal	The early age compressive strength of cement paste with the treated MSWI fly ash was lower than a control. The greater the replacement, the lower the strength. After 28 days, 10 and 20% replacement resulted in higher strength than the control due to enhanced C-S-H formation and ongoing strength development from the treated MSWI fly ash slag. Heavy metal leaching from the paste was less than regulatory limits.
[95]	Revasol Process	cement substitution with treated MSWI fly ash does not reduce the compressive strength of concrete more than the reduction in cement does. Treated MSWI fly ash does not deteriorate the physical properties of fresh or hardened concrete. Concrete made with treated MSWI fly ash leach less than MSWI bottom ash accepted for civil engineering work.
[73]	Calcination	MSWI fly ash contains an appreciable amount of metallic Al. Swelling was observed in cement paste and mortar containing MSWI fly ash during the first 24 hours of hydration. Ettringite formation occurs at the end of the swelling. The swelling leads to cracks in mortar and a significant decrease in strength.
[96]	Revasol Process Modified Revasol process	The treated MSWI residues contained a calcium aluminosilicate phase. The treated residue reacted with Ca(OH)2 hardened and formed calcium aluminate hydrates. The modified process lead to metal destabilisation
[97]	Revasol Process Modified Revasol process	The treated MSWI fly ash had a higher activity index than coal fly ash and had a pozzolanic effect through calcium aluminosilicate reactions but did not increase the compressive strength beyond the control. Paste with the treated MSWI fly ashes formed ettringite, unreacted anhydrite and calcium aluminium oxide hydrates.

3. Knowledge Gaps

The literature presented in Chapter 2 shows the following gaps (A-C) in our understanding of treating MSWI fly ash and utilising it in cement-based materials.

A. In the previous studies using MSWI fly ash residues, the origin of the MSWI fly ash is not always thoroughly elaborated. Furthermore, the results obtained regarding using untreated MSWI fly ash residues in cement-based materials varies from having adverse effects to being beneficial. This may be due to the variations in the different samples origin and chemical characteristics. To better understand the effect MSWI fly ash (untreated or treated) has on cement-based materials, there is a need for distinguishing the different samples from each other.
B. Thermally treating MSWI fly ash residues is a highly investigated method, showing great potential for using the treated residues in cement-based materials. However, thermally treating MSWI fly ash at high temperatures requires high amounts of fuel and power and does not recover the potentially valuable metals, traping the metals in the treated residue instead. Therefore, there is a need to test treatments that focuses on extracting the metals, such as combined acid leaching and solvent extraction. However, the treated residue should still be usable in cement-based materials. EDR may provide such treatment. The presented literature showed that the focus of previous EDR treatments was not on extracting as high a concentration of metals as possible but on reducing metal leaching. Moving forward, testing how large a concentration can be recovered with EDR is essential and whether such results are transferable from lab-scale to bench-scale.
C. The presented literature showed a trend in how treated MSWI fly ash residues are evaluated in terms of the feasibility of using it in cement-based materials. A blended binder with the treated residue is prepared, then subjected to standard compressive strength and leaching tests from which the results are evaluated. There remains a need to assess the hydration and phase development to understand better the residue's impact and how this affects the compressive strength. Additionally, the standard leaching test does not account for environmental exposure, requiring additional leaching tests to be performed.

4. Objectives & Limitations

Currently, MSWI fly ash residues in Denmark are not treated with the intent of extracting valuable resources. Instead, they are treated to deposit the residues safely. Nor are the residues utilised for concrete manufacturing. This thesis aims at developing a treatment process that may both recover valuable metals from MSWI fly ash residues and enable them to replace cement partially, thus valorising MSWI fly ash residue. The thesis focuses on the use of electrodialytic remediation to treat and recover metals.

As shown in Section 2.3, MSWI fly ash contains numerous metal species. It is beyond the scope of this thesis to investigate every metal. Therefore, the conducted experiments were limited to investigate Cd, Cr, Cu, Pb and Zn, which are present in relatively small and high amounts and range from easily leachable to hard to leach. As concrete manufacturing requires large machinery and a high amount of aggregates, it was decided to only work with cement paste and mortar to understand the effects EDR treated MSWI fly ash residues have on the hydration and mechanical properties of cement-based materials better. Typically, pozzolanic cement contains between 11-50% SCM and OPC, depending on the SCM used. As the optimal content of EDR treated MSWI fly ash is unknown, it was decided to replace 10% of the cement with MSWI fly ash and then increase the replacement percentage in the future if 10% was feasible. It was opted not to optimise particle packing or the rheological properties by changing the water/cement ratio. Therefore all pastes and mortar have been made with a water/cement ratio of 0.5. Furthermore, documenting the optimal residue replacement percentage, mechanical properties (except for mortar strength) and durability are beyond the scope of this thesis.

Part II
Experimental Approach & Methods

5. Research Methodology

The overall research methodology of the thesis is presented as a process diagram in Fig. 6. The figure also presents an overview of where the appended studies fit in the thesis and which knowledge gaps they were intended to address. The experimental work can be divided into four stages.

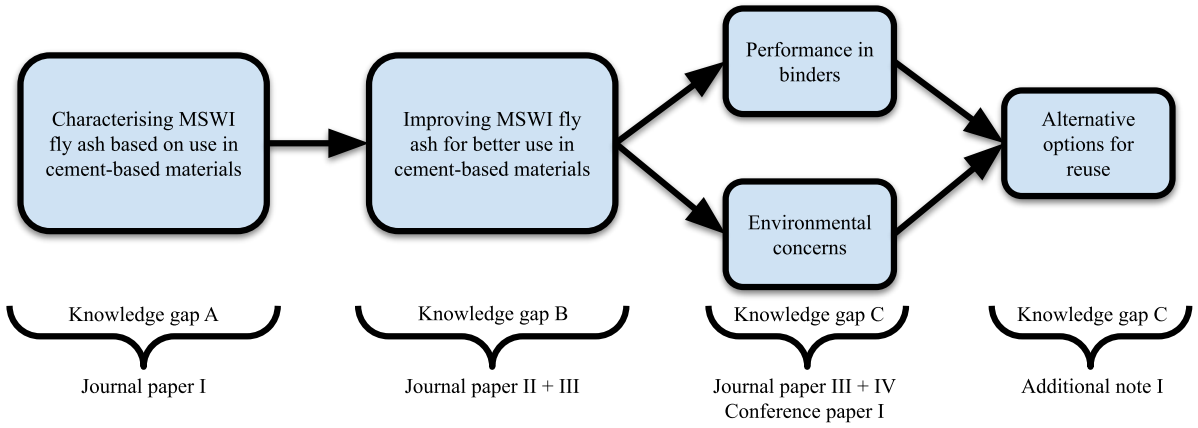

Figure 6: Process diagram of the research methodology.

In the first stages of the experimental work, five MSWI fly ash residues were characterised based on potential use in cement-based materials. In conjunction with this, a principal component analysis (PCA) was performed to ascertain how different the five residues were. Based on the characterisation and PCA results, three of the five residues were selected for the remaining stages of the experimental work. The second stage focused on treating the selected residues with electrodialytic remediation. First at lab-scale, then at bench-scale. To test the efficiency of EDR, the lab-scale results were compared with acid leaching. The bench-scale treated residues and untreated residues were then used to replace 10 wt% of cement paste and mortar cement as part of the third stage. The cement paste was used to test the phase development and bound water content, while the mortar was used to test the compressive strength and metal leaching. The metal leaching was performed using Cl^- and SO_4^{2-} as environmental agents. In the fourth final stage, ideas for alternative options for using MSWI fly ash residues in cement-based materials were explored. These ideas came from observations made during the experiments in the first three stages. The options investigated was using untreated MSWI fly ash as an accelerant and using the EDR treated MSWI fly ash as a gypsum replacement.

6. Summary of Materials & Methods

6.1 Materials

6.1.1 MSWI Fly Ash Residues

Five MSWI Fly ash residues were obtained from three commercial waste incinerators in the period 2017-2018. The residues were collected on-site by the operators.

Amager Bakke

Amager Bakke is a modern grate fired mass-burn incinerator located in Copenhagen, Denmark. Amager Bakke incinerates 1680 ton a day at approximately 1025˚C. Two residues (***AMA*** and ***AMA-X***) were extracted with an ESP before the APC system. After the first stage of characterising the residues based on use in cement-based materials, the residue AMA was chosen for further study. The treated AMA residue was designated **EDR AMA**. Fig. 7 shows the untreated residues macroscopic and microscopic appearance and the treated residues microscopic appearance.

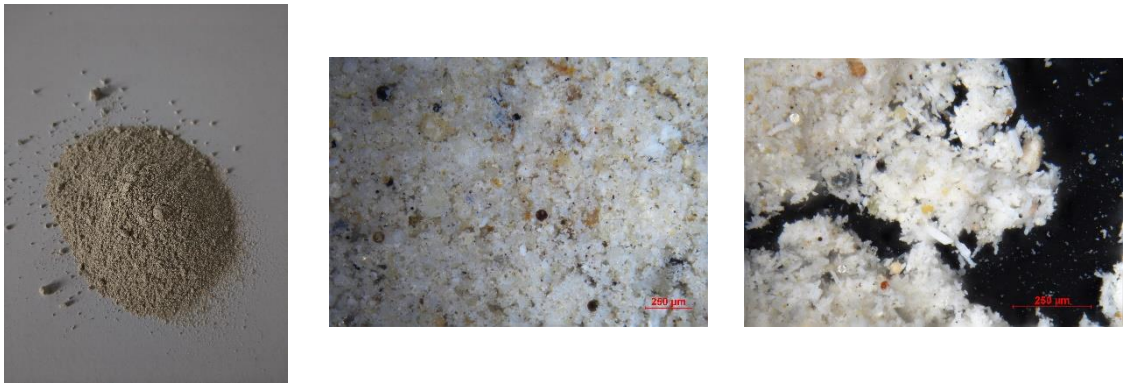

Figure 7: Collection of images of the untreated AMA residue at macroscopic range (left) and at microscopic range (middle), and the treated EDR AMA residue at microscopic range (right).

Nuuk Incineration

The incinerator in Nuuk, Greenland, is a grate fired mass-burn incinerator that incinerates 40 ton a day at approximately 1064˚C. Two residues (***NUU*** and ***NUU-X***) were extracted with an ESP. The incinerator does not have an APC system. After the first stage of characterising the residues based on use in cement-based materials, the residue NUU was chosen for further study. The treated NUU residue was designated **EDR NUU**. Fig. 8 includes images of the untreated residue at macroscopic and microscopic range and of the treated residue at microscopic range.

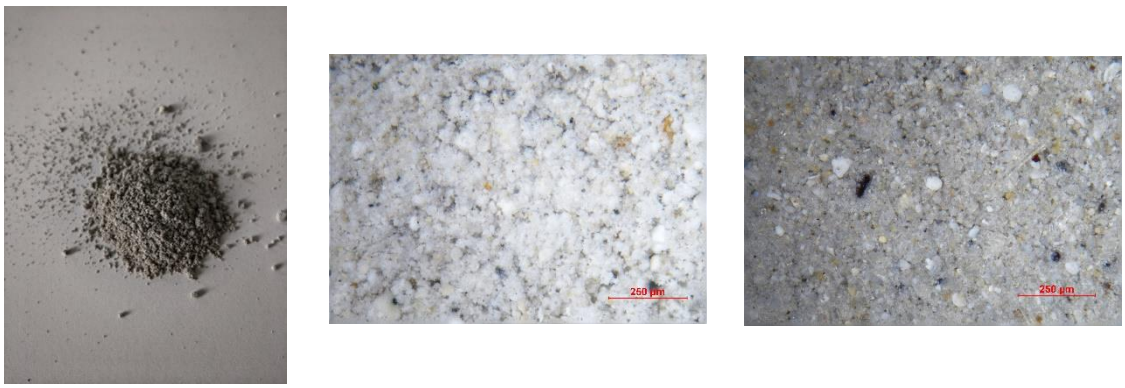

Figure 8: Collection of images of the untreated NUU residue at macroscopic range (left) and at microscopic range (middle), and the treated EDR AMA residue at microscopic range (right).

Ryaverket

Ryaverket is a circulating fluidised bed incinerator located in Borås, Sweden. Ryaverket incinerates 300 ton a day at approximately 900°C. One residue (***RYA***) was extracted with a textile filter after the APC system (lime and activated carbon injection). The treated RYA residue was designated **EDR RYA**. Fig. 9 shows the residues macroscopic and microscopic appearance and the treated residues microscopic appearance.

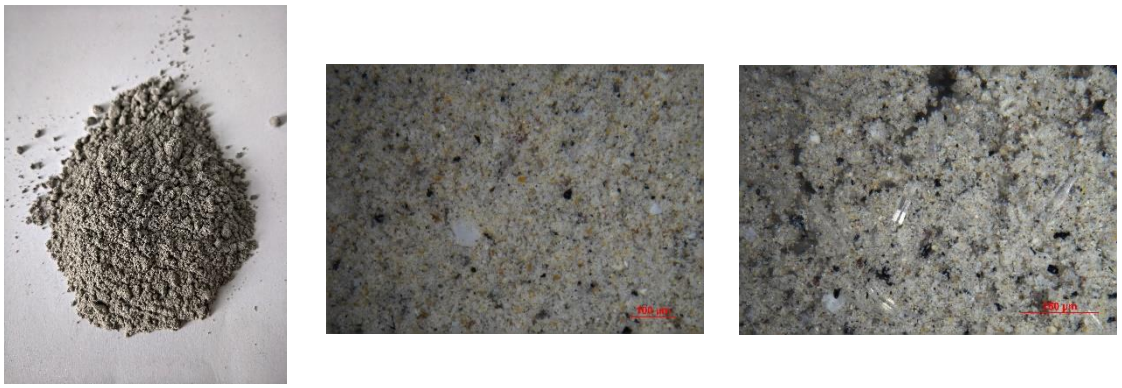

Figure 9: Collection of images of the untreated NUU residue at macroscopic range (left) and at microscopic range (middle), and the treated EDR AMA residue at microscopic range (right).

6.1.2 Cement

The cement used for the different experiments was a CEM I 52.5 N (MS/LA) OPC with a clinker content between 95-100 % and approximately 3.7% limestone filler. A CEM I 52.5 N cement containing no gypsum or limestone was used as part of the experiments for the additional note.

6.1.3 Sand

The sand used for the mortar was CEN standard sand that complies with the specifications in EN 196-1:2005 [98].

6.1.4 Quartz

The quartz used as an inert filler was M8 grade quartz that consists of 99.4% SiO_2.

6.2 Methods

6.2.1 Residue Characterisation

Batch Leaching

Batch leaching tests were performed according to EN 12457-1 [99] on the residues with deionised water (L/S 2).

Elemental Content Analysis

The elemental content of the materials used was determined using x-ray fluorescence (XRF) and inductively coupled plasma – optical emission spectrometry (ICP-OES).

Frattini Test

The Frattini test was performed according to the specifications of EN-196-5 2011 [100] using either 20g cement or a combination of 16g cement and 4g residue or quartz and used to assess the pozzolanic reactivity of the residues.

Loss On Ignition

The loss on ignition (LOI) of the residues was measured as the mass loss at 950˚C using a muffle furnace.

pH and Conductivity

The pH and conductivity of the residues were measured on samples suspended in deionised water (L/S 2.5) using a Radiometer analytical electrode and a conductivity meter, respectively.

Principal Component Analysis

The principal component analysis was performed using the statistical program Simca 14.1 by Sartorius Stedim Biotech. The variables in the PCA were Al_2O_3, CaO, Fe_2O_3, K_2O, MgO, Na_2O, SiO_2, SO_3, Cd, Cl, Cr, Cu, Pb and Zn. Appendix D provides more information about the analysis performed and the theory behind a PCA.

Thermogravimetric Analysis

Thermogravimetric analysis (TGA) was used to characterise the residues and measure their CO_2 content. A NETZSCH STA 449 F3 Jupiter, fitted with a silicon carbide furnace, top-loading,

aluminium oxide sample holders and nitrogen purge gas. The temperature range studied was 29-900°C at a 10°C increase per minute.

Water-Soluble Fraction

The wt% of the water-soluble fraction of the residues was measured as weight loss after three consecutive washings at L/S 5.

Water-Soluble Anion & Cation Content

The content of water-soluble anions of the residues was measured with ion chromatography after mixing with deionised water at L/S 2.5. The content of water-soluble cations in the residues was measured with ICP-OES after mixing with deionised water at L/S 2.0.

X-Ray Diffraction

The mineralogical phases in the residues were analysed with X-ray diffraction (XRD). The XRD analysis was performed using a Pan-Alytical X'pert Pro System (Cu metal anode), measuring the intensities between 4-100 °2θ with a step size of 0.002 °2θ and sampling time per step 24.8 s. Phase identification was performed using the ICDD PDF4 database.

6.2.2 Residue Treatment

HNO_3 Leaching

HNO_3 leaching at decreasing pH was performed on the residues using deionised water or increasing molarities of HNO_3 (L/S 25). This series of experiments was performed to assess the metals' release from the untreated residues at decreasing pH.

Combined HCl leaching & Solvent Extraction

HCl leaching experiments at constant pH were performed on the residues using a Metrohm 905 Titrando titrator. An initial suspension of residue and deionised water (L/S 5) had its pH reduced to 2 for an extended time using 3 M HCl. The titrator was programmed to initially stir the residue and deionised water suspension for an hour before lowering the pH to pH 2 with HCl.

The solvent extraction experiments were only performed using the residue RYA after leaching with HCl. LIX860N-I was used as the extractant and kerosene (solvent 70) as the organic phase. The experiments were performed with varying concentrations of LIX860N-I and with varying contact time. Appendix B provides additional information about the experiments.

Electrodialytic Remediation

Electrodialytic remediation experiments were performed at lab-scale and bench-scale. The lab-scale experiments were performed with both the two-compartment and three-compartment cells with a constant current of 1 mA. The bench-scale experiments were performed using the three-compartment set-up with a constant current of 1 A. Appendix A provides additional information about the performed experiments.

6.2.3 Binder Performance Assessment

Thermogravimetric Analysis

Thermogravimetric analysis was used to measure the bound water and portlandite content of crushed cement paste specimens containing the residues. The previously described equipment and procedure were also used for this series of experiments. The cement paste specimens were mixed using a Whip Mix Power Mixer Model B and then cast in 18 ml Nalgene LDPE sample vials and stored sealed at 20°C and >90% RH. The cement pastes hydration was stopped using a three-step procedure with isopropanol and diethyl ether.

Thermodynamic Modelling

The hydration phases formed in the various blended cement pastes were modelled using the Gibbs free energy minimisation program (GEMS). The standard thermodynamic data had been supplemented with cement specific database CEMDATA 18 [101]. Appendix C provides additional information regarding the thermodynamic modelling performed and the code used.

X-Ray Diffraction

The phases in the crushed cement paste specimens were identified using XRD analysis and the previously described Pan-Alytical X'pert Pro System. Phase identification was performed using the ICDD PDF4 database and a set of predefined patterns. The crushed cement paste specimens were prepared as described under the thermogravimetric analysis.

Mortar Compressive Strength

The compressive strength was determined per EN 196-1:2005 [98] using either an Instron 6025 or a Toni Technik 300 ton compression test machine. The mortar used for the tests were prepared following the specifications in EN 196-1:2005 [98] and stored for the first 24 hours of curing at 20°C and >90% RH followed by curing in a $Ca(OH)_2$ saturated solution until testing. The measured compressive strengths were normalised to air free compressive strength. The air

content was determined, and the subsequent normalisation was based on the study by Osbæck [102].

Cement Paste Setting Time

The initial and final setting time was determined per EN 196-3:2009 with a Matest E044N Vicatronic. The cement paste used was prepared per EN 196-3:2009 but used the mixing procedure outlined in EN 196-1:2005 [98].

Mortar Consistency

The mortar's consistency containing the residues was measured using a flow table using the techniques specified in EN 1015-3 [103].

6.2.5 Leaching Based on Environmental Concerns

Batch Leaching

Batch leaching tests were performed according to EN 12457-1 [99] on the residues with deionised water (L/S 2), a solution of 30 g NaCl per litre of deionised water (L/S 10), a solution of 30 g Na_2SO_4 per litre of deionised water (L/S 10) and deionised water acidified to pH 4 using 1M HNO_3 (L/S 10).

Mortar Leaching

Leaching experiments with mortar were performed on crushed and monolithic mortar cube specimens. The leaching experiments on crushed mortar were performed according to the specifications of EN 12457-1 [99] using a solution of 30 g NaCl per litre of deionised water (L/S 2), a solution of 30 g Na_2SO_4 per litre of deionised water (L/S 2) and deionised water acidified to pH 4 using 1M HNO_3 (L/S 2). The monolithic leaching experiments were performed using a modified version of the Dutch leaching test NEN 7345 [104–108] with the three solutions described previously at L/S 4. The mortar used was prepared according to EN 196-1:2005 [98]. The mortar was stored at 20°C and above 90% RH the first 24 hours of curing and were then stored in desiccators with 90% RH.

Part III
Results, Discussions & Conclusions

7. Main Findings

This chapter presents a resume of the main findings of the appended papers, beginning with the results of the first journal paper characterising and screening the MSWI fly ash residues based on use in cement-based materials.

7.1 Characterising MSWI Fly Ash based on use in Cement-Based Materials

7.1.1 Chemical Characteristics

MSWI fly ash residue is not a standardised material for use in cement-based materials. As such, there does not exist any guidelines or regulations on whether a residue can be used. However, fly ash originating from coal incineration is a standard material for concrete manufacturing and has regulatory guidelines that may be used instead. MSWI fly ash and CFA are very different materials and are not comparable, but using the requirements for CFA provides an indication of what may be required of MSWI fly ash residues before they can be used for concrete manufacturing. Table 4 shows an overview of the oxide content, Cl content and LOI of the five residues obtained for the project.

Table 4: Back calculated content of oxides (wt%), Cl content (wt%), CO_2 (wt%) and LOI (wt%) of the five residues. Included are data from journal paper I and III [109,110]. The requirements specified in EN 450-1[111] for CFA and the composition range for MSWI fly ash residues [45,50,112–128] and CFA [129] are also included.

	AMA	AMA-X	NUU	NUU-X	RYA	MSWI Residues	CFA	EN 450-1
SiO_2	4.6	4.9	6.1	4.7	6.4	2.4-33	15-57	≥25
Al_2O_3	1.4	2.3	4.6	4.0	4.7	0.5-15	3.4-38	-
Fe_2O_3	1.0	1.1	0.9	0.7	1.8	0.3-9.1	0.9-9.7	-
$\Sigma(SiO_2, Al_2O_3, Fe_2O_3)$	7.0	8.3	12	9.4	13	4.0-56	19-98	≥70
CaO	13	21	43	34	42	13-57	0.5-54	≤1.5/10*
MgO	0.6	0.8	1.4	0.9	1.8	0.1-8.1	0.2-9.1	≤4.0
K_2O	14	13	12	11	2.7	0.6-22	0.2-4.9	-
Na_2O	7.4	18	22	22	7.0	2.0-25	0.0-1.2	-
Na_2O_{eq}	17	26	29	29	8.8	1.5-39	0.2-4.5	≤5.0
P_2O_5	2.6	1.4	1.8	1.3	2.2	0.2-3.6	0.0-0.5	≤5.0
SO_3	34	23	8.9	7.7	8.9	2.2-21	0.2-22	≤3.0
Cl	2.8	8.9	24	20	13	3.1-42	-	≤0.1
CO_2	0.0	0.7	2.7	3.5	5.3	-	-	-
LOI	7.9	3.8	9.2	9.2	21	-	1.8-8.2	≤9.0**

* Free CaO limit/Reactive CaO limit
** Category C

The table includes the results for other MSWI fly ash residues and CFA residues found in the literature and the CFA requirements specified in EN 450-1[111]. The five residues did not fulfil the requirements for CFA, except for the MgO and P_2O_5 requirements. AMA-X also had an LOI that fulfilled the requirements. Instead of the desired SiO_2, Al_2O_3 and Fe_2O_3, the principal oxides

in the five residues are CaO, K_2O, Na_2O and SO_3. In general, the five residues contains less SiO_2, Al_2O_3 and Fe_2O_3 and more K_2O and Na_2O than what can be expected of CFA. The five residues have chemical compositions similar to other MSWI fly ash residues studied. However, the five residues contain SiO_2, Al_2O_3 and Fe_2O_3 in the low range of what can be expected. AMA's residue stands out because it has a higher SO_3 content than the previously measured residues and a low CaO content. RYA is the only residue extracted after the APC and differs from the other residues by having a low K_2O and Na_2O content. Furthermore, where the other four residues had a high Cl and low SO_3 content or a high SO_3 and low Cl content, RYA has a low Cl and SO3 content.

Table 5 contains a list of potential phases in the five untreated residues measured with x-ray diffraction. The residues NUU, NUU-X and RYA primarily contained $CaCO_3$, $CaSO_4$, KCl and NaCl, but may also have contained CaO, although harder to identify based on the peak identification. The residue RYA may also have contained CaClOH. AMA and AMA-X also contained $CaSO_3$ like the other residues. However, the two residues differed by containing other phases such as Na_2FeO_4. With its high SO_3 content, see table 5, AMA stood out further by potentially containing S phases not found in the other residues. The thermogravimetric analysis further highlighted the differences between the residues, where the residues NUU, NUU-X and Rya showed mass loss due to H_2O, CO_2 and SO_3 loss. AMA only showed mass loss due to SO_3 loss, while AMA-X had a similar mass loss as the other residues but with less intensity.

Table 5: List of measured phases with XRD in the five untreated residues. Included are data from journal paper I and III [109,110].

	AMA	AMA-X	NUU	NUU-X	RYA
$CaAl_2O_4$	✓				
CaClOH					✓
$CaCO_3$			✓	✓	✓
CaO			✓	✓	✓
$CaSO_4$	✓	✓	✓	✓	✓
KCl			✓	✓	✓
NaCl		✓	✓	✓	✓
Na_2FeO_4	✓	✓			
$Na_{21}Mg(SO_4)_{10}Cl$	✓				

Table 6 contains data on the pH, conductivity, water solubility and fraction of water-soluble Cl^-, SO_4^{2-}, Ca^{2+}, Na^+ and K^+ in the five untreated residues. The pH of the residues was alkaline, except for AMA that had a neutral pH, and their conductivities were between 90-150 ms/cm^2. The residues were highly soluble, with RYA having the lowest solubility (28 wt%) and AMA the highest solubility (56 wt%). The primary soluble ions in AMA were SO_4^2, Na^+ and K^+, suggesting that it may also contain K_2SO_4 and Na_2SO_4 in addition to the phases observed with XRD. AMA-X had a high content of soluble Cl^-, SO_4^{2-}, Na^+ and K^+, while both NUU and NUU-X had a high content of Cl^-, Na^+ and K^+. In this instance, RYA deviated from the other samples by having a

high soluble Cl^- and Ca^{2+} content compared to the other residues. This may be attributed to it being an APC residue.

Table 6: Measured pH, conductivity, water solubility and content of water-soluble Cl^-, SO_4^{2-}, Ca^{2+}, Na^+, K^+ ions. Included are data from journal paper I [109].

		AMA	AMA-X	NUU	NUU-X	RYA
pH	[-]	6.5	12	12	12	12
Conductivity	[ms/cm²]	95	110	150	150	94
Water Solubility	[wt%]	56	39	38	42	28
Cl^-	[wt%]	2.3	8.1	22	19	18
SO_4^{2-}	[wt%]	21	7.5	0.6	0.8	0.2
Ca^{2+}	[wt%]	0.1	0.1	1.8	0.7	6.0
K^+	[wt%]	3.1	3.9	6.8	5.6	1.3
Na^+	[wt%]	10	7.7	7.6	6.3	1.6

The total and leachable content of Cd, Cr, Cu, Pb and Zn in the five residues are included in Table 7. The order of the metals in terms of concentration was, in general, Zn>Pb>Cu>(Cr, Cd). AMA and AMA-X had a higher Cd content than Cr content, while NUU and RYA contained more Cr than Cd. NUU-X had a similar Cd and Cr content. The total concentration of Cd, Cr, Cu, Pb, and Zn in the residues was within the concentration range of what has previously been observed, except for RYA that had a higher Cu concentration than previously observed. Furthermore, the residue RYA contained more Cu than Zn and contained significantly less Zn than the other four residues. The metals in the residues were especially leachable in deionised water, exceeding the limit values for civil engineering work. This was especially the case for Pb and Zn and for four of the residues, Cr as well. The residues AMA, NUU and RYA all had particular metals they leached in high amounts. The residue AMA leached 90 % of its Cd and 42% of its Zn, while NUU and RYA leached 18 and 41% of their Pb.

Table 7:. The total and leached concentration of Cd, Cr, Cu, Pb and Zn in the five residues. Included are data from journal paper I, III and IV [109,110,130]. The total concentrations measured in previous research [45,50,112–128] and the limit values for non-hazardous waste [131] are included as well.

Total content (mg/kg)	AMA	AMA-X	NUU	NUU-X	RYA	MSWI Residues
Cd	480	280	420	205	80	22-580
Cr	300	130	800	206	400	47-2030
Cu	1400	1070	1300	760	7900	170-7800
Pb	12000	6300	3000	2800	3400	320-36000
Zn	55000	35000	33000	30000	6600	2.0-65000
Leachable (mg/kg)						Limit
pH [-]	6.5	12	12	12	12	
Cd	430	<0.01	<0.01	0.7	<0.01	0.6
Cr	1.0	1.5	39	20	0.1	4.0
Cu	2.6	0.2	0.4	0.3	52	25
Pb	5.0	50	530	16	1400	5.0
Zn	23000	10	5.8	4.0	20	25

7.1.2 Particle Size Distribution

The five residues particle size distributions are shown in Fig X. The residues vary significantly in size. AMA and AMA-X have d_{50} and d_{90} values above 40 and 200µm, and NUU, NUU-X and RYA have d50 values between 13-22µm and d90 values between 41-53µm. Due to the residues larger particle size than the CEM I cement, they are not expected to improve the packing density or enhance hydration through nucleation as filler. However, they may affect the degree of hydration through dilution. Likewise, the effect of the inert quartz as filler may be limited.

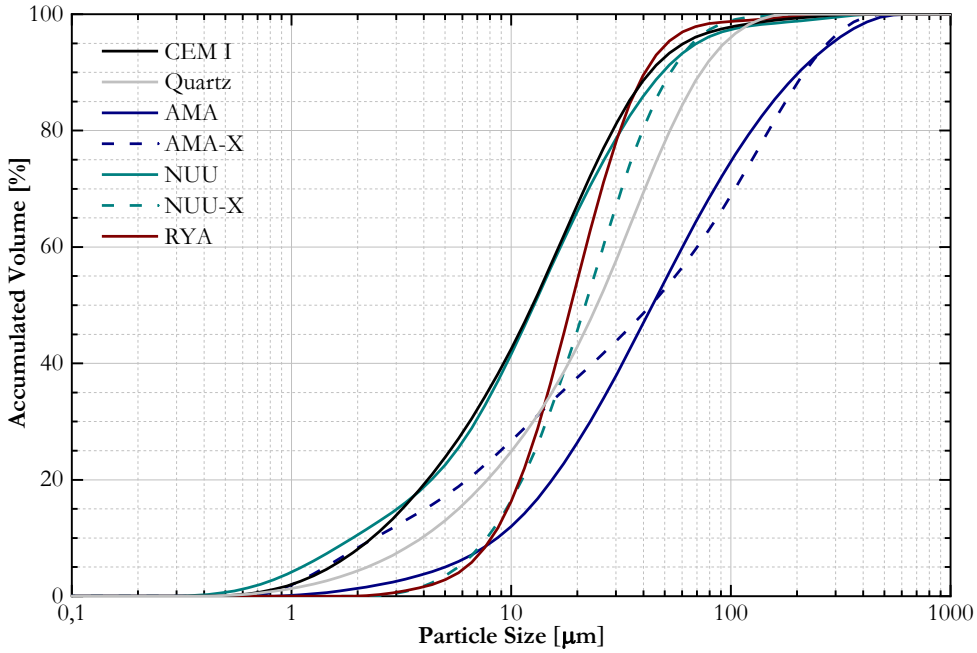

Figure 10: Particle size distribution of the five residues, CEM I cement and quartz. Recreated from journal paper I and IV [109,130].

7.1.3 Principal Component Analysis

The results of the principal component analysis shown in Fig. 11 for the 1st and 2nd components combined and in Fig. 12 for the 1st and 3rd components combined. Fig. 11a and Fig. 12a depicts the individual residues score and shows how some residues are clustered close to the origin of the plot and others are spread out in the plot. In a score plot, samples (residues) close to the origin has variables (oxide and heavy metal composition) close to the average of all the samples. Samples further from the origin are outliers or naturally extreme observations. A samples score and position in the score plot can be inferred from the loadings plot Fig. 11b and Fig. 12b. Variables in the loading plot close to the origin have little contribution to a samples score. Strongly correlated variables cluster together, while negatively correlated variables appear diagonally of each other.

Several of the studied dataset residues were clustered together close to the origin of the 1st and 2nd component score plot (group 1), suggesting that these residues have a representative and a typical composition for MSWI fly ash residues. This group includes residues from grate and fluidized bed incinerators and residues extracted with EPS, textile filters, or cyclone. These residues appear to have a high CaO content compared to Cd, Cr, Pb, Zn and SO_3 and tends towards more Cl, K_2O and Na_2O than a high content of Al_2O_3, Fe_2O_3, MgO and SiO_2. A second group (group 2) with a higher than average content of either Al_2O_3, Fe_2O_3, MgO or SiO_2 has also been identified. However, this group consist solely of Chinese fluidized bed incinerator residues.

The MSWI fly ash residues acquired for this project had significantly different score values. The APC residue RYA had a score close to the origin and was part of the group 1 cluster, indicating a typical and representative chemical composition for MSWI fly ash residues. However, the 1st and 2nd components do not account for the Cu content in the residue. See Fig. 11b. The 3rd component does account for the Cu content and in the score plot of the 1st and 3rd component scores, see Fig. 12a, RYA is part of a third cluster (group 3) with high Cu contents. Therefore, although RYA has a general chemical composition, it did have an atypical Cu content. Both NUU and NUU-X were clustered close together away from the origin and the typical chemical composition of MSWI fly ash residues, although the residues are not outliers. This may be due to a higher than average Cl, K_2O and Na_2O content. Therefore, NUU and NUU-X do not have a typical chemical composition but are still representative of MSWI fly ash residues. AMA-X and especially AMA are not representative of MSWI fly ash due to their high K_2O, SO_3, Cd, Pb and Zn content. Due to its higher content of Cd, Pb, Zn and SO_3 than AMA-X, AMA was outside

the 95% confidence limit of the PCA, making it an outlier in the dataset. Therefore, the residue AMA is not a typical or representative sample of MSWI fly ash residues.

Included in the score plots are a CFA that fulfils the specifications of EN 450-1 [111]. It is an outlier in the score plots, with a high Al_2O_3, Fe_2O_3 and SiO_2 content. None of the MSWI fly ash residues of the dataset were clustered with the CFA samples, suggesting that MSWI fly ash residue does not fulfil the EN 450-1 [111] requirement. The residues in group 2 may have the most similar composition to EN 450-1 CFA. Therefore, the MSWI fly ash residues of the project require treatment to improve their characteristics and to extract the valuable metals while reducing their hazardousness.

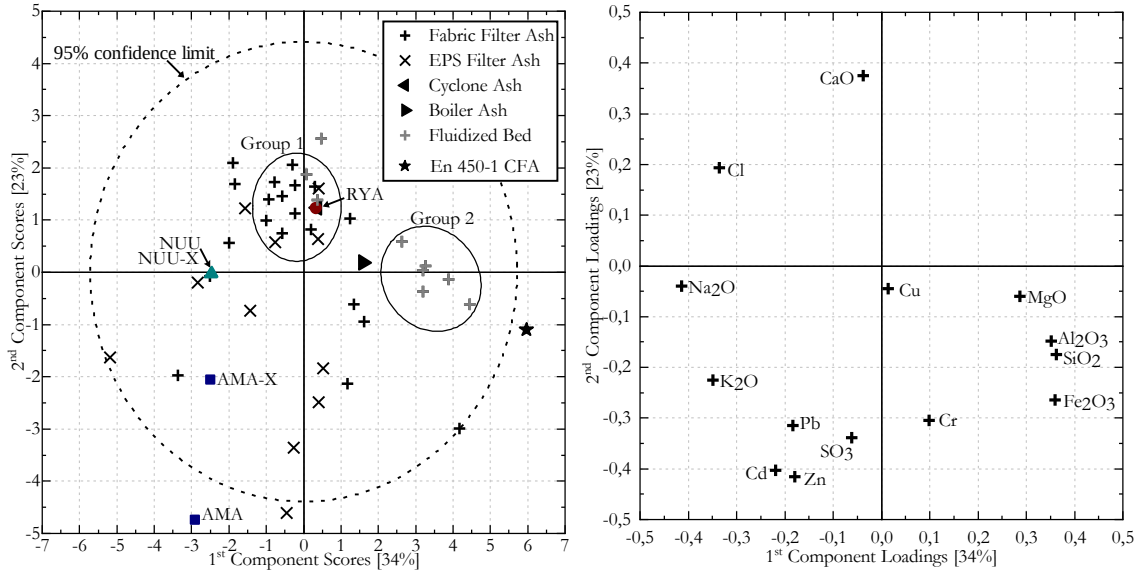

Figure 11: Score plot (left) and loading plot (right) of the 1st and 2nd principal components from the PCA. Points colored black are residues from grate furnaces, while points colored grey are filter ash residues from fluidized bed incinerators. Marked are two residue groupings. Recreated from journal paper I [109].

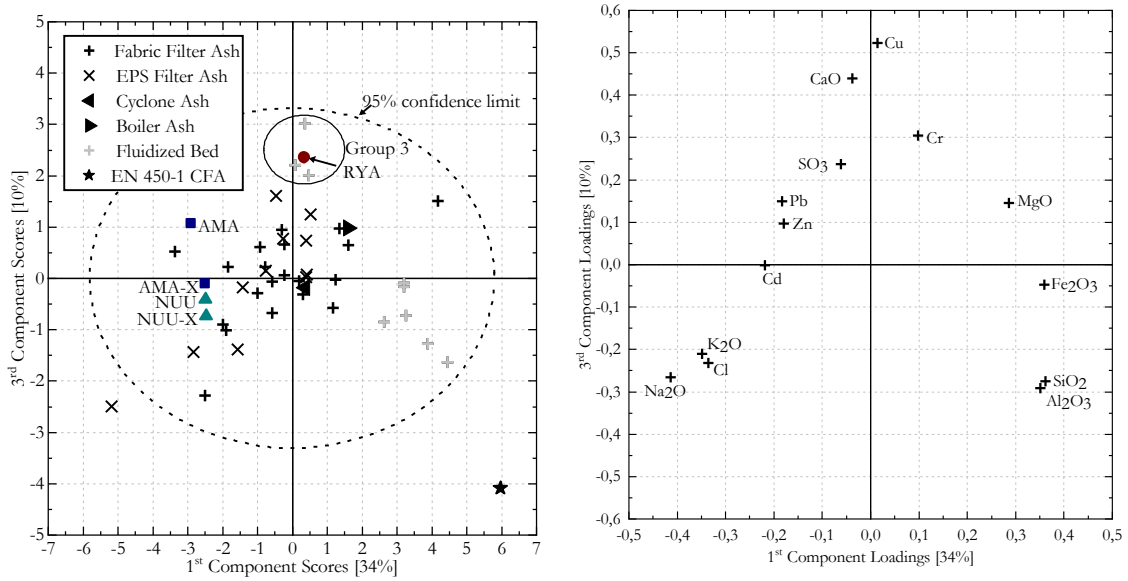

Figure 12: Score plot (left) and loading plot (right) of the 1st and 2nd principal components from the PCA. Points colored black are residues from grate furnaces, while points colored grey are filter ash residues from fluidized bed incinerators. A group of residues have been marked group 3. Recreated from journal paper I [109].

Therefore, the MSWI fly ash residues of the project require treatment to improve their characteristics and to extract the valuable metals while reducing their hazardousness.

7.2 Improving MSWI Fly Ash for Better Use in Cement-based Materials

Moving forward with treating and improving the residues, AMA, NUU and RYA were chosen for further study, based on the characterization and screening performed. Using these three residues, a broader interpretation of how MSWI fly ash residues perform may be acquired as they represent chemically common and uncommon residues. The first step in treating the studied residues was investigating the release of heavy metals as a function of decreasing pH.

7.2.1 HNO_3 Leaching: Decreasing pH

The results of the HNO_3 leaching experiments at an incrementally decreasing pH from journal paper II [23] are shown in Fig. 13. Cd leached from the residues at a pH below 8 and leached between 65-95 wt% at a pH below 4. Cr leached from the raw residues at a pH below 4, between 20-40 wt%, and above 6. Cu leached from the residues at a ph below 6 and at a pH of less than 1 had leached between 70-100 wt% of their Cu content. Pb leaching was found to vary between the three residues. From a pH of 5, NUU and RYA leached Pb and leached between 40-50 wt% at a low pH. However, the two residues also leached Pb at an alkaline pH. By comparison, the raw residue leached significantly less Pb (< 2 wt%). Similarly to Cd and Cu, Zn began leaching from the residues at a pH below 8 and leached between 70-100 wt% at an acidic pH.

By comparing Pourbiax diagrams of pure acidic and alkaline solutions and acidic and alkaline solutions containing C and S, it was surmised that Cd, Cu and Zn leach as ions with 2+ valency at a pH below 7-8 [132,133]. Furthermore, Pb would have been expected to be present as Pb^{2+} regardless of the pH. However, In solutions containing CO_2, a passivation zone occurs in the neutral pH range, which may account for Pb leaching below a pH of 5 and above a pH of 10 from NUU and RYA. In solutions with SO_4^{2-}, Pb precipitates as $PbSO_4$ at an acidic pH, which may account for the low wt% of Pb leached from AMA, as this was an S rich residue. The Pourbiax diagrams suggested that Cr leaches as Cr^{3+} at an acidic pH and does not account for Cr leaching at an alkaline pH. However, the solutions are not pure. Complexes may have formed. Differences in how the metals are bound may account for the differences in leaching yield between the residues. Lasssesson et al. [51] studied the influence of Cu's chemical speciation on its release. They found that Cu(II) species, e.g. sulphates, hydroxides and chlorides, resulted in 100% yield while Cu 0, I and II bound in phosphates and silicates resulted in a 60% yield [51].

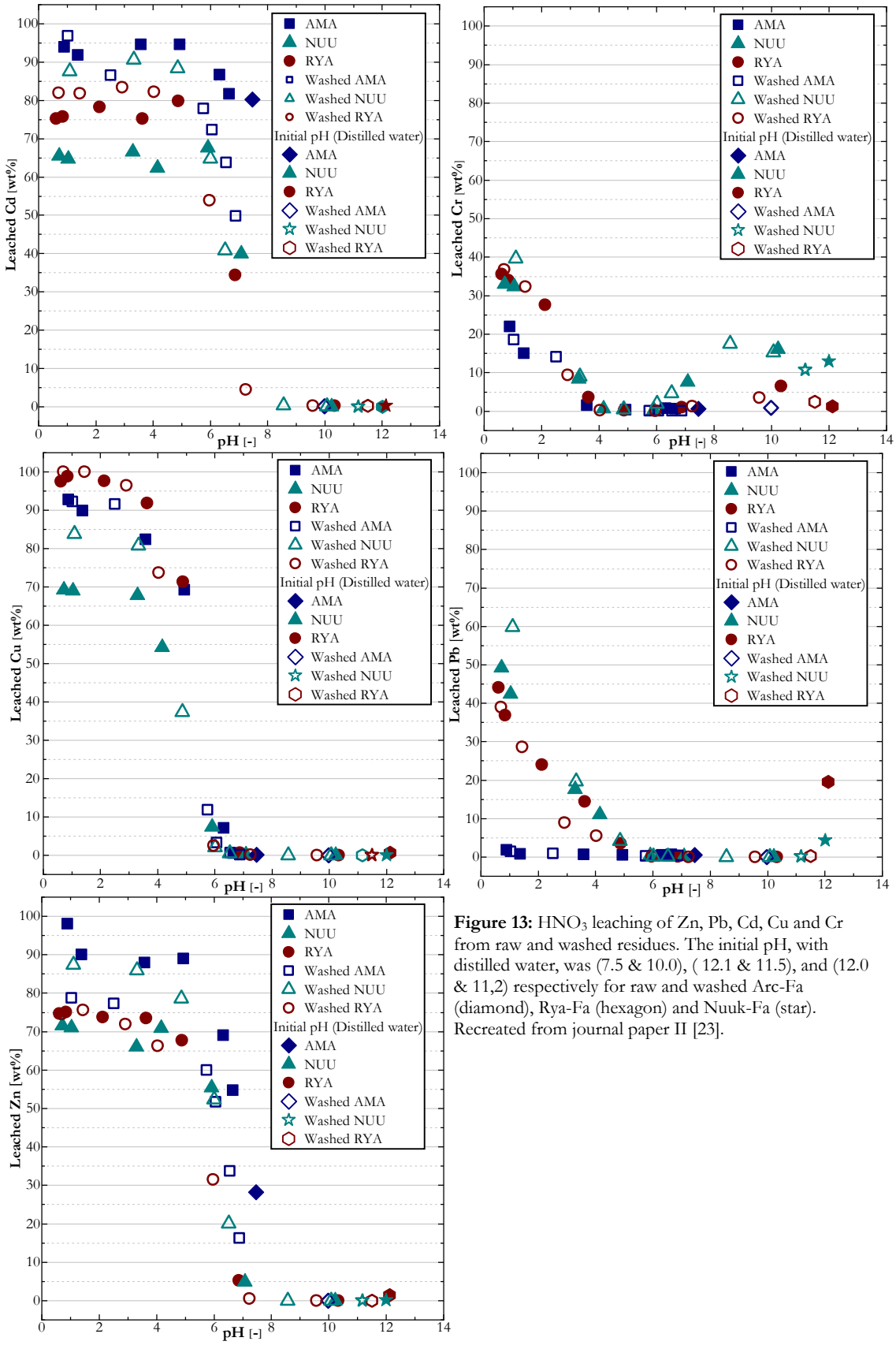

Figure 13: HNO_3 leaching of Zn, Pb, Cd, Cu and Cr from raw and washed residues. The initial pH, with distilled water, was (7.5 & 10.0), (12.1 & 11.5), and (12.0 & 11,2) respectively for raw and washed Arc-Fa (diamond), Rya-Fa (hexagon) and Nuuk-Fa (star). Recreated from journal paper II [23].

Washing the residues as part of the EDR treatment did, in general, not change the leaching yield. However, the leaching yield from NUU increased, suggesting that removing easily soluble elements such as Cl, K, Na, or S may have increased the yield. Additionally, the Zn leaching yield from AMA and Pb leaching from NUU and RYA at an alkaline pH was reduced. This may be due to a reduced pH of the washed NUU and RYA residues. Washing the AMA residue did not increase the Pb yield and may be due to the residue still containing high amounts of SO_4^{2-}.

7.2.2 Combined HCl Leaching & Solvent Extraction

Previous studies focused on metal leaching followed by solvent extraction experiments have found that HCl leaches more Cd, Cu, Pb and Zn from MSWI fly ash residues than HNO_3 at similar L/S ratios [49,50]. They found that close to 100% Cd and Pb were leachable, while between 80-100% Cu and 77-80% Zn was leachable at a pH of ≤ 2 [49,50]. The increased leachingyield from HCl leaching may be attributed to the formation of chloride complexes in the suspension [50,134,135]. Therefore, HCl was chosen for this series of experiments.

The results of the HCl Leaching at constant pH are presented in Fig. 14. At the end of the experiments, the suspension pH of AMA, NUU and RYA was 2.1, 2.2 and 2.3, respectively. The residues NUU and AMA required 9 and 10 mmol H^+/g ash, respectively, to maintain a pH close to 2, a similar concentration to a previous study by Tang et al. [50], while AMA required 3 mmol H^+/g ash. The difference in acid used was in journal paper II [23] attributed to the neutral pH of the AMA suspension and the residues low Ca content. The performed HCl leaching experiments deviated from the previous studies as the leaching yield of the three residues was lower. Between 60-90% Cd, 0.5-85% Cu, 0.1-55% Pb and 60-90% Zn were leachable at a constant pH of 2. At a pH of 2, the metal speciation in the leachates is expected to be Cd^{2+}, Cr^{3+}, Cu^{2+}, Pb^{2+} and Zn^{2+}, as discussed previously. The low Cu yield in the experiment with HCl, Compared to HNO_3, could be related to the initial decrease in Pb yield during the initial hours of the experiment. It may be the result of a high metallic Al content in NUU. In Greenland, metal from household waste is not separated before waste incineration [136], resulting in Al foil and cans incineration and a higher metallic Al content. During HCl leaching, Cu^{2+} and Pb^{2+} may react with solid Al and form precipitates. An oxidation agent prevents this from occurring, which HNO_3 may provide [136]. Leaching with HCl did not increase the Pb yield from AMA, suggesting that the Pb may have precipitated as $PbSO_4$ during this series of experiments as well. Although the experiments lasted up to 12 hours, the results showed that this was unnecessary as the maximum leaching yield could be reached within 4 hours. The highest Cu leaching yield was achieved from Raw RYA (85%). Raw RYA also had the highest Cu concentration of the investigated residues.

See Section 7.1. Raw RYA was, therefore, chosen for the subsequent solvent extraction experiments with LIX860N-I.

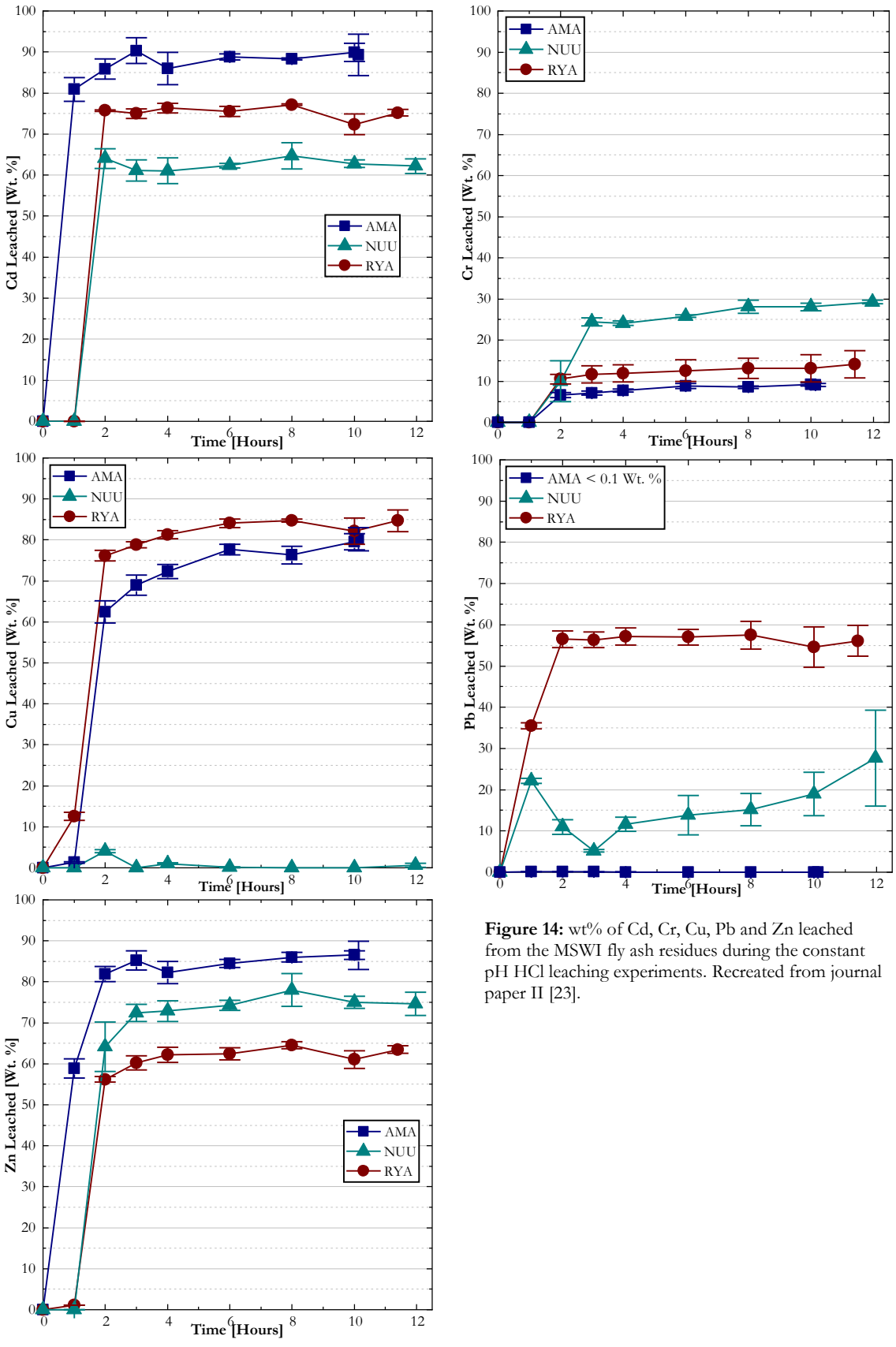

Figure 14: wt% of Cd, Cr, Cu, Pb and Zn leached from the MSWI fly ash residues during the constant pH HCl leaching experiments. Recreated from journal paper II [23].

The results of the solvent extraction experiments are shown in Fig. 15 as the extraction percentage E as a function of the concentration of LIX860N-I in the organic phase (solvent 70) and as a function of time. Using 0.1 M LIX860N-I and a contact time of 5 minutes between the aqueous and organic phases was sufficient to extract approximately 99 % of the Cu in the aqueous phase. A contact time of 5 minutes may have been too long, as the time-dependent investigation showed that a 3 minute contact time resulted in the highest extraction percentage at 0.01 M LIX860N-I

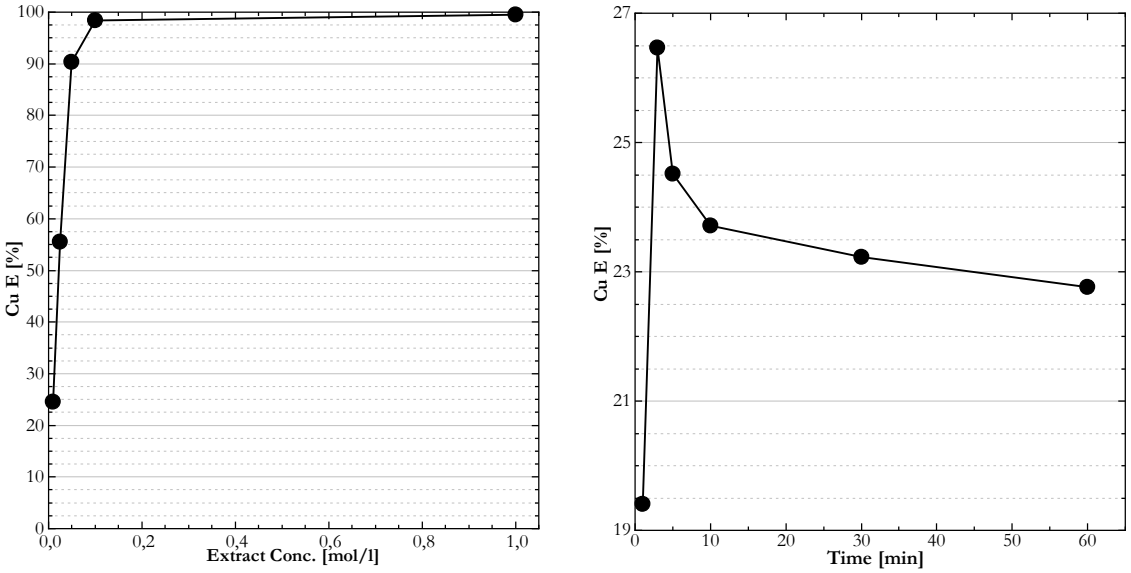

Figure 15: Extraction percentage of Cu from RYA's aqueous phase as a function of the extractant concentration in the organic phase (5 min extraction time) (left) and as a function of time (0.01 mol/l extraction concentration) (right). Recreated from journal paper II [23].

According to Tang et al. [44], LIX860N-I is very selective in extracting Cu, only extracting low concentrations of other metals, except for Fe. However, this appears to depend on the concentration of LIX860N-I used and the contact time. The solvent extraction experiments showed that at low LIX860N-I concentrations (0.01M) and short contact times (1 minute), more K, Na and Zn were extracted than Cu. At 1.00 M LIX860N-I and a 5 minute contact time, a low concentration of K, Na and Zn were extracted.

Tang et al. [44] also found that 85-95% of the Cu in the organic phase can be transferred to a new aqueous phase during a stripping stage with 1.5 M H_2SO_4 acid. Given that Raw RYA contains 7900 mg Cu/kg ash and 85% can be leached with HCl, 5700 mg Cu/kg residue may be extracted, suggesting it could be a valuable resource. The Cu content of the ore mined from the Swedish mine Aitik is approximately 2500 mg/kg [45], indicating that more Cu can be retrieved per kg MSWI fly ash residue than per kg ore. However, approximately 270,000 tonnes of MSWI fly ash residue is produced in Sweden annually compared to 36 million tonnes of ore from Aitik.

Although MSWI fly ash residues could be a valuable Cu source, they cannot replace current mining practices.

7.2.3 EDR: Lab-Scale

During the two- and three-compartment cell lab-scale EDR experiments, the pH of the various suspensions was acidified. The AMA suspensions reached a pH of 0.5, the NUU suspension a pH between 2 and 3 and the RYA suspension a pH of 1 at the end of the 28 days. However, AMA reached a pH of below 1 after 15 days, after which the pH was close to constant.

The wt% distribution of the studied metals Cd, Cr, Cu, Pb and Zn measured at the end of the EDR experiments is shown in Fig. 16. The concentration of metals removed and the removal order varied significantly between the three residues. Although the experiments with AMA achieved the lowest pH, they did not have the highest release of metals. Furthermore, although the pH was lower in the two-compartment cells, the release of metals varied between the two cell types and the residues. The highest metal removal was observed with Raw RYA, where up to 100 % Zn, 80 % Cu, 45 % Cd, 21% Pb and 11% Cr was removed with the two-compartment cell. The previous section discussed that the released metals had valencies of 2+ (Cd, Cu, Pb and Zn) and 3+ (Cr) at an acidic pH. Although most metals electromigrated to the cathode, see Fig. 16, 4-22 wt% of the metals electromigrated to the anode, depending on the residue and metal. In journal paper II [23], this was attributed to the formation of negatively charged metal Cl complexes, as the washing step before EDR may not have removed all of the Cl. The metals may also have been transferred due to interdiffusion between the membranes [24].

A higher removal wt% could be achieved with a longer remediation time and lower pH than previous EDR studies with MSWI fly ash residues. Previous studies by Kirkelund et al. [32] and Kirkelund et al. [37] found that 2-61% Cd, 1.1-6% Cr, 2-3.3% Cu, 2.5-5% Pb and 2-53% Zn were removable with the three-compartment cell (pH between 8.2-8.9) and that 56% Cd, 2.8% Cr, 15% Cu, 0.5% Pb and 4.6% Zn with the two-compartment cell (pH of 6.4). Although a higher removal percentage was achieved, lower removal percentages were also found, as seen with the residue AMA, despite the comparatively lower pH.

The concentration of Cu removed from NUU was not as high as the concentration leached during HNO_3 leaching. However, compared to HCl leaching, Cu was removable, suggesting an oxidising agent may not be required during EDR to leach metals such as Cu. EDR also resulted in a low Pb removal from AMA, compared to the other residues, suggesting that EDR cannot remove Pb from AMA and that it precipitates as $PbSO_4$ as well, during the EDR process.

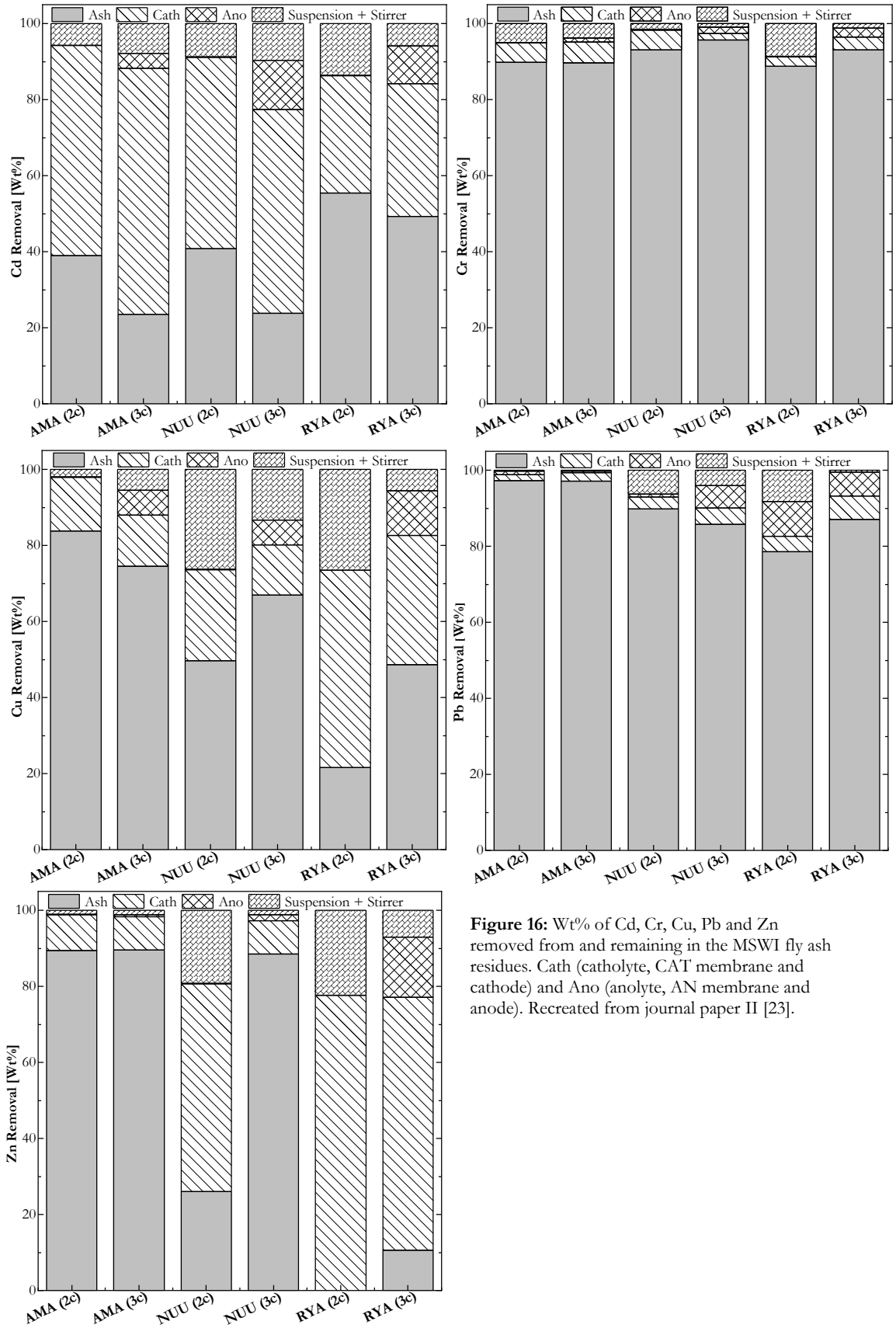

Figure 16: Wt% of Cd, Cr, Cu, Pb and Zn removed from and remaining in the MSWI fly ash residues. Cath (catholyte, CAT membrane and cathode) and Ano (anolyte, AN membrane and anode). Recreated from journal paper II [23].

7.2.4 EDR: Bench-Scale

Upscaling the three-compartment lab-scale cell to bench-scale affected the performance of the EDR process. The suspension pH developed similarly to the lab-scale experiments decreasing over time, although at a slower rate. After 28 days, the AMA suspension had a pH of 1.2, while NUU and RYA had pHs of 5.6. Furthermore, the AMA suspension had a close to constant pH after 16 days. This was attributed to differences in the L/S ratio, ion exchange membrane area, and current used between the lab-scale and bench-scale setup in journal paper III [110]. The bench-scale setup used may, therefore, not be as efficient as the lab-scale setup. A longer remediation time or higher current may therefore be a necessary change to the bench-scale setup.

The distribution of Cd, Cr, Cu, Pb and Zn at the end of the bench-scale experiments is shown in Fig. 17. The metal removal order was, as in the lab-scale tests, dependent on the residue. For AMA, the removal order was Cu>Zn>Cd>Cr>Pb, while for NUU and RYA, it was Cd>Zn>Cr>(Cu, Pb). A stark difference in metal removal was observed, attributed to the differences in pH between the residues. The highest removal percentage from AMA was 80 wt% Cu, while the highest removal percentage from NUU and RYA were 20 and 10 wt% Cd, respectively. As in the lab-scale tests, most of the removed metals migrated to the cathode, indicating a release of positively charged metals, while a small fraction migrated to the anode.

Due to the neutral final pH reached in the bench-scale experiments with NUU and RYA, only between 1-20 wt% of the metals were removed compared to 5-90 wt% lab-scale experiments. Furthermore, the final pH may have been too high for Cu release, given that the concentration of Cu removed was similar to the concentration of Pb removed, while some Cd and Zn were released. In contrast, the Cu and Zn concentration removed from AMA was up to 50 wt% higher at bench-scale than at lab-scale. As the pH was lower during the lab-scale tests with AMA, it may suggest that the lab-scale had removal issues that the bench-scale test did not. The previously discussed problem with removing Pb from AMA due to $PbSO_4$ precipitation was presumed to occur during the bench-scale test as well, explaining the minor release of Pb measured. Treating MSWI fly ash residues at bench-scale is, therefore, possible. However, the current setup needs to be modified to ensure a lower pH is reached. Furthermore, most of the metals removed from AMA were retained in the suspension instead of electromigrating to the electrodes. The bench-scale test with AMA was not hydraulically stable, causing liquid to flow from the electrolytes to the suspension compartments. The experiments metal distribution suggests that metals were transported with the liquid and represents another issue with the bench-scale setup that should be addressed.

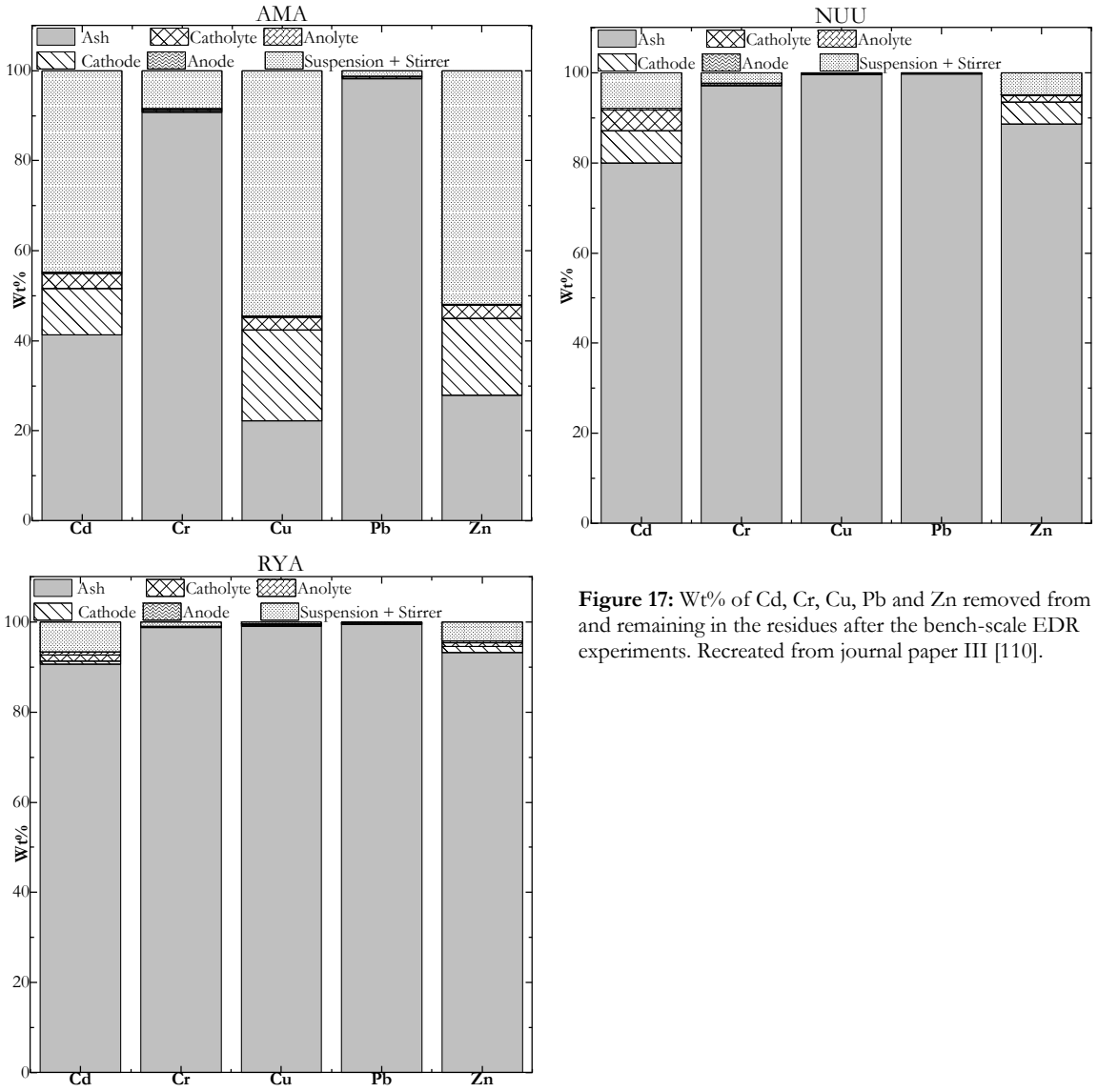

Figure 17: Wt% of Cd, Cr, Cu, Pb and Zn removed from and remaining in the residues after the bench-scale EDR experiments. Recreated from journal paper III [110].

7.2.4 Removal Efficiency: HNO_3 leaching, HCl leaching & EDR

A comparison of the wt% of metals removed with HNO_3 leaching (untreated and washed residues), HCl leaching and in the lab-scale and bench-scale EDR experiments is shown in Table 8. Included in the table is the average removal percentage from the three residues for each metal and all metals combined. The percentage of metals removed from the residues with the three methods was, in general, high, making them eligible methods for metal removal. However, leaching with acid removed more metals from the residues (combined average of 50-65 wt%) than what was removable with EDR (18-37 wt%). A lower pH was reached in the lab-scale EDR experiments (AMA and RYA) than in the acid leaching experiments, but this did not translate to higher metal removal, except for Zn removal from RYA. The wt% of metals leached with HNO_3 at a pH of 2 is slightly higher than the yield with HCl at a pH of 2, contrary to the results of [49,50]. This may be attributed to the ashes' chloride content being high, not requiring additional Cl to form complexes or the metal speciation in the ashes X. However, more Pb did leach from Raw RYA with HCl than with HNO_3, although it does not match the high leaching yield observed in the previous studies [49,50]. The combined average of removed metals with the lab-scale three-compartment cell was 32 wt% compared to 18 wt% with the bench-scale setup, highlighting that the bench-scale setup used may be half as efficient as the lab-scale setup. The experimental setup's inefficiency is further highlighted by comparison with the HNO_3 leaching experiment. At a pH of 5.6, the HNO_3 leaching experiment showed that more Cd, Cu and Zn should have leached from NUU and RYA than did in the bench-scale EDR experiment.

Given its higher removal, directly leaching metals from MSWI fly ash residues with acid appears to be a better-suited option for removing and recovering the metals. EDR may, therefore, be an inefficient treatment for recovering metals from MSWI fly ash residues. However, given that the residues are not in direct contact with acid during the EDR process, EDR treated residues may be better suited for use in cement-based material. The performance of EDR treated MSWI fly ash residues in cement-based materials was then subsequently tested.

Table 8: Removal efficiencies (%) of the HNO_3 leaching, HCl leaching and EDR experiments. Included are the average % for each metal and the average % for all metals combined. W HNO_3 refers to the washed ash experiment. Included are data from journal paper II and III [23,110].

					Lab-scale		Bench-scale
		HNO_3	W HNO_3	HCl	EDR 2c	EDR 3c	EDR 3c
pH	AMA	1.4	1.0	2.1	0.4	0.6	1.2
	NUU	1.0	1.1	2.3	2.2	2.9	5.6
	RYA	2.1	1.4	2.3	0.7	1.2	5.6
Cd	AMA	94	97	89	61	76	59
	NUU	65	88	62	59	76	20
	RYA	75	82	75	45	51	9.4
	Average	**78**	**89**	**75**	**55**	**68**	**27**
Cr	AMA	22	19	9.0	10	10	9.2
	NUU	33	40	29	7.0	4.0	2.8
	RYA	36	37	14	11	7.0	1.3
	Average	**30**	**32**	**14**	**9.3**	**7.0**	**4.4**
Cu	AMA	93	92	80	16	25	78
	NUU	69	84	0.6	50	33	0.4
	RYA	98	100	85	78	51	1.0
	Average	**87**	**92**	**55**	**48**	**36**	**26**
Pb	AMA	1.4	1.5	0.0	3.0	3.0	1.8
	NUU	49	60	28	10	14	0.2
	RYA	44	39	55	21	13	0.6
	Average	**31**	**33**	**28**	**11**	**10**	**0.9**
Zn	AMA	98	79	86	11	10	72
	NUU	72	87	75	73	11	11
	RYA	75	75	63	100	89	6.8
	Average	**82**	**80**	**75**	**61**	**37**	**30**
	Combined Average	***62***	***65***	***50***	***37***	***32***	***18***

7.2.5 Treated Residue Characterisation

Chemical & Physical Characteristics

Table 9 compares the oxide composition of the untreated residues with the bench-scale EDR treated residues. In general, the EDR treatment reduced K_2O, Na_2O and Cl concentration and resulted in SiO_2, Al_2O_3 and Fe_2O_3 accumulation. It also reduced the CaO concentration in NUU and RYA while increasing the concentration in AMA. For the untreated residues, phases such as $CaCO_3$, $CaSO_4$, KCl, NaCl and $Na_{21}Mg(SO_4)_{10}Cl_3$ were identified with XRD. After the treatment, $CaSO_4{\cdot}2H_2O$ and $CaCO_3$ were found in EDR NUU and EDR RYA instead, while EDR AMA contained $CaSO_4$, $CaSO_4{\cdot}0.5H_2O$ and $PbSO_4$. Corroborating that Pb may have precipitated as $PbSO_4$. The presence of these phases in the residues, except for $PbSO_4$, were confirmed with TGA in journal paper III [110].

Table 9: Back calculated content of oxides (wt%), and CO_2 (wt%) content, as measured with TGA, of the untreated and treated residues. Included are data from journal paper III [110].

	AMA	EDR AMA	NUU	EDR NUU	RYA	EDR RYA
SiO_2	4.6	14	6.1	14	6.4	12
Al_2O_3	1.4	2.3	4.6	9.6	4.7	5.3
Fe_2O_3	1.0	2.4	0.9	1.4	1.8	2.7
CaO	13	28	43	29	42	31
MgO	0.6	0.4	1.4	1.3	1.8	2.2
K_2O	14	1.0	12	0.4	2.7	0.7
Na_2O	7.4	0.7	22	-	7.0	-
P_2O_5	2.6	2.1	1.8	2.7	2.2	3.7
SO_3	34	30	8.9	9.7	8.9	8.7
Cl	2.8	0.1	24	0.1	13	0.2
CO_2	0.0	0.0	2.7	2.4	5.3	2.8

Table 10 compares the total concentration and leachable concentration of Cd, Cr, Cu, Pb and Zn in the untreated residues with the bench-scale EDR treated residues. As seen in subsection 7.2.4, the bench-scale treatment only removed Cd, Cu and Zn in high amounts from EDR AMA. EDR AMA is, therefore, the only treated residue with a reduced concentration of Cd, Cu and Zn. EDR NUU and EDR RYA had low removal percentages and subsequently increased metal concentrations. This may be attributed to removing the previously discussed phases and oxides, resulting in an accumulation of the metals. Cr and Cd were also accumulated in EDR AMA as the treatment did not reduce these metals.

Table 10: Total concentration and leachable concentration of Cd, Cr, Cu, Pb and Zn of the untreated end treated residues. Included are data from journal paper IV [130] and limit values for non-hazardous waste [131].

Total content (mg/kg)	AMA	EDR AMA	NUU	EDR NUU	RYA	EDR RYA	
Cd	480	60	420	460	80	100	
Cr	300	700	800	1100	400	600	
Cu	1400	520	1300	2000	7900	10200	
Pb	12000	31000	3000	3200	3400	3400	
Zn	55000	26000	33000	41000	6600	9100	
Leachable (mg/kg)							Limit
pH [-]	6.5	4.1	12	7.7	12	7.2	
Cd	430	4.2	0.03	0.01	0.00	0.02	0.6
Cr	1.0	0.1	39	23	0.1	2.6	4.0
Cu	2.6	23	0.4	0.07	52	0.01	25
Pb	5.0	4.3	530	0.01	1400	0.00	5.0
Zn	23000	1700	2.9	0.5	20	0.09	25

At the end of the bench-scale EDR treatment, the treated residue's had solidified, likely due to the formation of $CaSO_4 \cdot 2H_2O$ and $CaSO_4 \cdot 0.5H_2O$, requiring the residue to be ground before further use. Table 11 compares the particle density and size distribution of the untreated and bench-scale EDR treated residues. The treatment did not significantly affect the residues particle density, but the grinding did reduce the particle size of EDR AMA and EDR RYA. The untreated residue NUU had a small particle size before the treatment, which was smaller than what could be achieved during the grinding process. Furthermore, EDR RYA had a d_{90} value higher than the untreated residue.

Table 11: Particle density and size distribution of the untreated and treated residues. Included are data from journal paper IV [130].

		AMA	EDR AMA	NUU	EDR NUU	RYA	EDR RYA
ρ	[g/cm^3]	2.8	2.7	2.6	2.6	2.5	2.6
d_{10}	[µm]	8.7	2.9	1.9	2.4	8.2	2.4
d_{50}	[µm]	44	17	13	12	19	11
d_{90}	[µm]	204	120	49	56	41	130

New Principal Component Analysis & Ternary Diagram

A new PCA was performed using the previous dataset from journal paper I [109], expanded with the treated residues to see how they compared. Fig. 18 and Fig. 19 shows the new results for the 1st and 2nd component combined and the 1st and 3rd component combined. With an increased SiO_2, Al_2O_3 and Fe_2O_3 concentration and reduced K_2O, Na_2O and Cl concentration, the treated residues have scores closer to that of a CFA that fulfils the EN 450-1 [111] requirement. However, The requirement for CFA is $\sum SiO_2\text{-}Al_2O_3\text{-}Fe_2O_3 \geq 70$ wt%, where the sum of SiO_2-Al_2O_3-Fe_2O_3 in EDR Ama, EDR Nuu and EDR Rya remained less than 25 wt%. As the treated residues were within the 95% confidence limit, they can not be regarded as outliers and are still similar in chemical composition to untreated MSWI fly ash. Before the treatment, AMA was an

outlier in the analysis. Due to its oxide changes and reduced metal content, EDR AMA is now more similar to other MSWI fly ash residues. However, with the inclusion of the 3rd component, it is evident that the increased Cu concentration in EDR RYA almost makes it an outlier in the analysis. Furthermore, EDR AMA has a high positive 3rd component score, which may be attributed to its increased CaO concentration and high SO_3 concentration.

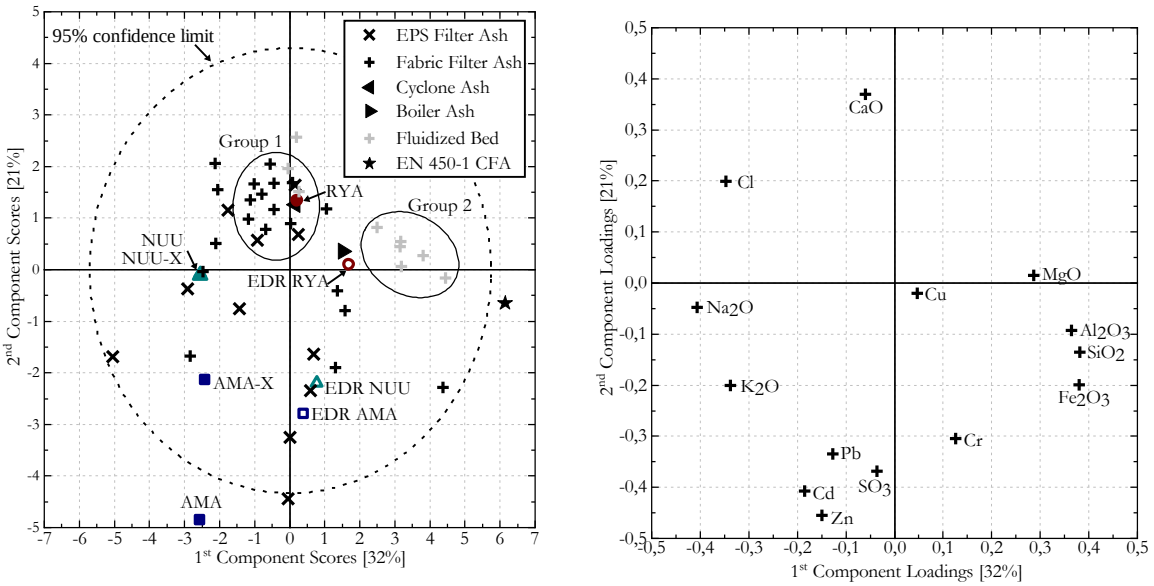

Figure 18: Score plot (left) and loading plot (right) of the 1st and 2nd principal components from the PCA. Points colored black are residues from grate furnaces, while points colored grey are filter ash residues from fluidized bed incinerators. Marked are two residue groupings. Included in this PCA are the treated residues and the dataset from journal paper I [109].

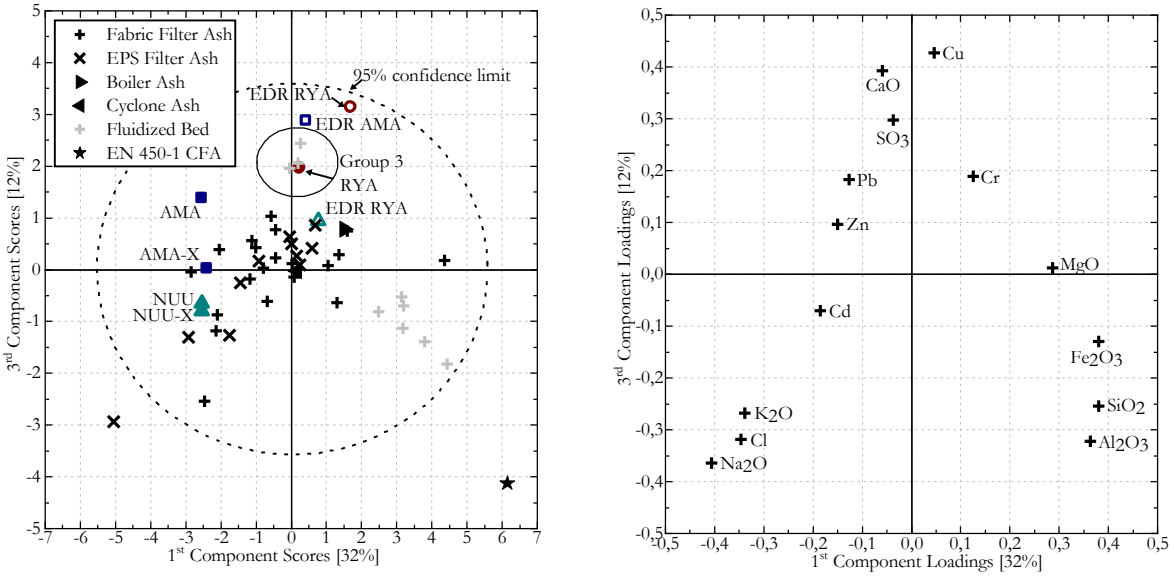

Figure 19: Score plot (left) and loading plot (right) of the 1st and 3rd principal components from the PCA. Points colored black are residues from grate furnaces, while points colored grey are filter ash residues from fluidized bed incinerators. Marked are two residue groupings. Included in this PCA are the treated residues and the dataset from journal paper I [109].

Fig. 20 shows the untreated and treated residues in a CaO-Al_2O_3-SiO_2 ternary diagram with OPC and the traditionally used SCMs. The untreated residues NUU and RYA had CaO-Al_2O_3-SiO_2 ratios close to limestone, while AMA had a ratio similar to portland cement. The diagram highlights how MSWI fly ash residues are different from traditionally used SCMs. After the bench-scale EDR treatment, the residues all had CaO-Al_2O_3-SiO_2 ratios similar to Portland cement, whereby the treated residues may be considered high-Ca mineral additions.

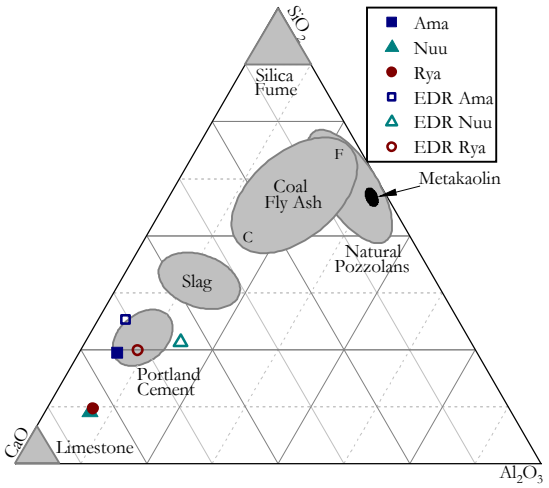

Figure 20: CaO-Al_2O_3-SiO_2 ternary diagram, with the ratios of the raw and EDR treated residues compared to Portland cement and selected SCMs from Lothenbach et al. [137] and Thomas et al. [15]. C: High calcium coal fly ash, F: Low calcium fly ash. Recreated from journal paper IV [130].

Pozzolanic Reactivity

Given the residues low SiO_2, Al_2O_3 and Fe_2O_3 concentration, they were not expected to have high pozzolanic reactivity. Fig. 21 depicts the results of the Frattini tests performed to assess the pozzolanic reactivity of the residues, where points in zone 1 indicate pozzolanic reactivity and points in zone 2 indicate no pozzolanic reactivity. The residue NUU is the only untreated residue included in the graphs, as the other residues produced results outside the area specified by the Frattini test. The cement paste with Ama was oversaturated with OH^- after eight and 15 days, while the paste with RYA was oversaturated with Ca^{2+} after eight and 15 days. The extended hydration time did reduce the OH^- and Ca^{2+} concentration in the paste with RYA but increased the OH^- concentration in the AMA paste. It was surmised that some phases in the two residues might have reacted with the solutions used in the Frattini test. However, this confirms that the untreated residues were not pozzolanic. The treated residues were likewise not pozzolanic, having a similar reactivity to the inert quartz instead after eight days. Although the treated residues did not exhibit pozzolanic reactivity, the pastes with the treated residue shifted towards zone 1 after 15 days, more than quartz, potentially indicating slow reactivity.

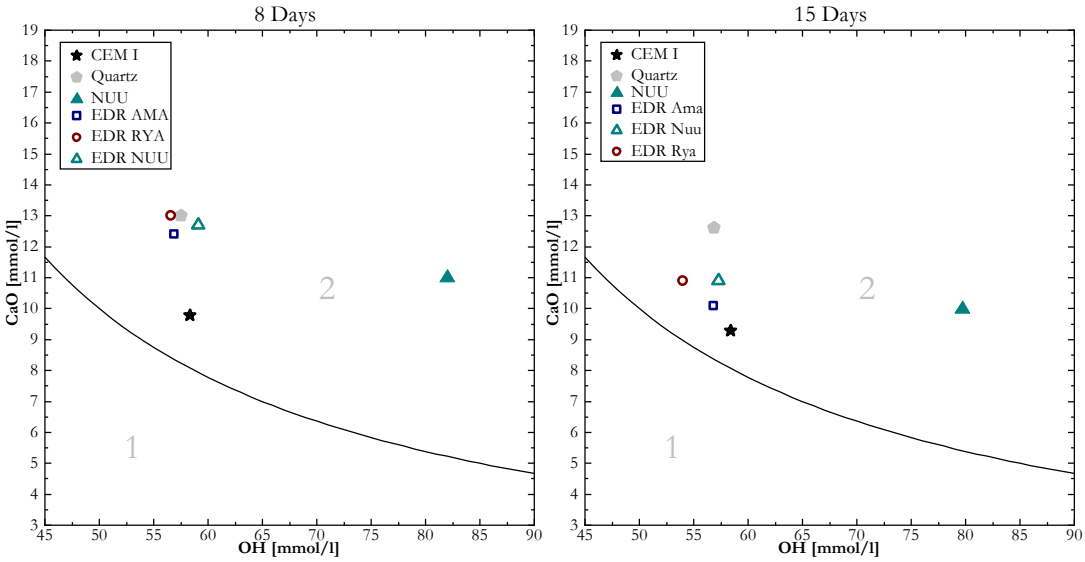

Figure 21: Frattini test results for 100 wt% CEM I cement paste and pastes with 10wt% quartz or residue after 8 days (left) and 15 days (right). Recreated from journal paper IV [130].

7.3 Performance in Binders

Section 7.3 explores the impact the bench-scale EDR treated residues has on hydration, phase development, setting time and compressive strength of cement-based materials. Starting with the hydration and phase development.

7.3.1 Effect on Hydration and Phase Development

The identified phases in the different cement pastes with either an untreated or treated residue after 1-90 days of hydration can be seen in Fig. 22 and Fig. 23, respectively, together with the results of the thermodynamic modelling. EDR treating the residues changed how they affected the hydration and phase development. Paste with either AMA or NUU had alite (A), belite (Be), tricalcium aluminate (Ta) and tricalcium aluminoferrite (Taf) peaks with high intensity and low-intensity portlandite peaks after one day of hydration, suggesting that the pastes hydration may be delayed after one day. However, ettringite had formed in the pastes, indicating that the aluminate/ferrite phases reacted partially. Over time the pastes did hydrate, where the AMA paste showed hemicarbonate formation after 90 days, while the NUU paste developed Friedel's salt. This was contrary to the development of the control paste with inert quartz that showed no delay and developed hemicarbonate and monocarbonate after three days of hydration. Paste with EDR AMA or EDR NUU exhibited only a slight delay in hydration based on the intensity of the initial clinker phases. Additionally, the paste with EDR NUU developed hemicarbonate and monocarboante similarly to the control paste, which may be attributed to its reduced chloride content. However, the paste with EDR did not develop hemicarbonate or monocarbonate. Ettringite was the only AFt/AFm phase formed. This was to EDR AMA's high Al_2O_3 and SO_3 content. The thermodynamic models corroborated the observed phase development, indicating that paste with AMA or EDR AMA will only develop ettringite as its AFt/AFm phase, while paste with NUU develop Friedel's salt and paste with EDR develops monocarbonate.

The residue RYA and the treated EDR RYA had a different effect on the hydration than the other residues but showed a similar phase development. Cement paste with RYA did not exhibit a delay by having similar peak intensities to the control. However, it still resulted in Friedel's salt development instead of hemicarbonate or monocarbonate. Like EDR NUU, EDR RYA did result in the development of hemicarbonate and monocarbonate. The thermodynamic model developed showed Friedel's salt formation with RYA and monocarbonate formation with EDR RYA, corroborating the observed development.

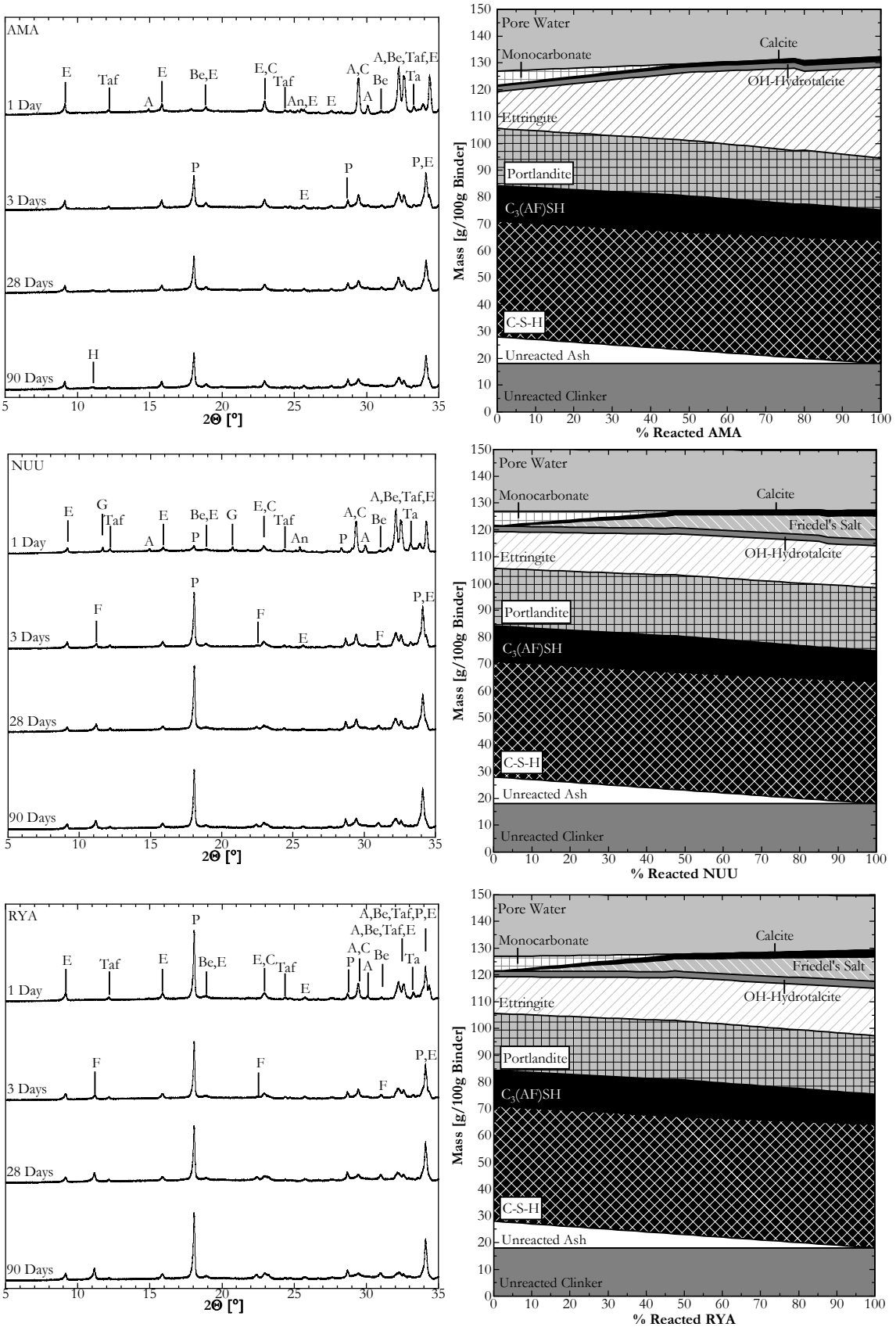

Figure 22: XRD patterns and Thermodynamic modelling of paste with Ama (top), Nuu (middle) and Rya (bottom). Alite (A), belite (Be), tricalcium aluminate (Ta), tricalcium aluminoferrite (Taf), portlandite (P), ettringite (E), hemicarbonate (H), Friedel's Salt (F), anhydrite (An), gypsum (G) and calcite (C). Recreated from journal paper [130].

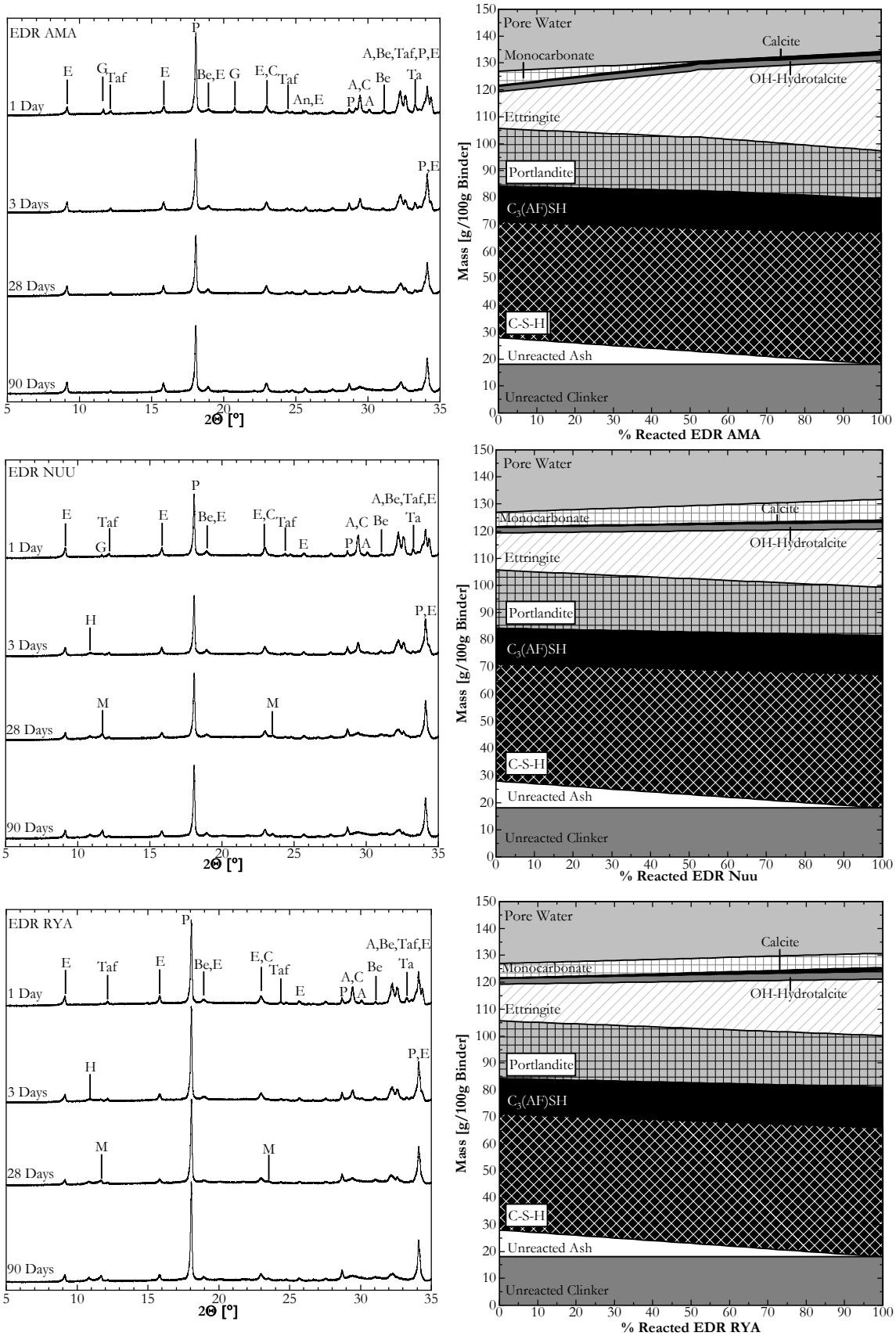

Figure 23: XRD patterns and Thermodynamic modelling of paste with EDR Ama (top), EDR Nuu (middle) and EDR Rya (bottom). Alite (A), belite (Be), tricalcium aluminate (Ta), tricalcium aluminoferrite (Taf), portlandite (P), ettringite (E), hemicarbonate (H), Friedel's Salt (F), anhydrite (An), gypsum (G) and calcite (C). Recreated from journal paper [130].

Fig. 24 shows the bound water and portlandite content in the cement paste specimens over time. The delayed hydration of the pastes with AMA or NUU is observable here as well, as the pastes bound water and portlandite content is low compared to the control specimens (CEM I and Quartz) after one day of hydration. After three days, when hydration has begun, the pastes with AMA or NUU had a higher bound water content than the control with quartz. However, after 28 and 90 days, it is again less. It was surmised that the residues had continued to inhibit the hydration of the clinker phases, as their peaks remained visible with XRD after 90 days of hydration. See Fig. 22. This also appears to have resulted in a low portlandite content.
In contrast, due to its uninhibited hydration, the paste with RYA binds more water than the control specimens, potentially as part of additional Friedel's salt and ettringite. However, the

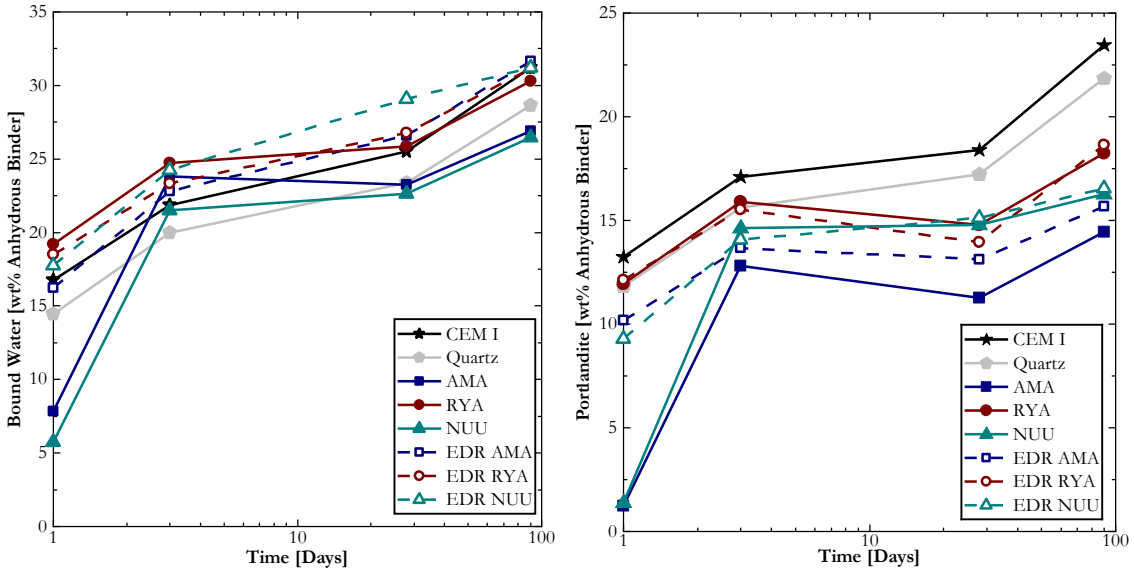

Figure 24: Bound water and portlandite conent as wt% of the anhydrous binder and function of time. Recreated from journal paper [130].

portlandite content is less than the control with quartz after three days. The pastes with the EDR treated residues all had a higher bound water content than both control specimens. This may be due to binding the water in ettringite and monocarbonate. However, the portlandite content remained less than the control with quartz after 90 days. The thermodynamic modelling showed an increase in C-S-H and a decrease in portlandite, which may be due to the increased SiO2 content in the treated residues. However, as evidenced by the Frattini test, the treated residues reactivity is slow, suggesting it has not occurred after 90 days of hydration.

7.3.2 Effect on Setting Time

The initial and final set of the various cement paste specimens are shown in Fig. 25. It was observed that the pastes with AMA or NUU exhibited delayed hydration during the hydration and phase development analysis.

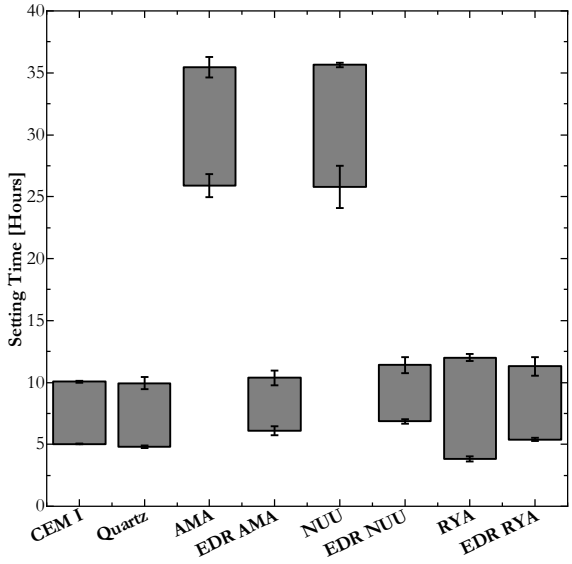

Figure 25: Initial and final setting times of cement pastes with the quartz and residues and a 100 CEM I cement paste. Error bars indicate standard variation. Recreated from journal paper [130].

The setting time tests showed that the pastes had their initial set after 25 hours and that their final set occurred after 35 hours. Treating the residues with EDR reduced the initial and final setting time delay by 19-20 and 24-25 hours, respectively, so that it conformed with the setting time of the control specimens. The treatment did not improve the setting time of the paste with RYA. The untreated RYA residue had an accelerative effect on the initial set but delayed the final set. After the treatment, the initial set was no longer accelerated, while the final setting time delay had been reduced.

Several possibilities for the delay and acceleration caused by the residues were explored in journal paper IV [130]. However, it was surmised that the metal content in the residues caused the delay. Fig. 26 compares the initial setting time of various pastes with the total metal molality and leached metal molality. Marked in the figure is the concentration of 0.18 mol/kg, at which a delayed setting has previously been observed. The total molality of metals in the pastes with untreated and treated residues was close to the concentration of 0.18 mol/kg, in that all pastes would have had a delayed set. However, only AMA and NUU resulted in a delayed set. The delay may instead depend on the leachable content of metals. This hypothesis may account for the residue AMA, where its high Zn content may be the cause. It does not account for NUU, as it

had the lowest leachable content of metals. The delay caused by the treated residues was attributed to the gypsum content extending the induction period of the early age hydration [130].

When working with mortar containing the untreated residue, the delay in setting had to be taken into account, along with other effects of the residues affecting the properties of the mortar. Fig 27 showcases some of the problems when the mortars with AMA or NUU were demoulded.

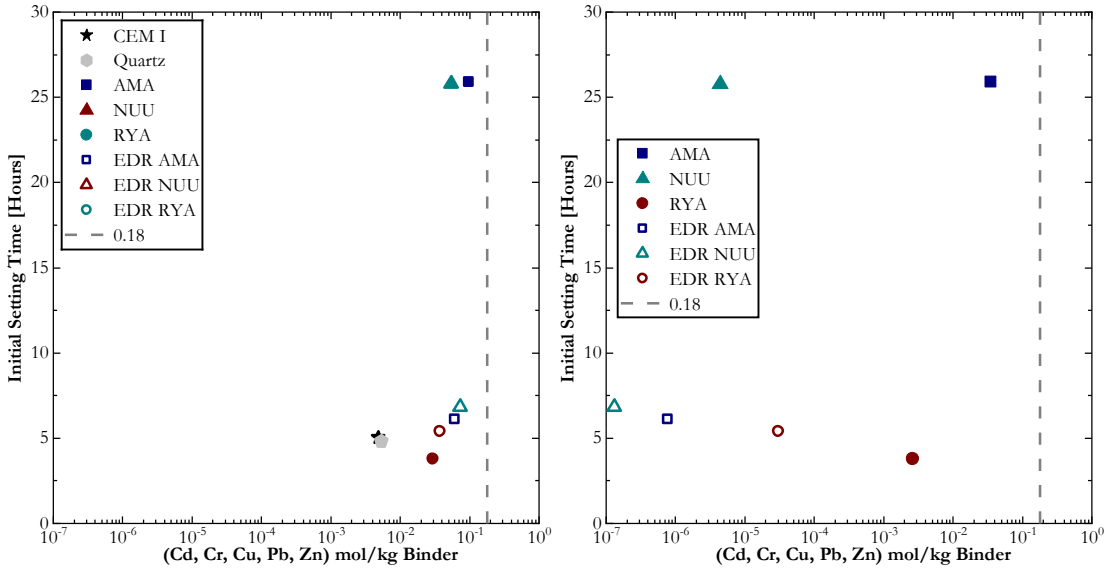

Figure 26: Initial and final setting versus (left) total metal content in the cement paste specimens and (right) content of leachable metals in the cement paste specimens. Recreated from journal paper [130].

Figure 27: Demoulding of mortar with AMA (left) and NUU (right) after 24 hours.

7.3.2 Effect on Compressive Strength

The residues impact on setting time is not the only effect that had to be accounted for while preparing the mortar for the compressive strength tests. The appended conference paper I [138] investigated the effect the residues had on mortar consistency, using a flow table, immediately after mixing and after 30 minutes. It was determined that a 10 wt% cement replacement with the residues reduced mortar flow by 30% and that the loss of consistency after 30 minutes is higher than for 100 wt% CEM I mortar. Therefore, a modified acrylic polymer-based superplasticizer was added to the mortar with the residues. This was shown to improve the flow and limit the loss of consistency over time [138].

Furthermore, the residues were shown to increase the macroporosity (based on a calculated air content). Using the residue, NUU resulted in 6% more macroporosity than the other residues and caused a visible volume expansion. See Fig. 28. It was surmised that as a Greenlandic residue, NUU had a higher metallic Al content and that the Al dissolved in the alkaline mortar causing H_2 gas to form and thereby increase the macroporosity, as discussed in [73]. The EDR treatment was shown to improve the macroporosity of the residues by reducing the porosity increase from the residues considerably. Therefore, the measured compressive strengths of the mortar were normalised to an air-free compressive strength using the method described in [102].

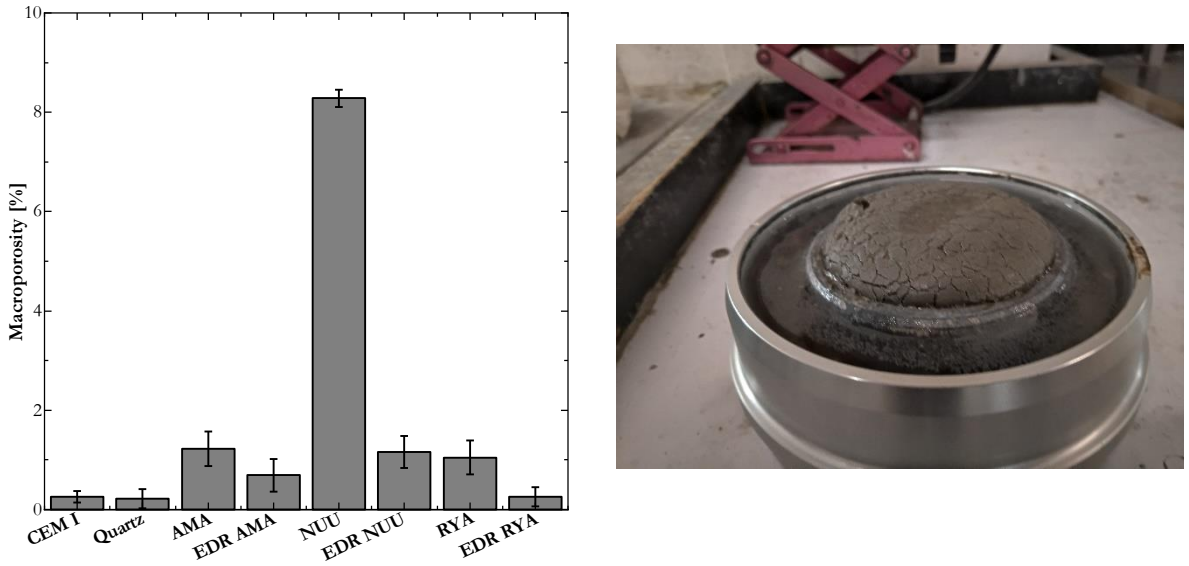

Figure 28: Calculated average macroporosity (air content) of the mortar specimens used for compressive strength testing (left) and example of the visible volume expansion caused by NUU (right). Recreated from journal paper [130].

The compressive strength results are shown in Fig. 29 as a function of time and bound water. Two control mortars were used, one without any cement replacement and one with 10 wt% inert quartz. The results are primarily compared with the mortar containing quartz, as this represents a

scenario where the residues do not affect the performance of the binder. Replacement with quartz reduced the compressive strength by 14% after one to three days and 21-23% after 28 and 90 days.

The delayed hydration and prolonged setting time of cement paste with AMA and NUU resulted in compressive strengths of less than 1 MPa. The continued inhibited hydration observed then resulted in compressive strengths that were lower than the mortar with quartz. The mortar with NUU achieved a compressive strength similar to the quartz mortar after 90 days, suggesting NUU do not inhibit hydration as much as AMA. In contrast, the mortar with RYA had a compressive strength similar to the control due to its accelerated initial set and uninhibited hydration.

EDR treating the residues improved the compressive strength of the mortar, except for EDR RYA, which now resulted in compressive strengths lower than the control. The strength of the mortars was still less than the mortar with quartz after one day, which may be due to the gypsum and bassanite in the residues prolonging the induction period [130]. The mortar with the treated residues then achieved compressive strengths between 70-75 MPa. Using the treated residues increased the bound water content and the compressive strength more than the quartz did. See Fig. 29b. It was, therefore, surmised that the treated residues resulted in increased bound water in the form of ettringite and monocarbonate, thereby increasing the strength. While the other untreated or treated residues may inhibit early hydration and C-S-H formation, Rya may promote C-S-H formation, thereby achieving a similar strength to the CEM I mortar.

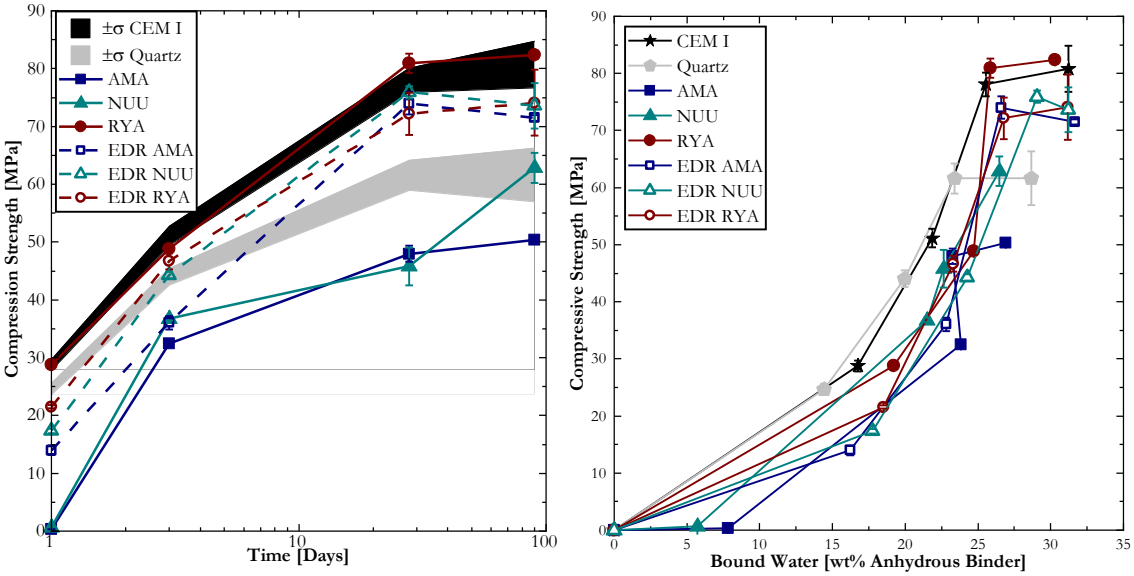

Figure 29: Compressive Strength (normalised to air free) of mortar specimens as a function of time and bound water content. Error bars and black/grey areas indicate standard deviation. Recreated from journal paper [130].

7.4 Environmental Concerns

Based on the previously presented results, EDR treated MSWI fly ash residues can be used in cement-based materials. However, the heavy metal content of the ashes may still pose an environmental risk. It has been demonstrated that cement-based materials effectively retain metals through chemical bonding and physical entrapment [139]. However, during a concrete structures lifetime, it is exposed to physical and chemical attack [140]. The environmental conditions at the surface of a concrete structure change how leaching occurs [140]. Environmental factors such as chlorides and sulphates have been shown to increase leaching. Therefore, two leaching scenarios were tested using a NaCl solution, Na_2SO_4 solution and deionised water adjusted to pH 4 with HNO_3. The scenarios tested were in-use (monolithic leaching) and end of life (crushed mortar leaching). However, the concentration of metals that can leach directly from the residues using the three solutions specified was investigated first using batch leaching.

7.4.1 Leaching Yield from the Raw Materials

The batch leaching results for the untreated and treated residues are shown in Fig. 30. The results are compared to the leaching criteria for granular hazardous waste acceptable at landfills for non-hazardous waste [131]. With the pH adjusted solute, AMA leached more Cd, Cr, Pb and Zn than the regulatory limit stipulates, NUU leached more Cr and Pb, while RYA leached more Cu and Pb. As demonstrated in Subsection 7.3.5, the treated residues leach less. However, EDR AMA still leached more Cd, Cr, Pb and Zn than the regulatory limit, while NUU and RYA leached more Cr and Pb, respectively. The NaCl and Na_2SO_4 solutions' effect on leaching is not easily discerned, as it varied depending on the metal and residue. In general, they leached more Cd and Cr than the pH 4 adjusted deionised water. For EDR NUU and EDR RYA specifically, more Cd leached with the NaCl solution than the Na_2SO_4 solution. For EDR AMA, NaCl increased Pb leaching, resulting in a higher yield than untreated AMA. Additional Cl^- and SO_4^{2-} may result in the formation of soluble (e.g. metal-chloride complexes) or insoluble complexes (e.g. $PbSO_4^{2-}$), thereby increase or decrease the leaching yield from the residues. In general, the NaCl and Na_2SO_4 solutions did not affect whether the leaching yield was higher than the regulatory limits. However, the two solutions did increase Cu leaching from EDR AMA, Cd from EDR NUU and Cr from EDR RYA beyond the limit.

7.4.2 Monolithic leaching (In-Use Scenario)

The results of the monolithic leaching experiments are presented in Table 12, as the maximum leaching measured between 0-4 days, 4-16 days and 16-70 days. The leaching results are compared to the leaching limits for construction materials specified in the Dutch building decree [141]. The impact of using the NaCl and $NaSO_4$ solutions to leach the metals is more discernable from the monolithic cubes than from the

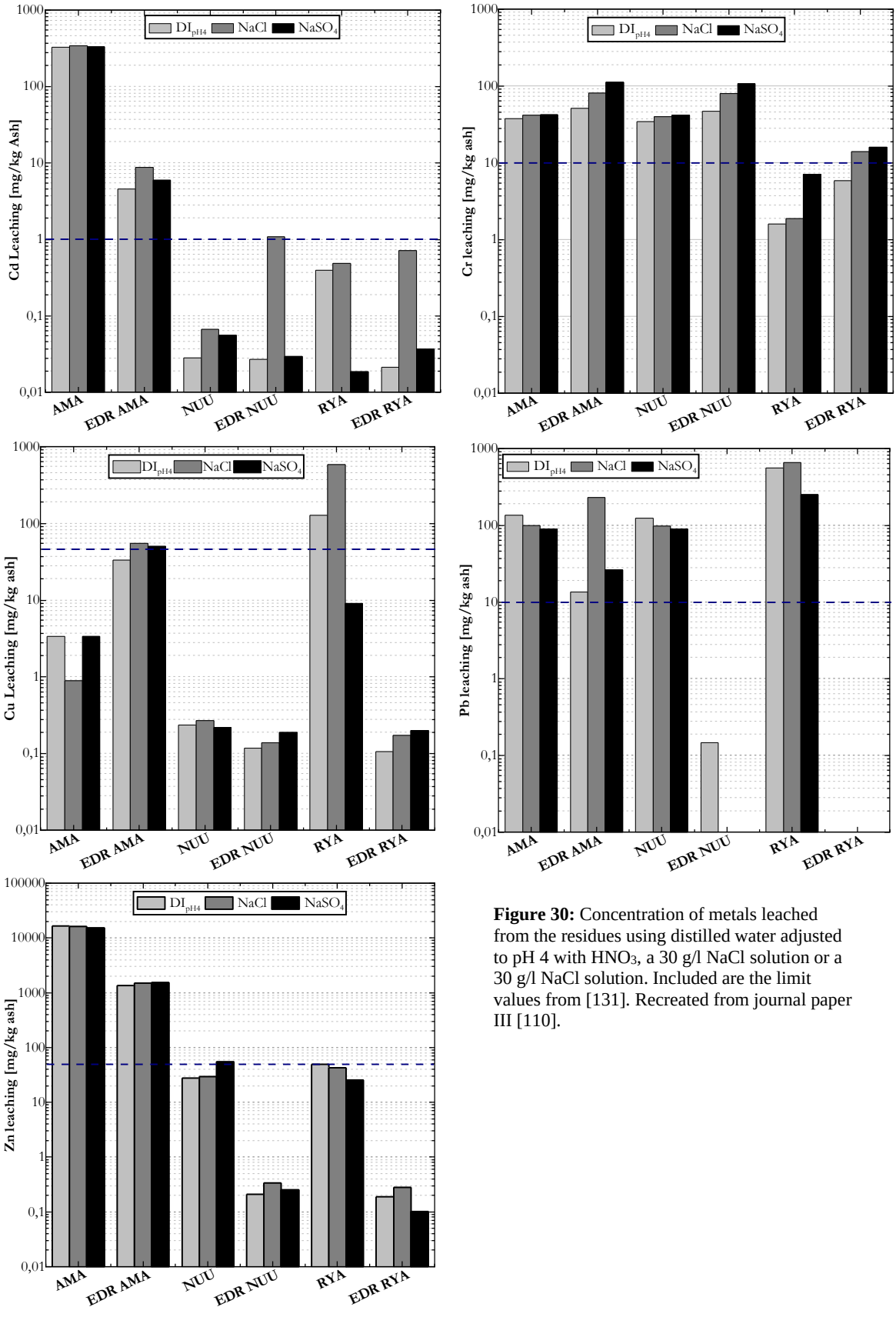

Figure 30: Concentration of metals leached from the residues using distilled water adjusted to pH 4 with HNO_3, a 30 g/l NaCl solution or a 30 g/l NaCl solution. Included are the limit values from [131]. Recreated from journal paper III [110].

Table 12: Maximum monolithic leaching (mg/m² surface) between 0-4 days, 4-16 days and 16-70 days. (-) below detection limit or no higher than solute concentration. The regulation limit values are from the Dutch building material degree, as presented in [141]. Included are data from journal paper III [110].

		Cd			Cr			Cu			Pb			Zn		
		0-4	4-16	16-70	0-4	4-16	16-70	0-4	4-16	16-70	0-4	4-16	16-70	0-4	4-16	16-70
DI_{pH4}	100 wt% CEM I	-	-	-	0.42	0.04	-	-	-	-	-	-	-	-	-	-
	Quartz	-	-	-	-	0.05	-	-	-	-	-	-	-	-	-	-
	Arc-Fa	0.35	0.24	0.21	0.75	0.79	1.0	0.49	0.66	0.75	0.82	1.8	3.3	0.15	2.3	4.0
	EDR-Arc-Fa	0.38	0.34	0.26	0.8	3.1	5.3	0.53	0.59	0.58	1.8	7.9	14	0.56	0.56	0.57
	Rya-Fa	0.37	0.18	0.16	0.66	0.68	0.63	0.51	0.84	0.51	-	-	-	-	0.60	0.46
	EDR Rya-Fa	0.04	0.28	-	-	-	-	-	0.08	0.16	-	-	-	0.16	-	-
	Nuuk-Fa	0.15	0.09	-	-	0.43	1-7	0.01	0.43	0.19	-	-	-	1.4	5.4	1.4
	EDR Nuuk-Fa	0.12	0.05	-	-	-	-	-	-	0.05	-	0.30	-	0.25	0.59	0.97
NaCl	100 wt% CEM I	-	-	-	2.0	5.7	8.9	-	-	-	0.61	-	-	-	-	-
	Quartz	-	-	-	2.3	5.1	10	-	-	-	-	0.18	-	-	-	-
	Arc-Fa	-	-	-	2.8	5.8	9.4	-	-	-	1.9	3.6	5.2	1.4	3.2	5.2
	EDR-Arc-Fa	0.31	0.38	0.24	1.1	3.4	6.3	0.26	0.61	0.30	4.9	11	18	0.37	1.5	0.32
	Rya-Fa	0.49	0.20	0.10	2.3	6.9	13	0.33	0.31	0.33	0.41	0.83	0.51	12	-	0.10
	EDR Rya-Fa	0.17	0.39	0.24	1.0	3.9	7.4	0.36	0.39	0.56	0.41	0.20	1.38	0.17	0.25	-
	Nuuk-Fa	-	0.10	0.01	3.3	7.2	11	0.93	1.2	1.1	-	-	-	0.79	2.2	2.2
	EDR Nuuk-Fa	0.24	0.01	0.01	2.4	5.5	9.9	0.85	1.1	1.6	0.48	0.03	0.25	1.3	1.9	2.2
Na_2SO_4	100 wt% CEM I	-	-	0.11	1.8	3.0	4.5	-	-	-	-	-	-	-	-	-
	Quartz	-	-	-	1.6	3.7	4.1	-	-	-	-	0.03	-	-	-	-
	Arc-Fa	-	-	-	3.8	5.5	7.2	-	-	-	1.5	2.4	3.0	3.1	8.7	6.0
	EDR-Arc-Fa	0.23	0.26	0.21	1.2	3.1	5.3	0.28	0.39	0.38	4.2	7.1	12	2.3	0.54	0.50
	Rya-Fa	0.20	0.22	0.25	1.3	3.8	7.2	0.17	0.16	0.44	0.11	0.18	0.83	0.39	1.7	-
	EDR Rya-Fa	0.15	0.09	-	1.2	3.0	3.7	0.93	2.04	1.49	0.76	0.53	1.4	0.54	0.93	-
	Nuuk-Fa	0.07	0.02	0.11	3.3	5.6	7.9	0.96	0.92	0.98	-	-	-	1.4	4.9	4.1
	EDR Nuuk-Fa	0.05	-	-	2.2	4.1	6.0	0.62	0.86	1.0	0.08	-	0.04	-	-	0.8
Regulation limit			12			1500			540			1275			2100	

residues directly. It has been demonstrated that Cl^- penetration results in the dissolution of the AFt and AFm phases and that it may be expected that both the major and trace elements change solubility [140]. Likewise, SO_4^{2-} penetration may lead to expansive gypsum and ettringite formation, while portlandite and the AFm and C-S-H phases dissolve [140]. Metals bound in dissolving phases may, therefore, be released.

No measurable Cd or Zn leached from the control specimen (100 wt% CEMI and quartz cubes). Cu and Pb leaching were measured. However, the measurements were erratic, suggesting that neither Pb nor Cu leach in significant concentrations. Cr leaching showed a similarly erratic behaviour when used the pH 4 deionised water. However, when using the NaCl or Na_2SO_4 solution, comparatively high concentrations of Cr leached. More Cr leached in the NaCl solution, suggesting that the diffusion of Cl^- has a more significant effect on Cr leaching than SO_4^{2-}. Cr may substitute Al^{3+} and SO_4^{2-} in the AFt and AFm phases, which may be released in higher amounts when AFt dissolves during Cl^- penetration.

The monolithic specimen containing the residues had a higher leaching yield than the controls when using either solution. However, the NaCl and Na_2SO_4 solutions resulted in a higher yield than the pH 4 adjusted deionised water. The yield was shown to depend on the metal and residue. Cd was the only metal to not leach in significant amounts, which may be attributed to it having almost the same ionic radius as Ca, resulting in strong incorporation or that it is encapsulated as $Cd(OH)_2$. Cr leached similarly to the control specimens, with an increased yield due to the additional Cr from the residues. Depending on the residue, either the NaCl or $NaSO_4$ solution resulted in the highest yield, suggesting that which phase Cu is predominantly incorporated in may depend on the residue. In contrast, the highest Pb yield was achieved with the NaCl solution, while the highest Zn yield was achieved with the Na_2SO_4 solution. As Pb and Zn may replace Ca in the AFt and C-S-H phase or be adsorbed to the C-S-H phase, the results suggest that Pb is predominantly found in the AFt phase and that Zn is predominantly found in the C-S-H phase.

The efficiency of the EDR treatment in reducing the leaching yield was also dependent on the metal studied. Generally, the treatment reduced the Zn and Cr yield, increased the Pb yield, while the Cu and Cd yield remained unchanged. This was contrary to the batch leaching experiments shown in Subsection 7.4.1, where an increase in Cr and a reduction in the Pb yield was observed. It should be noted that the treatment significantly increased the Pb yield from AMA, regardless of the solution used.

Despite the increase in metal leaching observed when using the residues and including environmental conditions in the leaching experiments, the metal emissions were up to a factor 1000 lower than the regulatory limits [141]. Therefore, substituting 10 wt% cement with MSWI fly ash residues may be feasible in terms of leaching during a structures lifetime, which may be attributed to how effectively heavy metals are retained in cement-based materials.

7.4.3 Crushed Mortar Leaching (End-of-Life Scenario)

The concentration of metals that leached during the experiments with crushed mortar is shown in Fig. 31. The crushed mortar represents construction waste at the end of a structures life and may be compared to the category three and category two leaching limits for construction and civil engineering waste.

Cd, Cu and Zn leaching were below the regulatory limits for all specimens tested (control and residue containing) regardless of the solution used, except for Cu leaching from the crushed mortar with AMA. Furthermore, 10 wt% cement replacement with the residues did not generally increase Cd, Cu and Cr leaching compared to what could leach from the control specimen. This was also the case for Pb leaching for NUU, EDR NUU, RYA and EDR RYA, where the measured yield was comparable to the 100 wt% CEM I control. Despite the significantly higher concentration of heavy metals in the residues than cement, the metal leaching was not increased, suggesting that the investigated metals were immobilised in the cement matrix. However, this was not the case for AMA and EDR AMA that increased the Pb and Zn yield compared to the control specimen. The residue NUU and the treated residue EDR NUU also increased the Zn yield compared to the control specimen. The increase in Pb and Zn with these residues may be related to their high metal concentrations. See Subsection 7.2.5.

The effect of the EDR treatment is not easily discernable for NUU and RYA but is discernable for Pb and Zn leaching from AMA. The EDR treatment increased the Pb concentration in AMA, thereby doubling the leaching yield while removing a fraction of the Zn reduced the Zn yield to below 20 μg/kg crushed mortar. Although not as pronounced as EDR AMA, the treatment also increased the Pb yield from NUU and RYA.

Using solutions containing NaCl or Na_2SO_4 resulted, in general, in higher leaching yields than using deionised water adjusted to pH 4, further suggesting that these simulated environmental factors may increase leaching. However, it depends on the metal and residue studied. The effect of the environmental factors on leaching, where very discernable for Cr leaching. Using the deionised water adjusted to pH 4, the leaching yield was within category three for all of the tested specimen but exceeded category 3 with the NaCl and Na_2SO_4 solutions.

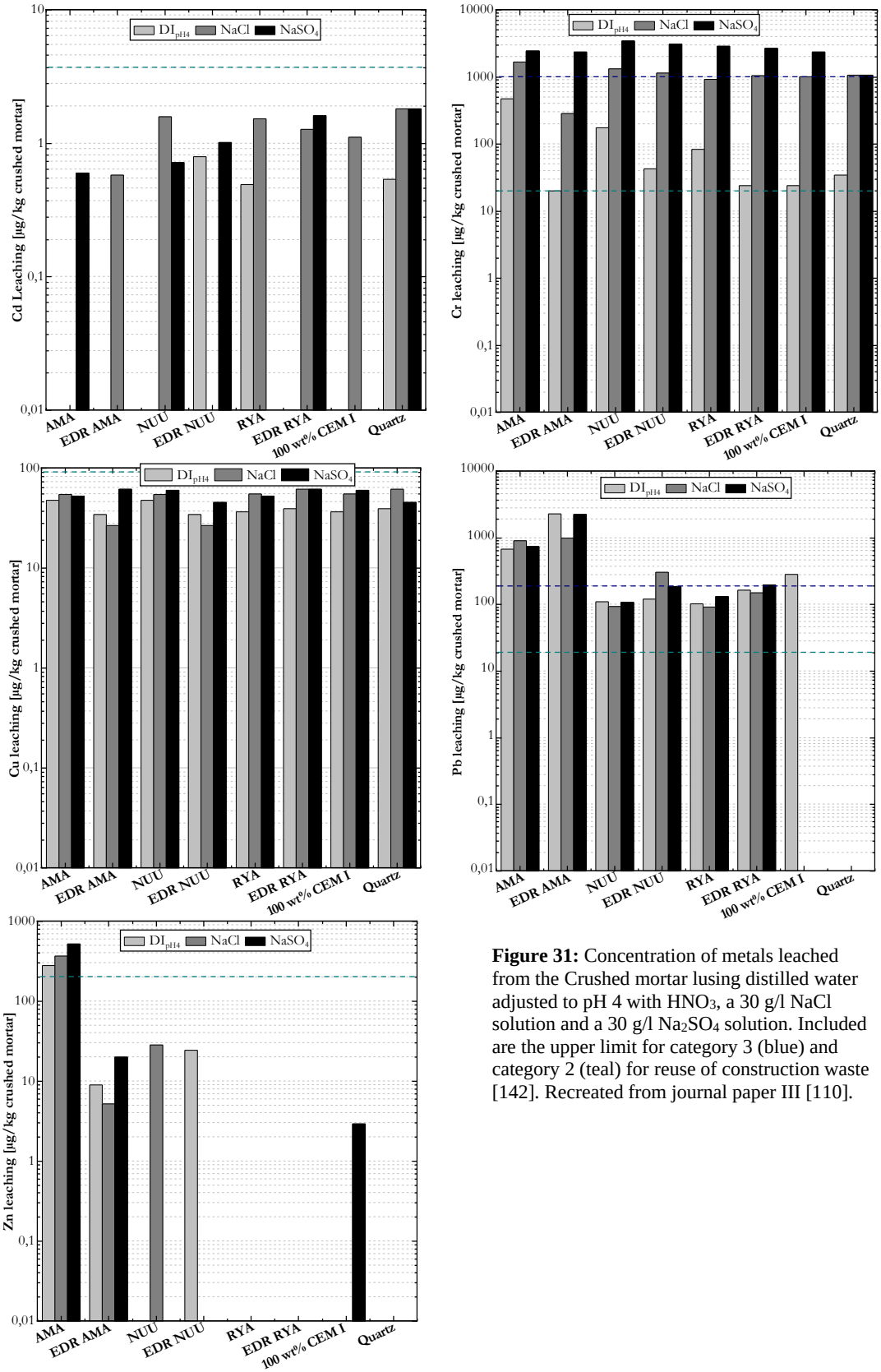

Figure 31: Concentration of metals leached from the Crushed mortar lusing distilled water adjusted to pH 4 with HNO_3, a 30 g/l NaCl solution and a 30 g/l Na_2SO_4 solution. Included are the upper limit for category 3 (blue) and category 2 (teal) for reuse of construction waste [142]. Recreated from journal paper III [110].

7.5 Alternative Options for Reuse

During the experiments with the residues, specific characteristics of the residues were observed that might enable the residues to be used in cement-based materials, but not as SCMs. It was noted that RYA might have an accelerative effect on cement hydration. EDR AMA's high sulphur content in the form of, among others, $CaSO_4 \cdot 0.5H_2O$ may be used to replace the gypsum used in cement. These potential alternatives were investigated by performing setting time experiments. 1-3 % RYA was added to cement paste to test its accelerative qualities compared with a commonly used accelerator, $CaCl_2$. A blend of cement without gypsum and EDR AMA was prepared so that the sulphur content was the same as in CEM I. The results of the accelerative test and gypsum replacement test are shown in Fig. 31.

Using RYA as an accelerator did decrease the initial and final set of a cement paste. However, the results had a higher standard deviation than and differed from $CaCl_2$. Using increasing amounts of $CaCl_2$ reduced the initial setting time and shortened the time to the final set. Using increasing amounts of RYA still decreased the initial setting time compared to the CEM I control. However, it was not as effective as using 1% and increased the time to the final set compared to using 1%.

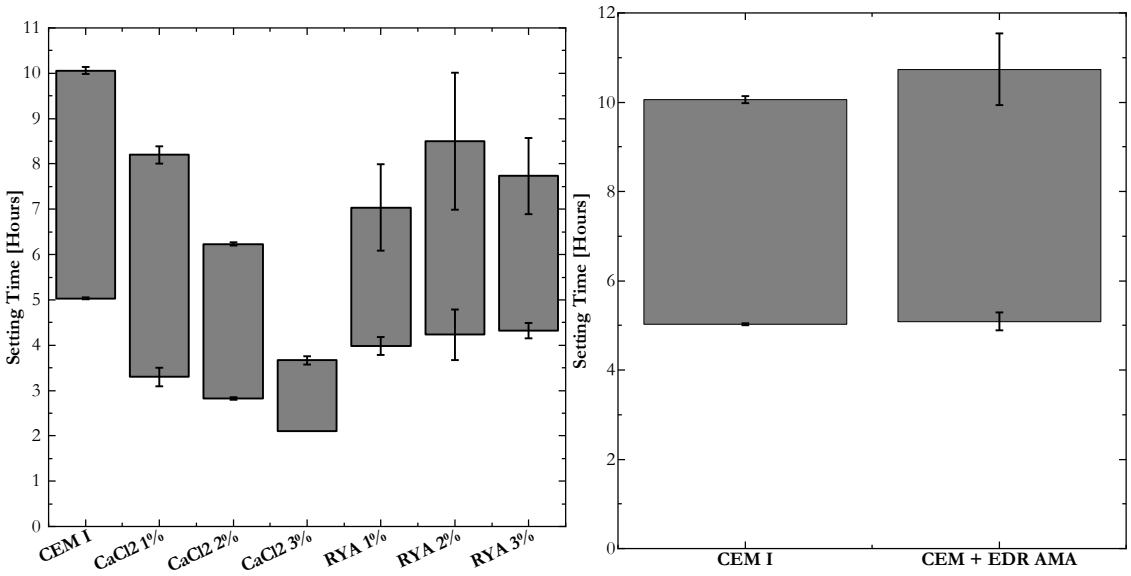

Figure 32: Setting time results from using RYA as an accelerator and using EDR AMA as a gypsum replacement. From additional note I.

The results of the gypsum replacement test showed that using sulphur-rich EDR treated MSWI fly ash residues is feasible as the EDR AMA blend had an initial set after 5 hours, the same as the control. However, the final set occurred after 10.5 hours instead of 10 and showed a large spread. It was hypothesised that the delay might be due to some of the sulphates being bound in $PbSO_4$ instead of $CaSO_4$. Furthermore, During the mixing process, small clumps were observed that was not observed in the control mixture, which may be hardened cement. However, despite these alterations to the set and the mixing process, gypsum replacement seems feasible. The resulting heavy metal content would still be an issue that will have to be accounted for.

8. Conclusions

The main conclusions of the research performed pertain to four stages of the PhD project; Charactering and screening the residues, treating and improving the residues, utilising the residues in cement-based materials and exploring additional options for reusing the residues.

The five MSWI fly ash residues obtained for the PhD project were very different from fly ash from coal incineration and did not fulfil the CFA requirements for concrete manufacturing. The principal oxides of the five residues were CaO, K_2O, Na_2O and SO_3 instead of the desired SiO_2, Al_2O_3 and Fe_2O_3. The potential phases in the five residues were mainly $CaCO_3$, $CaSO_4$, KCl and NaCl. A sulphur-rich MSWI fly ash was also found to contain sulphate phases such as $Na_{21}Mg(SO_4)_{10}Cl$. The five residues were characterised as highly soluble due to their content of water-soluble Cl^-, SO_4^{2-}, K^+ and Na^+. The residues were also found to contain high concentrations of toxic metals that leached in greater concentration than regulations permit. Therefore, the residues had to be treated to improve their characteristics and reduce metal leaching before they could be used in cement-based materials.

A principal component analysis showed that, although the five residues had oxide and metal concentrations within the range of previously studied MSWI fly ash residues in the literature, they were very different residues compared to each other. One residue, an MSWI APC residue, had a chemical composition similar to the average composition of the MSWI fly ash residues. Three residues, MSWI fly ashes, had chemical compositions less common for an MSWI fly ash residue. The fifth residue, the sulphur-rich MSWI fly ash, was an outlier in the analysis and had an uncharacteristic chemical composition for an MSWI fly ash residue.

It was decided to use the residue with an average composition, one of the residues with a less common composition and the outlier for the subsequent experiments. This would provide a broad interpretation of how MSWI fly ash residues perform in metal extraction methods, focusing on electrodialytic remediation (EDR) and as partial cement replacements in binders.

The EDR treatment improved the characteristics of the chosen residues. It reduced the K_2O, Na_2O and Cl concentration in the residues while accumulating SiO_2, Al_2O_3 and Fe_2O_3. After the treatment, the identified phases present in the sulphur-rich MSWI fly ash was $CaSO_4 \cdot 0.5H_2O$ and $PbSO_4$ and $CaSO_4 \cdot 2H_2O$ and $CaCO_3$ in the MSWI fly ash and MSWI APC residue. Furthermore, the treatment also reduced the metal leaching yield from the ashes. The EDR treated residues were more similar to CFA but did not fulfil the chemical requirements for CFA and had no

pozzolanic reactivity. Instead, the treated residues had a $CaO\text{-}SiO_2\text{-}Al_2O_3$ ratio similar to portland cement.

The EDR treatment was not successful in recovering large amounts of the valuable metals from the residues. The lab-scale and bench-scale EDR treatment had combined average removal percentages of Cd, Cr, Cu, Pb and Zn of 32-37% and 18% from the three residues, respectively, compared to 50-65% when leaching with acid. EDR may therefore be an inefficient treatment for recovering metals from MSWI fly ash residues.

The EDR treatment improved the performance of the residues when used in cement-based materials. The treatment reduced the delay in the initial setting time of blended cement pastes containing the two MSWI fly ashes from 20 to 1 hour and the delay in the final set from 25 to 2 hours. The improvement may be attributed to the treatment removing sufficient amounts of retarding compounds from the residue, e.g. heavy metals. A reduction in the macroporosity of blended mortars containing the residues was also observed. For one of the untreated MSWI fly ashes, the mortar expanded due to gas evolution from reacting metallic aluminium, which did occur with the treated ash. The EDR treatment increased the resulting compressive strength of blended mortar compared to blended mortar made with inert quartz. As the residues showed no pozzolanic reactivity, the contribution may be hydraulic, with slow reactivity. Combined XRD and thermodynamic modelling showed that the residues reacted to an extent and that an increase in ettringite and monocarbonate occurred, binding more water, which can contribute to the strength. The untreated MSWI APC residue also positively contributed to the strength, whereas the two untreated MSWI fly ashes resulted in a lower compressive strength than the blended mortar with quartz. Therefore, the EDR treatment may improve the performance of MSWI fly ash, while MSWI APC residues may be used without the treatment, based on the technical performance.

Although the technical performance of the blended mortar with the treated residues was promising, heavy metals leaching remained an environmental concern, especially how environmental factors may influence leaching. The use phase and end of life were subsequently tested by examing the metal leaching yield from the monolithic and crushed mortar. Using the treated MSWI fly ash residues increased the Cd, Cu, Pb and Zn yield from the monolithic mortar. Cr leached from the control specimens as well. Including environmental factors such as Cl^- and SO_4^{2-} increased Cr, Pb and Zn leaching, which may be attributed to the breakdown of the cement hydrates in the monolithic mortar over time. However, the yield was below regulatory limits, suggesting that the treated residues may be used as a partial cement replacement. Cr

leaching from the crushed mortar exceeded the regulatory limits for reuse when Cl^- and SO_4^{2-} were included in the experiments. This may be attributed to the cement used, as leaching from the control was high as well.

The experiments of the final stage showed that 1-3% of the untreated APC residue might be used as an accelerant, although not as effective as a common accelerator, while the sulphur-rich treated MSWI fly ash may substitute gypsum in cement. Substituting the gypsum may cause a delay in the cement-based materials final setting time.

9. Outlook

The thesis results were promising, demonstrating that using EDR treated MSWI fly ash residues as a partial cement replacement has potential. However, the presented research is not irrefutable, as there are still topics to be investigated further.

The EDR treatment removed lower amounts of metals from the MSWI fly ash residues than directly leaching with acid, despite similarities in pH. Why this was the case could be investigated further, and whether the EDR process can then be adjusted to account for it. Problems were encountered with the bench-scale EDR setup that may have hindered the treatment process. It may prove beneficial to rethink the bench-scale setup, improve the design and treat the MSWI fly ash residues again to reevaluate the setup.

The EDR treated residues were chosen for further study due to the treated residues not being in direct contact with acid. However, as the direct acid leaching was more effective at recovering metals from, it should be tested of the remaining residue after leaching performs in cement-based materials. Furthermore, to substantiate the findings of this thesis, residues that have only been water-washed should be studied as well, as water-washing the residues was part of the EDR treatment.

The EDR treated residues were found to have low pozzolanic reactivity but could be slowly reacting. The cement pastes and mortar tests were only performed after 1, 3, 28 and 90 days of hydration. Performing the same tests after 1-3 years may show if they have a slow reaction contributing to the results. Furthermore, previous studies have found that after 565 days of hydration, MSWI fly ash residues has a deteriorating effect on the performance of cement-based materials. Although the delay in setting time was attributed to the leachable heavy metal content of the residues, there were inconsistencies to this hypothesis, as one the fly ashes did not leach metals in as high amounts as the other residues, but caused a significant delay in the setting time. This may be accomplished by studying the various phases of the residues individually, testing their effect, and testing several phases together.

The APC residue resulted in a similar compressive strength as the tested control. Why this occurred was not thoroughly investigated and should be looked into further. The APC residue had an average composition for MSWI fly ash residues. Therefore, it should be investigated whether the positive results were due to its average composition or if it resulted from the APC.

The results of the final stage of the experiments showed that using the MSWI APC residue as an accelerant and the sulphur-rich MSWI fly ash as a gypsum replacement were possible. The only

experiments performed were setting time experiments. These alternative options should be further explored by performing additional experiments such as investigating the phase development or measuring the compressive strength.

References

[1] W.-Y. Chen, T. Suzuki, M. Lacker, eds., Handbook of Climate Change Mitigation and adaptation, Springer, 2017.

[2] UN, Introduction to Climate Action, (n.d.). https://unfccc.int/climate-action/introduction-climate-action (accessed May 6, 2021).

[3] UN, The 17 Goals, (n.d.). https://sdgs.un.org/goals accessed May 6, 2021).

[4] J.G.J. Olivier, P. J.A.H.W, TRENDS IN GLOBAL CO2 AND TOTAL GREENHOUSE GAS EMISSIONS, 2020 (2020). https://www.pbl.nl/sites/default/files/downloads/pbl-2020-trends-in-global-co2-and-total-greenhouse-gas-emissions-2019-report_4068.pdf.

[5] UN, Ikoner, (n.d.). https://www.verdensmaalene.dk/ikoner (accessed May 6, 2021).

[6] H. Justnes, How to Make Concrete More Sustainable, Journal of Advanced Concrete Technology. 13 (2015) 147–154. https://doi.org/10.3151/jact.13.147.

[7] Jos G.J. Olivier; Greet Janssens-Maenhout; Marilena Muntean; Jeroen A.H.W. Peters, Trends in global CO2 emissions 2016, (2016) 86.

[8] K.L. Scrivener, V.M. John, E.M. Gartner, Eco-efficient cements: Potential, economically viable solutions for a low-CO2, cement-based materials industry, (2016).

[9] C. Ferreira, A. Ribeiro, L. Ottosen, Possible applications for municipal solid waste fly ash, Journal of Hazardous Materials. 96 (2003) 201–216.

[10] G.M. Kirkelund, P.E. Jensen, Electrodialytic treatment of Greenlandic municipal solid waste incineration fly ash, Waste Management. 80 (2018) 241–251. https://doi.org/10.1016/j.wasman.2018.09.019.

[11] W. Chen, G.M. Kirkelund, P.E. Jensen, L.M. Ottosen, Electrodialytic extraction of Cr from water-washed MSWI fly ash by changing pH and redox conditions, Waste Management. 71 (2018) 215–223. https://doi.org/10.1016/j.wasman.2017.09.035.

[12] G.M. Kirkelund, M.R. Geiker, P.E. Jensen, Electrodialytically treated MSWI APC residue as substitute for cement in mortar, Nordic Concrete Research. (2014) 1–16.

[13] P.C. Hewlet, M. Liska, Lea's Chemistry of Cement and Concrete, Fifth Edit, Elsevier, 2019.

[14] K. de Weerdt, M. ben Haha, G. le Saout, K.O. Kjellsen, H. Justnes, B. Lothenbach, Hydration mechanisms of ternary Portland cements containing limestone powder and fly ash, Cement and Concrete Research. 41 (2011) 279–291. https://doi.org/10.1016/j.cemconres.2010.11.014.

[15] M. Thomas, Supplementary Cementing Materials in Concrete, CRC Press, 2013.

[16] H. Justnes, Influence of SCMs on hydration and durability of blended cements - Chemical and Physical Principles, Journal of the Chinese Ceramic Society. 13 (2554) 1359–1371.

[17] DS/EN 197-1: Cement - Part 1: Composition, Specifications and Conformity criteria for common cements, Dansk Standard, Denmark, 2012.

[18] M. Tokyay, Cement and Concrete Mineral Admixtures, CRC Press, 2018.

[19] A. Chandler, T. Eighmy, J. Hartlen, O. Hjelmar, D. Kosson, S. Sawell, H.A. van der Sloot, J. Vehlow, AN INTERNATIONAL PERSPECTIVE ON CHARACTERISATION AND MANAGEMENT OF RESIDUES FROM MUNICIPAL SOLID WASTE INCINERATION SUMMARY REPORT, THE INTERNATIONAL ASH WORKING GROUP, 1994.

[20] Teknik, (n.d.). https://a-r-c.dk/amager-bakke/teknik/ (accessed May 7, 2021).

[21] Y. Zhang, Z. Ma, Z. Fang, Y. Qian, P. Zhong, J. Yan, Review of harmless treatment of municipal solid waste incineration fly ash, Waste Disposal & Sustainable Energy. (2020). https://doi.org/10.1007/s42768-020-00033-0.

[22] H.K. Hansen, L.M. Ottosen, B.K. Kliem, A. Villumsen, Electrodialytic remediation of soils polluted with Cu, Cr, Hg, Pb and Zn, Journal of Chemical Technology and Biotechnology. 70 (1997) 67–73. https://doi.org/10.1002/(SICI)1097-4660(199709)70:1<67::AID-JCTB662>3.0.CO;2-V.

[23] B.A.R. Ebert, B.-M. Steenari, M. Petranikova, G.M. Kirkelund, "UNDER REVIEW" Electrodialytic Remediation and Combined Acid Leaching and Solvent Extraction - Potential Methods for Recovery of Metals from MSWI Fly Ash, Journal of Cleaner Production. (2021).

[24] A.J. Pedersen, L.M. Ottosen, A. Villumsen, Electrodialytic removal of heavy metals from municipal solid waste incineration fly ash using ammonium citrate as assisting agent, Journal of Hazardous Materials. 122 (2005) 103–109. https://doi.org/10.1016/j.jhazmat.2005.03.019.

[25] L.M. Ottosen, H.K. Hansen, C.B. Hansen, Water splitting at ion-exchange membranes and potential differences in soil during electrodialytic soil remediation, Journal of Applied Electrochemistry. 30 (2000) 1199–1207.

[26] A.J. Pedersen, L.M. Ottosen, Elemental analysis of ash residue from combustion of CCA treated wood waste before and after electrodialytic extraction, Chemosphere. 65 (2006) 110–116. https://doi.org/10.1016/j.chemosphere.2006.02.021.

[27] P.E. Jensen, L.M. Ottosen, H.K. Hansen, S. Bollwerk, L.J. Belmonte, G.M. Kirkelund, Suspended electrodialytic extraction of toxic elements for detoxification of three different mine tailings, International Journal of Sustainable Development and Planning. 11 (2016) 119–127. https://doi.org/10.2495/SDP-V11-N2-119-127.

[28] R. Parés Viader, P.E. Jensen, L.M. Ottosen, J. Ahrenfeldt, H. Hauggaard-Nielsen, Electrodialytic extraction of phosphorus from ash of low-temperature gasification of sewage sludge, Electrochimica Acta. 181 (2015) 100–108. https://doi.org/10.1016/j.electacta.2015.05.025.

[29] A.J. Pedersen, Characterization and electrodialytic treatment of wood combustion fly ash for the removal of cadmium, Biomass and Bioenergy. 25 (2003) 447–458. https://doi.org/10.1016/S0961-9534(03)00051-5.

[30] P.E. Jensen, L.M. Ottosen, C. Ferreira, Electrodialytic remediation of soil fines (<63 μm) in suspension-Influence of current strength and L/S, Electrochimica Acta. 52 (2007) 3412–3419. https://doi.org/10.1016/j.electacta.2006.03.116.

[31] L.M. Ottosen, A.T. Lima, A.J. Pedersen, A.B. Ribeiro, Electrodialytic extraction of Cu, Pb and Cl from municipal solid waste incineration fly ash suspended in water, Journal of Chemical Technology and Biotechnology. 81 (2006) 553–559. https://doi.org/10.1002/jctb.1424.

[32] G.M. Kirkelund, P.E. Jensen, L.M. Ottosen, Electrodialytic extraction of heavy metals from greenlandic MSWI Fly Ash as a function of remediation time and L/S ratio, in: ISCORD 2013: Planning for Sustainable Cold Regions - Proceedings of the 10th International Symposium on Cold Regions Development: American Society of Civil Engineers, 2013: pp. 87–96. https://doi.org/10.1061/9780784412978.009.

[33] A.J. Pedersen, L.M. Ottosen, A. Villumsen, Electrodialytic removal of heavy metals from different fly ashes: Influence of heavy metal speciation in the ashes, Journal of Hazardous Materials. 100 (2003) 65–78. https://doi.org/10.1016/S0304-3894(03)00064-5.

[34] R. Parés Viader, P.E. Jensen, L.M. Ottosen, Electrodialytic remediation of municipal solid waste incineration residues using different membranes, Chemosphere. 169 (2017) 62–68. https://doi.org/10.1016/j.chemosphere.2016.11.047.

[35] A.J. Pedersen, Evaluation of assisting agents for electrodialytic removal of Cd, Pb, Zn, Cu and Cr from MSWI fly ash, Journal of Hazardous Materials. 95 (2002) 185–198. https://doi.org/10.1016/S0304-3894(02)00138-3.

[36] G. Marie, P. Erland, M. Lisbeth, B. Alexandra, Comparison of two experimental set-ups for electrodialytic removal of heavy metals and Cl from MSWI APC residues, (2014).

[37] G.M. Kirkelund, C. Magro, P. Guedes, P.E. Jensen, A.B. Ribeiro, L.M. Ottosen, Electrodialytic removal of heavy metals and chloride from municipal solid waste incineration fly ash and air pollution control residue in suspension - Test of a new two compartment experimental cell, Electrochimica Acta. 181 (2015) 73–81. https://doi.org/10.1016/j.electacta.2015.03.192.

[38] G.M. Kirkelund, P.E. Jensen, L.M. Ottosen, K.B. Pedersen, Comparison of two- and three-compartment cells for electrodialytic removal of heavy metals from contaminated material suspensions, Journal of Hazardous Materials. 367 (2019) 68–76. https://doi.org/10.1016/j.jhazmat.2018.12.063.

[39] P.E. Jensen, C.M.D. Ferreira, H.K. Hansen, J.U. Rype, L.M. Ottosen, A. Villumsen, Electroremediation of air pollution control residues in a continuous reactor, Journal of Applied Electrochemistry. 40 (2010) 1173–1181. https://doi.org/10.1007/s10800-010-0090-1.

[40] P.E. Jensen, G.M. Kirkelund, K.B. Pedersen, C. Dias-Ferreira, L.M. Ottosen, Electrodialytic upgrading of three different municipal solid waste incineration residue types with focus on Cr, Pb, Zn, Mn, Mo, Sb, Se, V, Cl and SO4, Electrochimica Acta. 181 (2015) 167–178. https://doi.org/10.1016/j.electacta.2015.06.012.

[41] C. Dias-Ferreira, G.M. Kirkelund, P.E. Jensen, Mercury levels in fly ash and APC residue from municipal solid waste incineration before and after electrodialytic remediation, International Journal of Sustainable Development and Planning. 11 (2016) 672–682. https://doi.org/10.2495/SDP-V11-N5-672-682.

[42] G.M. Kirkelund, P.E. Jensen, A. Villumsen, L.M. Ottosen, Test of electrodialytic upgrading of MSWI APC residue in pilot scale: Focus on reduced metal and salt leaching, Journal of Applied Electrochemistry. 40 (2010) 1049–1060. https://doi.org/10.1007/s10800-009-0059-0.

[43] C. Dias-Ferreira, G.M. Kirkelund, P.E. Jensen, The influence of electrodialytic remediation on dioxin (PCDD/PCDF) levels in fly ash and air pollution control residues, Chemosphere. 148 (2016) 380–387. https://doi.org/10.1016/j.chemosphere.2016.01.061.

[44] J. Tang, B.-M. Steenari, Solvent extraction separation of copper and zinc from MSWI fly ash leachates, Waste Management. 44 (2015) 147–154. https://doi.org/10.1016/j.wasman.2015.07.028.

[45] K. Karlfeldt Fedje, C. Ekberg, G. Skarnemark, E. Pires, B.-M. Steenari, Initial studies of the recovery of Cu from MSWI fly ash leachates using solvent extraction, Waste Management and Research. 30 (2012) 1072–1080. https://doi.org/10.1177/0734242X12441385.

[46] V. Ramachandran, Recent advances in the solvent extraction of Cu, Ni, Co, Jom. 55 (2003) 23. https://doi.org/10.1007/s11837-003-0118-7.

[47] A. Rether, M. Schuster, Selective separation and recovery of heavy metal ions using water-soluble N-benzoylthiourea modified PAMAM polymers, Reactive and Functional Polymers. 57 (2003) 13–21. https://doi.org/10.1016/j.reactfunctpolym.2003.06.002.

[48] S. Schlumberger, M. Schuster, S. Ringmann, R. Koralewska, Recovery of high purity zinc from filter ash produced during the thermal treatment of waste and inerting of residual materials, Waste Management and Research. 25 (2007) 547–555. https://doi.org/10.1177/0734242X07079870.

[49] K.K. Fedje, C. Ekberg, G. Skarnemark, B.-M. Steenari, Removal of hazardous metals from MSW fly ash-An evaluation of ash leaching methods, Journal of Hazardous Materials. 173 (2010) 310–317. https://doi.org/10.1016/j.jhazmat.2009.08.094.

[50] J. Tang, B.-M. Steenari, Arie, Leaching optimization of municipal solid waste incineration ash for resource recovery : A case study of Cu , Zn , Pb and Cd, Waste Management. 48 (2016) 315–322. https://doi.org/10.1016/j.wasman.2015.10.003.

[51] H. Lassesson, K.K. Fedje, B.-M. Steenari, Leaching for recovery of copper from municipal solid waste incineration fly ash: Influence of ash properties and metal speciation, Waste Management and Research. 32 (2014) 755–762. https://doi.org/10.1177/0734242X14542147.

[52] M. Petranikova, C. Ekberg, J. Tang, R. Ylm, Comparative study of the application of traditional and novel extractants for the separation of metals from MSWI fly ash leachates, 172 (2018) 143–154. https://doi.org/10.1016/j.jclepro.2017.10.152.

[53] J. Rydberg, M. Cox, C. Musikas, G.R. Choppin, Solvent Extraction Principles and Practice, Second Edi, Marcel Dekker, Inc., 2004.

[54] D.S. Flett, Solvent extraction in hydrometallurgy: The role of organophosphorus extractants, Journal of Organometallic Chemistry. 690 (2005) 2426–2438. https://doi.org/10.1016/j.jorganchem.2004.11.037.

[55] J. Tang, M. Petranikova, C. Ekberg, B.-M. Steenari, Mixer-settler system for the recovery of copper and zinc from MSWI fly ash leachates: An evaluation of a hydrometallurgical process, Journal of Cleaner Production. 148 (2017) 595–605. https://doi.org/10.1016/j.jclepro.2017.02.015.

[56] W.J. Huang, S.C. Chu, A study on the cementlike properties of municipal waste incineration ashes, Cement and Concrete Research. 33 (2003) 1795–1799. https://doi.org/10.1016/S0008-8846(03)00203-5.

[57] H. Hou, X. He, S. Zhu, D. Zhang, H. Haobo, H. Xinghua, Z. Shujing, Z. Dajie, The cement solidification of municipal solid waste incineration fly ash, Journal of Wuhan University of Technology-Mater. Sci. Ed. 21 (2008) 137–140. https://doi.org/10.1007/bf02841224.

[58] R. Bie, P. Chen, X. Song, X. Ji, Characteristics of municipal solid waste incineration fly ash with cement solidification treatment, Journal of the Energy Institute. 89 (2016) 704–712. https://doi.org/10.1016/j.joei.2015.04.006.

[59] Q.Y. Chen, M. Tyrer, C.D. Hills, X.M. Yang, P. Carey, Immobilisation of heavy metal in cement-based solidification/stabilisation: A review, Waste Management. 29 (2009) 390–403. https://doi.org/10.1016/j.wasman.2008.01.019.

[60] T. Matschei, B. Lothenbach, F.P. Glasser, G. le Saout, E. Gallucci, K. Scrivener, K. de Weerdt, M. ben Haha, G. le Saout, K.O. Kjellsen, H. Justnes, B. Lothenbach, M. Zajac, A. Rossberg, G. le Saout, B. Lothenbach, H. sheng Shi, L. li Kan, T. Mangialardi, A.E. Paolini, A. Polettini, P. Sirini, R. Pomi, P. Sirini, F. Testa, G. Kakali, S. Tsivilis, E. Aggeli, M. Bati, Properties of Portland cement - Stabilised MSWI fly ashes, Cement and Concrete Research. 23 (2009) 2160–2166. https://doi.org/10.1016/j.conbuildmat.2008.12.016.

[61] A. Polettini, R. Pomi, P. Sirini, Fractional factorial design to investigate the influence of heavy metals and anions on acid neutralization behavior of cement-based products, Environmental Science and Technology. 36 (2002) 1584–1591. https://doi.org/10.1021/es010002z.

[62] G.X. Wei, H.Q. Liu, S.G. Zhang, Using of Different Type Cement in Solidification/Stabilization of MSWI Fly Ash, Advanced Materials Research. 291–294 (2011) 1870–1874. https://doi.org/10.4028/www.scientific.net/amr.291-294.1870.

[63] T. Mangialardi, A.E. Paolini, A. Polettini, P. Sirini, Optimization of the solidification/stabilization process of MSW fly ash in cementitious matrices, Journal of Hazardous Materials. 70 (1999) 53–70. https://doi.org/10.1016/S0304-3894(99)00132-6.

[64] X. Wang, A. Li, Z. Zhang, The Effects of Water Washing on Cement-based Stabilization of MWSI Fly Ash, Procedia Environmental Sciences. 31 (2016) 440–446. https://doi.org/10.1016/j.proenv.2016.02.095.

[65] Q. Xue, J. Li, Z. Hu, Compound stabilization/solidification of MSWI fly ash with trimercapto-s-triazine and cement, Water Science and Technology. 66 (2012) 689–694. https://doi.org/10.2166/wst.2012.226.

[66] Y. Su, J. Yang, D. Liu, S. Zhen, N. Lin, Y. Zhou, Effects of municipal solid waste incineration fly ash on solidification/stabilization of Cd and Pb by magnesium potassium phosphate cement, Journal of Environmental Chemical Engineering. 4 (2016) 259–265. https://doi.org/10.1016/j.jece.2015.11.025.

[67] L. Chen, L. Wang, D.W. Cho, D.C.W. Tsang, L. Tong, Y. Zhou, J. Yang, Q. Hu, C.S. Poon, Sustainable stabilization/solidification of municipal solid waste incinerator fly ash by incorporation of green materials, Journal of Cleaner Production. 222 (2019) 335–343. https://doi.org/10.1016/j.jclepro.2019.03.057.

[68] H. sheng Shi, L. li Kan, Characteristics of municipal solid wastes incineration (MSWI) fly ash-cement matrices and effect of mineral admixtures on composite system, Construction and Building Materials. 23 (2009) 2160–2166. https://doi.org/10.1016/j.conbuildmat.2008.12.016.

[69] X. Li, Z. Yu, B. Ma, B. Wu, Effect of MSWI fly ash and incineration residues on cement performances, Journal Wuhan University of Technology, Materials Science Edition. 25 (2010) 312–315. https://doi.org/10.1007/s11595-010-2312-0.

[70] J. Kim, J. An, B.H. Nam, K.M. Tasneem, Investigation on the side effects of municipal solid waste incineration ashes when used as mineral addition in cement-based material, Road Materials and Pavement Design. 17 (2016) 345–364. https://doi.org/10.1080/14680629.2015.1083463.

[71] L. Kan, L. Zhang, H. Shi, Hydration Kinetics of Municipal Solid Wastes Incineration (MSWI) Fly Ash-Cement, Journal Wuhan University of Technology, Materials Science Edition. 34 (2019) 596–603. https://doi.org/10.1007/s11595-019-2093-z.

[72] S. Remond, P. Pimienta, D.P.P. Bentz, S. Rémond, D.P.P. Bentz, P. Pimienta, Effects of the incorporation of Municipal Solid Waste Incineration fly ash in cement pastes and mortars I. Experimental study, Cement and Concrete Research. 32 (2002) 303–311. https://doi.org/10.3130/jaabe.3.1.

[73] J.E. Aubert, B. Husson, A. Vaquier, Metallic aluminum in MSWI fly ash: Quantification and influence on the properties of cement-based products, Waste Management. 24 (2004) 589–596. https://doi.org/10.1016/j.wasman.2004.01.005.

[74] T. MANGIALARDI, L. PIGA, G. SCHENA, P. SIRINI, Characteristics of MSW Incinerator Ash for Use in Concrete, Environmental Engineering Science. 15 (2009) 291–297. https://doi.org/10.1089/ees.1998.15.291.

[75] L. Bertolini, M. Carsana, D. Cassago, A.Q. Curzio, M. Collepardi, MSWI ashes as mineral additions in concrete, Cement and Concrete Research. 34 (2004) 1899–1906. https://doi.org/10.1016/j.cemconres.2004.02.001.

[76] Z. Yang, R. Ji, L. Liu, X. Wang, Z. Zhang, Recycling of municipal solid waste incineration by-product for cement composites preparation, Construction and Building Materials. 162 (2018) 794–801. https://doi.org/10.1016/j.conbuildmat.2017.12.081.

[77] X. Gao, W. Wang, T. Ye, F. Wang, Y. Lan, Utilization of washed MSWI fly ash as partial cement substitute with the addition of dithiocarbamic chelate, Journal of Environmental Management. 88 (2008) 293–299. https://doi.org/10.1016/j.jenvman.2007.02.008.

[78] T.C. Lee, Z.S. Li, Conditioned MSWI ash-slag-mix as a replacement for cement in cement mortar, Construction and Building Materials. 24 (2010) 970–979. https://doi.org/10.1016/j.conbuildmat.2009.11.021.

[79] T.C. Lee, W.J. Wang, P.Y. Shih, K.L. Lin, Enhancement in early strengths of slag-cement mortars by adjusting basicity of the slag prepared from fly-ash of MSWI, Cement and Concrete Research. 39 (2009) 651–658. https://doi.org/10.1016/j.cemconres.2009.02.005.

[80] K.S. Wang, K.L. Lin, Z.Q. Huang, Hydraulic activity of municipal solid waste incinerator fly-ash-slag-blended eco-cement, Cement and Concrete Research. 31 (2001) 97–103. https://doi.org/10.1016/S0008-8846(00)00423-3.

[81] K.-L. Lin, D.F. Lin, W.J. Wang, C.C. Chang, T.C. Lee, Pozzolanic reaction of a mortar made with cement and slag vitrified from a MSWI ash-mix and LED sludge, Construction and Building Materials. 64 (2014) 277–287. https://doi.org/10.1016/j.conbuildmat.2014.04.088.

[82] T.C. Lee, M.K. Rao, Recycling municipal incinerator fly- and scrubber-ash into fused slag for the substantial replacement of cement in cement-mortars, Waste Management. 29 (2009) 1952–1959. https://doi.org/10.1016/j.wasman.2009.01.002.

[83] T.C. Lee, W.J. Wang, P.Y. Shih, Slag-cement mortar made with cement and slag vitrified from MSWI fly-ash/scrubber-ash and glass frit, Construction and Building Materials. 22 (2008) 1914–1921. https://doi.org/10.1016/j.conbuildmat.2007.07.030.

[84] S. Rémond, D.P. Bentz, P. Pimienta, Effects of the incorporation of Municipal Solid Waste Incineration fly ash in cement pastes and mortars - II: Modeling, Cement and Concrete Research. 32 (2002) 565–576. https://doi.org/10.1016/S0008-8846(01)00722-0.

[85] M. Keppert, J.A. Siddique, Z. Pavlík, R. Černý, Wet-Treated MSWI Fly Ash Used as Supplementary Cementitious Material, Advances in Materials Science and Engineering. 2015 (2015). https://doi.org/10.1155/2015/842807.

[86] Z. Chen, S. Lu, M. Tang, J. Ding, A. Buekens, J. Yang, Q. Qiu, J. Yan, Mechanical activation of fly ash from MSWI for utilization in cementitious materials, Waste Management. 88 (2019) 182–190. https://doi.org/10.1016/j.wasman.2019.03.045.

[87] T. Lenormand, E. Rozière, A. Loukili, S. Staquet, Incorporation of treated municipal solid waste incineration electrostatic precipitator fly ash as partial replacement of Portland cement: Effect on early age behaviour and mechanical properties, Construction and Building Materials. 96 (2015) 256–269. https://doi.org/10.1016/j.conbuildmat.2015.07.171.

[88] S. Wan, X. Zhou, M. Zhou, Y. Han, Y. Chen, J. Geng, T. Wang, S. Xu, Z.D. Qiu, H. Hou, Hydration characteristics and modeling of ternary system of municipal solid wastes incineration fly ash-blast furnace slag-cement, Construction and Building Materials. 180 (2018) 154–166. https://doi.org/10.1016/j.conbuildmat.2018.05.277.

[89] P.Y. Shih, P.H. Lee, K.J. Nian, T.C. Lee, Characterization of a mortar made with cement and slag vitrified from a MSWI ash-mix and CMP sludge, Construction and Building Materials. 38 (2013) 22–30. https://doi.org/10.1016/j.conbuildmat.2012.07.083.

[90] T.C. Lee, C.J. Chang, M.K. Rao, X.W. Su, Modified MSWI ash-mix slag for use in cement concrete, Construction and Building Materials. 25 (2011) 1513–1520. https://doi.org/10.1016/j.conbuildmat.2010.08.007.

[91] T.C. Lee, Recycling of municipal incinerator fly-ash slag and semiconductor waste sludge as admixtures in cement mortar, Construction and Building Materials. 23 (2009) 3305–3311. https://doi.org/10.1016/j.conbuildmat.2009.06.043.

[92] K.-L. Lin, D.-F. Lin, S.-J. Chao, Effects of Municipal Solid Waste Incinerator Fly Ash Slag on the Strength and Porosity of Slag-Blended Cement Pastes, Environmental Engineering Science. 26 (2009) 1081–1086. https://doi.org/10.1089/ees.2008.0258.

[93] K.-L. Lin, The influence of municipal solid waste incinerator fly ash slag blended in cement pastes, Cement and Concrete Research. 35 (2005) 979–986. https://doi.org/10.1016/j.cemconres.2004.06.011.

[94] K.L. Lin, K.S. Wang, B.Y. Tzeng, C.Y. Lin, The reuse of municipal solid waste incinerator fly ash slag as a cement substitute, Resources, Conservation and Recycling. 39 (2003) 315–324. https://doi.org/10.1016/S0921-3449(02)00172-6.

[95] J.E. Aubert, B. Husson, A. Vaquier, Use of municipal solid waste incineration fly ash in concrete, Cement and Concrete Research. 34 (2004) 957–963. https://doi.org/10.1016/j.cemconres.2003.11.002.

[96] J.E. Aubert, B. Husson, N. Sarramone, Utilization of municipal solid waste incineration (MSWI) fly ash in blended cement. Part 1: Processing and characterization of MSWI fly ash, Journal of Hazardous Materials. 136 (2006) 624–631. https://doi.org/10.1016/j.jhazmat.2005.12.041.

[97] J.E. Aubert, B. Husson, N. Sarramone, Utilization of municipal solid waste incineration (MSWI) fly ash in blended cement. Part 2. Mechanical strength of mortars and environmental impact, Journal of Hazardous Materials. 146 (2007) 12–19. https://doi.org/10.1016/j.jhazmat.2006.11.044.

[98] DS/EN 196-1: Methods of testing cement – Part 1: Determination of strength, Dansk Standard, 2005.

[99] DS/EN 12457-1: Characterisation of waste - Leaching - Compliance test for leaching of granular waste materials and sludges - Part 1: One stage batch test at a liquid to solid ratio of 2 l/kg for materials with high solid content and with particle size bel, Dansk Standard, 2002.

[100] DS/EN 196-5: Methods of testing cement - Part 5: Pozzolanicity test for pozzolanic cement, Dansk Standard, 2011.

[101] B. Lothenbach, D.A. Kulik, T. Matschei, M. Balonis, L. Baquerizo, B. Dilnesa, G.D. Miron, R.J. Myers, Cemdata18: A chemical thermodynamic database for hydrated Portland cements and alkali-activated materials, Cement and Concrete Research. 115 (2019) 472–506. https://doi.org/10.1016/j.cemconres.2018.04.018.

[102] B. Osbæck, The influence of Air content by Assessing the pozzolanidc activity of fly ash by strength testing, Cement and Concrete Research. 15 (1985) 53–64.

[103] DS/EN 1015-3: Methods of test for mortar for masonry - Part 3: Determination of consistence of fresh mortar (by flow table), Dansk Standard, 1999.

[104] T. van Gerven, J. Moors, V. Dutré, C. Vandecasteele, Effect of CO2 on leaching from a cement-stabilized MSWI fly ash, Cement and Concrete Research. 34 (2004) 1103–1109. https://doi.org/10.1016/j.cemconres.2003.11.022.

[105] M. Andac, F.P. Glasser, The effect of test conditions on the leaching of stabilised MSWI-fly ash in Portland cement, Waste Management. 18 (1998) 309–319. https://doi.org/10.1016/S0956-053X(98)00041-5.

[106] T. van Gerven, D. van Baelen, V. Dutré, C. Vandecasteele, Influence of carbonation and carbonation methods on leaching of metals from mortars, Cement and Concrete Research. 34 (2004) 149–156. https://doi.org/10.1016/S0008-8846(03)00255-2.

[107] R. Malviya, R. Chaudhary, Evaluation of leaching characteristics and environmental compatibility of solidified/stabilized industrial waste, Journal of Material Cycles and Waste Management. 8 (2006) 78–87. https://doi.org/10.1007/s10163-005-0139-0.

[108] V. Dutre, C. Vandecasteele, An Evaluation of the Solidification/Stabilisation of Industrial Arsenic containing waste using extraction and semi-dynamic leach tests, Science. 16 (1997) 625–631.

[109] B.A.R. Ebert, B.-M. Steenari, M.R. Geiker, G.M. Kirkelund, Screening of untreated municipal solid waste incineration fly ash for use in cement-based materials: chemical and physical properties, SN Applied Sciences. 2 (2020). https://doi.org/10.1007/s42452-020-2613-7.

[110] B.A.R. Ebert, G.M. Kirkelund, "UNDER REVIEW" Effects of chlorides and sulphates on leaching from mortar with raw and electrodialytically treated MSWI fly ash, Journal of Hazardous Materials. (2021).

[111] DS/EN 450-1: Fly ash for concrete - Part 1: Definition, Specification and conformity criteria, Dansk Standard, 2012.

[112] P. Ni, H. Li, Y. Zhao, J. Zhang, C. Zheng, Relation between leaching characteristics of heavy metals and physical properties of fly ashes from typical municipal solid waste incinerators, Environmental Technology. 38 (2017) 2105–2118. https://doi.org/10.1080/09593330.2016.1246612.

[113] Q. Qiu, X. Jiang, Z. Chen, S. Lu, M. Ni, Microwave-Assisted Hydrothermal Treatment with Soluble Phosphate Added for Heavy Metals Solidification in MSWI Fly Ash, Energy and Fuels. 31 (2017) 5222–5232. https://doi.org/10.1021/acs.energyfuels.6b02516.

[114] W. Li, Y. Sun, Y. Huang, T. Shimaoka, H. Wang, Y. nan Wang, L. Ma, D. Zhang, Evaluation of chemical speciation and environmental risk levels of heavy metals during varied acid corrosion conditions for raw and solidified/stabilized MSWI fly ash, Waste Management. 87 (2019) 407–416. https://doi.org/10.1016/j.wasman.2019.02.033.

[115] Y. Mu, A. Saffarzadeh, T. Shimaoka, Influence of ignition of waste fishbone on enhancing heavy metal stabilization in municipal solid waste incineration (MSWI) fly ash, Journal of Cleaner Production. 189 (2018) 396–405. https://doi.org/10.1016/j.jclepro.2018.03.301.

[116] H. Kitamura, A.V. Dahlan, Y. Tian, T. Shimaoka, T. Yamamoto, F. Takahashi, Intra- and inter-particle heterogeneity of municipal solid waste incineration fly ash particles, Journal of Material Cycles and Waste Management. (2019) 925–941. https://doi.org/10.1007/s10163-019-00853-1.

[117] W. Ma, D. Chen, M. Pan, T. Gu, L. Zhong, G. Chen, B. Yan, Z. Cheng, Performance of chemical chelating agent stabilization and cement solidification on heavy metals in MSWI fly ash: A comparative study, Journal of Environmental Management. 247 (2019) 169–177. https://doi.org/10.1016/j.jenvman.2019.06.089.

[118] F. Zhu, Y. Xiong, Y. Wang, X. Wei, X. Zhu, F. Yan, Heavy metal behavior in "Washing-Calcination-Changing with Bottom Ash" system for Recycling of Four Types of Fly Ashes, Waste Management. 75 (2018) 215–225. https://doi.org/10.1016/j.wasman.2018.01.032.

[119] A. de Boom, J. Aubert, M. Degrez, Carbonation of municipal solid waste incineration electrostatic precipitator fly ashes in solution, (2014). https://doi.org/10.1177/0734242X14527637.

[120] G. Marie, P. Erland, Characterization of particulate residues from greenlandic mswi for use as secondary resources, (2016).

[121] G. Weibel, U. Eggenberger, S. Schlumberger, U.K. Mäder, Chemical associations and mobilization of heavy metals in fly ash from municipal solid waste incineration, Waste Management. 62 (2017) 147–159. https://doi.org/10.1016/j.wasman.2016.12.004.

[122] A.P. Bayuseno, W.W. Schmahl, T. Müllejans, Hydrothermal processing of MSWI Fly Ash-towards new stable minerals and fixation of heavy metals, 167 (2009) 250–259. https://doi.org/10.1016/j.jhazmat.2008.12.119.

[123] J.M. Chimenos, A.I. Ferna, Optimizing the APC residue washing process to minimize the release of chloride and heavy metals, 25 (2005) 686–693. https://doi.org/10.1016/j.wasman.2004.12.014.

[124] F. Liu, J. Liu, Q. Yu, Y. Jin, Y. Nie, F. Liu, J. Liu, Q. Yu, Y. Jin, Leaching Characteristics of Heavy Metals in Municipal Solid Waste Incinerator Fly Ash, Journal of Environmental Science and Health. 4529 (2005) 1975–1985. https://doi.org/10.1080/10934520500184707.

[125] L. Wang, R.-D. Li, L. Wei, Y. Li, Accelerated Carbonation of Municipal Solid Waste Incineration Fly Ash Using CO 2 as an Acidic Agent for Clinker Production, Environmental Engineering Science. 29 (2012) 677–684. https://doi.org/10.1089/ees.2011.0272.

[126] Z. Chen, S. Lu, Q. Mao, A. Buekens, W. Chang, X. Wang, Suppressing Heavy Metal Leaching through Ball Milling of Fly Ash, Energies. 9 (2016) 1–13. https://doi.org/10.3390/en9070524.

[127] Y.J. Park, Stabilization of a chlorine-rich fly ash by colloidal silica solution, 162 (2009) 819–822. https://doi.org/10.1016/j.jhazmat.2008.05.143.

[128] L. Zheng, W. Wang, Y. Shi, Chemosphere The effects of alkaline dosage and Si / Al ratio on the immobilization of heavy metals in municipal solid waste incineration fly ash-based geopolymer, Chemosphere. 79 (2010) 665–671. https://doi.org/10.1016/j.chemosphere.2010.02.018.

[129] M.L.D. Jayaranjan, E.D. van Hullebusch, A.P. Annachhatre, Reuse options for coal fired power plant bottom ash and fly ash, Reviews in Environmental Science and Biotechnology. 13 (2014) 467–486. https://doi.org/10.1007/s11157-014-9336-4.

[130] B.A.R. Ebert, W. Kunther, M.R. Geiker, G.M. Kirkelund, "UNDER REVIEW" Impact of Electrodialytic Remediation of MSWI Fly Ash on Hydration and Mechanical Properties of Blended Binders, Construction and Building Materials. (2021).

[131] Appendix 1: The Landfill Directive Council Directive 199/31/EC, 1999.

[132] P. Pedeferri, Pourbaix Diagrams, in: S.N. Switzerland (Ed.), Corrosion Science and Engineering, 2018: pp. 57–72. https://doi.org/10.1007/978-3-319-97625-9_4.

[133] D. Brookins, Geochemical Behaviour of Antimony, Arsenic, Camium and Thallium: E h - p H Diagrams for 25°C, 1-Bar Pressure, Chemical Geology. (1986) 271–278.

[134] G. Weibel, U. Eggenberger, D.A. Kulik, W. Hummel, S. Schlumberger, W. Klink, M. Fisch, U.K. Mäder, Extraction of heavy metals from MSWI fly ash using hydrochloric acid and sodium chloride solution, Waste Management. 76 (2018) 457–471. https://doi.org/10.1016/j.wasman.2018.03.022.

[135] A.E. Martell, R.M. Smith, Critical Stability Constants Volume 4: Inorganic Complexes, Springer Science + Business Media, LLC, 1976.

[136] R. Eisted, T.H. Christensen, Waste management in Greenland: Current situation and challenges, Waste Management and Research. 29 (2011) 1064–1070. https://doi.org/10.1177/0734242X10395421.

[137] B. Lothenbach, K. Scrivener, R.D. Hooton, Supplementary cementitious materials, Cement and Concrete Research. 41 (2011) 1244–1256. https://doi.org/10.1016/j.cemconres.2010.12.001.

[138] B.A.R. Ebert, B.-M. Steenari, M.R. Geiker, G.M. Kirkelund, THE EFFECT OF MSWI FLY ASH ON MORTAR WORKABILITY, in: ternational Conference on Sustainable Materials, Systems and Structures (SMSS 2019) New Generation of Construction Materials, 2019: pp. 180–186.

[139] R. Argane, M. Benzaazoua, R. Hakkou, A. Bouamrane, A comparative study on the practical use of low sulfide base-metal tailings as aggregates for rendering and masonry mortars, Journal of Cleaner Production. 112 (2016) 914–925. https://doi.org/10.1016/j.jclepro.2015.06.004.

[140] W. Müllauer, R.E. Beddoe, D. Heinz, Effect of carbonation, chloride and external sulphates on the leaching behaviour of major and trace elements from concrete, Cement

and Concrete Composites. 34 (2012) 618–626. https://doi.org/10.1016/j.cemconcomp.2012.02.002.

[141] N. Quijorna, A. Coz, A. Andres, C. Cheeseman, Recycling of Waelz slag and waste foundry sand in red clay bricks, Resources, Conservation and Recycling. 65 (2012) 1–10. https://doi.org/10.1016/j.resconrec.2012.05.004.

[142] Miljøministeriet, Bekendtgørelse om anvendelse af restprodukter og jord til bygge- og anlægsarbejder og om anvendelse af sorteret, uforurenet bygge- og anlægsaffald, 2010. https://www.retsinformation.dk/Forms/R0710.aspx?id=134831.

[143] K. G. Dunn, Process Improvements using Data, (2019). Learnch.mcmaster.ca/pid

[144] J. Tang, Removal and Recovery of Metals from Municipal Solid Waste Incineration Ashes by a Hydrometallurgical Process, 2017.

[145] D.A. Kulik, Improving the structural consistency of C-S-H solid solution thermodynamic models, Cement and Concrete Research. 41 (2011) 477–495. https://doi.org/10.1016/j.cemconres.2011.01.012.

Part IV
Appended Papers

Journal Paper I

Screening of untreated Municipal solid waste incineration fly ash for use in cement-based Material

Benjamin A. R. Ebert, Britt-Marie Steenari, Mette R. Geiker, Gunvor M. Kirkelund

Research Article

Screening of untreated municipal solid waste incineration fly ash for use in cement-based materials: chemical and physical properties

Benjamin A. R. Ebert[1] · Britt-Marie Steenari[2] · Mette R. Geiker[3] · Gunvor M. Kirkelund[1]

Received: 12 October 2019 / Accepted: 26 March 2020

Abstract
The environmental impact during concrete manufacturing can be reduced by using less cement or using types of cement with high amounts of secondary cementitious materials (SCMs) and fillers. Fly ash from municipal solid waste incineration (MSWI) is an unused material, which could potentially be used as an SCM or filler. The applicability of MSWI fly ash samples in cement-based materials was investigated through an indirect determination based on the chemical composition, toxic metal content and particle size distribution of the samples. Furthermore, how the samples compared to each other and how representative the samples were for MSWI fly ash, in general, were investigated by multivariate modelling. MSWI fly ash samples were obtained from Denmark, Sweden and Greenland. Comparing the chemical composition of the MSWI fly ash samples with the chemical requirements for coal fly ash to be used in concrete, specified in EN 450-1 2012, indicated a low potential as SCMs. Additionally, the MSWI fly ash contained and leached more toxic metals than the allowed limits. The particle size distributions were larger than cement and indicated limited potential as filler. A principal component analysis showed that the obtained samples were chemically different materials compared to each other and would have different effects if used in cement-based materials. Additionally, the samples from Denmark were unrepresentative of MSWI fly ash, while the Greenlandic and Swedish samples were comparable to previously studied MSWI fly ash samples.

Keywords Screening · Characterization · MSWI fly ash · Cement · Multivariate modelling

1 Introduction

Construction of new buildings and infrastructure consume large quantities of humanmade goods and raw materials, greatly impacting the environment and the sustainability of the construction industry. In 2016, the production of cement contributed to 8% of the global anthropogenic CO_2 emissions [1].

The environmental impact related to construction with cementitious materials, e.g. concrete, can be reduced by using less cement, and replacing Portland cement clinker with secondary cementitious materials (SCMs) [2] or fillers. However, limited availability of traditionally used SCMs such as ground granulated blast furnace slag and fly ash from coal incineration calls for the identification of new resources [3].

Several countries have in the past decades introduced changes to their municipal solid waste disposal, such as increased material recycling from the waste and waste incineration. However, incineration of municipal solid waste results in several by-products classified as hazardous materials [4]. It has been proposed that MSWI fly ash from waste incineration could be used in concrete as an SCM [5]. The high pH in Portland cement-based materials results in chemical binding of the toxic metals, reducing short term leaching [6]. However, later reduced pH due

✉ Benjamin A. R. Ebert, bareb@byg.dtu.dk | [1]Department of Civil Engineering, Technical University of Denmark, Kgs. Lyngby, Denmark. [2]Chemistry and Chemical Engineering, Chalmers University of Technology, Gothenburg, Sweden. [3]Department of Structural Engineering, Norwegian University of Science and Technology, Trondheim, Norway.

Published online: 03 April 2020

to, e.g. carbonation is likely to cause a release of the toxic metals.

Previous research on the utilisation of MSWI fly ash has evaluated the potential of the ashes as SCMs through direct methods, analysing the properties of cement-based materials made with MSWI fly ash [7–9]. The present study aimed at evaluating if samples of MSWI fly ash could be used as SCMs or filler in cement-based materials through an indirect determination. The indirect determination was performed by comparing the chemical properties of the samples with the chemical requirements in EN 450-1 2012 [10], evaluating the toxic metal content and by analysing the samples potential as filler materials, based on the particle size requirements presented by Moosberg-Bustnes et al. [11] and Scrivener et al. [12]. Furthermore, the present study evaluated how the samples compared to each other and previously studied MSWI fly ash samples based on their oxide and toxic metal content. Moreover, the influence of the type of furnace and flue gas filter used during waste incineration on the oxide and toxic metal content was evaluated. A principal component analysis (PCA) was used for this. A PCA is a multivariate statistical method that visualises the differences and similarities in large data sets [13]. Researchers have previously used PCA and other multivariate statistical methods when studying clustering trends and the most important characterisation properties in e.g. harbour sediments [13] and biomass ash [14, 15].

2 Methodology

2.1 Materials

Five MSWI fly ash samples were obtained from commercial MSW incineration heat and power plants. Two samples, designated Arc-Fa1 and Arc-Fa2, were obtained from Amager Bakke, Denmark, in early 2018 and late 2018 respectively. Two samples were collected from the incinerator in Nuuk, Greenland, designated Nuuk-Fa1 and Nuuk-Fa2, in 2017 and 2018 respectively. The final ash sample was obtained from Ryaverket in Sweden, designated Rya-Fa, in mid-2018. The five MSWI fly ash samples were sampled on-site by the operators. Information about the three incinerators is included in Table 1. The fly ash samples from Amager Bakke and Nuuk were extracted before any flue gas treatment, while the sample Rya-Fa was extracted after flue gas treatment with lime and active carbon.

2.2 Characterisation methods

The samples included in the evaluation were dried at 50 °C. Each analysis was made in triplicate, apart from the XRF and XRD analyses that were performed once.

2.2.1 Particle size distribution

The particle size distributions of the five MSWI fly ash samples were measured with a Malvern Mastersizer 2000 particle size analyser. The measurements were performed in a dry state, instead of as a wet slurry. CEM I 52.5 N (MS/LA/≤ 2) cement with a bulk and absolute density of 1.1 and 3.2 g/cm^3 was used for comparison between cement and the five MSWI fly ash samples. A Malvern Mastersizer 2000 determines the particle size distribution based on light scattering from spherical particles using Mie Theory [16].

2.2.2 Loss on ignition

Loss on ignition (LOI) was measured as the mass loss at 950 °C using a muffle furnace, equipped with temperature controls. Five gram of ash was ignited, in uncovered crucibles for 24 h, and subsequently cooled in a desiccator, ensuring that constant sample mass had been achieved.

2.2.3 pH and conductivity

The pH and conductivity of the ashes were measured on samples suspended in distilled water. Plastic bottles containing 5 g of ash and 12.5 ml distilled water (L/S 2.5) were shaken for an hour at 195 rpm. The pH and conductivity

Table 1 Average operating conditions of incineration plants during sampling

	Amager Bakke	Nuuk incineration	Ryaverket
Furnace	Grate fired	Grate fired	Fluidised bed
Incineration temp. (°C)	1025	1064	900
Waste type	Household/industrial	Household/construction	Household/industrial
Boiler ash separation	Gravitation	Gravitation/cyclone	Gravitation/cyclone
Flue gas filter type	Electrostatic	Electrostatic	Textile
Incineration capacity (ton/day)	1680	40	300
Fly ash (ton/day)	14.8	0.3	8.9
Bottom ash (ton/day)	237	4.7	17.8

were afterwards measured with a Radiometer analytical electrode and conductivity meter, respectively.

2.2.4 Water-soluble fraction

The weight percentage of the water-soluble fraction was measured at L/S 5 after three consecutive washings. The procedure used was the same as the L:S 3 × 5 washing procedure described in [17] by Chen et al. A 100 g of ash was mixed with 500 ml distilled water in an Erlenmeyer flask and shaken manually. The liquid phase was decanted through a Frisenette type 1125 filter, repeating for each wash. The entire sample was filtered and dried at 50 °C, after the third washing until a constant mass had been achieved.

2.2.5 Water-soluble anion content and batch leaching

The content of water-soluble anions was measured with Ion Chromatography (IC). Ten gram of ash was mixed with 25 ml distilled water (L/S 2.5) in 50 ml bottles and shaken for 12 h at 195 rpm. The liquid phase was extracted with a 0.45 µm filter syringe, and the content of Cl^- and SO_4^{2-} measured. A batch leaching test was performed to determine the leaching of Cd, Cr, Cu, Pb and Zn from the five MSWI fly ash samples as well as their content of water-soluble Ca, Na and K. The test was performed by mixing 40 g of ash with 80 ml distilled water (L/S 2). The mixture was shaken for 24 h at 195 rpm and then filtered using 0.45 µm syringe filters. The leached elements were measured using Inductively Coupled Plasma—Optical Emission Spectrometry (ICP-OES). The batch leaching test was performed according to EN 12457-1 [18].

2.2.6 Element content analysis

The elemental content of the five MSWI fly ash samples was determined using X-ray fluorescence (XRF) and ICP-OES analysis. The elements analysed with XRF were Si, Al, Fe, Ca, Mg, Na, K, S, Cl and P. The analysis was performed by an external laboratory using a SPECTRO Gmbh X-LAB 2000 with a Pd-tube on ash samples ground to a particle size below 200 µm. Based on the XRF analysis, the equivalent content of oxides was calculated for comparison with EN 450-1 2012 [10]. The elements analysed with ICP-OES were Cd, Cr, Cu, Pb and Zn. Samples for ICP-OES were prepared following the specifications of Danish Standard DS259 [19]. One gram of MSWI fly ash was mixed with 20 ml 7.3 M HNO_3 and heated at 120 °C and 200 kPa for 30 min. The liquid was then vacuum filtered through a 45-µm filter and diluted to 100 ml with distilled water and analysed with ICP-OES. The total content of Cd, Cr, Cu, Pb and Zn in the CEM I cement used during particle size measurements were analysed as well.

2.2.7 X-ray diffraction

X-ray diffraction (XRD) analysis was performed using a PanAlytical X'pert PRO Θ–Θ System, with a target metal anode made from Cu. Intensities were measured from 0° to 90°. Samples were pulverised in a mortar to increase the fineness and backloaded into sample holders. Peak and phase identification was performed using the ICDD PDF4 database. The detection limit of the XRD analysis was 2 wt%.

2.2.8 Thermogravimetric analysis

Thermogravimetric analysis (TGA) was performed using a NETZSCH STA 449 F3 Jupiter, fitted with a silicon carbide furnace and top-loading. Aluminium oxide sample holders were filled with approximately 35 mg of ash and heated to 29 °C. After 10 min at 29 °C, the temperature was raised to 900 °C, at 10 °C/min. Nitrogen was used as a purge gas, at a constant flow of 50 ml/min. The results of the analysis are included as the first derivative of the thermogravimetric mass loss (DTG).

2.3 Principal component analysis (PCA)

A principal component analysis (PCA) deals with possible collinearity between variables in a large data set [20]. Traditional statistical analysis, e.g. multiple regression analysis assumes that the variables of an observation are independent, potentially leading to biased results if the variables are correlated. A PCA can visualise the differences and similarities between observations by determining the principal components of the observations. A principal component is a vector that best explains the variance between observations. A PCA contains several principal components, each perpendicular to the previous. The 1st principal component accounts for the majority of the observations, while each subsequent principal component accounts for less. In this study, observations are referred to as the MSWI fly ash samples, variables as oxide composition and toxic metal content. Furnace and filter types are secondary input that characterises the samples.

The results of a PCA is given as loadings and scores. The principal component loadings are the weight of significance of the variables in the principal component vector and indicate if there is a positive or negative correlation between the variables. The principal component scores provide information on the individual observations with regard to their loadings. The scores are coordinates on the vector from the perpendicular projection of all points in the dataset. An observation's principal component score is

a linear combination of the observation's projected points, where the loadings are the weight of the projection. Each principal component has a series of loadings, equal to the number of variables, and scores equal to the number of observations. Combined plots of the loadings and the scores for two principal components provide information on how variables and observations correlate. Furthermore, similar observations (in the original dataset) will have similar scores.

2.3.1 Data compilation

Experimental data for the PCA covered MSWI fly ash samples from both the present study and literature [21–40]. The dataset for the PCA consisted of 51 MSWI fly ash samples and a coal fly ash, from Greenland, Europe and Asia. An MSWI fly ash sample was only included if the type of furnace and flue gas filter device of the incineration plant as well as the country of origin were specified in the reference. The composition of the incineration plant fuel was not considered due to inadequate reporting of the fuel composition in the literature.

The variables in the PCA were Al_2O_3, Fe_2O_3, SiO_2, CaO, MgO, Na_2O, K_2O, SO_3, Cl, Pb, Zn, Cu, Cr and Cd. Several references [22, 25, 27, 30, 31, 33, 36, 37, 39] reported elemental content instead of oxide content. The corresponding oxide content was calculated based on the reported elemental content. The furnace type of the included incineration plants was categorised as either a grate furnace or fluidised bed furnace. The flue gas filter was categorised as either an electrostatic precipitator (ESP) or a fabric filter. The PCA included, in addition to the samples from ESP or fabric filters, a cyclone and a boiler ash sample.

The PCA was performed using the statistical program Simca 14.1 by Sartorius Stedim Biotech. The PCA used standardised residual with R^2 specified as explained variance, as well as scaled and centred coefficients. Cross-validation was used when fitting with 7 cross-validation groups. A maximum of 200 iterations was used together with a missing data tolerance %(Var) of 5. The confidence level on parameters was set to 95%. The 1st, 2nd and 3rd principal components were used in the analysis and accounted for 67% of the variation in the dataset. The components each accounted for 34, 22 and 12% of the variance, respectively. The Q^2 of each component were 0.12, 0.13 and − 0.07, respectively.

Included in the analysis were the oxide composition and toxic metal content of a coal fly ash that fulfils the specifications of EN 450-1 2012 [10]. The oxide and toxic metal content of the coal fly ash were measured using the previously mentioned methods. The inclusion of the coal fly ash as an outlier in the PCA did not change the interpretation of the PCA results.

3 Results

3.1 Chemical properties

The calculated contents of oxides are shown in Table 2, together with the chloride content and LOI for the five MSWI fly ash samples. Included in Table 2 are the

Table 2 Calculated content of oxides (wt%) as well as Cl (wt%) and LOI (wt%)

	Arc-Fa1	Arc-Fa2	Nuuk-Fa1	Nuuk-Fa2	Rya-Fa	EN 450-1	MSWI [20–39]	Coal [42]
SiO_2	4.9	4.5	4.7	5.6	6.0	≥ 25	2.4–33.4	14.8–56.7
Al_2O_3	2.3	1.5	4.0	4.3	4.5	–	0.5–15.4	3.4–38.4
Fe_2O_3	1.1	1.0	0.7	0.8	1.7	–	0.3–9.1	0.86–9.7
Σ (SiO_2, Al_2O_3, Fe_2O_3)	8.3	7.0	9.4	10.7	12.2	≥ 70	4.0–56.0	19.1–97.6
CaO	21.0	13.4	33.6	40.6	40.6	≤ 1.5/10*	12.6–57.4	0.5–54.1
MgO	0.8	0.7	0.9	1.3	1.7	≤ 4.0	0.1–8.1	0.2–9.1
SO_3	22.5	35.0	7.7	8.2	8.7	≤ 3.0	2.2–20.5	0.2–22.1
K_2O	13.3	14.5	10.7	11.3	2.4	–	0.6–21.7	0.2–4.9
Na_2O	17.5	9.2	21.6	21.6	6.2	–	2.0–24.9	0.04–1.2
Na_2O_{eq}	26.3	18.7	28.6	29.0	7.8	≤ 5.0	1.5–38.6	0.2–4.5
P_2O_5	1.4	3.0	1.3	1.8	1.7	≤ 5.0	0.2–3.6	0.02–0.5
Cl	8.9	3.0	20.0	22.0	12.0	≤ 0.1	3.1–42.0	–
LOI	3.8	10.7	31.2	9.2	21.4	≤ 9.0**	–	1.8–8.2

Included are the requirements specified in En 450-1 as well as the composition of MSWI and Coal fly ash seen in the literature

*Free CaO limit/Reactive CaO limit

**Category C

requirements specified in EN 450-1 2012 [10] for using coal fly ash in cement-based materials, as well as the results found in other studies for MSWI fly ash [20–39] and coal fly ash [42]. The five MSWI fly ash samples evaluated in the present study only fulfilled the chemical requirements specified in EN 450-1 2012 [10], for MgO and P_2O_5. The five MSWI fly ash samples contained less SiO_2 than the limit of at least 25 wt% reactive SiO_2, regardless if the determined SiO_2 content is reactive or not, and had a combined content of SiO_2, Fe_2O_3 and Al_2O_3 of approximately one-seventh the lower limit of 70 wt%. The SiO_2 content was less than the range indicated for coal fly ash [42] and was in the low range of what was observed for MSWI fly ash [20–39]. The Al_2O_3 and Fe_2O_3 content were within the range of both MSWI and coal fly ash, with the exception of the Arc samples that contained less Al_2O_3 and the Nuuk samples that contained less Fe_2O_3 than the range for coal fly ash [42]. The content of Na_2O_{eq}, in the five fly ash samples, was within the range of MSWI fly ash [20–39]. However, the range for coal fly ash [42] was exceeded. The samples Arc-Fa1 and Arc-Fa2 both had low amounts of Cl and high amounts of SO_3, exceeding the SO_3 range for both MSWI and coal fly ash, while Nuuk-Fa1 and Nuuk-Fa2 contained high amounts of Cl and low amounts of SO_3. Compared to the Arc and Nuuk samples, Rya-Fa contained low amounts of both Cl and SO_3.

Large variations in LOI was observed for the five MSWI fly ash samples, between 3.8 and 31.2 wt%. Variations between samples obtained from the same incineration plant could be observed as well, with the LOI increasing by 6.9 wt% between Arc-Fa1 and Arc-Fa2 and decreasing by 22 wt% between Nuuk-Fa1 and Nuuk-Fa2. EN 450-1 2012 [10] specifies a maximum LOI limit of 9.0 wt%, all but Arc-Fa1 exceeded the limit as well as the range observed for coal fly ash.

The DTG curves of the five MSWI fly ash samples are shown in Fig. 1. The most extensive mass loss occurred between 500 and 700 °C. A second extensive mass loss was observed after 700 °C. According to Du et al. [43] carbonates in MSWI fly ash decompose between 402 and 725 °C, while mass loss observed between 725 and 1030 °C corresponds to the decomposition of sulphates. However, Galan et al. [44] suggest that $CaCO_3$ decomposes between 700 and 1000 °C in an N_2 atmosphere. The reduced decomposition temperature of CaCO3 could be caused by NaCl, as suggested by Wieczorek-ciurowa et al. [45]. The mass loss observed between 500 and 700 °C in the present study could, therefore, indicate the presence of $CaCO_3$ for Nuuk-Fa1, Nuuk-Fa2, Rya-Fa and Arc-Fa1. The second mass loss could be the result of sulphate phases decomposing. Several small mass losses could be observed between 0 and 500 °C, indicating potential loss of mass from several different phases, or the sequential decomposition of a single phase. Additionally, the samples Nuuk-Fa1 and Nuuk-Fa2 had similar DTG curves, while Arc-Fa1 and Arc-Fa2 had different peaks, indicating similarities and differences between the Nuuk and Arc samples respectively.

The XRD patterns of the five MSWI fly ash samples are shown in Fig. 2. Peaks for $CaSO_4$ and NaCl were found in all five fly ash samples, while peaks for $CaCO_3$ and KCl

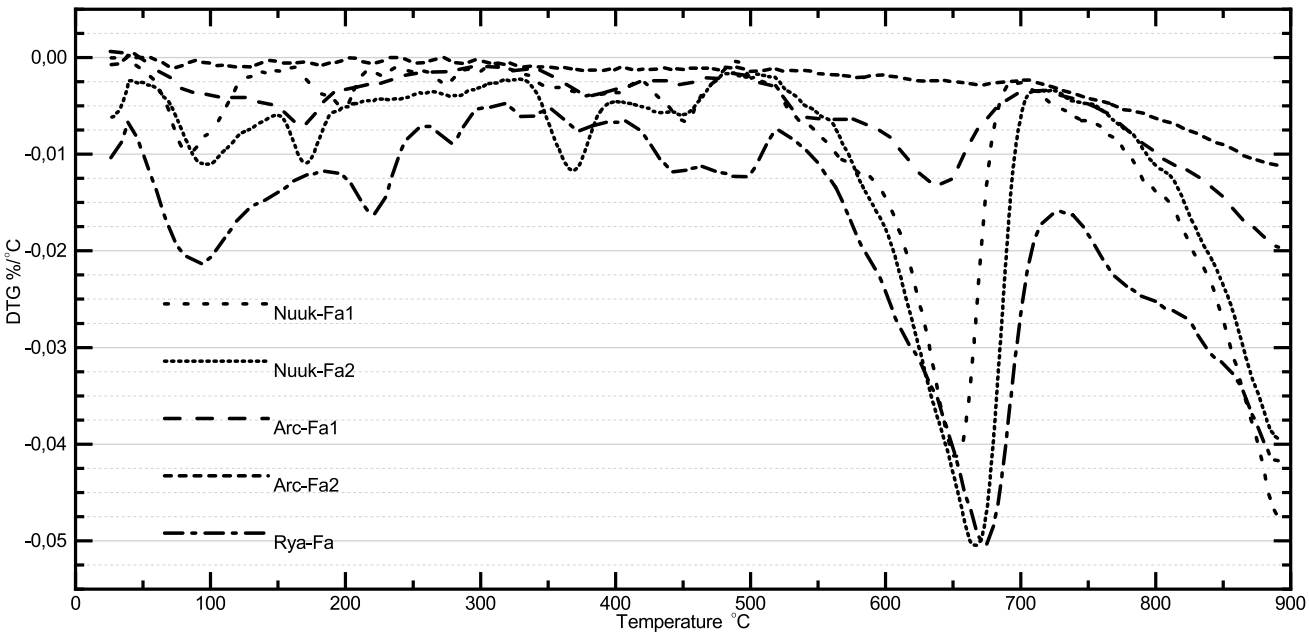

Fig. 1 DTG curves of the five MSWI fly ash samples

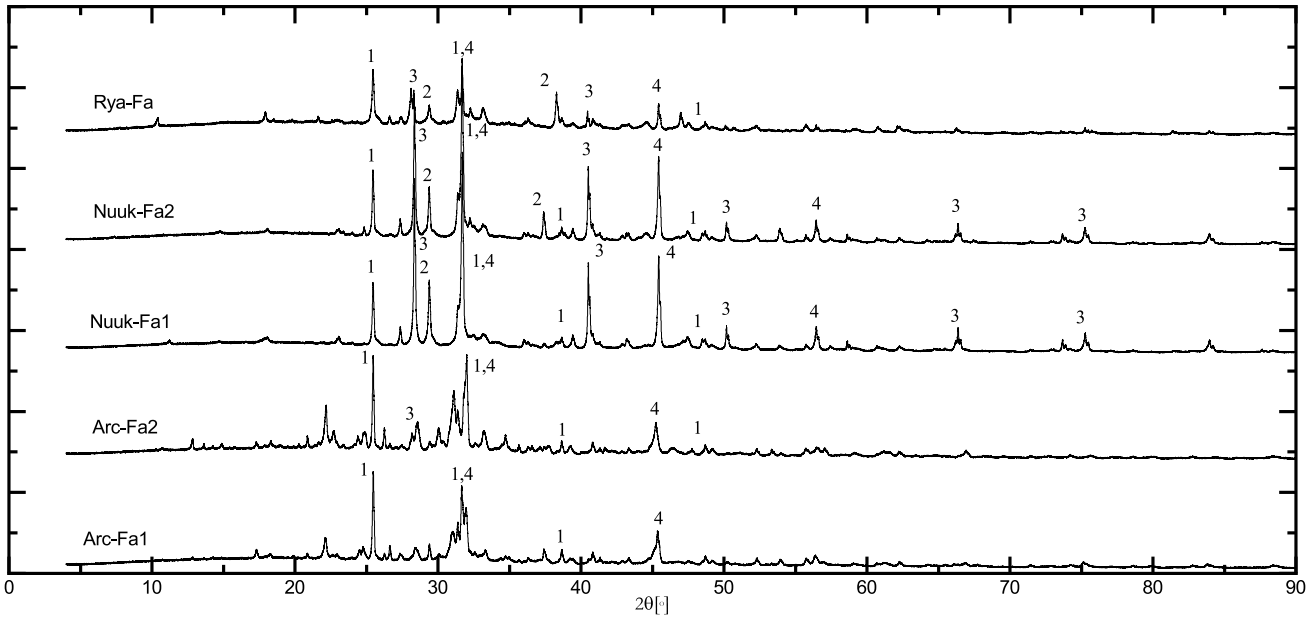

Fig. 2 X-ray diffractograms of the five MSWI fly ash samples. 1 = $CaSO_4$, 2 = $CaCO_3$, 3 = KCl and 4 = NaCl

were present in Nuuk-Fa1, Nuuk-Fa2 and Rya-Fa. The two Nuuk samples appeared to have similar diffraction patterns, diverging from each other in peaks for $CaCO_3$. The samples Arc-Fa1 and Arc-Fa2 showed several peak differences, between 20° and 35°, indicating differences in composition between the samples. The sample Arc-Fa2 could potentially contain several different sulphur compounds such as $KNaSO_4$ and $Mg_2NaOH(SO_3)_2{\cdot}H_2O$, not observed in the other ash samples.

The maximum limit for free and reactive CaO was exceeded in all five MSWI fly ash samples, see Table 3. However, as indicated by the TGA and XRD analysis, the Ca in the five MSWI fly ash samples can be present as $CaCO_3$ or $CaSO_4$.

Table 3 contains the measured pH, conductivity, water solubility and water-soluble content of the five MSWI fly ash samples. Four samples were alkaline, with a pH between 11 and 12, and electrical conductivities between 90 and 150 mS/cm^2. Pedersen et al. [46] measured the pH of two MSWI fly ash samples from different incineration plants and determined their pH to be 10.8 and 12.2, respectively. The pH of Arc-Fa2 differs from these results with a pH of 6.5, indicating that MSWI fly ash can have a neutral pH as well as alkaline pH. The lower pH of Arc-Fa2 could be a result of its high ratio of sulphur to other elements.

High solubility in water was observed for the five MSWI fly ash samples, varying between approximately 28 wt% and 56 wt%. The measured solubilities indicated that Cl^- was present in soluble form, matching the amounts measured with XRF, except for Rya-Fa, where the soluble Cl^- was 5 wt% higher, indicating that the measured Cl is higher in Rya-Fa than measured with XRF. The soluble Na^+ content measured in Arc-Fa2 did not match the XRF analysis either. The samples Arc-Fa1 and Arc-Fa2 contained a higher content of soluble SO_4^{2-} than the other samples. In comparison, Rya-Fa had a higher content of soluble Ca^{2+}, matching the results of the

Table 3 Measured pH, conductivity, water solubility and content of water-soluble Cl^-, SO_4^{2-} and NO_3^- anions and water-soluble Ca, Na and K of the five MSWI fly ash samples

	Arc-Fa1	Arc-Fa2	Nuuk-Fa1	Nuuk-Fa2	Rya-Fa
pH (–)	12.0 ± 0.1	6.5 ± 0.0	11.6 ± 0.0	11.9 ± 0.0	11.5 ± 0.0
Conductivity (mS/cm)	114 ± 4	94.7 ± 1.3	150 ± 21	147 ± 5	93.5 ± 1.2
Water Solubility (wt%)	39.4 ± 0.5	55. 7 ± 2.3	42.4 ± 1.3	38.0 ± 0.6	27.7 ± 0.9
Cl^- (wt%)	8.1 ± 0.1	2.3 ± 0.2	19.1 ± 0.9	22.2 ± 0.4	17.6 ± 0.5
SO_4^{2-} (wt%)	7.5 ± 0.0	21.1 ± 0.6	0.8 ± 0.0	0.6 ± 0.0	0.2 ± 0.0
Ca^{2+} (wt%)	0.1 ± 0.0	0.1 ± 0.0	0.7 ± 0.1	1.9 ± 0.1	6.0 ± 0.9
Na^+ (wt%)	7.7 ± 0.1	10.4 ± 0.2	6.3 ± 1.1	7.6 ± 0.2	1.6 ± 0.1
K^+ (wt%)	3.9 ± 0.1	3.1 ± 0.1	5.6 ± 1.0	6.8 ± 0.2	1.3 ± 0.1

XRF analysis where the samples from Arc had the highest content of Sulphur, and Rya-Fa the highest content of Calcium. The samples Nuuk-Fa1 and Nuuk Fa2 had similar water solubilities, while the sample Arc-Fa2 had approximately 16 wt% more soluble mass than Arc-Fa1.

The total content of toxic metals is shown in Table 4, together with the results of the batch leaching test, the total content measured in a CEM I cement and in previously studied MSWI fly ash samples [21–40]. The studied MSWI fly ashes were all characterised as having low amounts of Cd and Cr compared to Cu, Pb and Zn. The sample from the fluidised bed incinerator contained low total concentrations of Cd, Cr and Zn, and a higher total concentration of Cu compared to the other samples. In contrast, the samples from the large grate fired incinerator contained higher total concentrations of Pb and Zn. Arc-Fa2 differed further from Arc-Fa1 with an approximately twice as high total concentration of both Pb and Zn. The measured concentrations of toxic metals were within the range measured in other studies [21–40], except for the Cr content in Rya-Fa, that was less than previously observed and the Zn content in Arc-Fa2 that was higher than previously observed.

Cadmium leaching was below the detection limit of 0.01 mg/kg for the samples Arc-Fa1, Nuuk-Fa2 and Rya-Fa, while Nuuk-Fa1 leached 0.7 mg/kg and Arc-Fa2 leached 432.8 mg/kg. The leached amounts of Cr and Cu follow the total content measured, where the samples with the highest total concentration also had the highest leached concentration. This is not the case for Pb. The sample Arc-Fa2 had the highest concentration of Pb and leached the least, while Rya-Fa leached approximately a third of its concentration of Pb. The five fly ash samples all contained high amounts of Zn and leached between 4.0 and 19.8 mg Zn/kg, while Arc-Fa2 leached an exponentially high amount of Zn compared to the other samples at 22.9 g/kg.

No limits exist for toxic metal leaching from waste materials to be used as SCMs, the leaching limits for waste materials used for geotechnical purposes (Category 3, Restproduktbekendtgørelsen [47]) was therefore used instead. The specified limits were recalculated from µg/l to mg/kg. The studied MSWI fly ash samples exceeded the specified limits for Pb and Zn leaching, while Arc-Fa2 and Nuuk-Fa1 exceeded the limits for Cd. The sample Rya-Fa exceeded the limit for Cu leaching and was the only sample with leaching lower than the Cr limit.

3.2 Physical properties

The particle size distributions of the five MSWI fly ash samples are shown in Fig. 3, while the corresponding d-values are shown in Table 5. Arc-Fa1 consisted of finer particles than both Rya-Fa and Nuuk-Fa1, with a d_{10} similar to CEM I cement. Approximately 30% of Arc-Fa1 consisted of particles smaller than 10 µm, compared to around 10–15% for Nuuk-Fa1 and Rya-Fa. However, Arc-Fa1 also contained coarser particles than Rya-Fa and Nuuk-Fa1. The sample Arc-Fa2 deviated from Arc-Fa1 with a higher d_{10} value, smaller d_{50} and d_{90} values and approximately 13% of its particles less than 10 µm in diameter. Both Arc-Fa samples contained particles over the fine particle limit specified by Moosberg-Bustnes et al. [11]. The sample Nuuk-Fa2 deviated from Nuuk-Fa1 as well, resembling CEM-I cement instead. Approximately 40% of Nuuk-Fa2 consisted of particles with a diameter of less than 10 µm.

According to Moosberg-Bustnes et al. [11], the addition of fine particles, with a maximum size of 125 µm, to a cement-based material has a physical effect, filling intergranular voids, improving the packing density and

Table 4 Total toxic metal concentration in the five MSWI fly ash samples as well as leached concentrations

Total-content (mg/kg)	Arc-Fa1	Arc-Fa2	Nuuk-Fa1	Nuuk-Fa2	Rya-Fa	CEM I	MSWI [20–39]
Cd	280 ± 5	410 ± 9	205 ± 6	284 ± 7	62.7 ± 4.3	0.4 ± 0.3	22–578
Cr	126 ± 2	109 ± 2	206 ± 7	336 ± 9	23.1 ± 1.5	33.7 ± 0.7	47–2026
Cu	1070 ± 20	1360 ± 24	755 ± 16	940 ± 34	6940 ± 870	139.6 ± 3	168–7800
Pb	6250 ± 230	15,290 ± 780	2750 ± 61	3140 ± 96	3630 ± 450	16.7 ± 0.5	319–36,420
Zn	34,690 ± 1360	66,560 ± 2110	29,630 ± 830	23,070 ± 630	6860 ± 830	184 ± 15	2–65,170
Leached (mg/kg)						Category 3 [47]	
Cd	< 0.01	433 ± 10	0.7 ± 0.2	< 0.01	< 0.01	0.08	–
Cr	1.5 ± 1.6	0.9 ± 0.0	19.5 ± 2.7	39.2 ± 4.4	0.1 ± 0.0	1	–
Cu	0.2 ± 0.0	2.6 ± 0.1	0.3 ± 0.2	0.4 ± 0.2	51.7 ± 2.1	4	–
Pb	49.5 ± 3.4	5.0 ± 0.1	16.4 ± 1.8	530 ± 11	1400 ± 110	0.2	–
Zn	10.4 ± 0.6	22,950 ± 610	4.0 ± 0.7	5.8 ± 0.2	19.8 ± 0.9	3	–

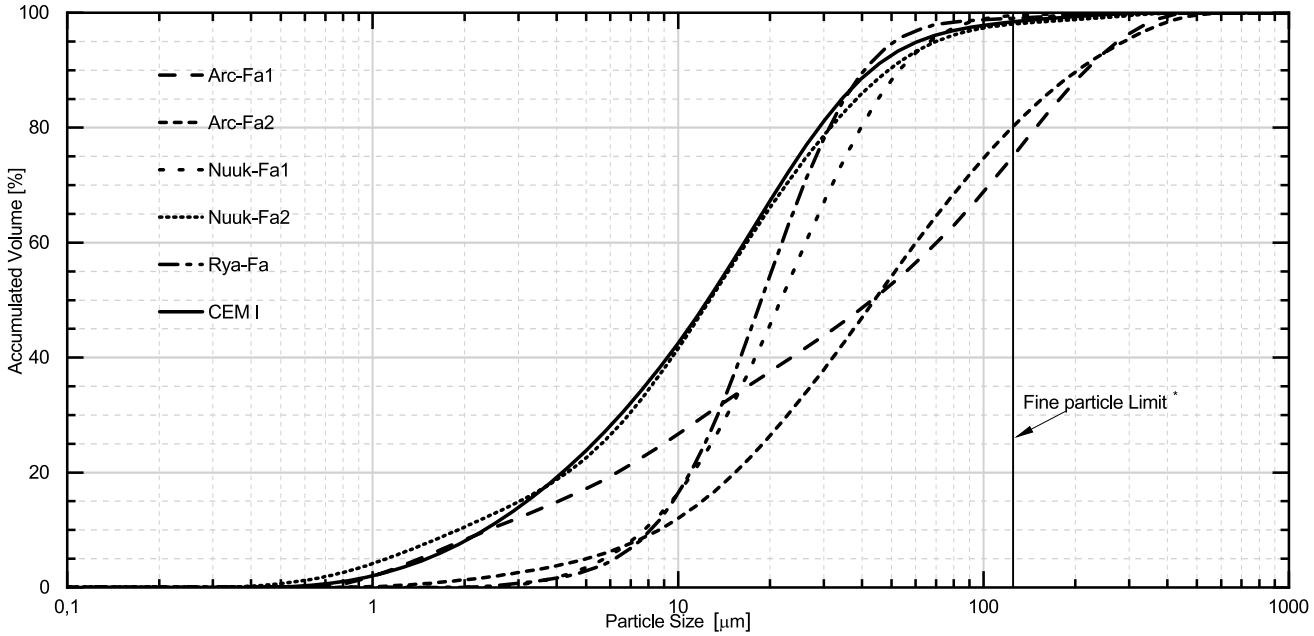

Fig. 3 The particle size distribution of the five MSWI fly ash samples and CEM I cement. *Fine particle limit as suggested by Moosberg-Bustnes et al. [11]

Table 5 d-Values (µm) of the five MSWI fly ash samples

	Arc-Fa1	Arc-Fa2	Nuuk-Fa1	Nuuk-Fa2	Rya-Fa
d_{10}	2.8 ± 0.2	8.7 ± 0.2	7.8 ± 0.3	1.9 ± 0.0	8.3 ± 0.7
d_{50}	49.6 ± 1.9	44.0 ± 0.9	21.7 ± 0.7	12.7 ± 0.2	18.7 ± 0.2
d_{90}	248 ± 5	204 ± 8	52.9 ± 1.2	48.8 ± 1.2	40.7 ± 2.7

a surface chemical effect enhancing the hydration by offering more nucleation sites. According to Scrivener et al. [12], the hydration enhancement is only possible for materials that have a finer particle size distributions than cement. Filler materials may also increase the degree of hydration through dilution by increasing the space for clinker hydrate formation [12]. The five MSWI fly ash samples had particle size distributions that were larger than or similar to CEM I cement and were within the fine particle limit, except the Arc samples. Although the samples are within the fine particle limit, they are not expected to improve the packing density or enhance hydration as nucleation sites, due to their larger particle size distribution than CEM I cement, except the sample Nuuk-Fa2. The sample Nuuk-Fa2 had a particle size distribution like CEM I and had a d_{10} value less than CEM and could potentially improve the packing density. The five MSWI fly ash samples would, therefore, be limited to increasing the degree of hydration through dilution.

3.3 Variability of MSWI fly ash

The results of the principal component analysis (PCA) are shown in Fig. 4 for the 1st and 2nd principal components and Fig. 5 for the 1st and 3rd components. Included are plots of the loadings and the scores.

In a loading plot, variables close to the origin has little contribution to a sample's score [48]; this was the case for Cu (see Fig. 4a) which has limited weight on the 1st and 2nd principal components. Strongly correlated variables cluster together in a loading plot [48], this is observable in Fig. 4a for (1) SiO_2, Al_2O_3, Fe_2O_3 and MgO and (2) Cd, Zn, Pb and SO_3. Samples with a high content of SiO_2 can be expected to have a high content of Al_2O_3, Fe_2O_3 and MgO as well, while samples with a high content of Cd, might contain a high amount of Zn, Pb and SO_3. Negatively correlated variables appear diagonally of each other in a loading plot [48]. This can be observed for Cl in Fig. 4a that is negatively correlated with SiO_2, Al_2O_3, Fe_2O_3 and MgO, indicating that MSWI fly ash with a high content of Cl contains less SiO_2, Al_2O_3, Fe_2O_3 and MgO.

In a score plot, samples with variables close to the average appear at the origin, while samples further out are outliers or naturally extreme observations in the data set [48]. This can be observed in Fig. 4b for the 1st and 2nd principal components. Several of the MSWI fly ash samples in the dataset were located close to the origin indicating that they have a common composition, while several samples are further away, indicating that those particular

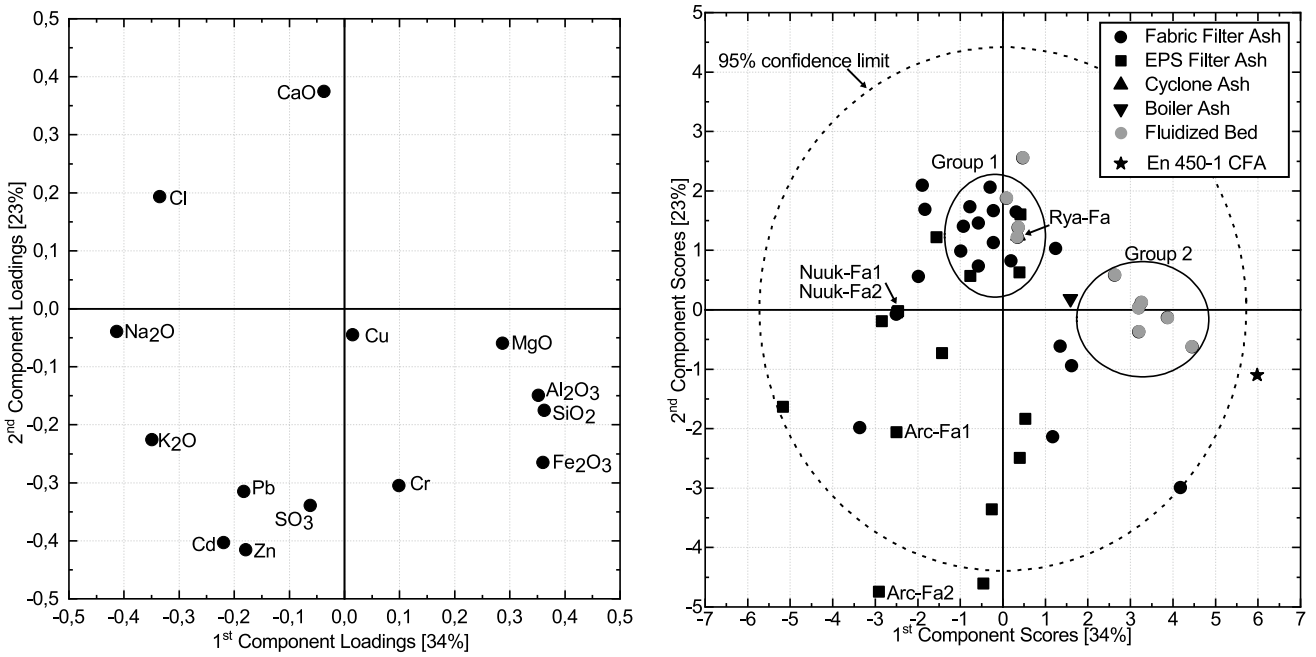

Fig. 4 PCA results for the 1st and 2nd principal components, loading plot (left, **a**) of the variables and score plot (right, **b**) of the observations. Black symbols are from grate furnaces, while grey symbols are fabric filter ash from fluidised bed furnaces. Included in the score plot is an EN 450-1 coal fly ash (CFA). Two clusters are marked as group 1 and 2

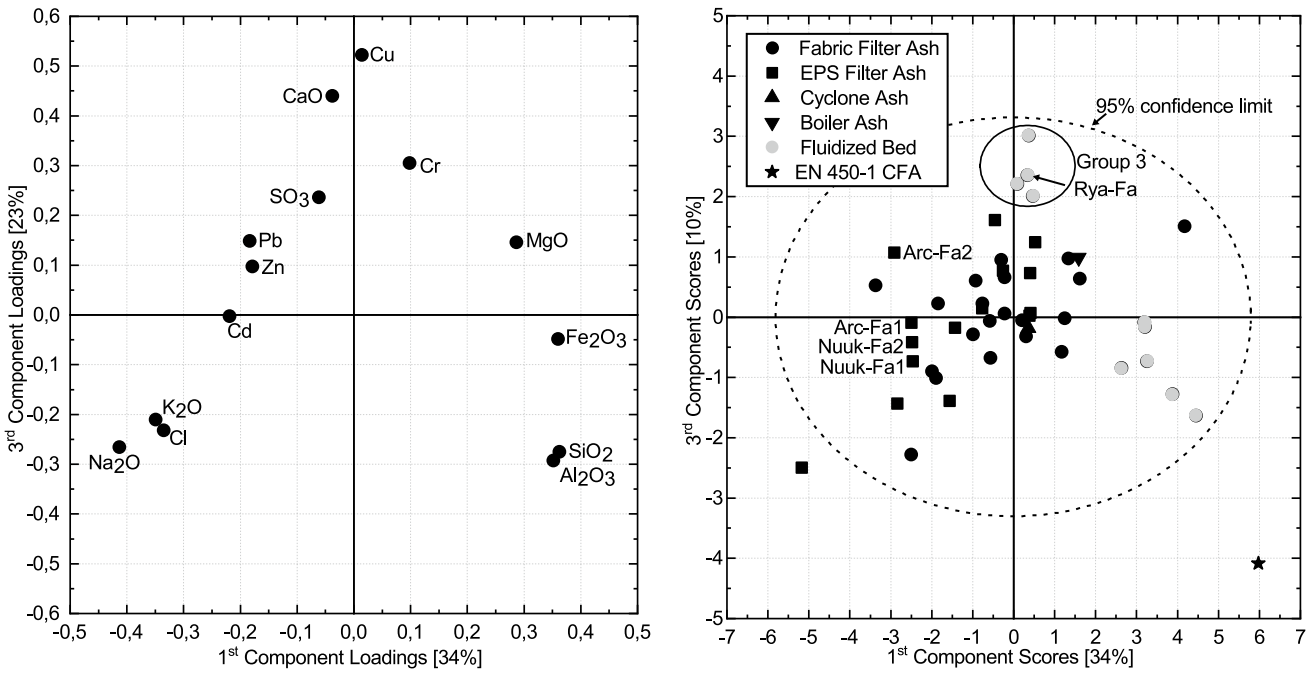

Fig. 5 PCA results for the 1st and 3rd principal components, loading plot (left, **a**) of the variables and score plot (right, **b**) of the observations. Black symbols are from grate furnaces, while grey symbols are fabric filter ash from fluidised bed furnaces. Included in the score plot is an EN 450-1 coal fly ash (CFA). A cluster of samples are marked as Group 3

MSWI fly ash samples have a unique composition. This can be observed for the included coal fly ash sample. The reason for a sample's score can, in general, be inferred by cross-referencing with the loading plot [48]. In Fig. 4b, samples with a high positive 1st principal component are therefore expected to have an above-average content of

SiO_2, Al_2O_3, Fe_2O_3 and MgO. In contrast, samples with a large negative 1st principal component are expected to have an above-average content of Na_2O, K_2O and Cl. Similar observations were made for the 2nd principal component where CaO is negatively correlated with Pb, Cd, Zn and SO_3.

The score plot in Fig. 4b for the 1st and 2nd principal components indicated that approximately half of the MSWI fly ash samples of the dataset had a negative 1st principal component, while the other half had a positive 1st principal component. This difference appears to partly depend on the furnace type used for incineration. The fluidised bed samples had positive 1st principal components indicating a higher than average content of SiO_2, Al_2O_3, Fe_2O_3 and MgO, while the majority of the grate furnace samples had a negative 1st principal component, indicating a higher than average content of Na_2O, K_2O and Cl. A difference between fabric filter ash and electrostatic precipitator (ESP) ash was observed for the 2nd principal component. Ash from a fabric filter appeared to have a higher content of CaO than ESP ash, while ESP ash had a higher content of Pb, Cd, Zn and SO_3 than fabric filter ash, which could be due to the addition of air pollution control products in the form of lime.

Marked in the score plot for the 1st and 2nd component, see Fig. 5b, are two clusters marked as Group 1 and 2. Group 1 consists of a third of the dataset and includes samples from both grate and fluidized bed incinerators as well as samples from fabric and EPS filters. The samples in Group 1 originated from several different countries and also included one cyclone ash from a grate fired furnace. Group 2 consists of a cluster of MSWI fly ash samples from Chinese fluidised bed incinerators with a higher than average content of SiO_2, Al_2O_3, Fe_2O_3 and MgO otherwise not observed in MSWI fly ash. This could be a result of the incinerator design or fuel used during incineration.

In the loading plot between the 1st and 3rd principal components, see Fig. 5a, Cu had a larger contribution to the samples' 3rd principal components score. The fluidised bed samples which were part of Group 1 in Fig. 4b were clustered separately along the 3rd principal component indicating a higher than average content of Cu in the samples, see Group 3 in Fig. 5b. The samples in Group 3 were from Swedish incinerators that the incinerator design or fuel used results in a higher Cu content.

The included coal fly ash sample was an outlier in both score plots, Figs. 4b and 5b, with a high content of SiO_2, Al_2O_3 and Fe_2O_3. The MSWI fly ash samples from fluidised bed incinerators in Group 2, had the closest scores to the coal fly ash sample, indicating the closest similar composition.

The sample Arc-Fa2 from the present study was an outlier in the dataset, with a 1st and 2nd principal component score of approximately − 3 and − 5, respectively. The sample Arc-Fa2 had an above-average content of SO_3, Pb, Zn and Cd not observed in other MSWI fly ash samples, that could be considered uncommon for MSWI fly ash. The sample Arc-Fa1 had a score closer to the rest of the samples. Although the sample Arc-Fa1 was not an outlier, it was not part of any cluster, suggesting a composition that is less common for MSWI fly ash. The samples Nuuk-Fa1 and Nuuk-Fa2 had similar scores, indicating that the two samples are similar in terms of oxide and toxic metal content. The two samples from Nuuk were outside of Group 1 with a higher than average content of Cl, Na_2O and K_2O compared to SiO_2, Al_2O_3 and Fe_2O_3 and could be considered less common of MSWI fly ash. The sample Rya-Fa was a part of Group 1, indicating a common chemical composition.

4 Discussion

Samples from fluidized bed incinerators had positive 1st components, while the majority of the grate furnace samples had negative 1st components. Samples from fabric filters had predominantly positive 2nd components, while samples from electrostatic precipitators had predominantly negative 2nd components. However, the scattering observed for dataset samples originating from grate furnaces and either EPS or fabric filters, suggested that similar chemical compositions can be found regardless of the incineration plant design. Parts of the dataset were clustered, while the rest of the dataset were scattered, indicating that a typical oxide composition and toxic metal content can to some extent be found for MSWI fly ash, regardless of the origins of the sample. The coal fly ash was an outlier compared to the MSWI fly ash samples of the dataset, indicating that the MSWI fly ash samples differed considerably from EN 450-1 2012 coal fly ash. The fluidised bed samples in Group 2 had the closest scores, suggesting that these samples were closest in chemical composition to EN 450-1 2012 coal fly ash. The samples in Group 2 could be the best suited MSWI fly ash samples for use in cement-based materials. None of the samples in the present study were found in this cluster.

The PCA indicated that the samples Arc-Fa1 and Arc-Fa2 differed significantly both from each other and previously studied MSWI fly ash samples, containing SO_3, Pb, Zn and Cd in high amounts. However, the total content of SO_3, Pb, Zn and Cd in Arc-Fa2 was noticeably higher than in Arc-Fa1, making it a different material as indicated by the differences in DTG curves and XRD patterns. The sample Arc-Fa2 was an outlier in the dataset, while Arc-Fa1 was spread out from any clustering, suggesting that the high contents of SO_3, Pb, Zn and Cd were uncommon for

MSWI fly ash and that the samples were unrepresentative of MSWI fly ash. The samples from Nuuk had similar PCA scores, indicating that the two samples were very similar in chemical composition. Their scores were closer to the majority of the dataset as well, indicating a less unique chemical composition compared to the Arc samples. The sample Rya-Fa was part of the cluster Group 1 and the closest to the dataset average out of the five MSWI fly ash samples in the present study and could be considered a representative sample for MSWI fly ash. Rya-Fa could, therefore, give a general impression of the effect MSWI fly ash has in cement-based materials. However, studying all five MSWI fly ash samples can give a deep impression of the impact MSWI fly ash has in cement-based materials.

Additionally, the PCA indicated that multivariate statistical methods could be used as a tool to evaluate how representative new MSWI fly ash samples are to previously studied samples. This is especially the case for the sample Arc-Fa2 that otherwise appeared to be within the limits of previously observed MSWI fly ash samples.

The five MSWI fly ash samples evaluated in the present study had PCA scores that varied from EN 450-1 coal fly ash and did not fulfil the chemical requirements specified in EN 450-1 2012 [10]. Using the five MSWI fly ash samples in cement-based materials could potentially result in several drawbacks. Pozzolanic reactions in cement-based materials occur between $Ca(OH)_2$ and amorphous SiO_2 forming C–S–H or with amorphous aluminosilicate forming C–A–H phases or C–A–S–H phases, Justness [2]. Hamernik and Frantz [41] studied MSWI fly ashes with a combined content of SiO_2, Fe_2O_3 and Al_2O_3 above 50 wt%. They analysed the pozzolanic activity index of paste samples with 35% cement replaced by MSWI fly ash and concluded that the MSWI fly ashes had pozzolanic activity indexes comparable to coal fly ash and showed no cementitious properties when mixed with water. The MSWI fly ashes of the present study had a low content of SiO_2, Fe_2O_3 and Al_2O_3 and would have limited pozzolanic activity if used in cement-based materials.

The differences between the particle size distributions of the five MSWI fly ash samples and CEM I cement indicate that the potential of the samples as filler materials are limited to increasing the degree of hydration through dilution. Although, with a small enough particle size distribution as observed for Nuuk-Fa2, the packing density could potentially be improved. However, the oxide composition and soluble content of Cl^- SO_4^{2-}, K^+, Na^+ and Ca^+ in the five MSWI fly samples indicates that they would not be inert filler, limiting their potential as filler materials.

Research has shown that an increasing sulphate level can reduce the heat of hydration, increase setting time and reduce the strength of a cement-based material [49]. The samples Arc-Fa1 and Arc-Fa2 could be expected to have a significant negative impact on these factors. Alkali-aggregate reactions occur in cement-based materials between alkalis (sodium and potassium) and specific aggregate types and may result in cracking [50]. The Arc and Nuuk samples all had a high Na_2O_{eq} content as well as soluble Na^+ and K^+ and could be expected to cause alkali-aggregate reactions if used in conjunction with reactive aggregates. The sample Rya-Fa exceeded the limit by 2.8 wt% and could cause alkali-aggregate reactions as well to a lesser extent. Chloride ions in reinforced cement-based materials can destroy the passive iron oxide film, leading to corrosion of the steel [50]. The measured calcium could be present as $CaCO_3$ in the fly ash samples. $CaCO_3$ can interact with the AFm and AFt phases in hydrating cement, resulting in the formation of carboaluminates, stabilizing the ettringite and improving the mechanical properties [51]. However, the interaction with $CaCO_3$ requires additional aluminates brought into the system [51]. The aluminate content range of MSWI fly ash is low compared to coal fly ash [42], limiting the beneficial interaction with the AFm and AFt phases.

No Danish standards exist regarding heavy metal content in cement-based materials when using MSWI ash. The limits for sewage sludge ash as specified in DS/EN 206 DK NA:2018 [52] are used for comparison instead. According to DS/EN 206 DK NA:2018 [52], using sewage sludge ash in concrete should not increase the heavy metal content by more than 25%. An increase of 50% can be accepted if the original heavy metal content in the concrete is low. The Cd content in the Arc and Nuuk samples was the most critical metal, exceeding the 50% criteria at 0.05–0.1% cement replacement. The sample Rya-Fa increases the Pb above 50% at 0.23% cement replacement. Toxic metals can be chemically bound in cement-based materials due to the high pH in Portland cement [6]. However, this does not account for decommissioning or reductions in pH due to, e.g. carbonation or chloride ingress [53].

Pre-treatment would be required before the studied MSWI fly ash samples can be used in cement-based materials. The pre-treatment method should reduce the toxic metal concentrations and leaching as well as improve the oxide composition. Additionally, the pretreatment could reduce the particle size distribution as well, improving the ashes potential as filler materials. Several potential methods of improving MSWI fly ash has been investigated, such as washing the MSWI fly ash to reduce chloride and toxic metal content [54] or thermal methods such as vitrification [55]. Another potential method is electrodialytic remediation that reduces the chloride and toxic metal content, increasing the fraction of SiO_2, Fe_2O_3 and Al_2O_3 [56]. Milling MSWI fly ash could be an effective method to both improve the particle size distribution and treat MSWI fly ash [57].

5 Conclusions

The multivariate modelling indicated that the samples Arc-Fa1 and Arc-Fa2 were not representative of MSWI fly ash due to their high content of SO_3, Pb, Zn and Cd and that the two samples were chemically different materials. The samples Nuuk-Fa1 and Nuuk-Fa2 were similar and more representative of MSWI fly ash. The sample Rya-Fa was the most common of the five MSWI fly ash samples investigated in the present study and could provide the most representative result if used in cement-based materials.

It was determined that the chemical composition was in part, dependent on the furnace and filter type used during incineration. However, similar MSWI fly ash samples could be found in literature, regardless of the furnace or filter type used during incineration.

MSWI fly ash differed significantly from a coal fly ash that fulfils the requirements of EN 450-1 2012. The five MSWI fly ash samples investigated did not fulfil eight of the ten chemical requirements specified in EN 450-1 2012. The investigated samples had particle sizes comparable to and slightly larger than cement and had limited potential as filler material. However, negative effects from the SO_3, Cl and alkali metal and the total toxic and leached metal concentrations limit their potential use in cement-based materials without pre-treatment.

Acknowledgements Amager Resource Center is acknowledged for their cooperation in obtaining ash from their facility. Furthermore, Kommuneqarfik Semersooq and Borås Energy och Miljö, are acknowledged for sampling and sending the MSWI fly ash samples from the Nuuk incinerator in Greenland and Ryaverket in Sweden. Finally, the lab technicians Ebba Schnell, Malene Møller, Anna Schroeder and Natasja Dueholm are recognised for their assistance in measuring the many properties of the MSWI fly ashes. The corresponding author would like to thank Nina Marie Sigvardsen and Kristine Bondo Pedersen for their support with the principal component analysis.

Compliance with ethical standards

Conflict of interest On behalf of all authors, the corresponding author states that there is no conflict of interest.

References

1. Olivier JGJ, Janssens-Maenhout G, Muntean M, Peters JAHW (2016) Trends in global CO_2 emissions, 86, PBL Netherlands environmental service
2. Justnes H (2015) Influence of SCMs on hydration and durability of blended cements—chemical and physical principles. J Chin Ceram Soc 2554(13):1359–1371
3. Scrivener KL, John VM, Gartner EM (2016) Eco-efficient cements: potential, economically viable solutions for a low-CO_2, cement based materials industry. United Nations Environment Program
4. Zhang H, Zhao Y (2009) Toxicity analysis of municipal solid waste incineration (MSWI) fly ash. In: 2009 3rd international conference on bioinformatics and biomedical engineering, pp 1–4
5. Ferreira C, Ribeiro A, Ottosen L (2003) Possible applications for municipal solid waste fly ash. J Hazard Mater 96:201–216
6. Kozakova L, Bakalar T, Zelenak M, Prascakova M (2013) Solidification of MSWI fly-ash with regard to hazardous metals leaching. Acta Montan Slov 18:129–139
7. Aubert JE, Husson B, Vaquier A (2004) Use of municipal solid waste incineration fly ash in concrete. Cem Concr Res 34:957–963
8. Aubert JE, Husson B, Sarramone N (2006) Utilization of municipal solid waste incineration (MSWI) fly ash in blended cement. Part 1: processing and characterization of MSWI fly ash. J Hazard Mater 136:624–631
9. Lenormand T, Rozière E, Loukili A, Staquet S (2015) Incorporation of treated municipal solid waste incineration electrostatic precipitator fly ash as partial replacement of Portland cement: effect on early age behaviour and mechanical properties. Constr Build Mater 96:256–269
10. DS/EN 450-1: Flyveaske til beton—Del 1 : Definition, specifikationer og overensstemmelses-kriterier; Dansk Standard (2012)
11. Moosberg-Bustnes H, Lagerblad B, Forssberg E (2004) The function of fillers in concrete. Mater Struct Constr 37:74–81
12. Scrivener KL, Lothenbach B, De Belie N, Gruyaert E, Snellings R, Vollpracht A (2015) TC 238-SCM: hydration and microstructure of concrete with SCMs state of the art on methods to determine degree of reaction of SCMs. Mater Struct 48:835–862
13. Pedersen KB, Kirkelund GM, Ottosen LM, Jensen PE, Lejon T (2015) Multivariate methods for evaluating the efficiency of electrodialytic removal of heavy metals from polluted harbour sediments. J Hazard Mater 283:712–720
14. Sigvardsen NM, Kirkelund GM, Jensen PE, Geiker MR, Ottosen LM (2019) Impact of production parameters on physiochemical characteristics of wood ash for possible utilisation in cement-based materials. Resour Conserv Recycl 145:230–240
15. Voshell S, Mäkelä M, Dahl O (2018) A review of biomass ash properties towards treatment and recycling. Renew Sustain Energy Rev 96:479–486
16. Javan H (1999) Application of Mie theory to large particle. In: Proceedings of the conference proceedings—IEEE SOUTHEASTCON, vol 1999-March, pp 237–241
17. Chen W, Kirkelund GM, Jensen PE, Ottosen LM (2017) Comparison of different MSWI fly ash treatment processes on the thermal behavior of As, Cr, Pb and Zn in the ash. Waste Manag 68:240–251
18. DS/EN 12457-1 (2002) Characterisation of waste—Leaching—Compliance test for leaching of granular waste materials and Sludges—Part 1: One stage batch test at a liquid to solid ratio of 2 l/kg for materials with high solid content and with particle size bel; Dansk Standard
19. DS 259 (2003) Vandundersøgelse—Bestemmelse af metaller i vand, jord, slam og sedimenter—Almene principper og retningslinjer for bestemmelse ved atomabsorptionsspektrofotometri i flamme Determination of metals in water, sludge and atomic absorption; Dansk Standard
20. Tefas A, Pitas I (2016) Principal component analysis. Intell Syst 2:37–52
21. Ni P, Li H, Zhao Y, Zhang J, Zheng C (2017) Relation between leaching characteristics of heavy metals and physical properties of fly ashes from typical municipal solid waste incinerators. Environ Technol 38:2105–2118
22. Qiu Q, Jiang X, Chen Z, Lu S, Ni M (2017) Microwave-assisted hydrothermal treatment with soluble phosphate added for heavy metals solidification in MSWI fly ash. Energy Fuels 31:5222–5232

23. Li W, Sun Y, Huang Y, Shimaoka T, Wang H, Wang YN, Ma L, Zhang D (2019) Evaluation of chemical speciation and environmental risk levels of heavy metals during varied acid corrosion conditions for raw and solidified/stabilized MSWI fly ash. Waste Manag 87:407–416
24. Mu Y, Saffarzadeh A, Shimaoka T (2018) Influence of ignition of waste fishbone on enhancing heavy metal stabilization in municipal solid waste incineration (MSWI) fly ash. J Clean Prod 189:396–405
25. Kitamura H, Dahlan AV, Tian Y, Shimaoka T, Yamamoto T, Takahashi F (2019) Intra- and inter-particle heterogeneity of municipal solid waste incineration fly ash particles. J Mater Cycles Waste Manag 21:925–941
26. Ma W, Chen D, Pan M, Gu T, Zhong L, Chen G, Yan B, Cheng Z (2019) Performance of chemical chelating agent stabilization and cement solidification on heavy metals in MSWI fly ash: a comparative study. J Environ Manag 247:169–177
27. Zhu F, Xiong Y, Wang Y, Wei X, Zhu X, Yan F (2018) Heavy metal behavior in "Washing–Calcination–Changing with Bottom Ash" system for recycling of four types of fly ashes. Waste Manag 75:215–225
28. De Boom A, Aubert J, Degrez M (2014) Carbonation of municipal solid waste incineration electrostatic precipitator fly ashes in solution. Waste Manag Res 32:406–413
29. Kirkelund GM, Dias-Ferreira C, Jensen PE (2016) Characterization of particulate residues from greenlandic mswi for use as secondary resources. In: Proceedings of the international conference materials, systems and structures in civil engineering 2016: workshop on cold region engineering, Nyt Teknisk Forlag, pp 27–36
30. Weibel G, Eggenberger U, Schlumberger S, Mäder UK (2017) Chemical associations and mobilization of heavy metals in fly ash from municipal solid waste incineration. Waste Manag 62:147–159
31. Bayuseno AP, Schmahl WW, Müllejans T (2009) Hydrothermal processing of MSWI fly ash-towards new stable minerals and fixation of heavy metals. J Hazard Mater 167:250–259
32. Chimenos JM, Ferna AI (2005) Optimizing the APC residue washing process to minimize the release of chloride and heavy metals. Waste Manag 25:686–693
33. Fedje KK, Ekberg C, Skarnemark G, Pires E, Steenari B (2012) Initial studies of the recovery of Cu from MSWI fly ash leachates using solvent extraction. Waste Manag Res 30:1072–1080
34. Liu F, Liu J, Yu Q, Jin Y, Nie Y (2007) Leaching characteristics of heavy metals in municipal solid waste incinerator fly ash. J Environ Sci Heal 40(10):1975–1985
35. Wang L, Li R-D, Wei L, Li Y (2012) Accelerated carbonation of municipal solid waste incineration fly ash using CO_2 as an acidic agent for clinker production. Environ Eng Sci 29:677–684
36. Chen Z, Lu S, Mao Q, Buekens A, Chang W, Wang X (2016) Suppressing heavy metal leaching through ball milling of fly ash. Energies 9:1–13
37. Park YJ (2009) Stabilization of a chlorine-rich fly ash by colloidal silica solution. J Hazard Mater 162:819–822
38. Zheng L, Wang W, Shi Y (2010) Chemosphere the effects of alkaline dosage and Si/Al ratio on the immobilization of heavy metals in municipal solid waste incineration fly ash-based geopolymer. Chemosphere 79:665–671
39. Tang J, Steenari B (2016) Leaching optimization of municipal solid waste incineration ash for resource recovery: a case study of Cu, Zn, Pb and Cd. Waste Manag 48:315–322
40. Song GJ, Kim KH, Seo YC, Kim SC (2004) Characteristics of ashes from different locations at the MSW incinerator equipped with various air pollution control devices. Waste Manag 24:99–106
41. Hamernik J, Frantz G (1991) Physical and chemical properties of municipal solid waste fly ash.pdf. ACI Mater J 88:294–301
42. Jayaranjan MLD, van Hullebusch ED, Annachhatre AP (2014) Reuse options for coal fired power plant bottom ash and fly ash. Rev Environ Sci Biotechnol 13:467–486
43. Du B, Li J, Fang W, Liu Y, Yu S, Li Y, Liu J (2018) Characterization of naturally aged cement-solidified MSWI fly ash. Waste Manag 80:101–111
44. Galan I, Glasser FP, Andrade C (2013) Calcium carbonate decomposition. J Therm Anal Calorim 111:1197–1202
45. Wieczorek-ciurowa K, Paulik J, Paulik F (1980) Influence of foreign materials upon the thermal decomposition of dolomite, calcite and magnesite part I. Influence of sodium chloride. Thermochim Acta 38:157–164
46. Pedersen AJ, Ottosen LM, Villumsen A (2003) Electrodialytic removal of heavy metals from different fly ashes: influence of heavy metal speciation in the ashes. J Hazard Mater 100:65–78
47. Miljøministeriet Bekendtgørelse om anvendelse af restprodukter og jord til bygge- og anlægsarbejder og om anvendelse af sorteret, uforurenet bygge- og anlægsaffald; 2010; Vol. 2010, pp 1–15
48. Dunn KG (2014) Latent Variable Modelling. In: Dunn KG (ed) Process improvement using data. pp 325–416
49. Paine K (2019) Physicochemical and mechanical properties of Portland cement. In: Hewlett P, Liska M (eds) Lea's chemistry of cement and concrete. Butterworth-Heinemann, Oxford, pp 285–332
50. Mindess S (2019) Resistance of concrete to destructive agencies. In: Hewlett P, Liska M (eds) Lea's chemistry of cement and concrete. Butterworth-Heinemann, Oxford, pp 251–283
51. De Weerdt K, Kjellsen KO, Sellevold E, Justnes H (2011) Synergy between fly ash and limestone powder in ternary cements. Cem Concr Compos 33:30–38
52. DS/EN 206 DK NA (2018) Beton - Specifikation, egenskaber, produktion og overensstemmelse—Regler for anvendelse af EN 206 i Danmark; Dansk Standard
53. Kurdowski W (2002) Chloride corrosion in cementitious system. In: Bensted J, Barnes P (eds) Structure and performance of cements. Taylor & Francis, New York, pp 295–310
54. Bertolini L, Carsana M, Cassago D, Curzio AQ, Collepardi M (2004) MSWI ashes as mineral additions in concrete. Cem Concr Res 34:1899–1906
55. Lee TC, Wang WJ, Shih PY (2008) Slag-cement mortar made with cement and slag vitrified from MSWI fly-ash/scrubber-ash and glass frit. Constr Build Mater 22:1914–1921
56. Belmonte LJ, Ottosen LM, Kirkelund GM, Jensen PE, Vestbø AP (2018) Screening of heavy metal containing waste types for use as raw material in Arctic clay-based bricks. Environ Sci Pollut Res 25:32831–32843
57. Chen Z, Lu S, Tang M, Ding J, Buekens A, Yang J, Qiu Q, Yan J (2019) Mechanical activation of fly ash from MSWI for utilization in cementitious materials. Waste Manag 88:182–190

Journal Paper II

Electrodialytic Remediation and Combined Acid Leaching and Solvent Extraction – Potential Methods for Recovery of Metals from MSWI fly Ash

Benjamin A. R. Ebert, Britt-Marie Steenari, Martina Petranikova, Gunvor M. Kirkelund

Electrodialytic Remediation and Combined Acid leaching and Solvent Extraction – Potential Methods for Recovery of Metals from MSWI Fly Ash

Benjamin A. R. Ebert[1*], Britt-Marie Steenari[2], Martina Petranikova[2], Gunvor M. Kirkelund[1]

[1]Department of Civil Engineering, Technical University of Denmark, Denmark

[2]Chemistry and Chemical Engineering, Chalmers University of Technology, Sweden

[*]Corresponding author email: bareb@byg.dtu.dk

Abstract

Municipal solid waste incineration results in metal-rich fly ashes that generally are landfilled, leading to a loss of valuable metals. However, some methods can be used to recover the metals present in the fly ashes. Two of these methods are electrodialytic remediation and acid leaching. The present work was made to compare these methods' efficiency in liberating Cd, Cr, Cu, Pb and Zn from fly ashes from three different municipal solid waste incineration units. Leaching with HNO_3 and HCl leaching at constant pH were tested. Solvent extraction was applied to recover Cu from one of the samples after HCl leaching. Leaching with HCl or HNO_3 resulted in a higher metal yield from the studied fly ash samples than electrodialytic remediation. Furthermore, by combining HCl leaching and solvent extraction with 0.1M LIX860N-I, it was possible to recover close to 100% of the Cu from the tested fly ash sample. However, the metal speciation and the chemical composition, e.g. SO_4^{2-} content, of the fly ash can affect the release of metal ions both in electrodialytic remediation and in acid leaching.

Keywords: Separation Processes, Electrokinetic Remediation, Acid Extraction, MSWI Fly Ash

Article Highlights

- Metals were removable with electrodialytic remediation and acid leaching.
- Acid leaching resulted in a higher leachate yield than electrodialytic remediation.
- The kinetics of acid leaching is faster than electrodialytic remediation.
- Metal extraction efficiency varies between the different MSWI fly ash samples.

Introduction

Increased population growth and urbanisation have led to a larger generation of waste that is not expected to decrease [1]. Unrecyclable waste is either landfilled or incinerated for heat and power production. Municipal solid waste incineration (MSWI) reduces the volume of waste by approximately 90%, recovering the majority of energy bound in the waste [2]. However, toxic residues, e.g. MSWI fly ash, are produced. Due to its content of toxic metal compounds, chlorides and dioxins, MSWI fly ash is commonly landfilled as hazardous waste. Landfilling incineration residues may have long-term environmental consequences due to contaminant leaching [2] and result in the loss of potential resources, e.g. salts and valuable metals in the fly ash. Treating the ash can reduce the ash's toxicity and potentially recover the valuable metals as secondary resources. Several potential treatments have been investigated, categorised as either solidification/stabilisation, thermal treatments or separation/extraction [3]. Solidification/stabilisation and thermal treatments focus on reducing contaminant leaching without recovering valuable metals. In contrast, separation/extraction procedures concentrate on separating the metals from the fly ash for later recovery [3].

Acid leaching can be used to produce metal-enriched solutions and can be optimised by using specific acids or complex-forming agents to target specific metals [4,5]. The solution can then enter a solvent extraction process where the targeted metal ions are transferred to an organic solvent by specially designed molecules that form complexes with these specific metal ions. The separation is possible since the aqueous solution and the organic solvent are immiscible [6]. The metals of value can be transferred from the organic phase to a new aqueous phase by reversing the extraction chemical reaction during a stripping step [6]. Solvent extraction has recently been used to recover metals from MSWI fly ash by first leaching the metals from the ash with acidic leaching optimised for MSWI fly ash, followed by metal recovery by solvent extraction [6,7]. Depending on the acid and L/S ratio used, close to 100 % of either Cd, Cu, Pb and Zn could be removed with acid leaching [4,5].

Electrodialytic remediation (EDR) is the combination of electrokinetic remediation and electrodialysis. It works by applying a direct current between two electrodes in electrolyte solutions, resulting in the electromigration of ions from a fly ash suspension towards the anode and cathode [8]. The migration of ions is controlled by anion and cation exchange membranes separating the electrolyte solutions from the fly ash suspension. At an acidic pH, the metal compounds will be dissolved, and their ions can electro migrate in the electric field. The

efficiency of EDR is, therefore, related to pH and total remediation time. EDR has been shown to remove between 1 and 61% at a neutral to slightly alkaline pH, depending on the metal [9,10].

Jensen et al. [11] determined that electrodialytic remediation had a higher extraction of up to 80% As and Zn, Cd, 70 % Cu, 50 % Cd, Cr and Ni and 20 % Pb from soil washing residue than batch acidic leaching with HNO_3 at around pH 2 for five different soils. Even though soil washing residue has a different chemistry than MSWI fly ash, the results of Jensen et al. [11] may suggest that EDR could remove more toxic metals from MSWI fly ash as well, compared to acid leaching, at an acidic pH. Testing the different alternatives for separating and extracting metals from MSWI fly ash is essential when determining the best treatment option.

The present study's objectives were twofold: 1) Testing the efficiency of electrodialytic remediation and leaching with HNO_3 or HCl, based on removing Cd, Cr, Cu, Pb and Zn from MSWI fly ash. 2) An additional objective was to determine the amount of Cu that can be extracted from an MSWI fly ash sample that had not been studied before by combining HCl leaching and solvent extraction, using different extractant concentrations and extraction times.

Materials and Methods

Materials

Three fly ash samples were obtained for this study in 2018 from commercial MSWI plants, incinerating waste for heat and power: 1) Arc-Fa was obtained from Amager Bakke in Copenhagen, Denmark; 2) Nuuk-Fa was obtained from the waste incinerator in Nuuk, Greenland; 3) Rya-Fa was obtained from Ryaverket in Borås, Sweden. The MSWI fly ash was sampled on-site by the operators. Information on the three incineration plants is included in Table 1. Fly ash is removed from the flue gas at Ryaverket after lime is injected into the flue gas.

Table. 1 Average operating conditions of incineration plants during sampling periods, as presented in [12].

		Amager Bakke	***Nuuk***	***Ryaverket***
Furnace		Grate	Grate	Fluidised bed
Waste type		Household/	Household/	Household/
Flue gas treatment		After fly ash removal	None	Before fly ash removal (lime injection)
Flue gas filter type		Electrostatic	Electrostatic	Textile
Incineration temp	[°C]	1025	1064	900
Incineration capacity	[ton/day]	1680	40	300
Fly ash	[ton/day]	14.8	0.3	8.9
Bottom ash	[ton/day]	237	4.7	17.8

Table 2 contains the element concentrations in the raw MSWI fly ash samples, as presented in [12] and also for water-washed ash. The main element and trace element concentrations were determined by X-ray fluorescence (XRF) analysis by an external lab. They measured the concentrations with a SPECTRO Gmbh X-LAB 2000 on ground samples (< 200 µm). The software used was TQ-3945r. The main element concentrations were back-calculated as oxides from the measurements. [12]The crystalline compounds present in the ashes, determined with X-ray diffraction, was described in [12] and performed using a Pan-Alytical X'pert PRO Θ–Θ System on samples ground in a mortar. Peak identification was performed using the ICDD PDF4 database. The samples Nuuk-Fa and Rya-Fa had similar $CaSO_4$, $CaCO_3$, KCl and NaCl peaks, while Arc-Fa had peaks for $CaSO_4$, KCl and NaCl as well as other minerals with S, not found in the other ashes [12].

Table. 2 Calculated oxide composition [12] and toxic metal concentration of the MSWI fly ash samples[12]. W-washed MSWI fly ash. (-) Below Detection Limit.

		Arc-Fa	***Arc-FaW***	***Nuuk-Fa***	***Nuuk-FaW***	***Rya-Fa***	***Rya-FaW***
SiO_2	[Wt%]	4.6	8.1	6.1	7.7	6.4	7.9
Al_2O_3	[Wt%]	1.4	1.9	4.6	4.9	4.7	5.3
Fe_2O_3	[Wt%]	1.0	1.4	0.9	1.0	1.8	2.1
CaO	[Wt%]	13	18	43	43	43	41
MgO	[Wt%]	0.6	0.8	1.4	1.8	1.8	2.2
SO_3	[Wt%]	34	28	8.9	8.5	8.9	8.7
K_2O	[Wt%]	14	10	12	1.3	2.7	1.0
Na_2O	[Wt%]	7.4	-	22	0.7	7.0	2.8
P_2O_5	[Wt%]	2.6	2.2	1.8	1.9	2.2	2.5
Cl	[Wt%]	2.8	0.8	24	1.5	13	3.6
Cd	[mg/kg]	480	290	420	420	80	90
Cr	[mg/kg]	300	500	800	800	400	500
Cu	[mg/kg]	1,400	2,300	1,300	1,400	7,900	8,600
Pb	[mg/kg]	12,000	20,000	3,200	2,200	3,400	3,000
Zn	[mg/kg]	55,000	61,000	33,000	33,000	6,600	7,500

The MSWI fly ash samples used for the EDR experiments were washed with distilled water in three stages to reduce their chloride content. During remediation, chloride ions may migrate towards the anode and evaporate as chlorine gas [13]. The changes in fly ash composition are included in Table 2. The fly ash samples were washed in three consecutive stages at L/S 5, filtered through a Frisenette type 1125 filter and dried at 50°C, using the procedure described in [12]. The fly ash samples' water-soluble mass was 56, 38 and 28 wt% for Arc-Fa, Nuuk-Fa and Rya-Fa, respectively [12].

Experiments

HNO_3 Leaching

The leaching of Cd, Cr, Cu, Pb and Zn from the studied ashes (both raw and water washed ash samples) at a decreasing pH was determined by mixing 1 g of sample with 25 ml of either distilled water or increasing molarities of HNO_3. The HNO_3 molarities used were dependent on the fly ash samples' pH when mixed with distilled water and is shown in Table 3. The final pH aimed at was 10, 8, 6, 4, 2, 1 and < 1. The samples were mixed on a shaking table at 200 rpm for seven days. After this period, the solution's pH was measured with a Radiometer electrode after the sample had settled for 15 minutes. The liquid phase was filtered using a 45 µm filter and analysed by ICP-OES.

Table. 3 HNO_3 concentrations used for HNO_3 leaching of the raw and washed samples.

Arc-Fa	***Nuuk-Fa***	***Rya-Fa***
0.02 M HNO_3	0.1 M HNO_3	0.1 M HNO_3
0.05 M HNO_3	0.2 M HNO_3	0.2 M HNO_3
0.08 M HNO_3	0.3 M HNO_3	0.3 M HNO_3
0.1 M HNO_3	0.35 M HNO_3	0.35 M HNO_3
0.2 M HNO_3	0.4 M HNO_3	0.4 M HNO_3
0.3 M HNO_3	0.5 M HNO_3	0.5 M HNO_3
	0.6 M HNO_3	0.6 M HNO_3

HCl Leaching

HCl leaching experiments at constant pH were performed using a programmable Metrohm 905 Titrando titrator, equipped with a Radiometer analytical electrode for pH measurements and a plastic propeller stirrer set to Methrohm 905 Titrando stirring rate 8. These experiments were only performed on the raw fly ash samples. The Radiometer analytical electrode was calibrated before each experiment using buffer solutions in the pH range 1 to 12. The titrator was programmed to reduce and maintain a suspension at pH 2 for an extended period. The suspension consisted of 10 g unwashed fly ash and 50 ml distilled water (L/S 5) at the experiments' start. The titrator was programmed to initially stir the suspension for one hour without adding acid while measuring the initial pH. The program comprised eight loops of reducing the pH to pH 2 and measuring the pH, ending the program after executing the eight loops. The time used for each consecutive loop varied for the three samples, depending on the volume of acid required to maintain a pH of 2.

A 3M HCl solution was used for the experiments. The end L/S ratio was 5.7, 7.8 and 8.3 for Arc-Fa, Rya-Fa and Nuuk-Fa, respectively. The concentrations of Cd, Cr, Cu, Pb and Zn in the suspension were determined after 1,

2, 3, 4, 6, 8, 10 hours and at the end of the program. Each experiment was performed in triplicate at ambient temperatures. The leachate was filtered after each experiment using a vacuum pump and a 45 µm filter.

Electrodialytic remediation

The electrodialytic remediation (EDR) cells (two-compartment and three-compartment cells) used in this study are illustrated in Fig. 1. Two experiments for each fly ash were performed, one for each of the cell setups. The cells were cylindrical and made from polymethyl methacrylate. The inner and outer diameter was 8 and 10 cm, respectively. Compartment II in Fig. 1a and Compartment I in Fig. 1b were stirred compartments containing the fly ash and distilled water suspension. The stirring setup consisted of a flexible plastic flap fastened to a glass rod connected to a Vos 14 overhead stirrer.

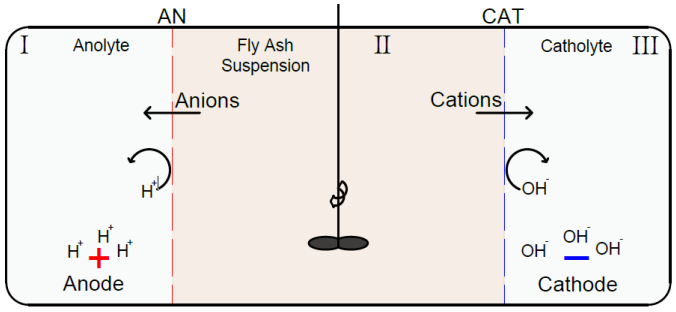

a

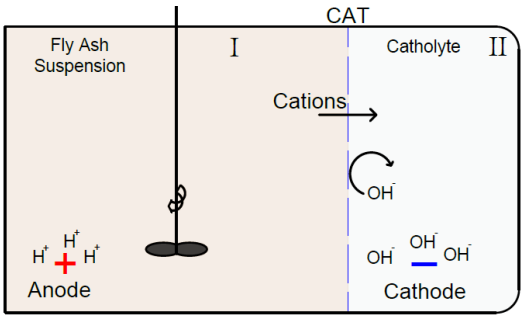

b

Fig. 1. Three compartment cell setup (a) and two-compartment cell setup (b).
AN – anion exchange membrane, CAT – Cation exchange membrane.

The remaining compartments, containing the cathode and anode (platinum-coated titanium wires with a diameter of 3 mm), were concentration compartments filled with an electrolyte solution (500 ml 0.01 M $NaNO_3$ solution adjusted to a pH of 2 with HNO_3). The anode and cathode compartments were separated from the fly ash suspension chamber by ion-exchange membranes ensuring that the direction of ion transport was outwards of the suspension. The anion exchange membranes were 204 SZRA B02249C, and the cation exchange membranes were CR67HUY N12116B. Both membrane types were from Ionics. In the two-compartment setup, the anode was placed directly in the fly ash suspension. The fly ash suspension compartment was 10 cm long,

and the electrolyte compartments were 5 cm long. During remediation, the pH of the fly ash suspension decreases due to the anode reaction ($H_2O \rightarrow ½\ O_2 + 2H^+ + 2e$) at the anode in the two-compartment cell and water splitting ($H_2O \rightarrow H^+ + OH^-$) at the anion exchange membranes in the three-compartment cell [14]. The catholyte's pH increases due to the cathode reaction ($2H_2O + 2e^- \rightarrow H_2 + 2OH^-$). During the experiments, the catholyte pH increase was adjusted to below pH 2 every day with HNO_3. The fly ash suspension consisted of 100 g ash and 350 ml distilled water (L/S 3.5). A DC power supply (HP E3612A) was used to maintain a constant current of 50 mA and monitor the voltage fluctuations. The conductivity and pH of the fly ash suspension were measured once per day, together with the voltage. The experiments lasted 28 days and were performed at ambient temperatures. Water flux occurred during the 28 days and was diminished by adjusting the pumping rate.

The fly ash suspension was filtered through a 45 µm filter at the end of each experiment. The treated material was dried at 50 °C, and its content of Cd, Cr, Cu, Pb and Zn analysed by ICP-OES, using the method described in [12]. The membranes and stirrer were submerged in 1M HNO_3 and the electrodes in 5M HNO_3 to release any accumulated metals. The concentrations of Cd, Cr, Cu, Pb and Zn in the liquids were then analysed with ICP-OES. The wt% metals removed using EDR are defined as the wt% metals removed from the ash to the fly ash suspension, membranes and electrolyte solutions.

An estimate of the total amount of mmol H^+/g ash used during electrodialytic remediation can be made based on the assumption that the electric current is used entirely to generate H^+. The total amount of H^+/g ash generated can then be estimated from:

$$Q = I \cdot t/F$$

F is faradays number, t is the length of the experiment, and I is the applied current.

Solvent extraction

The solvent extraction experiments were only performed on the filtered HCl leachate from the pH static experiment with Rya-Fa. The extractant used to recover Cu was an aldoxime extractant LIX860N-I (5-nonyl-salicyl-aldoxime) used in similar experiments [6,7]. The organic phase consisted of kerosene (Solvent 70) and LIX860N-I. The solvent extraction experiments were performed in triplicate with a phase ratio of 1 (aqueous volume = organic volume) in 3.5 ml glass vials sealed with plastic lids. An IKA Vibrax VXR Basic thermostat

sample shaker was used to mix the phases at 500 rpm. The temperature was set to 25 °C. The extraction of metals with an aldoxime can, in general, be described as:

$$M_{(aq)}^{z+} + zHA_{(org)} \leftrightarrow MA_{z(org)} + zH_{(aq)}^{+}$$

M is the metal, z is the valency, and HA is the protonated extractant [6]. The Cu extraction percentage *E* was calculated based on the distribution ratio D_M.

$$D_M = \frac{[M]_{org}}{[M]_{aq}}$$

$$E = \frac{D_M}{D_M + \frac{V_{aq}}{V_{org}}} \cdot 100$$

$[M]_{org}$ and $[M]_{aq}$ is the metal concentration in the organic phase and the aqueous phase, respectively. The Cu concentration in the organic phase could not be measured directly with ICP-OES. Instead, it was determined based on the measured concentration difference in the aqueous phase before and after the experiment. Two series of experiments were performed. The first using varying concentrations of LIX860N-I (0.01, 0.025, 0.05, 0.1 and 1 mol/l) in the organic phase and 5 minutes of contact time. The second with varying contact time (1, 3, 5, 10, 30 and 60 min) and a LIX860N-I concentration of 0.01 mol/l in the organic phase.

Results & discussion

HNO_3 leaching

The results of the HNO_3 leaching experiments are included in Fig. 2 for the raw and washed fly ash samples. Close to 100 wt% Cu could be removed from the unwashed samples at an acidic pH in the present study showing similarities to previous HNO_3 leaching experiments with MSWI fly ash [15,16]. However, the unwashed Nuuk-Fa sample deviated from the previous studies, with approximately 70 wt% Cu removed. The previous studies [15,16] also found that approximately 100 wt% Cd and Zn could be removed from MSWI fly ash. In contrast, between 65-95 wt% Cd and 70-100 wt% Zn could be removed from the unwashed samples at an acidic pH in the present study.

According to the Pourbiax diagrams for Zn and Cu in pure acidic and alkaline solutions [17], Zn and Cu are present as Zn^{2+} and Cu^{2+} at a pH below 7. At a pH above 7, Zn is present as $Zn(OH)_2$ and Cu as CuO or Cu_2O [17]. At a pH above 10, Zn is present as $HZnO_4^-$ or ZnO_2^{2-}, while Cu is present as CuO_2^{2-} or CuO_2^- at pH 14 [17]. Zn and Cu leached from the three samples in the present study at a pH below 8, suggesting that Zn and Cu could be present as Zn^{2+} and Cu^{2+} in the leachates as $Zn(OH)_2$, CuO or Cu_2O at higher pH. Brookins [18] investigated a Cd-S-C-O-H system and determined that depending on the Cd concentration, either $CdCO_3$ or $Cd(OH)_2$ is present at a pH above 10 and CdO_2^- at pH 14. A previous study using the same samples [12] determined that Rya-Fa and Nuuk-Fa contained carbonates, e.g. $CaCO_3$. In the present study, Cd leached from the three samples at a pH below 8, suggesting Cd is present as Cd^{2+} below pH 8 and as either $CdCO_3$, $Cd(OH)_2$ at a higher pH.

The previous studies [15,16] also determined that 10-50 wt% Cr and 50-75 wt% Pb can be leached at an acidic pH, while the results of the present study showed that 15-40 wt% Cr and 1-50 wt% Pb could be leached at an acidic pH from the unwashed samples. The sample Arc-Fa had a leaching yield of only 1 wt% Pb at a pH less than 1. Pb is present as Pb^{2+} at acidic, neutral and basic pH in pure acidic or alkaline solutions [17]. In the present study, Pb leached from Rya-Fa and Nuuk-Fa at a pH of 12 and a pH of less than 5. For Pb in a CO_2 containing solution, a passivation zone occurs close to neutral pH due to the formation of insoluble $PbCO_3$ [17]. At an alkaline pH, $HPbO^{2-}$ is present, while Pb^{2+} is present at a pH of less than 5 [17]. Furthermore, for Pb in an SO_4^{2-} containing solution, a passivation zone occurs at an acidic and neutral pH due to the formation of insoluble $PbSO_4$ [17]. The previous study by Ebert et al. [12] determined that the raw Arc-Fa sample contained

21 wt% water-soluble SO_4^{2-} anions, compared to 0.2 and 0.6 wt% for Rya-Fa and Nuuk-Fa, respectively, resulting in passivation. In the present study, Cr leached at an alkaline pH and an acidic pH. This was especially prevalent for the samples Rya-Fa and Nuuk-Fa. According to Pedeferri [17], at pH 0-5, Cr^{3+} is prevalent in the aerated Cr-O-H system and $Cr(OH)_3$ at pH 5-14. The leached Cr in the present study likely leached as Cr^{3+} at pH 0-5 and bound as $Cr(OH)_3$ at pH 5-6. The Pourbiax diagrams by Pedeferri [17] do not account for the leaching that occurred at pH 6-12. However, different ions may have affected the process, as observed for Pb.

Water washing the MSWI fly ash samples did, in general, not alter the leaching behaviour at the various pH values. However, the wt% of metals removed from Nuuk-Fa increased, suggesting that removing other soluble species, e.g. K, Na, Cl and S, increased metal removal. Additionally, Zn removal from Arc-Fa was reduced. The most notable difference is the loss of Zn leaching from Rya-Fa and Pb leaching from Rya-Fa and Nuuk-Fa at an alkaline pH. The initial pH in distilled water for the washed Rya-Fa and Nuuk-Fa is below pH 12, suggesting a pH reduction could have reduced the yield in the alkaline range. The washing process mainly removed the soluble K, Na, Cl and S from the fly ash samples see Table 2. Therefore, Cl and S's removal has not affected leaching, or the concentration of these ions in the ash is perhaps still high enough to affect leaching. Although soluble sulphate was removed from Arc-Fa, the Pb leaching remained unchanged. The sample Arc-Fa still contained high amounts of S, compared to the other samples, suggesting that additional SO_4^{2-} could be released at an acidic pH, binding the Pb as $PbSO_4$.

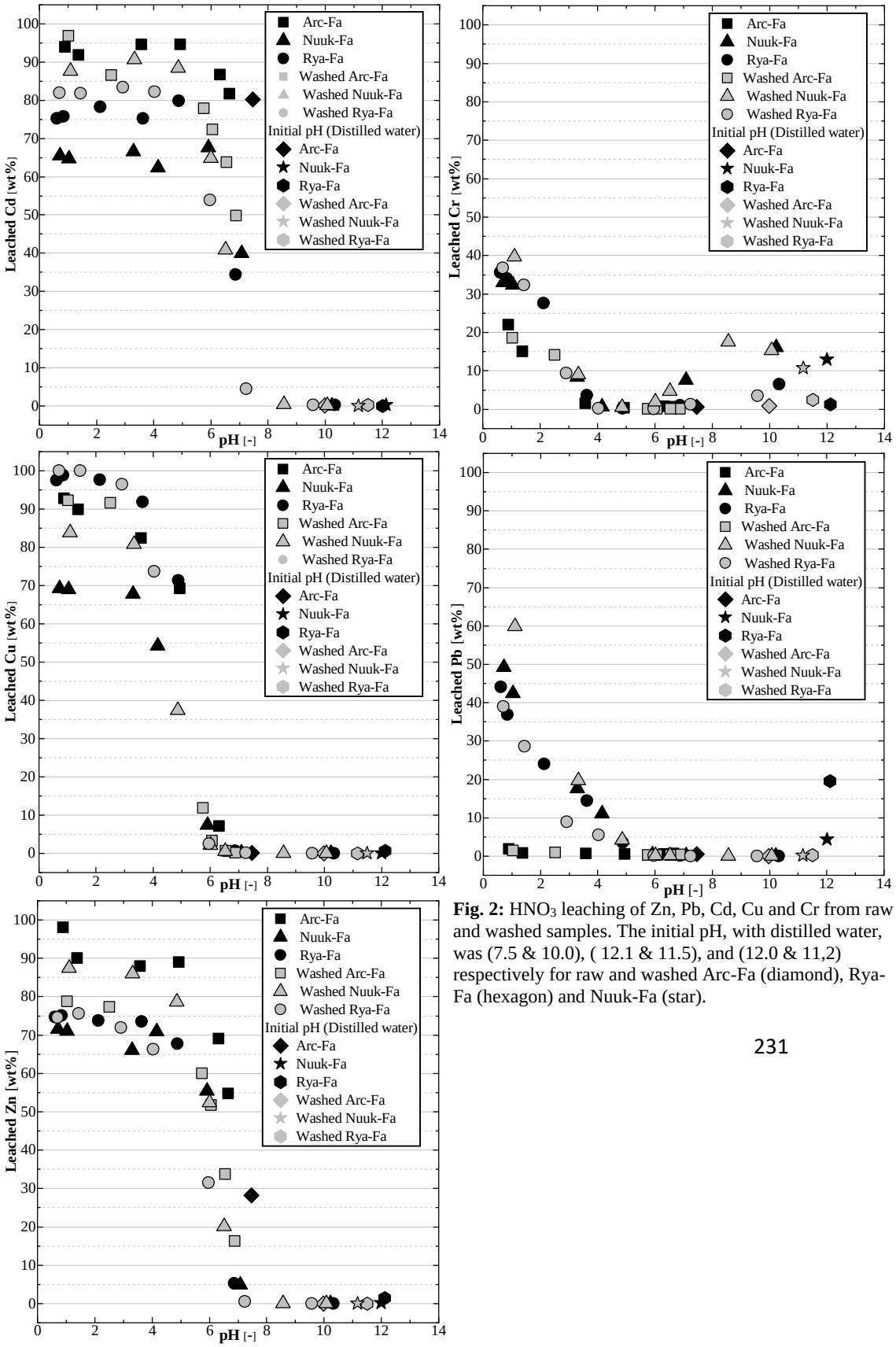

Fig. 2: HNO_3 leaching of Zn, Pb, Cd, Cu and Cr from raw and washed samples. The initial pH, with distilled water, was (7.5 & 10.0), (12.1 & 11.5), and (12.0 & 11,2) respectively for raw and washed Arc-Fa (diamond), Rya-Fa (hexagon) and Nuuk-Fa (star).

231

HCl Leaching

The average pH development during the HCl leaching experiments is depicted in Fig. 3, together with the total number of acid equivalents used to maintain a pH close to 2. The suspensions' final pH levels were 2.1, 2.3 and 2.23, respectively, for Arc-Fa, Rya-Fa and Nuuk-Fa. The samples Rya-Fa and Nuuk-Fa required 9 and 10 mmol H^+/g ash, respectively, while less than 3 mmol H^+/ g ash was required for Arc-Fa to reach pH 2. Previous acid leaching experiments by Tang et al. [4] showed that approximately 9 mmol H^+/ g ash were required to maintain a pH of approximately 2. Furthermore, Fedje et al. [5] determined that the acid neutralising capabilities of MSWI fly ash is high. The neutral pH of Arc-Fa in distilled water compared to the alkaline pH of the samples Rya-Fa and Nuuk-Fa could explain the differences in acid equivalents required to reach a pH of 2. The sample Arc-Fa consisted of less Ca than Rya-Fa and Nuuk-Fa and would, therefore, not contain as much CaO, $Ca(OH)_2$ or $CaCO_3$. Hydrochloric acid reacts with $CaCO_3$ under the following reaction:

$$2HCl_{(aq)} + CaCO_{3(s)} \rightarrow CaCl_{2(aq)} + H_2O_{(l)} + CO_{2(g)}$$

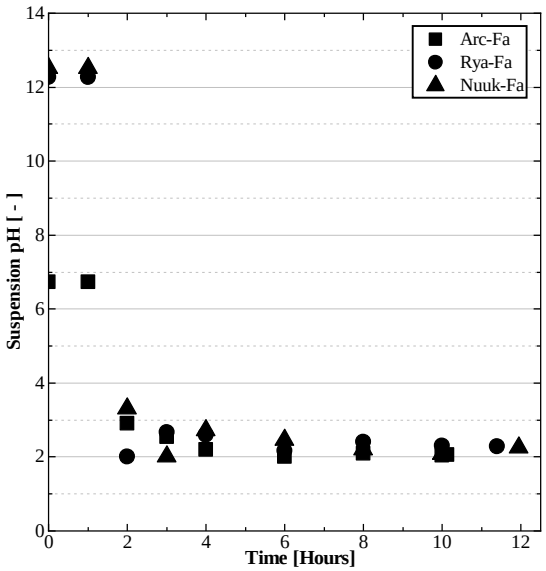

FIG. 3: pH DURING HCL ACID LEACHING EXPERIMENTS.

The wt% of Zn, Pb, Cd, Cu and Cr leached during the HCl leaching experiments are depicted in Fig. 4. As observed for the HNO_3 leaching experiments, several metals leached when the samples were mixed with distilled water at pH 6.7, 12.2 and 12.5 for Arc-Fa, Rya-Fa and Nuuk-Fa, respectively. However, the majority of the metals were leached when the pH approached 2. At a pH of 2, the leachate metal speciation is expected to be Cd^{2+}, Cr^{3+}, Cu^{2+}, Pb^{2+} and Zn^{2+}, as discussed for HNO_3 leaching. A previous study has shown that 77 wt% Zn, 75 wt% Cu [4,5] and 100 wt% Cd [4] could be leached when using HCl at L/S ratios of 5, 20 and 50, whereas Pb leaching was higher with a lower L/S ratio [4]. Additionally, 100 wt% Cu could be leached from MSWI fly ash at an L/S of 5 with 3 M HCl [4,5]. The present study deviates from the previous results, as between 60-90 wt% Cd, 0.5-85 wt% Cu and 60-90 wt% Zn was removed from the unwashed samples. Cu removal deviated significantly from previous research, as less than 5% Cu leached from Nuuk-Fa, while 85 and 80 wt% leached from Rya-Fa and Arc-Fa, respectively. The sample Nuuk-Fa had an initial increase in leached Cu between the first and second hour of the leaching experiment, followed by a decrease in leached Cu. Previous studies determined that 100% Pb can be leached from MSWI fly ash using 3M HCl at an L/S of 5 [4,5]. The highest concentration of Pb leached was 55 wt% from Rya-Fa in the present study, while 30 wt% leached from the sample Nuuk-Fa and less than 0.1 wt% leached from the sample Arc-Fa. As with the HNO_3 leaching, this may be attributed to the precipitation of $PbSO_4$, as previously discussed.

Additionally, Pb leaching from Nuuk-Fa decreased during the first 2 hours of acidification, followed by an increase during the remainder of the experiments. Cr leaching varied between the three samples. The sample Nuuk-Fa leached 30 wt%, while 10 and 15 wt% leached from Arc-Fa and Rya-Fa, respectively. The previous experiments [4,5] lasted between 24-72 hours. Had the present study's experiments continued for up to 72 hours, the leached concentrations might have been higher. A difference in the chemical speciation of the metals could affect the leaching as well. Lassesson et al. [19] studied the influence of chemical speciation on Cu's release from MSWI fly ash. MSWI fly ash containing Cu (II) species, e.g. sulphates, hydroxides and chlorides, leached 100 % of its Cu, while fly ash with Cu oxidation states 0, I and II, e.g. phosphates or silicates, leached 60 % of its Cu. Differences in the metal's chemical speciation between the present study's samples could explain the differences in leached concentration between the samples in the present study and previous studies.

Similar metal leaching yields as HNO_3 batch leaching could, in general, be achieved. Although higher concentrations of Zn and Cr was leached from Rya-Fa than with HCl since HNO_3 is an oxidizing acid. Higher concentrations of Cu were leached from Arc-Fa and Nuuk-Fa with HNO_3 than with HCl as well. However, a

higher concentration of Pb was leached from Rya-Fa with HCl. HCl has previously been shown to leach more Pb, Zn [4,5], Cd [4] than HNO_3 and either more Cu [4] or a similar concentration to HNO_3 [5]. The increased leaching yield with HCl can be attributed to the formation of chloride complexes in the solution [4] and [20], where chloride ions can form several different complexes with Cd^{2+}, Cr^{3+}, Cu^{2+}, Cu^{+}, Pb^{2+} and Zn^{2+} [21]. The increased leaching yield with HNO_3 seen in the present study could result from the longer experiment time or that the chloride content in the ashes is enough to form chloride complexes without external chlorides. However, the increased Pb leaching yield with HCl could be due to Pb chloride complexes' formation.

The low Cu and Pb leaching from Nuuk-Fa with HCl acid could result from a higher metallic aluminium content than in the other fly ashes. Metal from household waste is not separated in Greenland before incineration [22], whereas Al cans will go into the incineration plants, which is opposite the waste management systems in Denmark and Sweden[22], implying a higher metallic aluminium content in Greenlandic MSWI fly ash. During HCl leaching, more noble metal ions such as Cu^{2+} and Pb^{2+} react with less noble metals such as Al^{0}, forming reduced precipitates, Weibel et al. [20]. The addition of an oxidising agent, e.g. HNO_3, suppresses this type of precipitation due to the metallic components in the fly ash being oxidised. During leaching with HCl, Cu^{2+} and Pb^{2+} could have precipitated as Cu^{0} and Pb^{0} due to the reducing conditions in Nuuk-Fa, while HNO_3 ensures oxidising conditions and prevents precipitation. Leaching with HCl did not increase the Pb yield from raw Arc-Fa, suggesting the Pb is bound as $PbSO_4$ during HCl leaching as well. The solubility of $PbCl_2$ is 9.9 g/l [23] compared to 0.4 g/l for $PbSO_4$ [24].

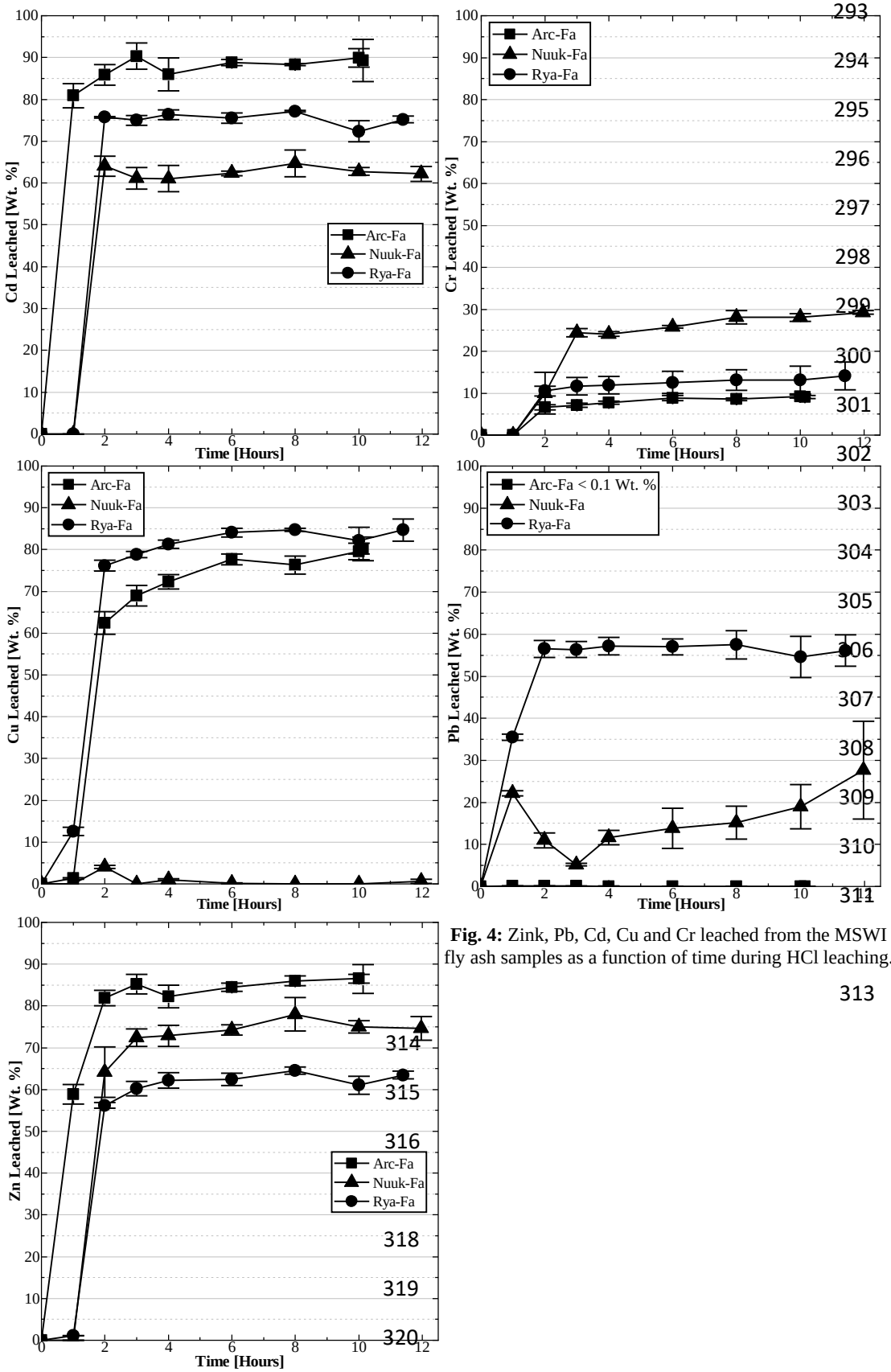

Fig. 4: Zink, Pb, Cd, Cu and Cr leached from the MSWI fly ash samples as a function of time during HCl leaching.

Electrodialytic remediation

The pH development in the suspension chamber during the electrodialytic remediation experiments is shown in Fig. 5. The sample Arc-Fa reached a pH of 0.5, Rya-Fa, a pH of 1 and Nuuk-Fa, a pH between 2 and 3, depending on the experiment cell setup. The applied current during each EDR experiment and each experiment's length were the same for each sample, resulting in 12.5 equivalent mmol H^+/g ash used during remediation. The differences in pH development are due to the ash samples' acid buffering differences as observed for the HCl leaching. The fly ash suspensions pH of the six experiments decreased as in previous studies [9,13]. However, the sample Arc-Fa reached a pH below 2 faster than Rya-Fa and Nuuk-Fa and had an almost constant pH after 15 days of remediation not observed in previous studies. Higher metal removal is therefore expected in the electrodialytic experiments with Arc-Fa. [13]

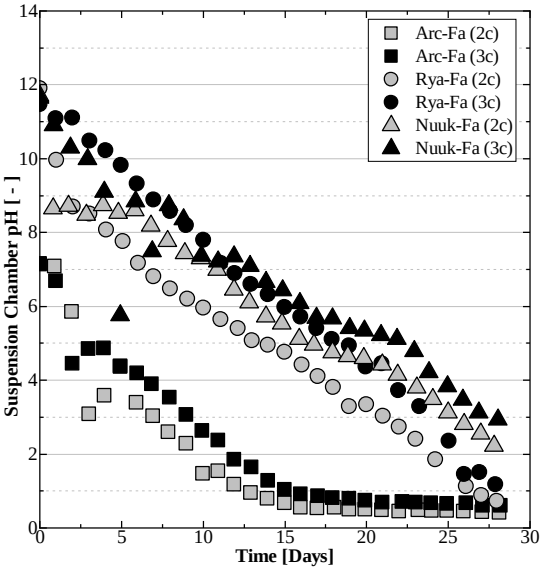

FIG. 5: PH IN THE MSWI FLY ASH SUSPENSIONS DURING THE EXPERIMENTS. 2C - 2 COMPARTMENT CELL, 3C– 3 COMPARTMENT CELL.

The wt% distribution of Cd, Cr, Cu, Pb, and Zn at the end of the electrodialytic remediation (EDR) experiments are shown in Fig. 6. Generally, the removal order was Cd > Zn > Cu > Pb, Cr. Higher removal rates were achieved in the 2 compartment cell (2c) setup compared to the 3 compartment cell (3c) setup. The highest metal removal was observed for Rya-Fa, 2 compartment cell, where up to 100 % Zn, 80 % Cu, 45 % Cd, 21% Pb and 11% Cr was removed. The majority of the metals electromigrated towards the cathode, indicating mainly positively charged metal ions. However, during the 3c remediation experiments, 4-22 wt% of the metals migrated towards the anode, depending on the sample and metal investigated. According to the Pourbiax diagrams of Pedeferri [17], the studied metals would have a valency of 2+ (Cd, Cu, Pb, Zn) or 3+ (Cr) in an aqueous solution at the experimental pH. At high enough potentials, negative Cr phases could occur. However,

348 this only occurs outside the water stability zone E (V SHE) > 1. Previous research [25] have shown that the
349 redox potential in the suspension chamber of a 3c setup is between 0.15 and 0.45 V (within water stability).
350 Washing the MSWI fly ash samples reduced the Cl content in the ashes. However, it did not remove all Cl
351 present in the samples, as seen in Table 2. Therefore, negatively charged metal chloride complexes such as
352 MCl_3^- and $M_2Cl_4^-$ can be formed and move toward the anode [21]. Metals can be transferred due to
353 interdiffusion [26], which also could be the reason for finding metals in the anode compartment.

354 Previous electrodialytic remediation studies with MSWI fly ash have shown varying degrees of metal removal at
355 L/S 3.5, 50 mA current and 14 days duration. In the study by Kirkelund et al. [9], 2 % Zn, Cd and Cu, 5% Pb
356 and 6 % Cr were removed in the 3c setup for Greenlandic fly ash. Another study by Kirkelund et al. [10]
357 showed that 53 % Zn, 2.5 % Pb, 61 % Cd, 3.3 % Cu and 1.1 % Cr could be removed in the 3c setup after 14
358 days and that 4.6 % Zn, 0.5 % Pb, 56 % Cd, 15 % Cu and 3.8 % Cr could be removed in the 2c setup from
359 another Danish fly ash. The final pH reached in the fly ash suspension in these studies was 8.9 [9], 8.2 (3c) and
360 6.4 (2c) [10]. Higher removal percentages to both the anode and cathode side were observed in the present study
361 than the previous studies [9] and [10] due to the lower pH in the fly ash suspension. As the efficiency of EDR is
362 related to the pH of the suspension and the duration of the EDR, higher removal percentages would be expected
363 for the experiments of the present study lasting 28 days compared to the previous reported lasting 14 days. The
364 efficiency of EDR also seems to be dependent on the fly ash sample as indicated by the lower Cr removal from
365 Rya-Fa compared to previous studies and higher Pb removal from Arc-Fa than other fly ash samples.

366 Electrodialytic remediation could remove Cu from Nuuk-Fa, suggesting that an oxidising agent, e.g. HNO_3, is
367 not required during remediation. However, less Cu could be removed from Nuuk-Fa using EDR compared to
368 HNO_3 leaching. As observed during the experiments with HNO_3 and HCl, Pb could not be removed Arc-Fa in
369 significant amounts, suggesting that Pb may precipitate as $PbSO_4$ during electrodialytic remediation.
370 Furthermore, Arc-Fa had the lowest Cu and Zn removal of the samples, despite reaching the lowest pH,
371 suggesting that the metal removal is not entirely pH-dependent.

372

373

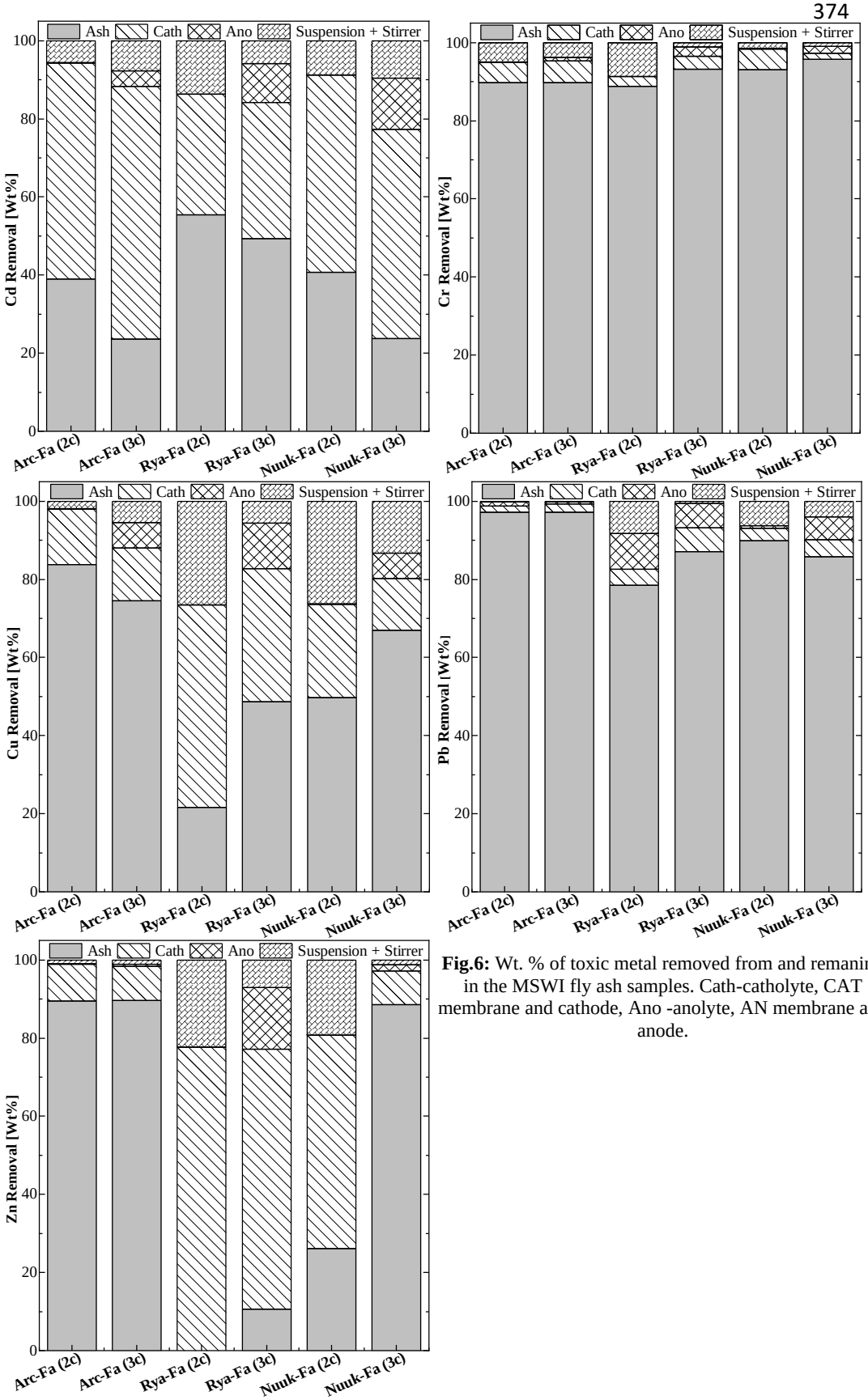

Fig.6: Wt. % of toxic metal removed from and remaning in the MSWI fly ash samples. Cath-catholyte, CAT membrane and cathode, Ano -anolyte, AN membrane and anode.

Removal Efficiency

A comparison of the removed wt% between the samples using HNO_3 on raw (HNO_3) and washed (HNO_3 W) samples, HCl leaching (HCl) and 2 or 3 compartment cell electrodialytic remediation (EDR) is shown in Table 4. The results (Fig. 2 and Fig. 3) showed that 80-81 wt% Cd, 0-1 wt% Cr, 0-1 wt% Cu, 0-1 wt% Pb and 28-60 wt% Zn leached from Arc-Fa, 0 wt% Cd, 0-1 wt% Cr, 1-13 wt% Cu, 20-35 wt% Pb and 1 wt% Zn leached from Rya-Fa and that 0 wt% Cd, 0-13 wt% Cr, 0 wt% Cu, 4-22 wt% Pb and 0 wt% Zn leached from Nuuk-Fa when mixed with distilled water. Although the washing water was not analysed, these metals could still have been partially removed during the pre-washing step before EDR and are for this comparison considered part of the removed amounts.

Table 4: Removal efficiencies (%) from the experiments.

		HNO_3	W HNO_3	HCl	EDR 2c	EDR 3c
pH	Arc-Fa	1.4	1.0	2.1	0.4	0.6
	Rya-Fa	2.1	1.4	2.3	0.7	1.2
	Nuuk-Fa	1.0	1.1	2.3	2.2	2.9
Cd	Arc-Fa	94	97	89	61	76
	Rya-Fa	75	82	75	45	51
	Nuuk-Fa	65	88	62	59	76
	Average	**78**	**89**	**75**	**55**	**68**
Cr	Arc-Fa	22	19	9.0	10	10
	Rya-Fa	36	37	14	11	7.0
	Nuuk-Fa	33	40	29	7.0	4.0
	Average	**30**	**32**	**14**	**7.1**	**3.5**
Cu	Arc-Fa	93	92	80	16	25
	Rya-Fa	98	100	85	78	51
	Nuuk-Fa	69	84	0.6	50	33
	Average	**87**	**92**	**55**	**48**	**36**
Pb	Arc-Fa	1.4	1.5	0.0	3.0	3.0
	Rya-Fa	44	39	55	21	13
	Nuuk-Fa	49	60	28	10	14
	Average	**31**	**33**	**28**	**10**	**9.0**
Zn	Arc-Fa	98	79	86	11	10
	Rya-Fa	75	75	63	100	89
	Nuuk-Fa	72	87	75	73	11
	Average	**82**	**80**	**75**	**61**	**37**
	Average	***62***	***65***	***49***	***36***	***31***

Generally, all three extraction methods' removal efficiency was high, and all methods are eligible for metal extraction. However, leaching with HNO_3 or HCl resulted in higher metal removal from the samples than electrodialytic remediation. Similar Cd (98-100 wt%) and Zn (90-100 wt%) removals could be achieved between the extraction methods. This could be expected; as Zn and Cd are generally leachable in higher percentages than Pb, Cu and Cr [15,16], they should be the more easily removable metals. Differences in leaching yield could be observed for Cu, Pb and Cr between acid leaching and EDR. This was especially apparent for Cr removal from Nuuk-Fa, where 92 wt% could be removed with HNO_3 and 16 wt% with EDR. The final suspension pH measured was lower with EDR than in acid leaching, except for the sample Nuuk-Fa,

suggesting that more metals can be removed using direct acid leaching at lower pH than EDR. Furthermore, 28 days of EDR were required to obtain the results, compared to 7 days of HNO_3 batch leaching or approximately 12 hours of pH static HCl leaching, suggesting that more metals can be removed using direct acid leaching in less time than EDR. Similar results, as in the previously discussed articles [9,10], might have been obtained at a reduced remediation time. If the present study's results were to be reproduced in less than 28 days, the experimental conditions should be optimised by, e.g. using a higher current density.

Directly leaching the toxic metals from MSWI fly ash is, therefore, the better-suited method for toxic metal removal from MSWI fly ash. This result is contrary to the study by Jensen et al. [11] that determined EDR to have a higher removal percentage of Zn, Pb, Cd, Cu and Cr from soil washing residues instead of HNO_3 leaching. A potential reason for the difference in leaching between MSWI fly ash and soil washing residues could be the speciation of the metals in the two materials, where the metals in soil washing residues are more readily extracted with EDR.

Solvent Extraction

The sample Rya-Fa was chosen to determine how extractable Cu is after HCl leaching due to its higher Cu content (7 g/kg ash) and leached Cu (almost 7 g/kg ash). The solvent extraction results are included in Fig. 7, depicting the Cu extraction percentage E as a function of the concentration of LIX860N-I in the organic phase (a) and time (b). The results showed that a concentration of 0.1 M LIX860N-I was sufficient to extract approximately 99 % of the Cu from the aqueous phase with 5 minutes of contact time. A concentration increase to 1 mol/l increased the extraction percentage close to 100 %. However, the time-dependent extraction experiment (Fig. 7b) showed that 3 minutes of contact time gave the highest Cu extraction and that longer contact times reduced the Cu extraction efficiency.

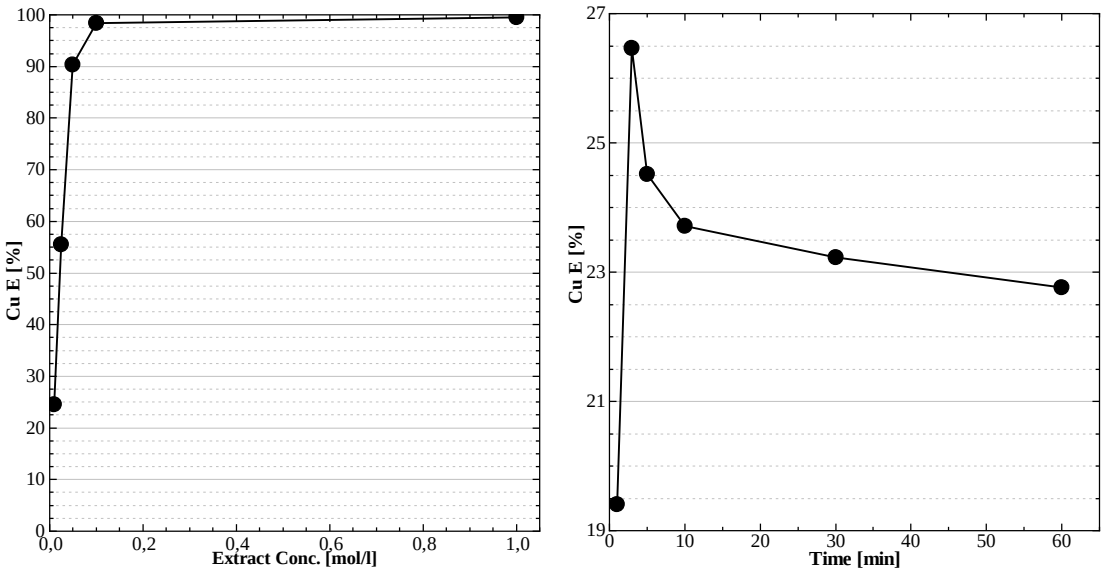

414

FIG.7: EXTRACTION PERCENTAGE OF CU FROM RYA-FA AQUEOUS PHASE AS A FUNCTION OF THE EXTRACTANT CONCENTRATION IN THE ORGANIC PHASE (EXTRACTION TIME 5 MIN) (A) AND AS A FUNCTION OF TIME (EXTRACTION CONCENTRATION 0.01 [MOL/L]) (B).

415

416

417 The influence of the LIX860N-I concentration in the organic phase on the distribution ratio for the Cu extraction
418 is shown in Fig. 8, with added trend line. The slope of the trend line is 1.41, suggesting that 1.5 LIX860N-I
419 molecules are required per extracted Cu transferred. However, Cu^{2+} requires 2 LIX860N-I molecules per
420 extracted Cu transferred, as previously shown by Tang et al. [6], suggesting that Cu(I) could be present and
421 extracted as well in this study.

422

423

424

425

426

427

428

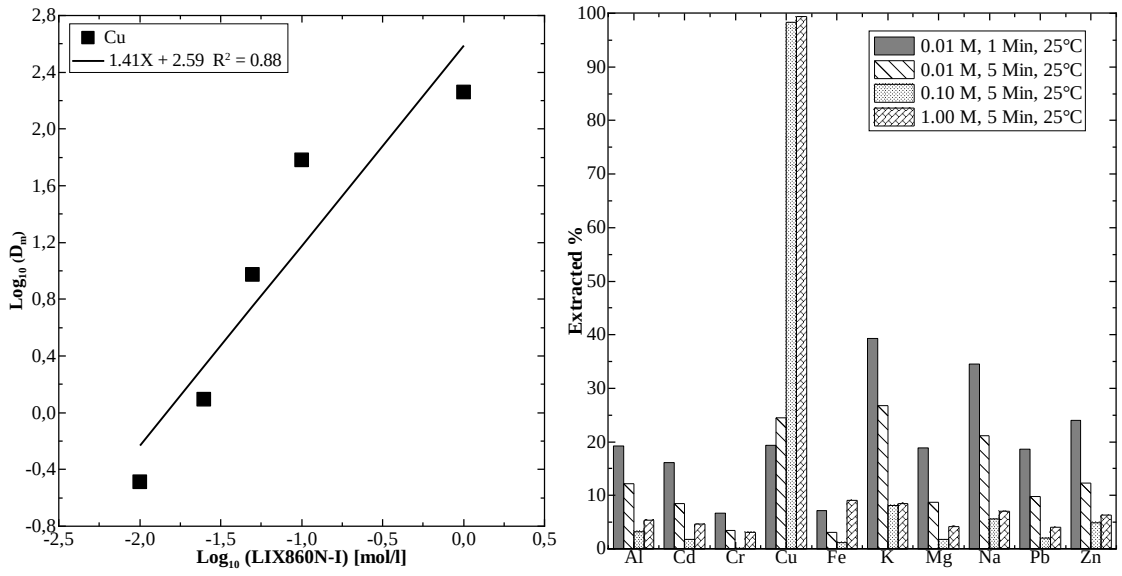

429

Fig. 8: (a) Influence of LIX860N-I concentration on the extraction of Cu, WITH ADDED TREND LINE $LOG_{10}(D) = 1.41\ LOG_{10}(LIX860N\text{-}I) + 2.59$. PERCENTAGE OF METALS EXTRACTED FROM THE ASH LEACHATE WITH VARYING CONCENTRATIONS OF LIX860N-I AND OVER TIME.

430

The percentage of other elements extracted from the ash leachate is shown in Fig. 8b for different concentrations of LIX860N-I in the organic phase and for 1 minute and 5 minutes of contact time. Increasing the contact time between the two phases from 1 minute to 5 minutes increased the Cu extraction and reduced the other elements' extraction. At an extractant concentration of 0.01 mol/l Al, Cd, K, Na, Pb and Zn were extracted in similar concentrations as Cu. LIX became more selective at higher concentrations, where approximately 100% of the Cu was extracted. At a concentration of 0.1 mol/l, other metals' extraction was less than 9 % and the Cu extraction close to 100 %. At a concentration of 1 mol/l, the extraction of other metals was slightly higher than at 0.1 mol/l, suggesting that the extractant concentration can be too high, unnecessarily extracting other metals, indicating that the optimal extractant concentration is 0.1 mol/l. The observed differences between the extracted concentrations of other metals could be related to the organic phase's pH. However, the pH of the organic phase was not measured. Tang et al. [6] determined that LIX860N-I was very selective, extracting none or low concentrations of other metals, except for Fe from one of the leachates. The differences in extracted metals between the leachate of the present study and Tang et al. [6] suggest that the Cu extraction selectivity depends on the MSWI fly ash leachate studied.

With an additional stripping step, Cu can be transferred to a new aqueous phase and be recovered with electrowinning. Tang et al. [6] determined that 85-95% of Cu can be transferred to a new aqueous phase with 1.5 M H_2SO_4 acid. The amount of other metals' co-extraction can be reduced further by reducing the contact time between the organic and aquatic phase from 5 minutes to 3 minutes. Furthermore, the solvent extraction can be upscaled using the industrial mixer settler system to increase resource recovery efficiency [27]. Therefore, acid leaching followed by solvent extraction could represent an effective method for recovering Cu from MSWI fly ash and be implemented as a viable option like the already utilised FLUWA process used to recover Zn in Switzerland [28]. Electrodialytic remediation could potentially be combined with solvent extraction of metals from the catholyte as well. However, if solvent extraction should be combined with EDR, it is recommended to use an alternative setup where an anion-exchange membrane prevents the metal ions from electrodepositing on the cathode. Furthermore, FLUWA uses acidic scrubber water (similar to dilute hydrochloric acid) from the combustion unit to leach metals from MSWI fly ash [28], limiting the need for additional chemicals and materials, further incentivising the use of an acid to recover the metals.

The Cu content in Rya-Fa was 6900 mg/kg indicating that MSWI fly ash can be a valuable source of Cu. If a subsequent stripping step can reverse the extraction as efficiently as seen in previous research by Tang et al. [6],

approximately 85 % of the 7900 mg/kg Cu in the Rya-Fa fly ash can be refined as usable Cu. The Cu content of ore mined from Aitik in Sweden is approximately 2500 mg/kg [7], indicating that more Cu can be retrieved per kg MSWI fly ash than per kg mined ore. However, the Aitik mine is estimated to produce 36 million tonnes of ore yearly [29](approximately 90,000 tonnes of Cu a year), compared to an approximate yearly production of 270,000 tonnes of MSWI fly ash in Sweden [30] (approximately 1800 tonnes of Cu a year, assuming 6900 mg Cu per kg ash). Although MSWI fly ash can be a valuable source of Cu, it cannot replace current mining practices. Furthermore, the Cu concentration in MSWI fly ash varies depending on the origin, as evidenced by the measured Cu concentration in the present study, see Table 2.

Conclusions

Comparable removal efficiencies of Zn, Cd could be achieved from three MSWI fly ash samples from different combustion units, using either HNO_3 leaching, HCl leaching or electrodialytic remediation. The highest removal percentages of Cu, Pb and Cr were achieved by leaching with acid rather than electrodialytic remediation. The higher leaching yield with acid was achieved at a higher pH and in less time, suggesting that direct acid leaching is, in general, the better-suited option for recovering valuable metals from MSWI fly ash than electrodialytic remediation. Depending on the fly ash sample's chemical composition and the targeted metal, electrodialytic remediation could be the better option, e.g. MSWI fly ash with high sulphur concentrations.

Using a concentration of 0.1 mol/l LIX860N-I and 5 minutes of contact time between the aqueous and organic phases is enough to recover 99 % of the leached Cu from Rya-Fa with solvent extraction. The experiments with varying contact time showed that this could be improved by reducing the contact time to 3 minutes. With an additional stripping step, the Cu can be transferred to a new aqueous solution (xg/L) and recovered with electrowinning making it an efficient method for recovering and potentially reusing the Cu. Although the Cu concentration can be higher in MSWI fly ash than in mined ore, the annual amount of fly ash produced is not enough to replace Cu from mined ore. Still, it represents a potential significant secondary source of Cu.

Acknowledgements

The many people working at the Department of Chemistry and Chemical Engineering – Nuclear Chemistry and Industrial Materials Recycling at the Chalmers University of Technology are each acknowledged for their assistance with the acidic leaching and batch extraction experiments. The lab technicians at the Department of Civil Engineering at the Technical University of Denmark are acknowledged for their assistance with the electrodialytic experiments. Finally, Amager Resource Center is recognised for its cooperation in obtaining ash from their facility. Kommuneqarfik Semersooq and Borås Energy och Miljö are recognised for sampling and sending the MSWI fly ash samples from the Nuuk incinerator in Greenland and Ryaverket in Sweden, respectively.

References

[1] S. Das, S.H. Lee, P. Kumar, K.H. Kim, S.S. Lee, S.S. Bhattacharya, Solid waste management: Scope and the challenge of sustainability, Journal of Cleaner Production. 228 (2019) 658–678. https://doi.org/10.1016/j.jclepro.2019.04.323.

[2] O. Hjelmar, Disposal strategies for municipal solid waste incineration residues, Journal of Hazardous Materials. 47 (1996) 345–368. https://doi.org/10.1016/0304-3894(95)00111-5.

[3] Y. Zhang, Z. Ma, Z. Fang, Y. Qian, P. Zhong, J. Yan, Review of harmless treatment of municipal solid waste incineration fly ash, Waste Disposal & Sustainable Energy. (2020). https://doi.org/10.1007/s42768-020-00033-0.

[4] J. Tang, B.-M. Steenari, Arie, Leaching optimization of municipal solid waste incineration ash for resource recovery : A case study of Cu , Zn , Pb and Cd, Waste Management. 48 (2016) 315–322. https://doi.org/10.1016/j.wasman.2015.10.003.

[5] K.K. Fedje, C. Ekberg, G. Skarnemark, B.-M. Steenari, Removal of hazardous metals from MSW fly ash-An evaluation of ash leaching methods, Journal of Hazardous Materials. 173 (2010) 310–317. https://doi.org/10.1016/j.jhazmat.2009.08.094.

[6] J. Tang, B.-M. Steenari, Solvent extraction separation of copper and zinc from MSWI fly ash leachates, Waste Management. 44 (2015) 147–154. https://doi.org/10.1016/j.wasman.2015.07.028.

[7] K. Karlfeldt Fedje, C. Ekberg, G. Skarnemark, E. Pires, B.-M. Steenari, Initial studies of the recovery of Cu from MSWI fly ash leachates using solvent extraction, Waste Management and Research. 30 (2012) 1072–1080. https://doi.org/10.1177/0734242X12441385.

[8] H.K. Hansen, L.M. Ottosen, B.K. Kliem, A. Villumsen, Electrodialytic remediation of soils polluted with Cu, Cr, Hg, Pb and Zn, Journal of Chemical Technology and Biotechnology. 70 (1997) 67–73. https://doi.org/10.1002/(SICI)1097-4660(199709)70:1<67::AID-JCTB662>3.0.CO;2-V.

[9] G.M. Kirkelund, P.E. Jensen, L.M. Ottosen, Electrodialytic extraction of heavy metals from greenlandic MSWI Fly Ash as a function of remediation time and L/S ratio, ISCORD 2013: Planning for Sustainable Cold Regions - Proceedings of the 10th International Symposium on Cold Regions Development. (2013) 87–96. https://doi.org/10.1061/9780784412978.009.

[10] G.M. Kirkelund, C. Magro, P. Guedes, P.E. Jensen, A.B. Ribeiro, L.M. Ottosen, Electrodialytic removal of heavy metals and chloride from municipal solid waste incineration fly ash and air pollution control residue in suspension - Test of a new two compartment experimental cell, Electrochimica Acta. 181 (2015) 73–81. https://doi.org/10.1016/j.electacta.2015.03.192.

[11] P.E. Jensen, L.M. Ottosen, B. Allard, Electrodialytic versus acid extraction of heavy metals from soil washing residue, Electrochimica Acta. 86 (2012) 115–123. https://doi.org/10.1016/j.electacta.2012.07.002.

[12] B.A.R. Ebert, B.-M. Steenari, M.R. Geiker, G.M. Kirkelund, Screening of untreated municipal solid waste incineration fly ash for use in cement-based materials: chemical and physical properties, SN Applied Sciences. 2 (2020). https://doi.org/10.1007/s42452-020-2613-7.

[13] G.M. Kirkelund, P.E. Jensen, L.M. Ottosen, K.B. Pedersen, Comparison of two- and three-compartment cells for electrodialytic removal of heavy metals from contaminated material suspensions, Journal of Hazardous Materials. 367 (2019) 68–76. https://doi.org/10.1016/j.jhazmat.2018.12.063.

[14] L.M. Ottosen, H.K. Hansen, C.B. Hansen, Water splitting at ion-exchange membranes and potential differences in soil during electrodialytic soil remediation, Journal of Applied Electrochemistry. 30 (2000) 1199–1207.

[15] A.J. Pedersen, Evaluation of assisting agents for electrodialytic removal of Cd, Pb, Zn, Cu and Cr from MSWI fly ash, Journal of Hazardous Materials. 95 (2002) 185–198. https://doi.org/10.1016/S0304-3894(02)00138-3.

[16] A.J. Pedersen, L.M. Ottosen, A. Villumsen, Electrodialytic removal of heavy metals from different fly ashes: Influence of heavy metal speciation in the ashes, Journal of Hazardous Materials. 100 (2003) 65–78. https://doi.org/10.1016/S0304-3894(03)00064-5.

[17] P. Pedeferri, Pourbaix Diagrams, in: S.N. Switzerland (Ed.), Corrosion Science and Engineering, 2018: pp. 57–72. https://doi.org/10.1007/978-3-319-97625-9_4.

[18] D. Brookins, Geochemical Behaviour of Antimony, Arsenic, Cadmium and Thallium: Eh -pH Diagrams for 25°C, 1-Bar Pressure, Chemical Geology. (1986) 271–278.

[19] H. Lassesson, K.K. Fedje, B.-M. Steenari, Leaching for recovery of copper from municipal solid waste incineration fly ash: Influence of ash properties and metal speciation, Waste Management and Research. 32 (2014) 755–762. https://doi.org/10.1177/0734242X14542147.

[20] G. Weibel, U. Eggenberger, D.A. Kulik, W. Hummel, S. Schlumberger, W. Klink, M. Fisch, U.K. Mäder, Extraction of heavy metals from MSWI fly ash using hydrochloric acid and sodium chloride solution, Waste Management. 76 (2018) 457–471. https://doi.org/10.1016/j.wasman.2018.03.022.

[21] A.E. Martell, R.M. Smith, Critical Stability Constants Volume 4: Inorganic Complexes, Springer Science + Business Media, LLC, 1976.

[22] R. Eisted, T.H. Christensen, Waste management in Greenland: Current situation and challenges, Waste Management and Research. 29 (2011) 1064–1070. https://doi.org/10.1177/0734242X10395421.

[23] Lead Chloride, National Library of Medicine. (2021). https://pubchem.ncbi.nlm.nih.gov/compound/Lead-chloride (accessed January 11, 2021).

[24] Lead Sulphate, National Library of Medicine. (2021). https://pubchem.ncbi.nlm.nih.gov/compound/Lead-sulfate (accessed January 11, 2021).

[25] G.M. Kirkelund, L.M. Ottosen, A. Villumsen, Electrodialytic remediation of harbour sediment in suspension-Evaluation of effects induced by changes in stirring velocity

and current density on heavy metal removal and pH, Journal of Hazardous Materials. 169 (2009) 685–690. https://doi.org/10.1016/j.jhazmat.2009.03.149.

[26] A.J. Pedersen, L.M. Ottosen, A. Villumsen, Electrodialytic removal of heavy metals from municipal solid waste incineration fly ash using ammonium citrate as assisting agent, Journal of Hazardous Materials. 122 (2005) 103–109. https://doi.org/10.1016/j.jhazmat.2005.03.019.

[27] J. Tang, M. Petranikova, C. Ekberg, B.-M. Steenari, Mixer-settler system for the recovery of copper and zinc from MSWI fly ash leachates: An evaluation of a hydrometallurgical process, Journal of Cleaner Production. 148 (2017) 595–605. https://doi.org/10.1016/j.jclepro.2017.02.015.

[28] G. Weibel, U. Eggenberger, S. Schlumberger, U.K. Mäder, Chemical associations and mobilization of heavy metals in fly ash from municipal solid waste incineration, Waste Management. 62 (2017) 147–159. https://doi.org/10.1016/j.wasman.2016.12.004.

[29] History and Development, (n.d.). https://web.archive.org/web/20150417162758/http://www.boliden.com/Operations/Mines/Aitik/Allmant/ (accessed November 10, 2020).

[30] Avfall Sverige, Swedish Waste Management 2018, 2018.

Journal Paper III

Effects of Chloride and Sulphates on Leaching from Mortar with Raw and Electrodialytically Treated MSWI Fly Ash

Benjamin A. R. Ebert, Gunvor M. Kirkelund

Effects of chlorides and sulphates on metal leaching from mortar with raw and electrodialytically treated MSWI fly ash

Benjamin A. R. Ebert, Gunvor M. Kirkelund*

[1]Department of Civil Engineering, Technical University of Denmark, Brovej, building 118, 2800 Kgs. Lyngby, Denmark

*corresponding author: gunki@byg.dtu.dk

Abstract

Municipal solid waste incineration (MSWI) fly ash could be used in cement-based materials, although metal leaching from both the MSWI fly ash and the cement-based materials remains a persistent obstacle. Here, electrodialytic treatment was used as pre-treatment to remove metals from MSWI fly ash before the fly ash was used mortar and the mortar exposed to different leaching solutions for testing the effect of varying environmental conditions in different scenarios. Mortar samples with 10 wt% replacement of cement with either raw or electodialytically treated MSWI fly ash were subjected to monolithic (in-use scenario) and crushed mortar (end-of-life scenario) leaching tests under exposure of acidified H_2O, NaCl or Na_2SO_4 solutions. The present study showed up to 80 % metal removal by the electrodialytic pre-treatment. Both NaCl and Na_2SO_4 generally increased the metal leaching yield from fly ash and cement-based materials compared to leaching with H_2O. Regulatory limits for disposing of the MSWI fly ash in non-hazardous waste landfills were exceeded, even if metals were removed by the electrodialytic treatment. Contrarily, leaching from monolithic mortar samples complied with the regulatory limits. Cr leaching exceeded the regulatory limits for all of the crushed mortar samples when using the NaCl or Na_2SO_4 solutions.

Keywords: Electrokinetic remediation, bench-scale, leaching, cement-based materials, Environmental Factors

Article Highlights

- Cd, Cu, Pb and Zn leaching decreased by electrodialytic treatment
- Leaching scenarios in-use and end-of-life for mortars with MSWI fly ash
- NaCl and Na_2SO_4 resulted in increased leaching from the tested materials

1 Introduction

Cement is regarded as the second most used material globally, after water, and the most produced material in terms of mass [1]. The production of ordinary Portland cement clinker represents a significant environmental issue due to high CO_2 emissions. It has been estimated that cement production accounted for 8% of the global anthropogenic CO_2 emissions in 2015 [2]. A well-established strategy to reduce CO_2 emissions is to partly replace cement clinker with supplementary cementitious materials (SCMs) [1]. However, limited supplies of commonly used SCMs restricts reducing CO_2 emissions further in this way, requiring the identification of new SCMs.

Municipal solid waste incineration (MSWI) is a preferred waste management solution in many countries, reducing the non-recyclable waste volume combined with energy recovery. However, MSWI results in fly ash residues classified as hazardous waste disposed of at controlled hazardous waste disposal sites. Disposing MSWI fly ash may have long term environmental consequences due to contaminants leaching, e.g. toxic metals [3], and results in the loss of any valuable metals in the fly ash.

A treatment process that can reduce MSWI fly ash's hazardousness, recover any valuable metals, and enable the treated ash to replace cement clinker partially is, therefore, of interest. Several treatment methods (e.g. solidification/stabilisation, separation/extraction or thermal treatments) have been investigated previously [4]. One of the methods that can remove metals from contaminated materials [5] and potentially enable MSWI fly ash for use in cement-based materials [6] is electrodialytic remediation (EDR). Electrodialytic remediation uses a direct current to remove metals from a suspension of the contaminated material into electrolyte solutions separated from the suspension by ion-exchange membranes. The process acidifies the suspension, releasing the metals in the material as ions that can migrate in the electric field.

Electrodialytic remediation has been used in lab-scale to remove toxic metals from MSWI fly ash [7–10], investigating the method's efficiency and potential improvements. A sketch of a laboratory-scale electrodialytic remediation cell is included in Fig. 1. The cell consists of three compartments. Compartment I and III are concentration compartments filled with a circulating electrolyte solution (0.01 M $NaNO_3$ adjusted to a pH < 2 with HNO_3) and contains the anode and cathode, respectively. Compartment II contains a suspension of the material to be remediated, and the suspension is kept stirred. The anode and cathode compartments are separated from the suspension compartment by ion-exchange membranes, ensuring that ion transport is outwards of the suspension. During remediation, the pH of the suspension decreases due to water splitting ($H_2O \rightarrow H^+ + OH^-$) at the anion exchange membrane [11]. During remediation, soluble chlorides can migrate towards the anode as Cl^- and form toxic chlorine gasses if present [8]. Previous lab-scale experiments have shown that after 28 days of electrodialytic treatment at an applied current of 600 C/g MSWI fly ash, removal percentages of 51-75 wt% Cd, 5-10 wt% Cr, 25-50 wt% Cu, 2-15 wt% Pb and 10-90 wt% Zn could be achieved for three characteristically very different MSWI fly ash samples [12].

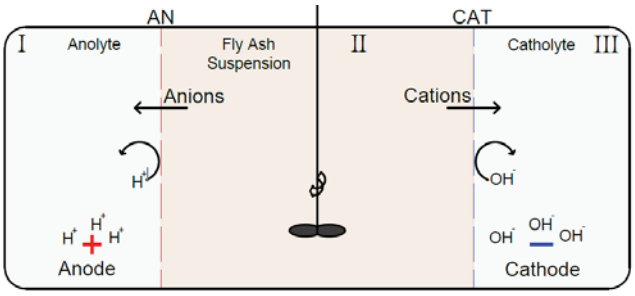

Figure 1: Principal sketch of the electrodialytic remediation set-up.
AN – anion exchange membrane, CAT – Cation exchange membrane, as presented in [12].

For EDR to be a viable treatment process for metal removal and improving fly ash properties, the process needs to be up-scalable while retaining its efficiency. Efforts have been made in up-scaling the technology to treat MSWI fly ash in bench-scale [13,14] and pilot-scale [15,16] based on the set-up principles used for the electrodialytic treatment of liquid solutions. However, the purpose of the experimental set-up used in the previous studies was to remove the easily mobile parts of toxic metals from the MSWI fly ash and reduce the potential leaching instead of investigating the metals' total recovery from the fly ash (metal removals were typically below 5 % [13]). Further investigating the total recovery of metals possible in bench-scale is therefore of interest.

Although EDR can remove metals from MSWI fly ash, the residue could still leach toxic metals. Furthermore, if the treated MSWI fly ash is used to partially replace cement in cement-based material, metals could potentially leach from the cement-based material. Investigating the content of metals leaching from EDR treated MSWI fly ash and cement-based materials with EDR treated MSWI fly ash is required. Elements that can potentially leach from MSWI fly ash are typically studied through batch leaching methods with deionised water [17] or the toxic characteristic leaching procedure (TCLP) [18].

Evaluating the environmental risk of the treated MSWI fly ash based on leaching alone is not enough. Leaching from cement-based materials should also be evaluated [19]. It has been

93 proven that cement-based materials effectively retain toxic metal through chemical bonding
94 and physical entrapment [20]. Waste solidification/stabilisation research has shown that in a
95 cement-based material, metal ions from the waste may chemisorp, precipitate, form a surface
96 compound with the cement component surface, form an inclusion or be chemically
97 incorporated into the cement structure [21]. Leaching characteristics of cement-based
98 materials containing raw or treated MSWI fly ash have been investigated for both crushed or
99 monolithic samples, e.g. [18,22–25]. Typically these leaching tests have been performed
100 using the same leaching tests for the raw materials with distilled/deionised water [22–24] or
101 the TCLP test [18]. Concrete structures are subjected to many different forms of physical and
102 chemical attacks during their lifetime, e.g. carbonation and external sulphate attack [26].
103 Leaching is affected by the concrete surface's environmental conditions that the standard
104 leaching tests do not consider, leading to a wrong assessment [19]. Müllauer et al. [19]
105 investigated the leaching yield from concrete containing coal incineration fly ash. They
106 determined that environmental factors such as chloride (contact with deicing salts or the
107 ocean) and sulphate exposure (ocean water, groundwater or soil contact) or carbonation
108 affected the leaching yield. When SO_4^{2-} penetrate cement-based materials, expansive gypsum
109 and ettringite forms, while $Ca(OH)_2$, AFm (e.g. monosulphate), and the C-S-H phase tends to
110 dissolve [19]. Exposure to Cl^- may lead to Friedel's salt formation at the expense of the AFt
111 (e.g. ettringite) and AFm phases and may be expected to change the solubility of both major
112 and trace elements. In the study by Müllauer et al. [19] chloride and sulphate exposure
113 increased Ba, Cr, Sr and V leaching from concrete samples.

114 To further advance the research, treating the three characteristically very different MSWI fly
115 ash samples [12] at bench-scale is therefore required, focusing not just on leaching reduction,
116 but also on metal removal. Furthermore, if EDR treated MSWI fly ash is to be used in

cement-based materials, the effect environmental factors would have on the metal leaching yield and scenarios for in-use and end-of-life should be investigated.

The objectives of the present study were, therefore 1) to further evaluate the potential of electrodialytically treating MSWI fly ash, investigating if previously obtained lab-scale results can be replicated in bench-scale in terms of both total metal recovery and leaching reduction and 2) to determine the effect environmental properties have on cement-based materials containing treated MSWI fly ash, measuring the Cd, Cr, Cu, Pb and Zn leaching yield during exposure to HNO_3 pH adjusted distilled water, chlorides or sulphates.

2 Materials and methods

2.1 Experimental MSWI fly ash

The experimental MSWI fly ash samples used in this study were acquired in 2018 from three different incineration plants. Six samples were used in this study; three untreated and three EDR treated MSWI fly ash samples.

- **Amager Bakke:** Large scale state-of-the-art grate fired incinerator located in Copenhagen, Denmark. The incinerator is equipped with electrostatic precipitators followed by a wet scrubber system for flue gas treatment. The incinerator incinerates approximately 440,000 tons of household/industrial waste annually at an approximate temperature of 1025°C. One fly ash sample was acquired from the electrostatic precipitators denoted Arc-Fa. The EDR treated fly ash was denoted EDR Arc-Fa.
- **Ryaværket:** Medium-scale fluidised bed incinerator located in Borås, Sweden. It uses a dry scrubber system with lime and activated carbon injection followed by a textile filter for flue gas treatment. The incinerator incinerates approximately 110,000 tons of household/industrial waste annually at approximately 900°C. One fly ash sample was

acquired from the textile filter denoted Rya-Fa. The EDR treated fly ash was denoted EDR Rya-Fa.

- **Nuuk:** Small scale grate fired incinerator located in Nuuk, Greenland. The incinerator uses an electrostatic precipitator to capture its fly ash and treat its flue gas. Its incineration capacity is approximately 15,000 tons of household/construction waste annually at approximately 1064°C. One fly ash sample was acquired from its electrostatic precipitators denoted Nuuk-Fa. The EDR treated fly ash was denoted EDR Nuuk-Fa.

The MSWI fly ash samples used for the bench-scale EDR experiments were washed with distilled water in three stages to remove easily soluble salts detrimental to the electrodialytic process. The L/S ratio was 5 for each stage of washing. The washing procedure was the same, as described by Chen et al. [27]. The three samples' water-soluble mass has been determined to be 56, 38 and 28 wt% for Arc-Fa, Nuuk-Fa and Rya-Fa, respectively [28].

2.2 Bench scale electrodialytic remediation

Three electrodialytic treatment experiments, one with each MSWI fly ash sample, were performed using the bench-scale experimental set-up shown in Fig. 2. The bench-scale set-up was built in a PVC plastic container (60x40x32 cm^3). The suspension was a mixture of MSWI fly ash and distilled water at a liquid to solid (L/S) ratio of 10. First, 27 L distilled water was added to the suspension chamber (II), gradually followed by a slurry of 3 L distilled water and 3 kg MSWI fly ash. The MSWI fly ash was kept suspended to avoid sedimentation in the container by three propellers connected to Vos 14 overhead stirrers from VWR. The anode and cathode were placed in electrode units (I and III), plastic boxes with circulating electrolytes. The unit's side facing the MSWI suspension contained a 27x37 cm^2 anion exchange membrane (20 SZRA B02249) or cation exchange membrane (CR67 HUY N12116B) from Ionics. Each

electrode unit had a separate electrolyte circulating system (5 L of 0.01 M $NaNO_3$ adjusted to a pH < 2 with HNO_3) and one electrode. The electrodes were platinum-coated titanium meshes (4x20 cm^2) from durAnode®. A power supply (Blanko- Model Q J-3003C III) maintained a constant current of 1 A. The applied current and membrane area of ~1000 cm^2 corresponded to a current density of 1 mA/cm^2.

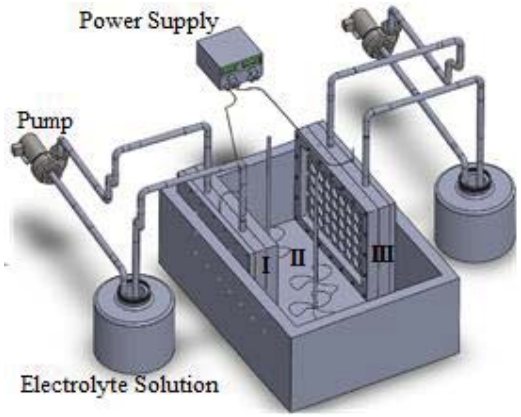

Fig. 2: Principal sketch of the EDR bench-scale set-up
Anode compartment (I), suspension chamber (II) and cathode compartment (III).

During the electrodialytic experiments, the suspension chamber's pH was measured daily by Radiometer electrodes in the suspensions. The pH in the catholyte was adjusted daily during the experiments to pH~2 with 7 M HNO_3. The experiments lasted 28 days, and the current applied was equivalent to 800 C/g ash.

The fly ash suspension was filtered through 45 µm filters at the end of each experiment. The treated ash was then dried at 50°C then crushed. Afterwards, the toxic metal content was measured with XRF analysis. The membranes and stirrer were submerged in 1 M HNO_3 and the electrodes in 5 M HNO_3 to release any accumulated metals. The toxic metal accumulations were then analysed with ICP-OES.

The wt% distribution of metals removed from the fly ash, e.g. in the suspension, catholyte or anolyte, were calculated based on the initial concentration of metals in the MSWI fly ash before the EDR treatment, measured with x-ray fluorescence (XRF)analysis.

185 *2.2.1 Treated ash characterisation*

186 The elements in the EDR treated MSWI fly ash were analysed with x-ray fluorescence
187 analysis.

188 The content of Al, Ca, Fe, K, Mg, Na, P, S and Si were back-calculated as oxides, while Cl
189 and the studied metals Cd, Cr, Cu, Pb and Zn are presented as-is. Furthermore, the
190 mineralogy and phase composition were analysed using x-ray diffraction (XRD) and
191 thermogravimetric (TG) analysis. The XRF analysis was performed on samples ground to a
192 particle size below 200 μm, by an external laboratory that used a Pd-tube equipped
193 SPECTRO Gmbh X-LAB 2000[27]. The XRD analysis was performed using a Pan-Alytical
194 X'pert PRO Θ–Θ System (2 wt% detection limit) on backloaded samples. The ICDD PDF4
195 database was used for peak and phase identification. The TG analysis was performed using a
196 NETZSCH STA 449 F3 Jupiter, aluminium oxide sample holders and 50 ml/min of nitrogen
197 purge gas. The samples were heated from 29°C to 900°C at 10°C/min. The TG analysis
198 results are included as the 1st derivative of the thermogravimetric graph (DTG).

199 **2.3 Leaching experiments**

200 Leaching experiments were performed on the raw and treated MSWI fly ash samples, and on
201 mortar cubes made with 10 wt% MSWI fly ash substituting cement. In addition to the mortar
202 cubes with MSWI fly ash, two reference cubes were made, one without cement replacement
203 andon with 10 wt% inert M8 quartz filler substituting cement. The reference samples were
204 included to test the metal content that could be expected to leach from a mortar with 100 wt%
205 cement and a mortar containing less cement. The cement used was a CEM I 52.5 N
206 (MS/LA/≤2) with a bulk and absolute density of 1.1 and 3.2 g/cm^3, respectively. Portland
207 cement contains toxic metals in varying concentrations due to the raw materials used during
208 cement production, bound during cement hydration or dissolved in the pore solution [29].

Table 1 contains the toxic metal concentration of the cement and quartz used. The cement was treated with Fe(II) to reduce Cr(VI) to Cr(III) by the cement production plant.

Table 1: Toxic metal concentration (mg/kg) in CEM I cement and quartz.

	Pb	Zn	Cd	Cu	Cr
CEM I	17	180	0.4	140	33
Quartz	1.2	6.2	0.0	0.4	0.4

The leaching experiments were performed using three different solutions, based on Müllaur et al. [19] and the commonly used Dutch diffusion test NEN 7345 [25,30–33] and EN 12457-1 [34].

1. NaCl dissolved in distilled water at a concentration of 30 g/L. Simulates deicing salt for concrete highways in moderate and cold climates [19].
2. Na_2SO_4 dissolved in distilled water at a concentration of 30 g/L. It corresponds to the upper limit of exposure class XA2 according to EN 206 and is the most often concentration used to test resistance to sulphate attack [19].
3. Distilled (DI) water acidified to pH 4 using 1M HNO_3 [25,30–33].

Fig. 3 shows an overview flow chart of the leaching experiments performed.

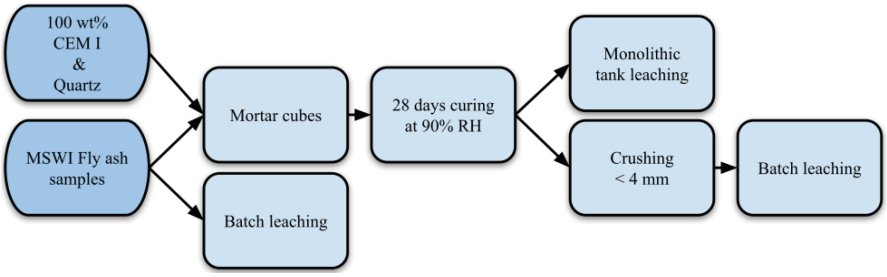

Fig. 3. Flow chart of the performed leaching experiments

2.3.1 Fly ash

Leaching experiments on untreated and treated MSWI fly ash were performed according to the batch leaching test described in EN 12457-1 [34], although modified to study the potential influence of environmental factors on leaching by using the solvents 1-3. The experiments were performed by mixing 5 g of ash with 50 ml of solvent (L/S ratio of 10).

The mixture was shaken for 24 hours at 195 rpm and then filtered using 0.45 µm syringe filters before pH and metal analysis with a Radiometer electrode and ICP-OES. Duplicate experiments were performed.

2.3.2 Mortar cubes

The mortar cube specimens were prepared according to EN 196-1 [35]. A total of sixteen cubes were prepared, eight for measuring leaching from crushed mortar and eight for measuring monolithic (in-use scenario) leaching. Mortar cubes with 10 wt% cement replaced by either MSWI fly ash or inert quartz (admixtures) were a mix of 45 g admixture, 405 g cement, 1350 g Cen standard sand and 225 g distilled water. The 100 wt% cement cubes contained 450 g cement, 1350 g Cen standard sand, and 225 g distilled water. The mixtures were vibrated and moulded in 5 x 5 x 5 cm^3 cubical fibre wood moulds at 50 Hz for 2 minutes after mixing the ingredients. The cubes were demolded after 20-24 hours of curing at >90 % relative humidity and 20°C and stored to hydrate further for 28 days in desiccators with 90% relative humidity at 20°C.

Leaching experiments on crushed (end-of-life scenario mortar cube specimens were performed according to the one-stage batch test described previously. The mortar cubes were crushed to a particle size below 4 mm with a hammer after 28 days of curing. The experiments were performed by mixing 175 g of the crushed specimen with solutions 1-3 at an L/S ratio of 2. The volume of solution used was adjusted for each specimen to account for each crushed specimen's water content.

The monolithic leaching experiments were performed using a modified version of the Dutch leaching test NEN 7345 described in [32] by submerging the cubes in one of the solvents 1-3 at an L/S ratio of 4. The submerged cubes were stored in 1.4 L sealed containers for 70 days at ambient temperatures. The cubes were placed flat on the containers' bottom, exposing five of the cubes' sides. After 6 hours, 24 hours, 54 hours, 4 days, 9 days, 16 days, 36 days and 64

days, 20 ml of the effluent was extracted from the containers and replaced with 20 ml fresh solution. The extracted effluent's pH and metal content were then measured with a Radiometer electrode and ICP-OES, respectively. The measured concentration of metals was corrected to account for the initial concentration of metals in the solvents. One experiment with crushed and monolithic mortar was performed for each raw and EDR treated MSWI fly ash samples.

3 Results and discussion

3.1 Bench scale electrodialytic remediation

3.1.1 Experimental conditions

The pH development in the suspension chamber during the bench-scale electrodialytic remediation experiments is shown in Fig. 4. During the experiments, pump failures for the circulating electrolytes occurred, resulting in an unwanted flow of liquids between the

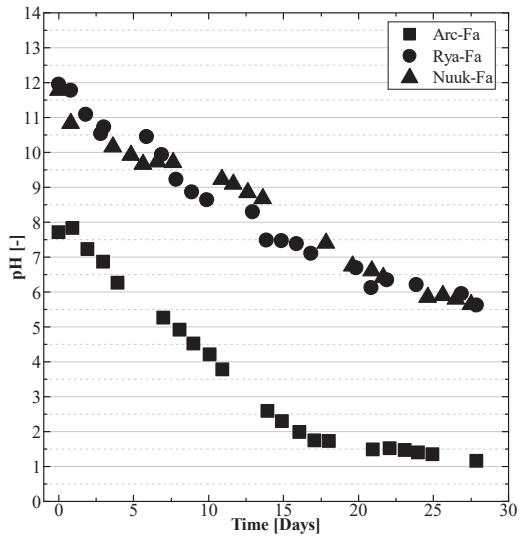

Fig. 4: Suspension chamber pH during bench-scale EDR experiments.

chambers. Additional liquid was, therefore, added to the electrolytes over the course of the experiments. However, this did not influence the pH of the fly ash suspensions.

In the electrodialytic remediation experiments, the final pH in the fly ash suspensions was pH 1 for Arc-Fa and pH 5.5 for Rya-Fa and Nuuk-Fa. The differences in final suspension pH

between the fly ash samples may be attributed to their initial pH differences (pH 6 for Arc-FA and pH 12 for Rya-Fa and Nuuk-Fa) and their buffer capacities. Therefore, a longer remediation time would be required for Rya-Fa and Nuuk-Fa to reach an acidic pH similar to Arc-Fa. The pH in the three experiments decreased at an almost constant rate. However, after 15 days, Arc-Fa's pH rate of decrease changed, stabilising at a pH of 1.5.

The pH decrease observed in the present study is similar to the development observed in lab-scale [12]. However, the acidification occurred slower during the bench-scale experiments than lab-scale, potentially due to the L/S ratio differences (3.5 in lab-scale and 10 in bench-scale) or the ion exchange membrane area and current compared to the amount of fly ash remediated. In the previously performed lab-scale experiments with Rya-Fa and Nuuk-Fa, the pH in the fly ash suspensions reached a pH of 1 and 3, respectively, after 28 days of remediation [12].

3.1.2 Metal removal

The distribution of Cd, Cu, Cr, Pb and Zn after the three electrodialytic experiments is shown in Fig. 5. The metal removal order varied between the three MSWI fly ash samples. For Arc-Fa, it was Cu>Zn>Cd>Cr>Pb, while for Nuuk-Fa and Rya-Fa, it was Cd>Zn>Cr>(Cu, Pb). A stark difference was observed between the percentage of metals removed from Arc-Fa and those removed from Rya-Fa and Nuuk-Fa. For Arc-Fa, the highest removal was 80 wt% Cu, while the highest for Nuuk-Fa and Rya-Fa were 20 and 10 wt% Cd, respectively. The differences in metal removal between the experiments correlate with the differences in pH. A final pH of 5.5 was insufficient to remove high concentrations of metals from Nuuk-Fa and Rya-Fa. HNO_3 batch leaching experiments with MSWI fly ash [10,36] have shown that Cd leach below pH 8, Zn below pH 7, Cu below pH 5, and Pb Cr below pH 4 and, therefore, high metal removal could only be expected in the experiment with Arc-Fa. Due to the higher pH in Rya-Fa and Nuuk-Fa, more than 28 days of remediation would be required to treat these more alkaline MSWI fly ashes under the current bench-scale experimental conditions.

Although a final suspension pH of 1.5 was maintained in the experiment with Arc-Fa, less than 10 wt% Cr and 2 wt% Pb were removable from the fly ash, matching the observed lab-scale results [12]. However, more Pb was removable from Nuuk-fa and Rya-Fa during the lab-scale experiments than Arc-Fa, despite maintaining a lower suspension pH with Arc-Fa. This was attributed to Arc-Fa's high sulphate content, potentially resulting in the precipitation of $PbSO_4^{2-}$ at a low pH [12], which may have occurred at bench-scale as well. The bench-scale results differ from the lab-scale results in terms of Cd, Cu and Zn from Arc-Fa. Close to 80 wt% Cd, 26 wt% Cu and 10 wt% Zn could be removed from Arc-Fa during the lab-scale experiments [12].

The Cu and Zn removal in the bench-scale experiment was 40 wt% and 60 wt% higher, respectively than in the lab-scale experiments, suggesting that the lab-scale experiment had removal issues that the bench-scale experiment did not. In contrast, the lab-scale experiments with Nuuk-Fa and Rya-Fa removed between 5-90 wt% of the metals, compared to 1-20 wt% at bench-scale [12]. The pH reached in the lab-scale experiments for Rya-Fa and Nuuk-Fa was lower, suggesting that the observed differences are because the bench-scale experiments did not reach an acidic pH.

At the near-constant pH reached in the Arc-Fa experiment, the valency of metals in a pure acidic and aerated solution could be expected to be 2+ (Cd, Zn, Pb and Cu) or 3+ (Cr) [37], suggesting a release to the suspension and subsequent removal to the cathode. The majority of the removed metals migrated to the catholyte, indicating the release of positively charged metals. However, most of the metals released from Arc-Fa remained in the suspension instead of migrating to the electrodes, whereas the majority migrated to the cathode in the lab-scale experiment [12]. The experiment with Arc-Fa was not hydraulically stable. As previously mentioned, a significant amount of liquid flowed from the electrolytes to the

suspension compartment. This experiment's metal distribution indicates that the metals were transported with the liquid instead of being retained in the electrolytes.

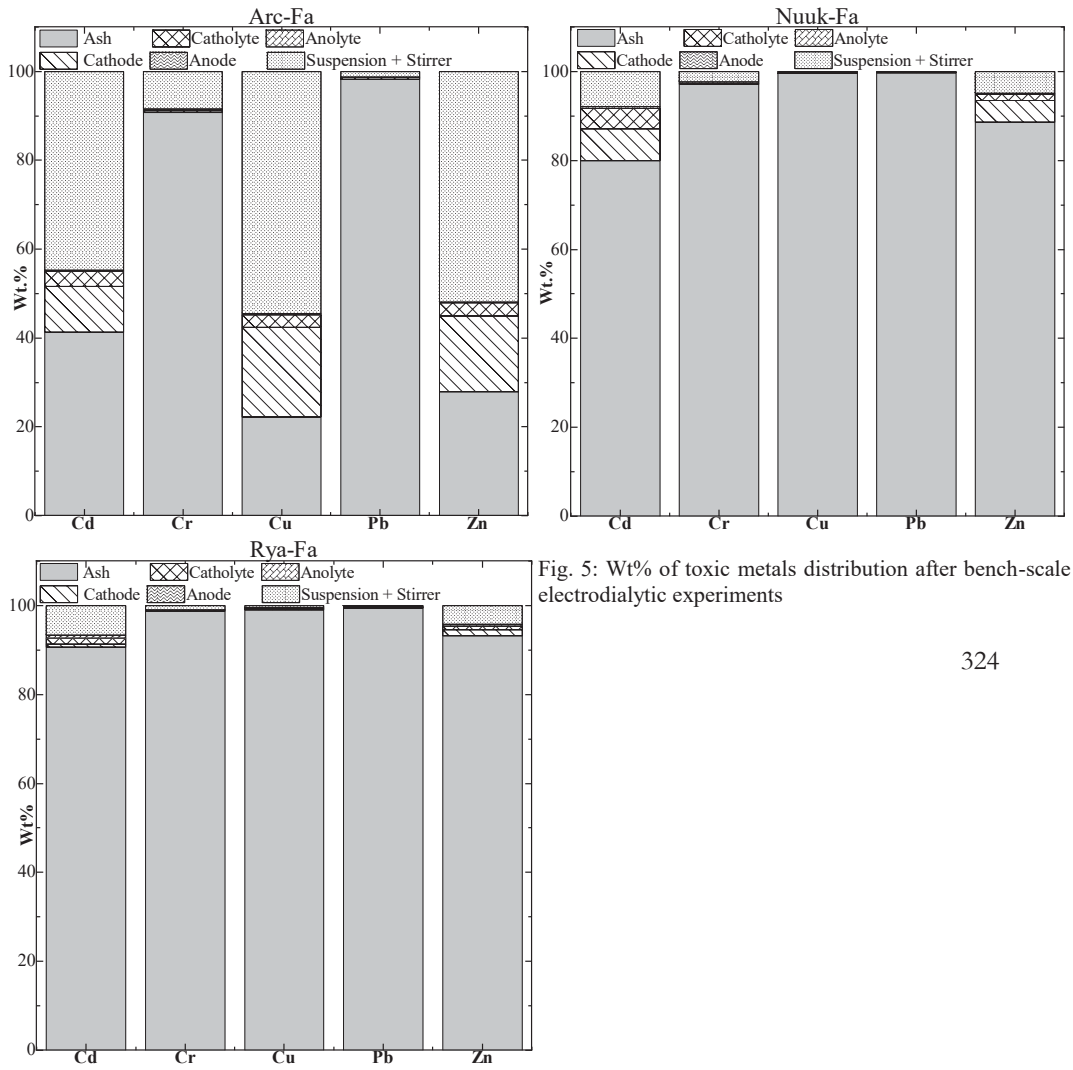

Fig. 5: Wt% of toxic metals distribution after bench-scale electrodialytic experiments

The bench-scale experiments' experimental performance showed that further developments and adjustments of the experimental set-up and conditions are needed 1) to obtain hydraulically stable experiments and 2) to achieve faster acidification and higher metal removal. This development is essential to properly assess technical concerns that can increase the

technological readiness level (TRL) of electrodialytic remediation for MSWI fly ash treatment and enable full-scale treatment [38].

3.1.3 Characteristics of treated fly ash

The element concentrations of the raw [28] and EDR treated MSWI fly ash samples are included in Table 2. The EDR treatment reduced the K, Na and Cl concentrations of the fly ash samples due to the dissolution of easily soluble salts, which decreased the fly ash mass after the experiments. Even if metals were removed from the fly ash samples (Fig. 5), the EDR treated Arc-Fa was the only sample with reduced toxic metal concentrations (Cd, Cu, Zn). The Cr and Pb concentration in Arc-Fa were concentrated. The EDR treatment also concentrated the metals in Rya-Fa and Nuuk-Fa, except Pb, while reducing the fly ashes' Ca content. The Ca concentration in Arc-Fa increased after the treatment and may be attributed to an insoluble Ca content in Arc-Fa. Furthermore, the EDR treatment concentrated the Si, Al and Fe in the fly ashes, which are advantageous for cement-based materials.

Table. 2 Calculated oxides composition of the raw MSWI fly ash samples, as presented in [28], and EDR treated samples, with trace elements, measured with XRF analysis and pH. (-) below the detection limit.

		Raw Arc-Fa	**EDR Arc-Fa**	**Raw Nuuk-Fa**	**EDR Nuuk-Fa**	**Raw Rya-Fa**	**EDR Rya-Fa**
pH	[-]	6.5	4.1	12	7.7	12	7.2
Al_2O_3	[Wt%]	1.4	2.3	4.6	9.6	4.7	5.3
CaO	[Wt%]	13	28	43	29	43	31
Fe_2O_3	[Wt%]	1.0	2.4	0.9	1.4	1.8	2.7
K_2O	[Wt%]	14	1.0	12	0.4	2.7	0.7
MgO	[Wt%]	0.6	0.4	1.4	1.3	1.8	2.2
Na_2O	[Wt%]	7.4	0.7	22	-	7.0	-
P_2O_5	[Wt%]	2.6	2.1	1.8	2.7	2.2	3.7
SO_3	[Wt%]	34	30	8.9	9.7	8.9	8.7
SiO_2	[Wt%]	4.6	14	6.1	14	6.4	12
Cl	[Wt%]	2.8	0.1	24	0.1	13	0.2
Cd	[mg/kg]	480	60	420	460	80	100
Cr	[mg/kg]	300	700	800	1,100	400	600
Cu	[mg/kg]	1,400	520	1,300	2,000	7,900	10,200
Pb	[mg/kg]	12,000	31,000	3,200	3,200	3,400	3,400
Zn	[mg/kg]	55,000	26,000	33,000	41,000	6,600	9,100

Fig. 6 depicts the XRD diffractograms of the raw and EDR treated MSWI fly ash samples. The XRD diffractograms showed that the mineral phases of raw Arc-Fa were $CaSO_4$, Na_2SO_4,

353 Na_2FeO_4 and $CaAl_2O_4$, while raw Rya-Fa contained CaClOH, $CaSO_4$ NaCl, KCl and $CaCO_3$,
354 and raw Nuuk-Fa contained NaCl, KCl, $CaCO_3$, $CaSO_4$ and CaO. After the EDR treatment, Cl
355 containing mineral phases could no longer be identified. Instead, treated Arc-Fa contained
356 $CaSO_4 \cdot 0.5H_2O$, $CaSO_4$, $PbSO_4$ and SiO_2, while both treated Rya-Fa and Nuuk-Fa contained
357 $CaSO_4 \cdot 2H_2O$, $CaCO_3$. Arc-Fa may not contain $CaSO_4$ as the peaks for $CaSO_4$ overlap with
358 $CaSO_4 \cdot 0.5H_2O$. As hypothesised in [12], EDR treated Arc-Fa does contain $PbSO_4$ explaining
359 the low Pb removal observed in both lab-scale and bench-scale.

360 Fig. 7 depicts the DTG graphs of the raw and EDR treated MSWI fly ash samples. In a previous
361 study by Ebert et al. [28] it was determined that raw Rya-Fa and Nuuk-Fa contained $CaCO_3$
362 (mass loss at 650-700°C) and that all three samples potentially contained sulphate phases that
363 started decomposing above 700°C. The mass losses observed between 0 and 500°C for Rya-
364 Fa and Nuuk-Fa indicate water loss from several different phases not present in Arc-Fa. The
365 DTG curves of the EDR treated MSWI fly ash samples suggest that the samples still contain
366 $CaCO_3$ and various sulphate phases, as supported by the XRD graphs. However, EDR treated
367 Nuuk-Fa did not show the same mass loss after 700°C as raw Nuuk-Fa. Furthermore, the mass
368 losses between 0 and 500°C is no longer observable. Instead, the three samples show a mass
369 loss between 100 and 150°C, corresponding to $CaSO_4 \cdot 2H_2O$ [39]. The mass loss size suggests
370 that Rya-Fa and Nuuk-Fa contain a higher concentration of $CaSO_4 \cdot 2H_2O$ than Arc-Fa, despite
371 containing less sulphur. The XRD analysis showed that Arc-Fa contained $CaSO_4 \cdot 0.5H_2O$
372 instead of $CaSO_4 \cdot 2H_2O$, suggesting that the smaller mass loss is due to less H_2O per $CaSO_4$.
373 Treated Rya-Fa and Nuuk-Fa also have a mass loss at 70°C and 300°C, which is not as easily
374 identified but could be due to monosulphate [39].

After EDR treatment, the different MSWI fly ash samples become more uniform at K, Na and Cl phases are removed together with the removable Ca. The unremovable Ca then remains as $CaCO_3$ or as either unhydrated or hydrated $CaSO_4$, together with the Al, Fe and Si phases.

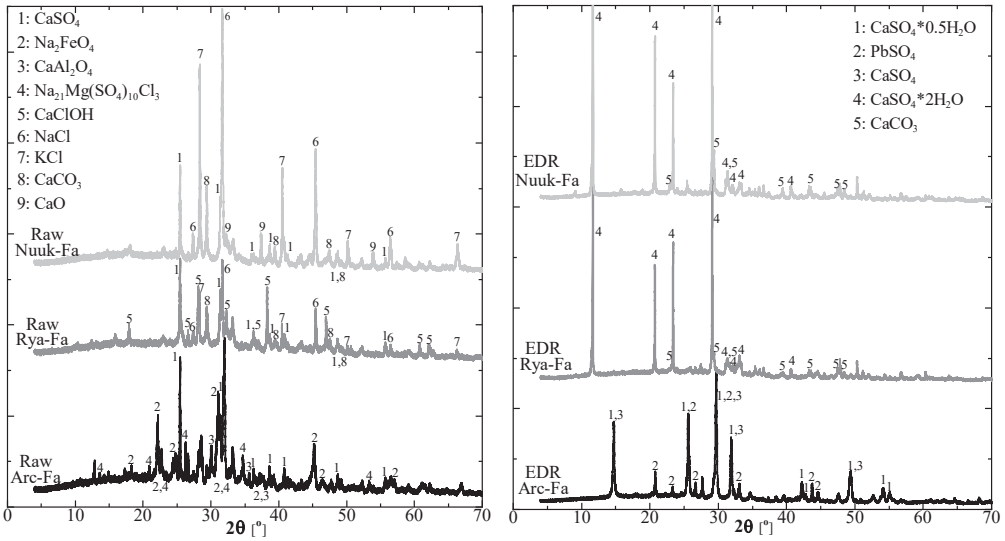

Fig. 6. XRD diffractograms of the raw and EDR treated MSWI fly ash samples.

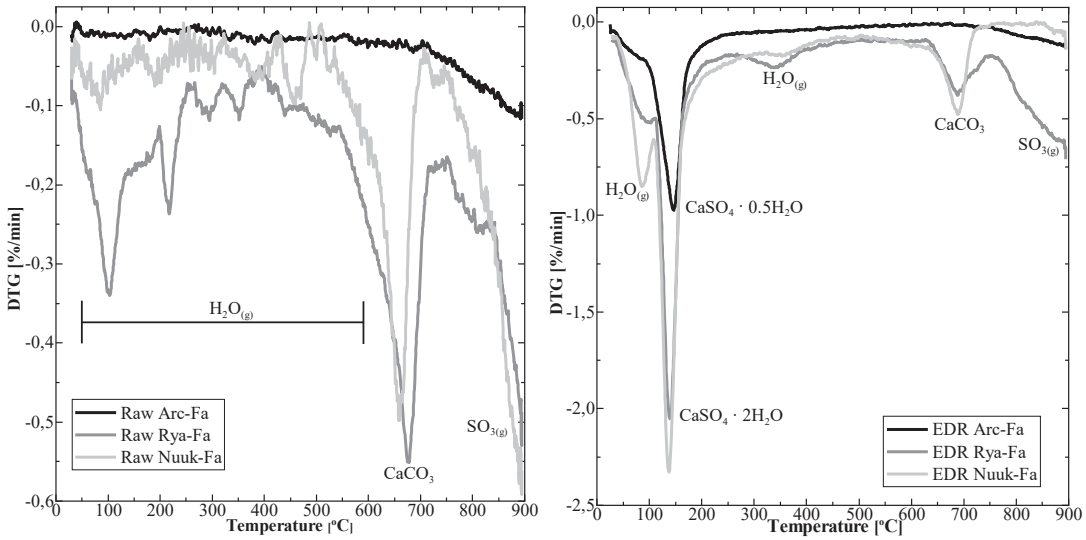

Fig. 7. DTG patterns of the raw and EDR treated MSWI fly ash samples.

3.2 Leaching experiments

3.2.1 Raw materials

The pH of the batch leaching experiments with the raw and treated fly ash samples are included in Table 3. The pH of the leachate varied between 6.4 and 12.0, depending on the sample.

Table 3: Resulting pH in the raw and treated batch leaching experiments.

	$DI_{pH\ 4}$	NaCl	Na_2SO_4
Arc-Fa	6.6	6.4	6.6
EDR Arc-Fa	5.1	4.9	5.3
Rya-Fa	11.5	11.6	11.5
EDR Rya-Fa	8.3	8.3	8.8
Nuuk-Fa	11.9	11.8	12.0
EDR Nuuk-Fa	9.1	9.1	9.9

The batch leaching results with the raw and EDR treated MSWI fly ash samples are shown in Fig. 8. The figure includes the criteria for granular hazardous waste acceptable at landfills for non-hazardous waste [40]. The leaching yield of the raw MSWI fly ash samples exceeded the regulatory limit for landfilling at the non-hazardous waste for some of the metals. Untreated Arc-Fa leached more Cd, Cr, Pb and Zn than the regulatory limit, while untreated Nuuk-Fa leached more Cr and Pb, and untreated Rya-Fa leached more Cu and Pb. Treating the MSWI fly ash with electrodialytic remediation generally resulted in a reduced (Cd, Cu, Pb and Zn) or increased (Cr) leaching yield, although depending on the fly ash and the leaching solution. Leaching results of Arc-Fa EDR was still above the limit values, except for Cu leaching with distilled water with pH 4 and the Cu leaching for Arc-Fa also increased with electrodialytic treatment. For Nuuk-Fa EDR and Rya-Fa EDR only Cr leaching was above the specified limit. The observed differences in leaching concentrations may be attributed to the decreased pH after the EDR treatment (Table 3). In pure acidic or alkaline solutions within the water stability range, Zn and Cu are present as Zn^{2+} and Cu^{2+} below a pH of 7, while Cr is present as Cr^{3+} below a pH of 4 and Pb is present as Pb^{2+} in the entire pH range [37]. In carbon dioxide containing solutions, Pb can be passivated as PbO_2 at a pH between 5-10 and as $PbSO_4$ at a pH between 0-10 in sulphate containing solution [37]. The fly ashes' characterisation showed the presence of $CaCO_3$ and SO_4, with $PbSO_4$ being identified for Arc-Fa. In a Cd-S-C-O-H system, Cd is present as Cd^{2+} below a pH of 8 [41]. Furthermore, Zn and Pb can be present as oxyanions at a pH above 11 [37]. This may be why Zn and Pb's higher release from untreated Rya-Fa and Pb from untreated Nuuk-Fa was

observed regardless of the solution used compared to the electrodialytically treated samples, where the Pb and Zn leaching was significantly reduced.

The NaCl and Na_2SO_4 solutions effect on the leaching is not easily discerned, as the leaching varied depending on the metal and sample. Generally, the NaCl and Na_2SO_4 solutions leached more Cd and Cr than with the pH 4 adjusted solution. In the case of EDR treated Nuuk-Fa and Rya-Fa, NaCl showed a significantly higher Cd leaching compared to Na_2SO_4. The NaCl solution also increased the Pb leaching yield from the EDR treated Arc-Fa sample, resulting in a higher yield than the untreated sample. The addition of extra Cl^- and SO_4^{2-} could result in additional soluble (e.g. metal-chloride complexes) or insoluble complexes (e.g., $PbSO_4$) and, therefore, increasing or decreasing the leaching yield. Generally, the NaCl and Na_2SO_4 solutions did not affect whether the leaching yield was above or below the regulatory limits, except for Cd leaching from EDR treated Nuuk-Fa, Cr leaching from EDR treated Rya-Fa, and Cu leaching EDR treated Arc-Fa, where the leaching increased to above the limit with these solutions compared to acidified water.

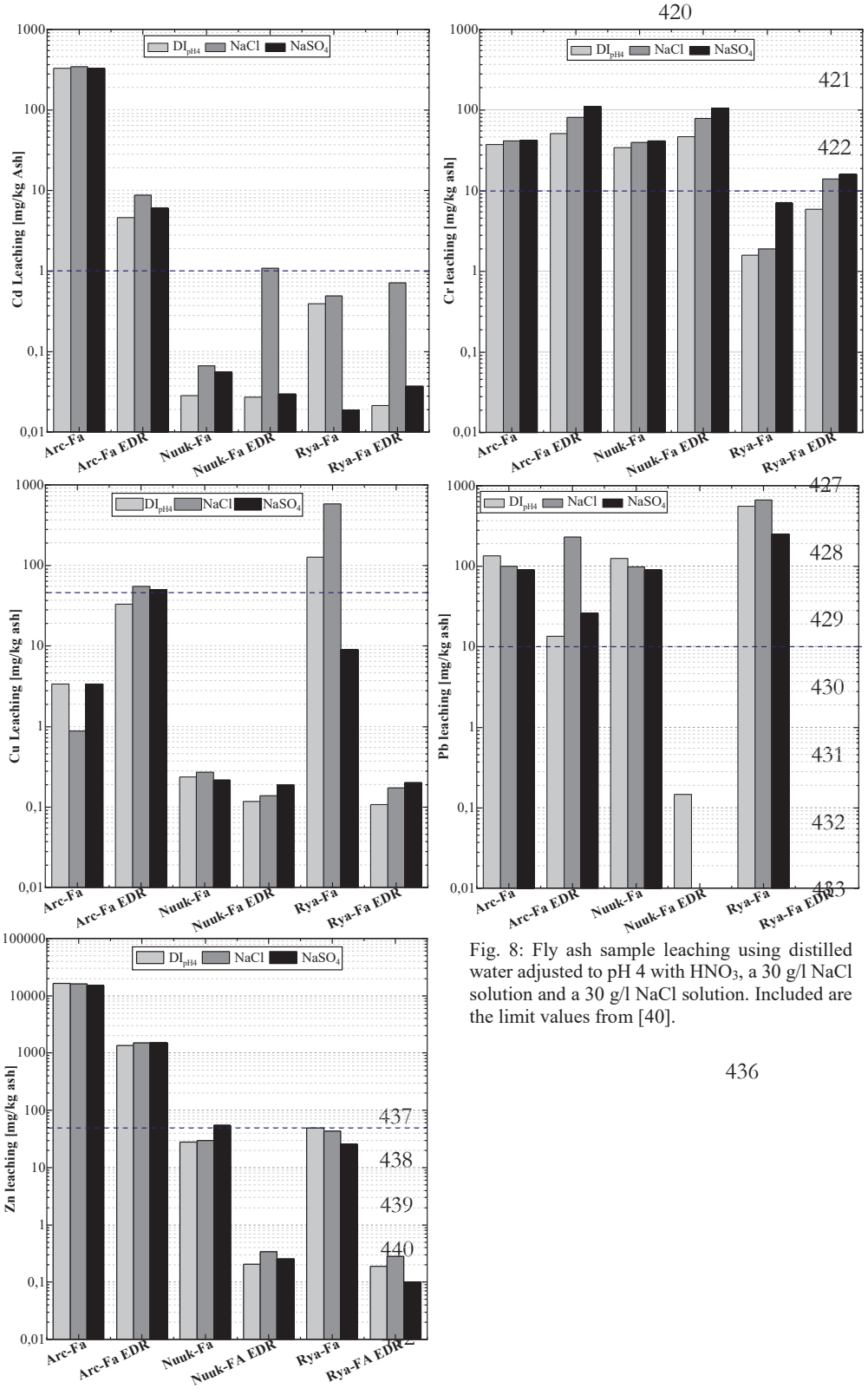

Fig. 8: Fly ash sample leaching using distilled water adjusted to pH 4 with HNO_3, a 30 g/l NaCl solution and a 30 g/l NaCl solution. Included are the limit values from [40].

3.2.2 *Monolithic leaching test (in-use scenario)*

Table 4 shows the monolithic leaching experiments' results as the maximum leaching measured between 0-4 days, 4-16 days and 16-70 days. Monolithic leaching tests represent an in-use scenario for the mortars and can be compared to leaching limits for construction materials. The leaching results are compared to the regulatory limit for total leachability specified in the Dutch building decree [42]. The pH after 6 hours to 70 days was between 11.4 and 12.5 for all experiments performed. Carbonation of cement-based materials can affect leaching by reducing the pore solution pH, changing the porosity and pore size distribution and causing the dissolution of the hydration products [19]. Uncontrolled uptake of CO_2 has been shown to have a negligible effect on the leaching conditions in the NEN 7345 test [25]. Therefore, any observed increase in leaching yield is attributed to the effect of the solutions used exclusively.

No measurable Zn or Cd leached from the 100 wt% cement or quartz mortar cubes regardless of the solution used, while Pb and Cu leached from the reference samples when using the pH 4 adjusted solute. The measured Pb and Cu leaching yield with the NaCl or Na_2SO_4 solutions were erratic, with only one measurement above the detection limit or the solution's initial concentration, suggesting that neither Pb nor Cu leached significantly from the 100 wt% CEM I or quartz cubes. Cr leached from the 100 wt% CEM I and the quartz cubes in the pH 4 adjusted solute showed similarly erratic behaviour, as Pb and Cu. Comparatively, a high concentration of Cr leached when using the NaCl and Na_2SO_4 solutions for the reference samples. More Cr leached in the NaCl solution than the Na_2SO_4 solution, suggesting that the diffusion of Cl^- into the cement matrix has a larger effect on Cr leaching than SO_4^{2-}. It has been well documented that Cr may be incorporated into the AFt and AFm through Al^{3+} and SO_4^{2-} substitution [22,29,43–45] but may also be chemically incorporated into all cement hydration products [46]. The higher Cr leaching yield with NaCl may be attributed to a higher Cr concentration in the

AFt phase, which would fit with Cr(III) substituting Al^{3+} in ettringite, where the Cr is subsequently released due to AFt dissolution.

Substituting cement with MSWI fly ash increased the monolithic leaching of the studied heavy metals, with the measured concentrations depending on the MSWI fly ash samples and solution used. As could be observed with the 100 wt% CEM I and quartz cubes, parts of the measurements were inconsistent, as observed for Zn leaching from Rya-Fa in the NaCl solution (12 mg/m^2 between 0-4 and 4 days, 0 mg/m^2 between 4-16 days and 0.10 mg/m^2 between 16-70 days). It was also observed that the leaching yield did not increase after the initial 0-4 days, suggesting that the metal leached through surface wash only. In some cases, a leaching yield could not be measured between 4-16 or 16-70 days following surface wash-off and may be attributed to the metals' precipitating. In a previous study, Ca precipitation was observed on the tank walls [25]. Although the leaching yield increased with the three leachate solutions used, the Cl^- and SO_4^{2-} enhanced solutions resulted in a higher leaching yield than the pH 4 adjusted solution. Using MSWI fly ash may result in swelling and cracking in a mortar bar [49] and may make mortar more susceptible to Cl- and SO_4^{2-} penetration, resulting in an increased leaching yield.

Leaching with Na_2SO_4 increased the Zn leaching yield more than NaCl, while the opposite was seen for Pb. Zn and Pb can both replace Ca^{2+} in the AFt or C-S-H phase or may be adsorbed to the C-S-H phase [21,29,44,47,48]. The higher Zn leaching yield with NaCl may be attributed to a higher concentration in the AFt phase, similarly to Cr. In comparison, the higher Pb leaching yield with Na_2SO_4 may be attributed to a higher concentration of Pb adsorbed or in the C-S-H phase, as C-S-H may dissolve during SO_4^{2-} penetration. The Cu leaching yield showed the most dependence on the fly ash type, as NaCl resulted in a higher leaching yield from Nuuk-Fa and for Na_2SO_4, the highest leaching yield was seen from Rya-Fa. For the sample Arc-Fa, using either NaCl or Na_2SO_4 reduced Cu leaching compared to

the acidified water, suggesting that which phase Cu is predominantly associated to may depend on the fly ash used. Although cement replacement with MSWI fly ash did result in Cd leaching, the measured leaching yield was low compared to the other metals. Leaching appeared unaffected when using NaCl or Na_2SO_4, suggesting that Cd has a stronger incorporation into the cement matrix than the other metals studied [28,42,46,49,50]. Ca^{2+} and Cd^{2+} have the same charge and almost the same ionic radius and may have a stronger incorporation or be encapsulated as $Cd(OH)_2$ by C-S-H and $Ca(OH)_2$ efficiently [49]. Cr leaching from cubes with MSWI fly ash behaved similarly to the 100 wt% CEM I and quartz cubes. However, the leaching yield increased, due to the higher Cr content in the fly ash samples than in the cement. The efficiency of EDR treating MSWI fly ash in reducing the leaching yield was also dependent on the metal studied. In general, electrodialytic treatment reduced the Zn and Cr leaching yield from the mortars, increased the Pb leaching yield, while the Cu and Cd leaching yield was unchanged. This was contrary to the batch leaching experiments with the fly ash samples, where an increase in Cr and a reduction in Pb leaching were observed. The Pb leaching yield from mortars with Arc-Fa significantly increased after EDR treatment, even with the pH 4 adjusted solute.

Despite the increase in leaching yield observed in this study using MSWI fly ash in cement-based materials, including environmental conditions, the metals' total emissions were up to a factor 1000 lower than the specified regulatory limits [42]. This would suggest that substituting 10 wt% cement with MSWI fly ash is feasible in terms of metal leaching, during the cement-based materials lifetime, despite the environmental conditions and may be attributed to how effectively heavy metals are retained in cement-based materials [20].

517

Table 3: Maximum monolithic leaching (mg/m^2 surface) between 0-4 days, 4-16 days and 16-70 days. (-) below detection limit or no higher than solute concentration. The regulation limit values are from the Dutch building material degree, as presented in [42].

518

519

		Cd			Cr			Cu			Pb			Zn		
		0-4	4-16	16-70	0-4	4-16	16-70	0-4	4-16	16-70	0-4	4-16	16-70	0-4	4-16	16-70
DI_{pH4}	100 wt% CEM I	-	-	-	0.42	0.04	-	-	-	-	-	-	-	-	-	-
	Quartz	-	-	-	-	0.05	-	-	-	-	-	-	-	-	-	-
	Arc-Fa	0.35	0.24	0.21	0.75	0.79	1.0	0.49	0.66	0.75	0.82	1.8	3.3	0.15	2.3	4.0
	EDR-Arc-Fa	0.38	0.34	0.26	0.8	3.1	5.3	0.53	0.59	0.58	1.8	7.9	14	0.56	0.56	0.57
	Rya-Fa	0.37	0.18	0.16	0.66	0.68	0.63	0.51	0.84	0.51	-	-	-	-	0.60	0.46
	EDR Rya-Fa	0.04	0.28	-	-	-	-	-	0.08	0.16	-	-	-	0.16	-	-
	Nuuk-Fa	0.15	0.09	-	-	0.43	1-7	0.01	0.43	0.19	-	-	-	1.4	5.4	1.4
	EDR Nuuk-Fa	0.12	0.05	-	-	-	-	-	-	0.05	-	0.30	-	0.25	0.59	0.97
NaCl	100 wt% CEM I	-	-	-	2.0	5.7	8.9	-	-	-	0.61	-	-	-	-	-
	Quartz	-	-	-	2.3	5.1	10	-	-	-	-	0.18	-	-	-	-
	Arc-Fa	-	-	-	2.8	5.8	9.4	-	-	-	1.9	3.6	5.2	1.4	3.2	5.2
	EDR-Arc-Fa	0.31	0.38	0.24	1.1	3.4	6.3	0.26	0.61	0.30	4.9	11	18	0.37	1.5	0.32
	Rya-Fa	0.49	0.20	0.10	2.3	6.9	13	0.33	0.31	0.33	0.41	0.83	0.51	12	-	0.10
	EDR Rya-Fa	0.17	0.39	0.24	1.0	3.9	7.4	0.36	0.39	0.56	0.41	0.20	1.38	0.17	0.25	-
	Nuuk-Fa	-	0.10	0.01	3.3	7.2	11	0.93	1.2	1.1	-	-	-	0.79	2.2	2.2
	EDR Nuuk-Fa	0.24	0.01	0.01	2.4	5.5	9.9	0.85	1.1	1.6	0.48	0.03	0.25	1.3	1.9	2.2
Na_2SO_4	100 wt% CEM I	-	-	0.11	1.8	3.0	4.5	-	-	-	-	-	-	-	-	-
	Quartz	-	-	-	1.6	3.7	4.1	-	-	-	-	0.03	-	-	-	-
	Arc-Fa	-	-	-	3.8	5.5	7.2	-	-	-	1.5	2.4	3.0	3.1	8.7	6.0
	EDR-Arc-Fa	0.23	0.26	0.21	1.2	3.1	5.3	0.28	0.39	0.38	4.2	7.1	12	2.3	0.54	0.50
	Rya-Fa	0.20	0.22	0.25	1.3	3.8	7.2	0.17	0.16	0.44	0.11	0.18	0.83	0.39	1.7	-
	EDR Rya-Fa	0.15	0.09	-	1.2	3.0	3.7	0.93	2.04	1.49	0.76	0.53	1.4	0.54	0.93	-
	Nuuk-Fa	0.07	0.02	0.11	3.3	5.6	7.9	0.96	0.92	0.98	-	-	-	1.4	4.9	4.1
	EDR Nuuk-Fa	0.05	-	-	2.2	4.1	6.0	0.62	0.86	1.0	0.08	-	0.04	-	-	0.8
Regulation limit			12			1500			540			1275			2100	

3.2.3 *Crushed mortar (end-of-life scenario)*

The concentration of metals that leached during batch leaching on the crushed mortar is shown in Fig. 9. Batch leaching on crushed mortar represents an end-of-life scenario and can be compared to the leaching limits for reusing inert construction and civil engineering waste, where Category 3 covers more restricted use than Category 2 [50]. The pH of leachate in the experiments was 12.6-12.9. The results show that Cd, Cu and Zn leaching for all samples were generally below the regulatory limits regardless of the solution, except for Cu leaching from crushed mortar with Arc-Fa that exceeded the limit. Cr leached from all samples in similar concentrations, regardless if the mortar contained MSWI fly ash or not, probably due to the Cr content in the cement (Table 1) and exceeded the Category 2 or 3 limit. Whether Pb leaching was above the regulatory limit depended on the fly ash sample. Both untreated and treated Arc-Fa exceeded the Category 3 limit, whereas mortars with Rya-Fa were below the limit and for Nuuk-Fa only one sample was above the limit.

The crushed 100 wt% CEM I cube exceeded the Category 3 limit for Pb leaching with the pH 4 adjusted solution and Cr leaching with $NaSO_4$, all the other CEM I samples were below the Category 3 limit or even the detection limit. Furthermore, leaching from the crushed mortar cube with 10 wt% quartz did not leach measurable Pb or Zn and Cd, Cr and Cu leaching was below the Category 3 limit.

A 10 wt% replacement of cement with MSWI fly ash did not, in general, increase Cd, Cu and Cr leaching, despite the substantially higher concentration of toxic metals in MSWI fly ash than cement, suggesting that the investigated metals were immobilised in the cement matrix. Also, the leaching concentrations from the crushed mortar with MSWI fly ash was significantly lower than the leaching from the MSWI fly ash itself (Fig. 8), so the metals were incorporated into the mortar matrix. The use of raw and treated Arc-Fa resulted in the highest concentrations of leached Zn and Pb. Both Arc-Fa and Nuuk-Fa contained more Zn than Rya-Fa, while Arc-

Fa contained fivefold the Pb concentration than Rya-Fa and Nuuk-Fa, and may explain the higher leaching yield measured from the Arc-Fa samples.

The effect of electrodialytically treating the MSWI fly ash is not easily discernible for Rya-Fa and Nuuk-Fa, yet can be discerned for Zn and Pb leaching from Arc-Fa. Removing some of the Zn in Arc-Fa reduced the leaching yield to below 20 µg/ kg crushed mortar. Electrodialytically treating Arc-Fa increased the Pb concentration from 12,000 to 31,000 mg/kg fly ash and more than doubled the leaching yield with the pH 4 adjusted solute or Na_2SO_4 solute. An increase in Pb leaching was also observed with treated Rya-Fa and Nuuk-Fa compared to untreated.

In general, NaCl and Na_2SO_4 resulted in a higher leaching yield than the pH 4 adjusted solute, further suggesting that these simulated environmental parameters can increase leaching. However, this effect depended on the metal and MSWI fly ash studied. A previous study with crushed mortar containing a MSWI fly ash treated with phosphation and calcination showed an increase in Cr and Pb leaching [50], suggesting that these metals might not be as efficiently bound in cement-based materials as the other metals. The effect of environmental factors on leaching was very apparent for Cr leaching from the crushed mortar, where Cr leaching was below Category 3 for all samples when using distilled water adjusted to pH 4 alone. However, with NaCl and especially Na_2SO_4, the Cr leaching yield was above than the Category 3 for most mortar samples, also the reference samples without MSWI fly ash. Pb was the only other metal than Cr to leach in concentrations higher than the Category 3 upper limit. Cd, Cu and Zn (after EDR treatment) were within the upper limit of Category 2.

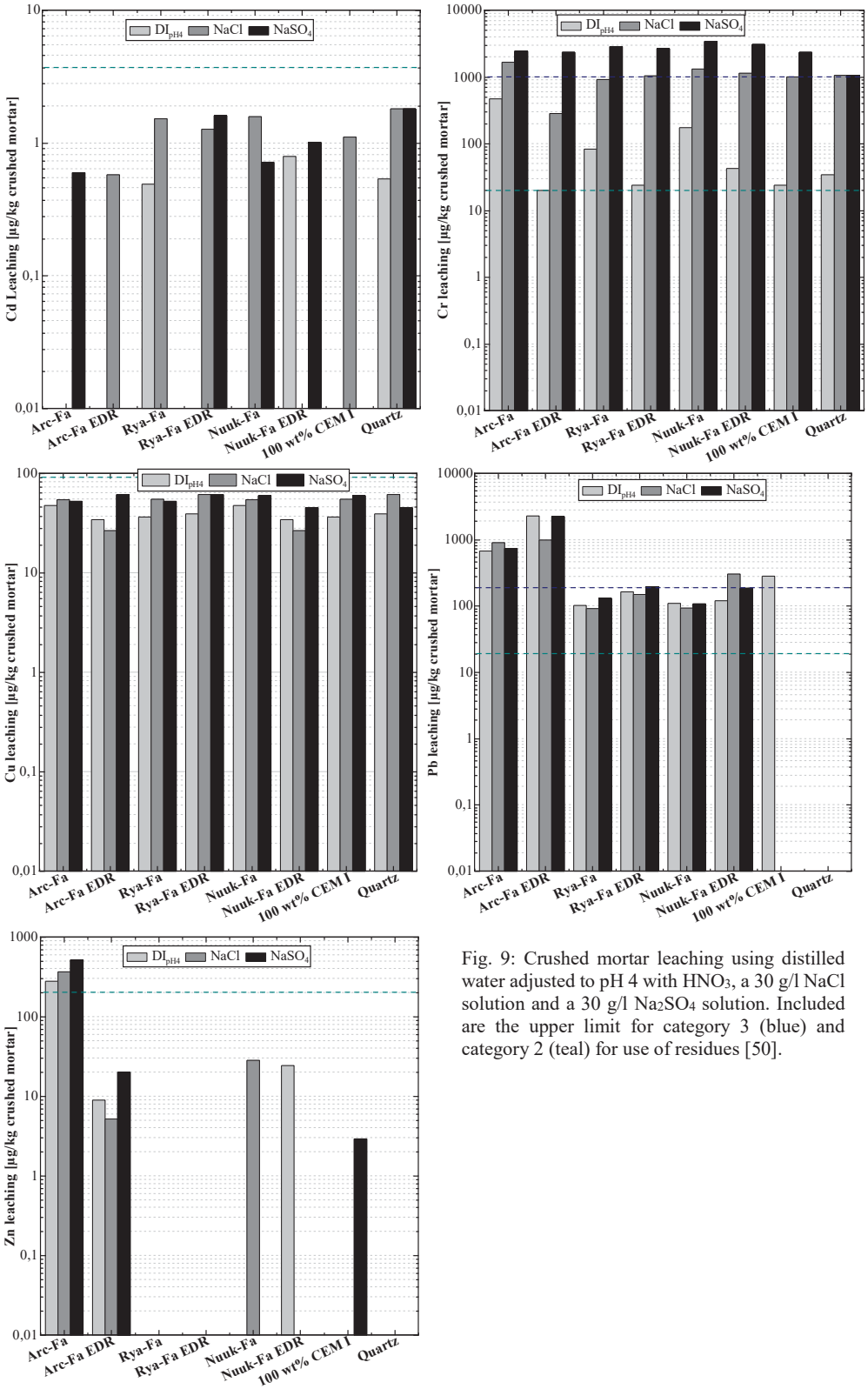

Fig. 9: Crushed mortar leaching using distilled water adjusted to pH 4 with HNO_3, a 30 g/l NaCl solution and a 30 g/l Na_2SO_4 solution. Included are the upper limit for category 3 (blue) and category 2 (teal) for use of residues [50].

4 Conclusions

Treating MSWI fly ash to remove toxic metal with electrodialytic remediation at bench-scale was feasible if a low pH is reached, e.g. pH 1.5, with a removal order Cu>Zn>Cd>Cr>Pb and removing close to 80 wt% Cu in bench-scale experiments. The effect of simulated environmental factors by NaCl and Na_2SO_4 on leaching behaviour was tested on both fly ash and monolithic and crushed mortar with fly ash. The electrodialytic treatment generally reduced the leaching yield of Zn, Pb, Cd and Cu and increased Cr leaching, although an increase in the Cu leaching yield for treated Arc-Fa was observed.

The metal leaching yield from monolithic mortar, representing the use phase of the mortar, was higher for Cd, Cu, Pb and Zn in the samples MSWI fly ash with compared to references made with 100 wt% CEM I cement of 10 % cement replacement with quartz. For Cr, leaching was also seen for the reference samples and is also attributed to the Cr content in cement. Higher leaching of Cr, Pb and to some extent Zn by NaCl and Na_2SO_4 was also observed in the monolithic time-dependent leaching test and may be attributed to the accelerated breakdown of the cement hydration phases over time. However, the monolithic leaching test showed that the leaching was within regulatory limits during the mortars service life when both raw and electrodialytically treated MSWI fly ash was used.

The leaching test on the crushed mortar, representing an end-of-life scenario, showed that Pb leaching from the untreated and treated Arc-Fa sample exceeded the regulatory limit with all leaching solutions, while Cr leaching only exceeded the regulatory limits when the NaCl and Na_2SO_4 solutions were used. Metal leaching from the other samples was below the limit values for reuse. For future studies, it is suggested to supplement the commonly used leaching tests using distilled water with other liquids that can simulate environmental factors to investigate

592 the environmental performance further when using potentially using MSWI fly ash for
593 construction.

594 5 Acknowledgements

595 This study would not have been possible if not for the lab technicians Ebba Schnell and Natasja
596 Due to the Department of Civil Engineering at the Technical University of Denmark during the
597 COVID-19 lockdown period. Their continued lab work was invaluable. The people working at
598 Amager Resource Center, Borås Energi och Miljö and Kommuneqarfik Semersooq are
599 acknowledged for their interest in the study, their cooperation and help with sampling and
600 sending the MSWI fly ash to the Technical University of Denmark. Finally, Erasmus + is
601 acknowledged for providing a scholarship for Nuria Bernárdez Rodas to help conduct the
602 bench-scale experiments.

603

6 References

[1] K.L. Scrivener, V.M. John, E.M. Gartner, Eco-efficient cements: Potential, economically viable solutions for a low-CO2, cement-based materials industry, (2016).

[2] Jos G.J. Olivier; Greet Janssens-Maenhout; Marilena Muntean; Jeroen A.H.W. Peters, Trends in global CO2 emissions 2016, (2016) 86.

[3] O. Hjelmar, Disposal strategies for municipal solid waste incineration residues, Journal of Hazardous Materials. 47 (1996) 345–368. https://doi.org/10.1016/0304-3894(95)00111-5.

[4] Y. Zhang, Z. Ma, Z. Fang, Y. Qian, P. Zhong, J. Yan, Review of harmless treatment of municipal solid waste incineration fly ash, Waste Disposal & Sustainable Energy. (2020). https://doi.org/10.1007/s42768-020-00033-0.

[5] H.K. Hansen, L.M. Ottosen, B.K. Kliem, A. Villumsen, Electrodialytic remediation of soils polluted with Cu, Cr, Hg, Pb and Zn, Journal of Chemical Technology and Biotechnology. 70 (1997) 67–73. https://doi.org/10.1002/(SICI)1097-4660(199709)70:1<67::AID-JCTB662>3.0.CO;2-V.

[6] G.M. Kirkelund, M.R. Geiker, P.E. Jensen, Electrodialytically treated MSWI APC residue as substitute for cement in mortar, Nordic Concrete Research. (2014) 1–16.

[7] G.M. Kirkelund, P.E. Jensen, L.M. Ottosen, Electrodialytic extraction of heavy metals from greenlandic MSWI Fly Ash as a function of remediation time and L/S ratio, ISCORD 2013: Planning for Sustainable Cold Regions - Proceedings of the 10th International Symposium on Cold Regions Development. (2013) 87–96. https://doi.org/10.1061/9780784412978.009.

[8] W. Chen, G.M. Kirkelund, P.E. Jensen, L.M. Ottosen, Electrodialytic extraction of Cr from water-washed MSWI fly ash by changing pH and redox conditions, Waste Management. 71 (2018) 215–223. https://doi.org/10.1016/j.wasman.2017.09.035.

[9] G.M. Kirkelund, C. Magro, P. Guedes, P.E. Jensen, A.B. Ribeiro, L.M. Ottosen, Electrodialytic removal of heavy metals and chloride from municipal solid waste incineration fly ash and air pollution control residue in suspension - Test of a new two compartment experimental cell, Electrochimica Acta. 181 (2015) 73–81. https://doi.org/10.1016/j.electacta.2015.03.192.

[10] A.J. Pedersen, Evaluation of assisting agents for electrodialytic removal of Cd, Pb, Zn, Cu and Cr from MSWI fly ash, Journal of Hazardous Materials. 95 (2002) 185–198. https://doi.org/10.1016/S0304-3894(02)00138-3.

[11] L.M. Ottosen, H.K. Hansen, C.B. Hansen, Water splitting at ion-exchange membranes and potential differences in soil during electrodialytic soil remediation, Journal of Applied Electrochemistry. 30 (2000) 1199–1207.

[12] B.A.R. Ebert, B.-M. Steenari, M. Petranikova, G.M. Kirkelund, "UNDER REVIEW" Electrodialytic Remediation and Combined Acid Leaching and Solvent Extraction - Potential Methods for Recovery of Metals from MSWI Fly Ash, Journal of Cleaner Production. (2021).

[13] G.M. Kirkelund, P.E. Jensen, Electrodialytic treatment of Greenlandic municipal solid waste incineration fly ash, Waste Management. 80 (2018) 241–251. https://doi.org/10.1016/j.wasman.2018.09.019.

[14] P.E. Jensen, C.M.D. Ferreira, H.K. Hansen, J.U. Rype, L.M. Ottosen, A. Villumsen, Electroremediation of air pollution control residues in a continuous reactor, Journal of Applied Electrochemistry. 40 (2010) 1173–1181. https://doi.org/10.1007/s10800-010-0090-1.

[15] G.M. Kirkelund, P.E. Jensen, A. Villumsen, L.M. Ottosen, Test of electrodialytic upgrading of MSWI APC residue in pilot scale: Focus on reduced metal and salt leaching, Journal of Applied Electrochemistry. 40 (2010) 1049–1060. https://doi.org/10.1007/s10800-009-0059-0.

[16] P.E. Jensen, G.M. Kirkelund, K.B. Pedersen, C. Dias-Ferreira, L.M. Ottosen, Electrodialytic upgrading of three different municipal solid waste incineration residue types with focus on Cr, Pb, Zn, Mn, Mo, Sb, Se, V, Cl and SO4, Electrochimica Acta. 181 (2015) 167–178. https://doi.org/10.1016/j.electacta.2015.06.012.

[17] A. de Boom, M. Degrez, Belgian MSWI fly ashes and APC residues: A characterisation study, Waste Management. 32 (2012) 1163–1170. https://doi.org/10.1016/j.wasman.2011.12.017.

[18] K.L. Lin, K.S. Wang, B.Y. Tzeng, C.Y. Lin, The reuse of municipal solid waste incinerator fly ash slag as a cement substitute, Resources, Conservation and Recycling. 39 (2003) 315–324. https://doi.org/10.1016/S0921-3449(02)00172-6.

[19] W. Müllauer, R.E. Beddoe, D. Heinz, Effect of carbonation, chloride and external sulphates on the leaching behaviour of major and trace elements from concrete, Cement and Concrete Composites. 34 (2012) 618–626. https://doi.org/10.1016/j.cemconcomp.2012.02.002.

[20] R. Argane, M. Benzaazoua, R. Hakkou, A. Bouamrane, A comparative study on the practical use of low sulfide base-metal tailings as aggregates for rendering and masonry mortars, Journal of Cleaner Production. 112 (2016) 914–925. https://doi.org/10.1016/j.jclepro.2015.06.004.

[21] D.L. Cocke, The binding chemistry and leaching mechanisms of hazardous substances in cementitious solidification/stabilization systems, Journal of Hazardous Materials. 24 (1990) 231–253. https://doi.org/10.1016/0304-3894(90)87013-8.

[22] H.S. Shi, L.L. Kan, Leaching behavior of heavy metals from municipal solid wastes incineration (MSWI) fly ash used in concrete, Journal of Hazardous Materials. 164 (2009) 750–754. https://doi.org/10.1016/j.jhazmat.2008.08.077.

[23] J.E. Aubert, B. Husson, A. Vaquier, Use of municipal solid waste incineration fly ash in concrete, Cement and Concrete Research. 34 (2004) 957–963. https://doi.org/10.1016/j.cemconres.2003.11.002.

[24] M. Dell'Orso, T. Mangialardi, A.E. Paolini, L. Piga, Evaluation of the leachability of heavy metals from cement-based materials, Journal of Hazardous Materials. 227–228 (2012) 1–8. https://doi.org/10.1016/j.jhazmat.2012.04.017.

[25] T. van Gerven, J. Moors, V. Dutré, C. Vandecasteele, Effect of CO2 on leaching from a cement-stabilized MSWI fly ash, Cement and Concrete

Research. 34 (2004) 1103–1109. https://doi.org/10.1016/j.cemconres.2003.11.022.

[26] C. Baldermann, A. Baldermann, O. Furat, M. Krüger, M. Nachtnebel, H. Schroettner, J. Juhart, V. Schmidt, J. Tritthart, Mineralogical and microstructural response of hydrated cement blends to leaching, Construction and Building Materials. 229 (2019) 116902. https://doi.org/10.1016/j.conbuildmat.2019.116902.

[27] W. Chen, G.M. Kirkelund, P.E. Jensen, L.M. Ottosen, Comparison of different MSWI fly ash treatment processes on the thermal behavior of As, Cr, Pb and Zn in the ash, Waste Management. 68 (2017) 240–251. https://doi.org/10.1016/j.wasman.2017.07.011.

[28] B.A.R. Ebert, B.-M. Steenari, M.R. Geiker, G.M. Kirkelund, Screening of untreated municipal solid waste incineration fly ash for use in cement-based materials: chemical and physical properties, SN Applied Sciences. 2 (2020). https://doi.org/10.1007/s42452-020-2613-7.

[29] A. Vollpracht, W. Brameshuber, Binding and leaching of trace elements in Portland cement pastes, Cement and Concrete Research. 79 (2016) 76–92. https://doi.org/10.1016/j.cemconres.2015.08.002.

[30] M. Andac, F.P. Glasser, The effect of test conditions on the leaching of stabilised MSWI-fly ash in Portland cement, Waste Management. 18 (1998) 309–319. https://doi.org/10.1016/S0956-053X(98)00041-5.

[31] T. van Gerven, D. van Baelen, V. Dutré, C. Vandecasteele, Influence of carbonation and carbonation methods on leaching of metals from mortars, Cement and Concrete Research. 34 (2004) 149–156. https://doi.org/10.1016/S0008-8846(03)00255-2.

[32] R. Malviya, R. Chaudhary, Evaluation of leaching characteristics and environmental compatibility of solidified/stabilized industrial waste, Journal of Material Cycles and Waste Management. 8 (2006) 78–87. https://doi.org/10.1007/s10163-005-0139-0.

[33] V. Dutre, C. Vandecasteele, An Evaluation of the Solidification/Stabilisation of Industrial Arsenic containing waste using extraction and semi-dynamic leach tests, Science. 16 (1997) 625–631.

[34] DS/EN 12457-1: Characterisation of waste - Leaching - Compliance test for leaching of granular waste materials and sludges - Part 1: One stage batch test at a liquid to solid ratio of 2 l/kg for materials with high solid content and with particle size bel, Dansk Standard, 2002.

[35] DS/EN 196-1: Methods of testing cement – Part 1: Determination of strength, Dansk Standard, 2005.

[36] A.J. Pedersen, L.M. Ottosen, A. Villumsen, Electrodialytic removal of heavy metals from different fly ashes: Influence of heavy metal speciation in the ashes, Journal of Hazardous Materials. 100 (2003) 65–78. https://doi.org/10.1016/S0304-3894(03)00064-5.

[37] P. Pedeferri, Pourbaix Diagrams, in: S.N. Switzerland (Ed.), Corrosion Science and Engineering, 2018: pp. 57–72. https://doi.org/10.1007/978-3-319-97625-9_4.

[38] E. Lacasa, S. Cotillas, C. Saez, J. Lobato, P. Cañizares, M.A. Rodrigo, Environmental applications of electrochemical technology. What is needed

to enable full-scale applications?, Current Opinion in Electrochemistry. 16 (2019) 149–156. https://doi.org/10.1016/j.coelec.2019.07.002.

[39] B. Lothenbach, P. Durdzinski, K. de Weerdt, Thermogravimetric Analysis, in: K. Scrivener, R. Snellings, B. Lothenbach (Eds.), A Practical Guide to Microstructural Analysis of Cementitious Materials, CRC Press, 2016: pp. 177–213.

[40] Appendix 1: The Landfill Directive Council Directive 199/31/EC, 1999.

[41] D. Brookins, Geochemical Behaviour of Antimony, Arsenic, Camium and Thallium: E h -p H Diagrams for 25°C, 1-Bar Pressure, Chemical Geology. (1986) 271–278.

[42] N. Quijorna, A. Coz, A. Andres, C. Cheeseman, Recycling of Waelz slag and waste foundry sand in red clay bricks, Resources, Conservation and Recycling. 65 (2012) 1–10. https://doi.org/10.1016/j.resconrec.2012.05.004.

[43] K. You, J. Ahn, H. Cho, G. Han, D.-Y. Han, K.-H. Cho, Competing ion effect of stabilization by Cr(III) & Cr(VI) in ettringite crystal structure, Solid State Phenomena. (2007) 1629–1632. http://library1.nida.ac.th/termpaper6/sd/2554/19755.pdf.

[44] M.L.D. Gougar, B.E. Scheetz, D.M. Roy, Ettringite and C-S-H portland cement phases for waste ion immobilization: A review, Waste Management. 16 (1996) 295–303. https://doi.org/10.1016/S0956-053X(96)00072-4.

[45] M. Chrysochoou, D. Dermatas, Evaluation of ettringite and hydrocalumite formation for heavy metal immobilization: Literature review and experimental study, Journal of Hazardous Materials. 136 (2006) 20–33. https://doi.org/10.1016/j.jhazmat.2005.11.008.

[46] B. COHEN, J. PETRIE, CONTAINMENT OF CHROMIUM AND ZINC IN FERROCHROMIUM FLU DUSTS BY CEMENT-BASED SOLIDIFICATION, Canadian Metallurgical Quarterly. 36 (1997) 251–260. https://doi.org/10.1081/E-EEE2-120046011.

[47] D.L. Cocke, M.Y.A. Mollah, J.R. Parga, T.R. Hess, J.D. Ortego, An XPS and SEM/EDS characterization of leaching effects on lead- and zinc-doped portland cement, Journal of Hazardous Materials. 30 (1992) 83–95. https://doi.org/10.1016/0304-3894(92)87076-R.

[48] I. Serclerat, P. Moszkowicz, Retention mechanisms in mortars of the trace metals contained in Portland cement clinkers, Studies in Environmental Science. 71 (1997) 339–347. https://doi.org/10.1016/S0166-1116(97)80216-6.

[49] F.K. Cartledge, L.G. Butler, D. Chalasani, H.C. Eaton, F.P. Frey, E. Herrera, M.E. Tittlebaum, S.L. Yang, Immobilization Mechanisms in Solidification/Stabilization of Cd and Pb Salts Using Portland Cement Fixing Agents, Environmental Science and Technology. 24 (1990) 867–873. https://doi.org/10.1021/es00076a012.

[50] Miljøministeriet, Bekendtgørelse om anvendelse af restprodukter og jord til bygge- og anlægsarbejder og om anvendelse af sorteret, uforurenet bygge- og anlægsaffald, 2010. https://www.retsinformation.dk/Forms/R0710.aspx?id=134831.

Journal Paper IV

Impact of Electrodialytic Remediation of MSWI Fly Ash on Hydration and Mechanical Properties of Blended Binders

Benjamin A. R. Ebert, Wolfgang Kunther, Mette R. Geiker, Gunvor M. Kirkelund

Impact of electrodialytic remediation of MSWI fly ash on hydration and mechanical properties of blends with Portland cement

Benjamin A. R. Ebert[1], Mette R. Geiker[2], Wolfgang Kunther[1], Gunvor M. Kirkelund[1*]

[1]Department of Civil Engineering, Technical University of Denmark, Brovej, building 118, 2800 Kgs. Lyngby, Denmark

[2]Department of Structural Engineering, Norwegian University of Science and Technology, Richard Birkelands Vei 1a, 7491 Trondheim Norway

[*]Corresponding author email: gunki@byg.dtu.dk

Abstract

Municipal solid waste incineration (MSWI) residues such as fly ash and air pollution control (APC) residues may serve as new secondary cementitious materials (SCM). These SCMs may, however, require a pre-treatment to improve material properties. This study investigates the impact of electrodialytically remediated (EDR) MSWI residues to remove heavy metals and salts, on the phase development, setting, and compressive strength development of composite cements with 10 wt% cement replacement, compared to inert quartz or untreated (raw) MSWI residues. All treated MSWI residues showed reactivity in mortar, resulting in higher compressive strength than inert quartz, attributed to additional ettringite and monocarbonate formation. The results indicate that electrodialytical remediation improves the performance of MSWI fly ash in blends with Portland cement, while MSWI APC residues might be used without pre-treatment.

Keywords: Portland cement, secondary cementitious materials, phase characteristics, reactivity, thermodynamic modelling, compressive strength

Article highlights

- EDR MSWI residues contributed to the strength development of PC mortar
- XRD/TGA and thermodynamic modelling showed changes in AFm/AFt quantities
- EDR shortened setting time and reduced gas evolution in mortars with MSWI FA

1 Introduction

Portland cement clinker production has been estimated to account for approximately 8% of the global anthropogenic CO_2 emissions, representing a significant environmental issue [1]. Research into replacing Portland cement with other cement types, e.g. belite cement, and magnesium-based cement, is ongoing [2]. However, concrete based on Portland cement clinker is estimated to dominate in the foreseeable future [2]. A well-established strategy for reducing Portland cement clinker use is to partially replace it with supplementary cementitious materials (SCMs). Limited potential for reducing CO_2 emission further with commonly used SCMs such as ground granulated blast furnace slag or fly ash from coal incineration has been identified because of limited supplies of these SCMs [2]. The introduction of new sources of SCMs is therefore needed.

Municipal solid waste incineration (MSWI) residues as fly ash and air pollution control (APC) residues could potentially be a new SCM source [3]. However, MSWI fly ash's chemical composition differs considerably from coal fly ash, suggesting a low potential as an SCM [4]. Untreated MSWI fly ash has a high content of chlorides, sulphates, heavy metals and organic compounds and is considered as hazardous material that is landfilled [4]. On the other hand, landfilling the MSWI fly ash results in the loss of a potential new SCM and valuable metals seen as hazardous in landfills, but if extracted a resource. Furthermore, due to its high content of chlorides, sulphates and metals, MSWI fly ash could be expected to retard the setting [5–8], lower the compressive strength [8] and cause volume expansion [9] of cement-based materials. Various treatment processes to reduce the ashes hazardousness by demobilisation or extraction of metals (e.g. solidification/stabilisation [10,11], milling [12], separation [13,14] or thermal treatments [15,16]) or to improve its use in cement-based materials (e.g. combined phosphonation and calcination [17], melting [18], combined sieving and washing [19] or mechanical chemical stabilisation [20]) have been investigated. Treating MSWI fly ash with these methods have shown promising results when used in cement-based materials, such as increased compressive strength

[17–20] and reduced metal leaching [17–19]. However, these treatments do not recover the valuable metals in the ash. A method that can recover the valuable metals, remove soluble salts and improve MSWI fly ash for use in cement-based materials is electrodialytic remediation (EDR) [21,22]. EDR combines electrokinetic remediation and ion-exchange membranes to separate ions from a particulate suspension into different electrolyte solutions, using a low electric current. The metals are released through acidification and migrate as ions in the electric field. EDR does not reduce the concentration of organic contaminants [23]. Partially replacing cement with raw or EDR treated MSWI residue was previously studied by Kirkelund et al. [24]. They studied an MSWI air pollution control (APC) residue (with flue gas cleaning products) before and after electrodialytic upgrading. They found that mortar made with EDR treated MSWI APC residue achieved higher compressive strength and had reduced metal leaching compared to an untreated APC residue.

Recent research by Ebert et al. [25] identified similarities and differences in the chemical composition of a large dataset of MSWI residues using a principal component analysis. Based on this analysis, one MSWI residue close to; one MSWI residue deviating and one MSWI residue deviating considerably to the average chemical composition of MSWI residues were chosen for electrodialytic remediation at bench-scale [26]. Subsequently, the electrodialytically treated MSWI residues metal leaching when used in cement-based materials was tested for crushed and monolithic mortar [26]. It was found that if a low pH could be maintained during the electrodialytic treatment process, 60 wt% Cd, 80 wt% Cu and 75 wt % Zn could be removed from the investigated MSWI residues and leaching from the mortar containing 10 % electrodialytic treated MSWI fly ash was below the regulatory limits for both monolithic and crushed mortar samples [26].

To further improve our understanding of how EDR treated MSWI residues behaves in cement-based materials, the present study's objective is to determine the impact of EDR of MSWI residues on cement hydration and the development of mechanical properties. The performance is compared to mixtures with an inert material (quartz).

This is accomplished by investigating the development of the hydrate phases with x-ray diffraction (XRD), thermogravimetric analysis (TGA) and thermodynamic modelling, and measuring the development of mechanical properties in the form of initial and final setting time and compressive strength after 1, 3, 28 and 90 days. Thermodynamic modelling of the cement hydration can serve as a powerful tool for further understanding and complements experimental hydration studies and provides a better understanding of the chemical interactions of the solid and aqueous phases during cement hydration and the influence of added SCMs [27]. Thermodynamic modelling has been used to model cement hydration with commonly used SCMs such as blast furnace slag, metakaolin and coal fly ash [27,28]. Thermodynamic modelling has also been used to model the effect of incorporating raw MSWI fly ash in cement pastes and mortar [28] and model the hydration characteristics of ternary blends of raw MSWI fly ash, blast furnace slag and cement. However, it has not been used to investigate the hydration differences between binders with raw or treated MSWI fly ash.

2 Materials and methods

2.1 Materials

Three MSWI residues were in 2018 acquired from two grate fired and one fluidised bed commercial MSWI plants:

1) **Fly ash from Amager Bakke (*Ama*):** A state-of-the-art grate fired incinerator (1680 tons/day) in Copenhagen, Denmark. The facility incinerated household and industrial waste at an average temperature of 1025°C. The MSWI fly ash sample was extracted before the addition of APC products with an electrostatic precipitator.

2) **Fly ash from Nuuk incineration (*Nuu*):** A grate fired incinerator (40 tons/day) located in Nuuk, Greenland. The facility incinerated household and construction waste at an average temperature of 1060°C. The MSWI fly ash sample was extracted with an electrostatic precipitator. The facility does not have APC.

3) **APC residue from Ryaverket (*Rya*):** A fluidised bed incinerator (300 tons/day) located in Borås, Sweden. The facility had an average furnace temperature of 900°C and incinerated household and

industrial waste. The APC residue sample was extracted with a textile filter after the APC (a dry scrubber system with lime and activated carbon injection), consisting of fly ash and APC products.

Since the experimental samples were both fly ash and APC residue, the term MSWI residues will be used in this paper when referring to both types of samples. The MSWI residues were treated with EDR using a three-cell bench-scale setup, the treatment method is summarised below, and the treatment details can be viewed in [26]. The MSWI residues used in the bench-scale EDR treatment were first washed three times with deionised water at a liquid/solid ratio of 5. 3 kg of the washed MSWI residue were then mixed with 30 litres of deionised water in a stirred container to avoid sedimentation. A constant current of 1 A was then maintained for 28 days to leach and separate the MSWI residues' metals into the electrolyte solutions. The MSWI residue suspension was then filtered through 45 μm filters and dried at 50°C. The MSWI residue was then crushed manually with a mortar and pestle.

2.2 Preparation of pastes and mortars

Paste or mortar with 10 wt% of the raw MSWI residues are denoted *Raw*, while paste or mortar with 10 wt% of the EDR treated MSWI residue are denoted *EDR*.

A Portland cement, inert quartz, sand and a superplasticiser were also used as part of this study.

- The Portland cement was a CEM I 52,5 N (MS/LA) consisting of 95-100% Portland cement clinker and 3.7% limestone filler (TGA measurement). Paste or mortar made with 100 wt% cement as a binder are denoted *CEM I*.
- The inert quartz filler was M8 grade quartz, consisting of 99.4 % SiO_2. Paste or mortar made with 10 wt% quartz are denoted *Qua*.
- The sand was CEN standard sand that complies with EN 196-1:2005 [29].
- The superplasticiser was a modified acrylic polymer based on designed performance polymers, with a viscosity of <30 MPa, a pH of 6.5±1 and a density of 1.06±0.02 g/cm^3.

The oxide composition (back-calculated from an x-ray fluorescence analysis) and physical characteristics of the raw and EDR treated MSWI residues, CEM I cement, and quartz used are given

in Table 1 and 2, respectively. The CO_2 content was measured with TGA, using the mass loss between 600-750**°C**. The total concentration of Cd, Cu, Pb, and Zn, determined with x-ray fluorescence, is given in Table 3, together with the metals' leachable content. The content of leachable metals was determined using the batch leaching test as specified in EN 12457-1 [30].

Table 1
Calculated oxide composition and physical characteristics of the raw [25] and treated MSWI residues [26] and CEM I.

		Raw Ama	EDR Ama	Raw Nuu	EDR Nuu	Raw Rya	EDR Rya	CEM I
SiO_2	[Wt%]	4.6	14	6.1	14	6.4	12	20
Al_2O_3	[Wt%]	1.4	2.3	4.6	9.6	4.7	5.3	5.4
Fe_2O_3	[Wt%]	1.0	2.4	0.9	1.4	1.8	2.7	3.8
CaO	[Wt%]	13	28	43	29	42	31	61
MgO	[Wt%]	0.6	0.4	1.4	1.3	1.8	2.2	1.0
SO_3	[Wt%]	34	30	8.9	9.7	8.9	8.7	3.2
K_2O	[Wt%]	14	1.0	12	0.4	2.7	0.7	0.4
Na_2O	[Wt%]	7.4	0.7	22	-	7.0	-	0.3
P_2O_5	[Wt%]	2.6	2.1	1.8	2.7	2.2	3.7	0.3
Cl	[Wt%]	2.8	0.1	24	0.1	13	0.2	0.04
CO_2	[Wt%]	0.0	0.0	2.7	2.4	5.3	2.8	1.6

Table 2
Density and particle size distribution d values of the MSWI residues, CEM I and quartz.

		Raw Ama	EDR Ama	Raw Nuu	EDR Nuu	Raw Rya	EDR Rya	CEM I	Quartz
ρ	[g/cm^3]	2.8	2.7	2.6	2.6	2.5	2.6	3.2	2.7
d_{10}	[µm]	8.7	2.9	1.9	2.4	8.2	2.4	2.7	4.5
d_{50}	[µm]	44	17	13	12	19	11	14	28
d_{90}	[µm]	204	120	49	56	41	130	49	84

Table 3
Total concentration and leachable concentration of Cd, Cr, Cu, Pb and Zn of the raw [25], treated MSWI residues [26] and CEM I.

		Raw Ama	EDR Ama	Raw Nuu	EDR Nuu	Raw Rya	EDR Rya	CEM I
Total								
Cd	[mg/kg]	480	60	420	460	80	100	0.4
Cr	[mg/kg]	300	700	800	1100	400	600	33
Cu	[mg/kg]	1400	520	1300	2000	7900	10200	140
Pb	[mg/kg]	12000	31000	3000	3200	3400	3400	17
Zn	[mg/kg]	55000	26000	33000	41000	6600	9100	180
Leachable								
Cd	[mg/kg]	430	4.2	0.03	0.01	0.00	0.02	-
Cr	[mg/kg]	1.0	0.1	39	23	0.1	2.6	-
Cu	[mg/kg]	2.6	23	0.4	0.07	52	0.01	-
Pb	[mg/kg]	5.0	4.3	530	0.01	1400	0.00	-
Zn	[mg/kg]	23000	1700	2.9	0.5	20	0.09	-

2.3 Frattini test

The Frattini test was performed per EN-196-5 2011 [31] using 20g cement or 16g cement and 4g MSWI residue or quartz, and 100 ml deionised water at 40°C. The results are presented as CaO (mmol/l) as a function of OH^- (mmol/l). Included is the saturation concentration curve of the calcium ion (expressed as CaO) as a function of the OH^- concentration, estimated for a 40°C solution:

$$[\mathrm{CaO}] = \frac{350}{[\mathrm{OH}^-] - 15} \quad \textbf{(1)}$$

The curve is valid over the range of 45 mmol/l to 90 mmol/l OH^- [31]. Results at or above the solubility curve (zone 2) indicate low to no pozzolanic activity due to saturation with $Ca(OH)_2$. Results below the solubility curve (zone 1) indicate pozzolanic activity due to $Ca(OH)_2$ reduction.

2.4 Setting time

The cement paste for the setting time test was prepared per EN 196-3:2009 [32] with the following deviations. 500g of cement (Ref) or 450g + 50g quartz or MSWI residue were mixed with 250g of deionised water. The mixing process used follows the procedure outlined in EN 196-1:2005 [29], instead of EN 196-3:2009 [32], with cement added to a 5-litre stainless steel bowl first and then mixed with deionised water. For the paste with 10 wt% admixture and cement, the admixture and cement were mixed for 2 minutes before adding water.

The initial and final setting time of the cement paste and paste with MSWI residue or quartz were determined per the method specified in EN 196-3:2009 [32] using an automatic Vicat apparatus Matest E044N Vicatronic. The mould was not inverted during the test after the initial setting had been measured as specified in EN 196-3:2009 [32].

2.5 Phase development

The cement paste used for the phase development assessment was prepared using the quantities for setting time determination. However, the paste was mixed using a high shear mixer (Whip Mix Power Mixer Model B). The paste was first mixed manually for 30 s, then left to rest for 30 s and finally mixed for 180 s with the high shear mixer. The paste samples were then cast in 18 ml (27.1 mm diameter)

Nalgene LDPE sample vials with snap closure and stored sealed at 20°C and >90% relative humidity. Paste samples were only repeated once per date tested.

The pastes' hydration was stopped after 1, 3, 28 and 90 days using a three-step procedure with isopropanol and diethyl ether, as described in [33]. Several slices (approximately 2 mm thick) were cut from the middle part of the paste sample and crushed in a porcelain mortar to a particle size below 1 mm. Approximately 4 g of crushed paste was immersed in 67 ml isopropanol, shaken for 30 s and left to rest for 5 minutes before decanting the isopropanol. This step was performed twice. After the second washing with isopropanol, the sample and isopropanol were vacuum-filtered. The crushed paste was then immersed in 13 ml diethyl ether, shaken for 30 s and left to rest for 5 minutes before vacuum-filtering the solution. The crushed paste was then dried at 40°C for 8 minutes to remove any remaining ether—the crushed paste was then ground to a particle size below 63 µm.

2.5.1 X-ray diffraction

The crystalline phases in the crushed paste were identified with XRD. A Pan Analytical x-ray diffractometer equipped with a PW3064 Spinner stage was used for the measurements. The x-ray source was Cu-Kα with a wavelength of 1.54 Å. The crushed paste was backloaded into the sample holder and measured between 4° 2θ - 100° 2θ. The step size and sampling time per step were 0.002°2θ and 24.8s, respectively. The crystalline phases were identified from the XRD plots by comparing the pure crystalline phase plots shown in Table 4 in conjunction with the ICDD PDF4 database.

Table 4: Crystalline phases and corresponding ICSD and PDF number.

Name	**Formula**	**ICSD number**	**PDF number**
Alite M3	Ca_3SiO_5	94742	85-1378
Alite M	Ca_3SiO_5	81100	42-551
Belite β	Ca_2SiO_4	81096	33-302
C_3A cub.	$Ca_3Al_2O_6$	1841	38-1429
Brownmillerite	$Ca_2Al_{1.35}Fe_{0.651}O_5$	98839	01-074-3675
α-Quartz	SiO_2	174	46-1045
Anhydrite	$CaSO_4$	15876	37-1496
Bassanite	$CaSO_4{\cdot}0.5(H_2O)$	79529	41-224
Gypsum	$CaSO_4{\cdot}2(H_2O)$	409581	33-311
Calcite	$CaCO_3$	73446	5-586
Portlandite	$Ca(OH)_2$	202220	4-733
Ettringite	$Ca_6Al_2(SO_4)_3(OH)_{12}(H_2O)_{26}$	155395	41-1451
Friedel's salt	$Ca_2Al(OH)_6Cl(H_2O)_2$	62363	01-078-1219
Hemicarbonate	$Ca_4Al_2(OH)_{12}(OH)(CO_3)_{0.5}(H_2O)_5$	-	41-0221
Monocarbonate	$Ca_4Al_2(OH)_{12}(CO_3)(H_2O)_5$	59327	01-087-0493

2.5.2 Thermogravimetric analysis

Thermogravimetric analysis (TGA) was performed with a NETZSCH STA 449 F3 Jupiter to assess the bound water and portlandite content in the paste samples. Approximately 50 mg of the crushed paste was placed into 85 µl aluminium oxide crucibles (diameter 6.8 mm). The weight loss was measured from 29°C to 900°C, a heating rate of 10°C/min, in a nitrogen atmosphere (50 ml/min of nitrogen gas was used as purge gas). The results were analysed using the Proteus Analyzer software. The crushed paste's bound water content was determined as the mass loss between 50°C and 550°C (H_2O_g). The portlandite content was determined based on the mass loss between 400°C and 550°C (H_2O_g) using tangential quantification to exclude any C-S-H loss [33]. The portlandite content was calculated using the molar masses of portlandite and water. The results were normalised as mass relative to the mass of the anhydrous binder in the paste (weight at 550°C).

2.5.3 Thermodynamic modelling

The Gibbs free energy minimization program (GEMS) [34] was used to model the cement paste phase development as a function of the % of reacted MSWI residue. The program computes equilibrium phase assemblages and speciation in complex chemical systems. The standard PSI-GEMS database in GEMS was supplemented with the CEMDATA18 database [35]. The C-S-H phase was modelled using the CSHQ model proposed by Kulik [36]. The databases used do not account for heavy metals, such as Zn or Pb, on the resulting phase assemblage. The following phases were excluded from the modelling: M-S-H, $Al(OH)_{3am}$, $Al(OH)_{3mic}$, gibbsite, graphite, C_3AH_6, anhydrite, thaumasite, iron, hematite, magnetite, geothite, quartz and silica-amorph. The MSWI residues and CEM I cement input was calculated from the XRF results as listed in Table 1, scaled so that the oxides shown were equal to 100 wt%. For the performed calculations, a reaction degree of 80% was used for the cement without accounting for the differences in the different clinker phases degree of reaction.

2.6 Compressive strength

Mortar prisms (4x4x16 cm^3) for compressive strength testing were prepared per EN 196-1:2005 [29]. The CEM 1 sample was made with 450g cement, 225g deionised water and 1350g CEN standard sand. Mortar with 10 wt% cement replacement was made with 405g cement, 45g MSWI residue or quartz,

225g deionised water and 1350g CEN standard sand. Superplasticiser was added to the deionised water for mortar prisms made with the MSWI residues to maintain a consistency equal to the CEM 1 and Qua mortar's consistency, as determined by the fall table test EN 1015-3: 1999 [37]. Superplasticiser was added to the mortar with Raw Ama (5.4g), Raw Nuu (0.3g), Raw Rya (0.5g), EDR Ama (1.4g), EDR Nuu (1.5g) and EDR Rya (1.3g). The prism moulds were filled with mortar halfway and vibrated for 15s at 50hz, then filled over the following 15s and finally vibrated for a total of 120 s. The prisms were stored covered in their moulds for 24 hours at 20°C and ~90% relative humidity. After 24 hours, the prisms were demoulded and submerged in containers with a solution of 3g $CaOH_2$ per litre deionised water until testing. The prisms from the different mortar mixtures were stored in separate containers. The mixes for the CEM I mortar and mortar with quartz was repeated 3 times per date tested.

The compressive strength of mortar prisms was measured after 1, 3, 28 and 90 days of curing per EN 196-1:2005 [29]. All samples were tested perpendicular to the casting orientation after splitting the prisms in two with an electro-mechanic test machine (Instron 6025, 100 kN) followed by compressive strength testing with the Instron 6025 or a Toni Technik 300 ton compression test machine. The as measured compressive strength (σ) were normalised to the air free compressive strength (σ_0), using the equation by Osbæck [38]:

$$\sigma = \sigma_0 - e^{-\varphi \cdot p} \quad \textbf{(2)}$$

The air content (p) of the mortar, after one day of curing, was determined using an indirect method, based on the difference in density of the mortar immediately after demoulding (ρ) and the theoretical mortar density (ρ_0), according to the equation by Osbæck [38]:

$$p = 1 - \frac{\rho}{\rho_0} \quad \textbf{(3)}$$

The density of the mortar prism's was calculated immediately after demoulding based on the difference in weight (w_{ow}) above water and submerged in water (w_{uw}), and the density of water (ρ_w):

$$\rho = \frac{w_{ow}}{w_{ow} - w_{uw}} \cdot \rho_w \quad \textbf{(4)}$$

The theoretical density of the mortar was calculated based on the density and mass of the mortar ingredients:

$$\rho_0 = \frac{m_c + m_s + m_w + m_a}{\frac{m_c}{\rho_c} + \frac{m_s}{\rho_s} + \frac{m_w}{\rho_w} + \frac{m_a}{\rho_a}} \quad \textbf{(5)}$$

Where m_c and ρ_c is mass and density of the cement, m_s and ρ_s is the mass and density of the sand, m_w and ρ_w is the mass and density of water and m_a and ρ_a is the mass and density of the admixture. The measured air content is an indication of the macroporosity of the mortar prisms.

3 Results and discussion

3.1 Impact of EDR on MSWI residue composition and pozzolanic reactivity

The general changes to the oxide composition and Cl after the electrodialytic remediation treatment were reduced K_2O, Na_2O and Cl concentrations and an accumulation of SiO_2, Al_2O_3 and Fe_2O_3, see Table 1. A reduced concentration of CaO could be observed for EDR Nuu and EDR Rya, while EDR Ama had an increased CaO concentration. Furthermore, EDR Nuu and EDR Rya had an accumulation of SO_3, while EDR Ama had a 4% reduction in SO_3. Previous work by Ebert et al. [25] found that Raw Nuu and Raw Rya contained 1.9 wt% and 6.0 wt% water-soluble Ca^{2+}, and 0.6 wt% and 0.2 wt% water-soluble SO_4^{2-} respectively, while raw Ama contained 0.1 wt% water-soluble Ca^{2+} and 21 wt% water-soluble SO_4^{2-}. Therefore, the EDR treatment would have removed low amounts of Ca^{2+} compared to SO_4^{2-} from Raw Ama while removing high amounts of Ca^{2+} compared to SO_4^{2-} from Raw Nuu and Raw Rya.

Previous work by Ebert et al. [26] also showed that the raw MSWI residues contained $CaSO_4$, NaCl, KCl and $CaCO_3$. Raw Ama also contained other SO_4 bearing phases, such as $NaSO_4$, and no $CaCO_3$, while Raw Rya also contained CaClOH. After the EDR treatment, $CaSO_4$, $CaSO_4{\cdot}2H_2O$ and $CaCO_3$ were found in EDR Nuu and EDR Rya, while EDR Ama contained $CaSO_4$, $CaSO_4{\cdot}0.5H_2O$ and $PbSO_4$. Therefore, the treatment process reduced the K_2O, Na_2O, Cl and SO_4^{2-} (Raw Ama) content by removing NaCl, KCl, CaClOH (Raw Rya) and $NaSO_4$ (Raw Ama). The high CaO and SO_3 observed in the treated MSWI residues could result from $CaSO_4{\cdot}0.5H_2O$, $CaSO_4{\cdot}2H_2O$, $PbSO_4$ formation and $CaCO_3$

accumulation. However, EDR Nuu and EDR Rya had reduced concentrations of CO_2. Their CO_2 content was measured with TGA, see [26], as the mass loss occurring around 650-750°C, and were interpreted as CO_2 bound in $CaCO_3$, potentially indicating a reduction in $CaCO_3$ after EDR.

Reduced K_2O, Na_2O and Cl concentrations are desirable for cement-based materials due to the risk of alkali-silica reactions and reinforcement corrosion [39]. The requirement for coal fly ash used as an SCM is less than 5 wt% Na_2O_{eq} [40], which the treated MSWI residues are within. However, the requirement for Cl is 0.01 % [40], which the treated MSWI residues exceed by a magnitude of 10. An increase of SiO_2-Al_2O_3-Fe_2O_3 is desired as these are the pozzolanic reactive oxides in SCMs [41]. The requirement for coal fly ash is $\sum SiO_2$-Al_2O_3-$Fe_2O_3 \geq 70$ wt% [40]. The sum of SiO_2-Al_2O_3-Fe_2O_3 in EDR Ama, EDR Nuu and EDR Rya was less than 25 wt%. Therefore, it was expected that the treated MSWI residues were not as pozzolanic as coal fly ash. Fig. 1 depicts the raw and treated MSWI residues in a CaO-Al_2O_3-SiO_2 ternary diagram.

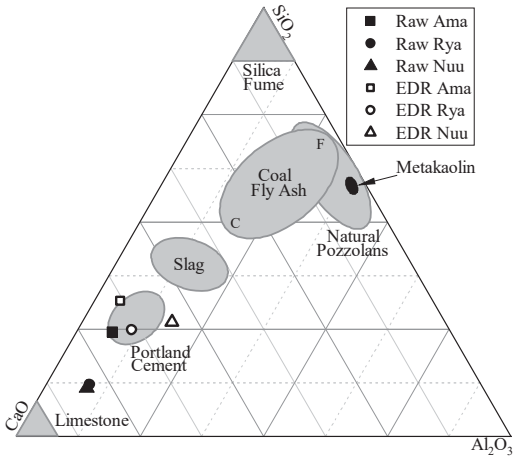

Fig. 1. CaO-Al_2O_3-SiO_2 ternary diagram, with the ratios of the raw and EDR treated residues compared to Portland cement and selected SCMs from Lothenbach et al. [42] and Thomas et al. [43]. C: High calcium coal fly ash, F: Low calcium fly ash.

Raw Nuu and Raw Rya had CaO-Al_2O_3-SiO_2 ratios close to limestone, while Raw Ama had a ratio matching Portland cement. After the EDR treatment, the treated MSWI residues had ratios similar to Portland cement. Therefore, the MSWI residues may be categorised as high-Ca mineral additions.

Fig. 2 shows the results of the Frattini test characterising pozzolanic reactivity. All MSWI residues were within zone 2, indicating no pozzolanic activity, as suggested by their low SiO_2-Al_2O_3-Fe_2O_3 content. However, only the cement paste with Raw Nuu was within the area specified by the test. The cement paste with Raw Ama was highly saturated with OH^- (256 mmol/l after 8 days), while the Ca^{2+} had been consumed (3 mmol/l after 8). In contrast, the paste with Raw Rya was undersaturated with OH^- (41 mmol/l) and oversaturated with Ca^{2+} (25 mmol/l). Extended hydration time reduced the Ca^{2+} and OH^- content, except for Raw Ama, where OH^- increased to 266 mmol/l after 15 days. Some phases in these two raw MSWI residues could have reacted with the hydrochloric acid and EDTA solutions, interfering with the results.

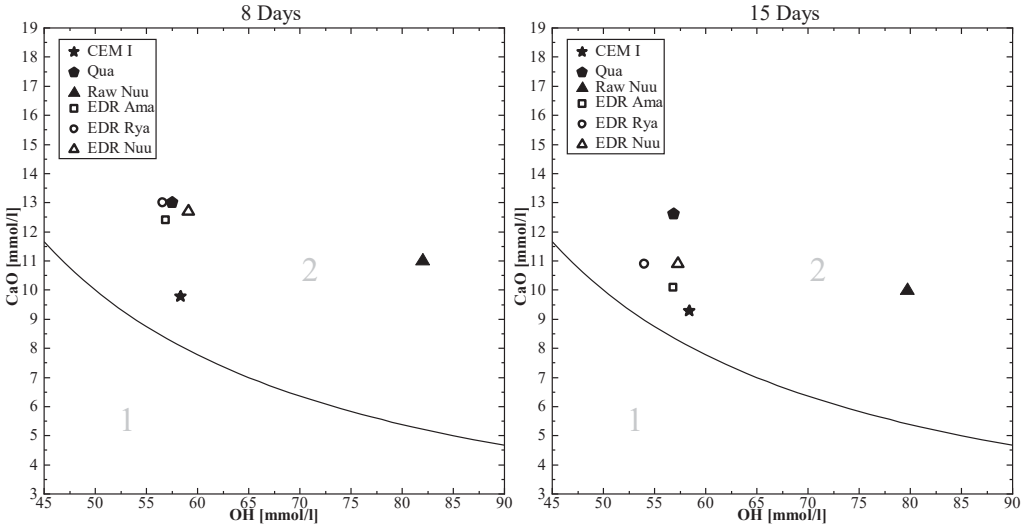

Fig. 2. Frattini test results for the CEM I paste, and paste with quartz and the MSWI fly ash residus after 8 days (left) and 15 days (right).

Although the pastes with treated MSWI residue did not show any pozzolanic reactivity, the results shifted towards zone 1 after 15 days, more than the quartz paste, potentially indicating slow reactivity.

The EDR treatment did not reduce the heavy metal concentration in the MSWI residues, but the concentrations increased instead, except for Cd, Cu and Zn from Raw Ama, see Table 3. This may be attributed to removing the previously discussed phases with high solubility (e.g. KCl, NaCl and Na_2SO_4), resulting in an accumulation of the studied heavy metals, despite removing part of the metals.

Previous experiments have shown that the MSWI residues contain compounds that may accelerate or retard hydration [44]. The impact of different components is briefly summarised in Table 5.

Table 5
Components influencing hydration reactions.

Element/compound	Main hydration effect	Described effects
Alkalis	Acceleration	May accelerate alite hydration leading to higher early strength but less strength at later ages [45,46].
$CaCO_3$	Acceleration	Leads to hemicarbonate and monocarbonate formation. May accelerate hydration due to nucleation and dilution effects [45,46].
Cl^-	Acceleration	$CaCl_2$ is a commonly used accelerator that reduces the initial and final setting due to C-S-H supersaturation [47–49]. NaCl may accelerate alite and aluminate hydration (class G cement) [7,50]. More 20-36 % NaCl and 34% may retard instead [7,50].
SO_4^{2-}	Acceleration	Na_2SO_4 and $CaSO_4$ may accelerate hydration, increasing alite hydration during the first days. Gypsum may lengthen the induction period while increasing the hydration rate in the acceleration period. [6,45,51]
Cd^{2+}	Retardation	Cd may or may not retard setting time. 0.18 mol Cd^{2+}/kg binder may delay setting by 3 hours. It may also reduce the compressive strength [8,52].
Cr^{3+}	Retardation	Cr(III) may significantly hinder C-S-H and CH formation after 1 day while leading to accelerated CH growth after 31 days [53].
Cu^{2+}	Retardation	Cu may result in large variation in setting time. 0.18 mol Cu^{2+}/kg binder may delay setting by 98 hours. Low levels of Cu may increase compressive strength while high levels reduce compressive strength [8,52,54].
Pb^{2+}	Retardation	Pb may coat cement clinker and block hydration, causing a drop in strength. 0.18 mol Pb^{2+}/kg binder may delay setting by 23 hours. Reasonably normal hydration reactions occur after 3 days delay with less C-S-H and CH after 28 days. Small quantities may accelerate setting [8,52,54–56].
Zn^{2+}	Retardation	It has been reported that 0.18 Zn^{2+} mol/kg binder delays setting by 360 hours. The retardation has been shown to have no long-term effect on the product quality. Low Zn levels may increase strength, while higher levels inhibit strength [8,54,57].

The present study's raw MSWI residues contained compounds that could make them function as hydration accelerators, e.g. $CaCO_3$, NaCl, or Na_2SO_4. However, given the MSWI residues high content of heavy metals, they could retard the hydration instead if the blended binders metal concentration is high enough. Although the EDR treatment did not reduce the metal concentrations as intended, this may not be a problem when using the treated MSWI residues. Previous research by Kirkelund et al. [24] suggests that metal leaching after EDR is reduced and does not affect the blended binders compressive strength as drastically as raw MSWI residues when compared to a 100 wt% cement sample. As indicated in Table 3, the studied MSWI residues leach less after EDR, which would also imply the lower reactivity of heavy metals in the cement blends.

3.2 Hydration and phase development

3.2.1 CEM I and quartz paste

Fig. 3 combines the XRD diffractograms of the CEM I and quartz cement pastes. The cement pastes without MSWI residues showed a decreasing peak intensity of the initial Portland clinker phases alite (A), belite (Be), tricalcium aluminate (Ta) and brownmillerite (Br) from 1 to 90 days of hydration. The crystalline phases formed after 1 day of hydration were portlandite (P) and ettringite (E), followed by hemicarbonate (H) after 3 days, and monocarbonate (M) after 28 days. The continued reaction of tricalcium aluminate in cement paste after gypsum has been consumed would, under different conditions, lead to the destabilisation of ettringite and the formation of monosulphate. However, in the presence of limestone, hemicarbonate and monocarbonate form instead of monosulphate, stabilising ettringite [58,59]. Experimental studies have shown that hemicarbonate is initially formed [51], which may be due to the slow dissolution of limestone at high pH [9].

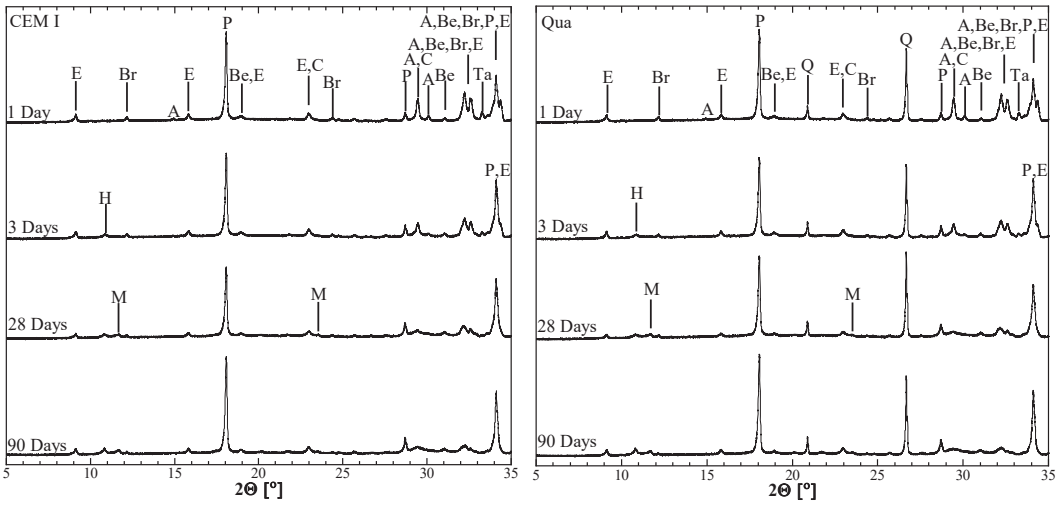

Fig. 3. XRD patterns for the CEM I (left) and quartz (right) pastes cured 1, 3, 28 and 90 days. Alite (A), belite (Be), tricalcium aluminate (Ta), brownmillerite (Br), portlandite (P), ettringite (E), hemicarbonate (H), monocarbonate (M), calcite (C) and quartz (Q).

The results of the quantification of bound water and portlandite content with TGA are shown in Fig. 4. The CEM 1 paste and paste with quartz had an increasing content of bound water and portlandite, as suggested by decreasing peak intensity of the initial clinker phases with XRD. The cement paste with quartz had the same bound water and portlandite development over time as the CEM I paste, albeit at a reduced quantity due to the reduced cement content. After 90 days, the CEM I paste

contained 31 wt% bound water, while the paste with quartz contained 29 wt%. The portlandite content in the CEM I paste and paste with quartz was 23 and 22 wt%, respectively.

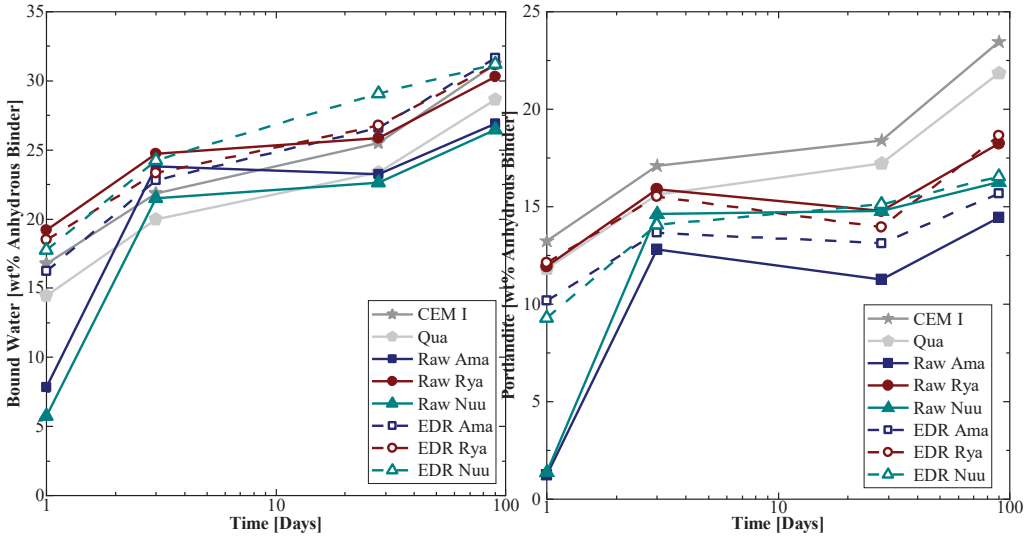

Fig. 4. Bound water and portlandite content as wt% of the experimental pastes.

3.2.2 Raw MSWI residues

Fig. 5 shows the XRD diffractograms and thermodynamic modelling results of the cement pastes with Raw Ama, Raw Nuu and Raw Rya. The pastes with Raw Ama or Raw Nuu had peaks of alite (A), belite (Be), tricalcium aluminate (Ta) and brownmillerite (Br) with high intensity compared to the Qua paste after 1 day of hydration, suggesting that the cement was largely unhydrated after 1 day. This is further evidenced by the low intensity of the portlandite peak, indicating that only a small amount of alite had reacted after 1 day. However, the paste with Raw Nuu had portlandite peaks with higher intensity than the paste with Raw Ama, suggesting a higher degree of reaction after 1 day. Ettringite (E) was present after 1 day of hydration, indicating that the aluminate/ferrite phases react partially.

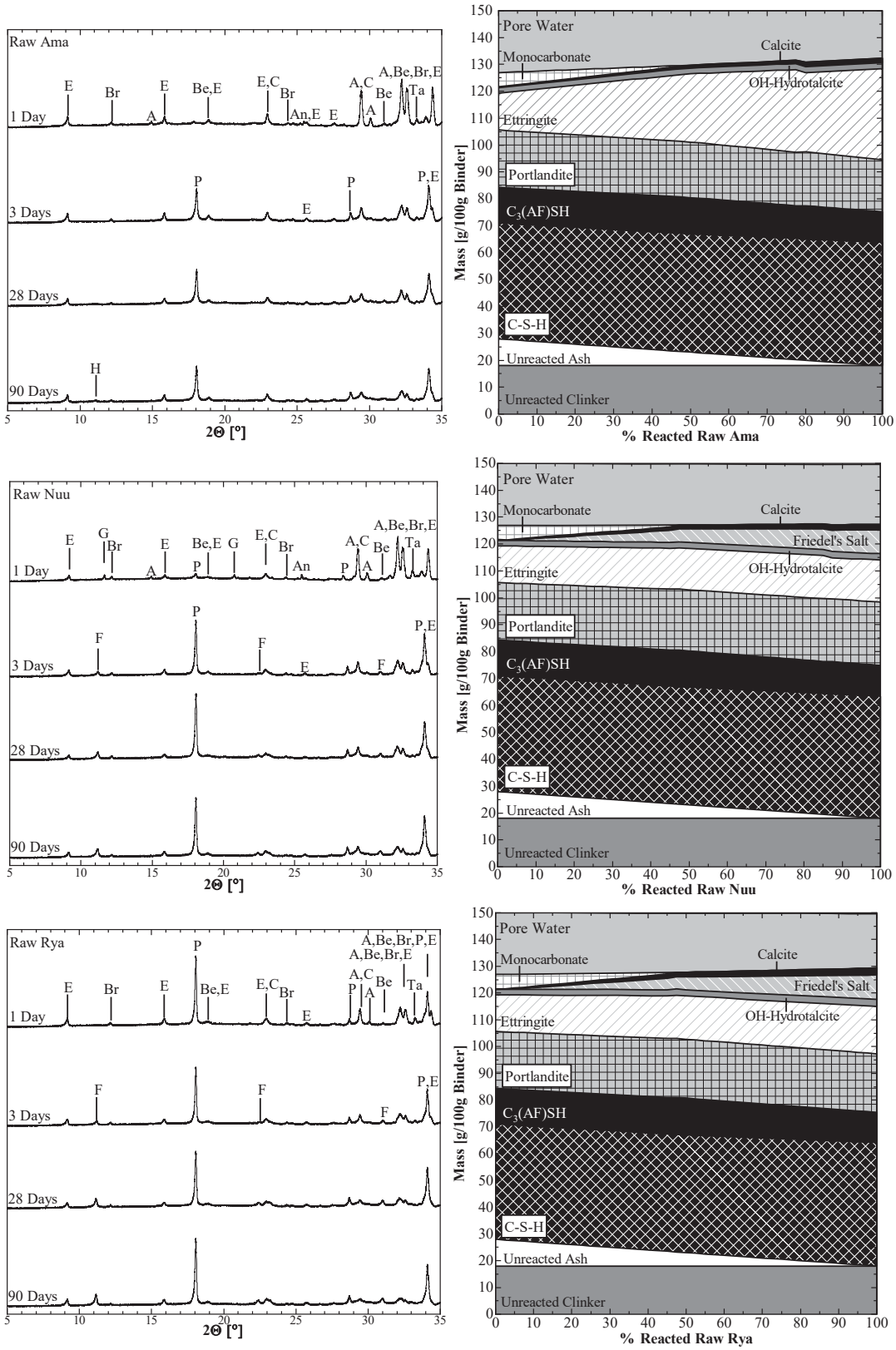

Fig. 5. XRD patterns and Thermodynamic modelling of paste with Raw Ama (top), Raw Nuu (middle) and Raw Rya (bottom). Alite (A), belite (Be), tricalcium aluminate (Ta), brownmillerite (Br), portlandite (P), ettringite (E), hemicarbonate (H), friedel's Salt (F), anhydrite (An), gypsum (G) and calcite (C).

Furthermore, gypsum (G) peaks could be found in the paste with Raw Nuu, indicating an excess of sulphate after 1 day of hydration, suggesting either a lower degree of reaction than paste with Raw Ama or that the tricalcium aluminate reaction is retarded. Raw Ama and Raw Nuu contained compounds that could have accelerated the hydration, e.g. NaCl, KCl or Na_2SO_4. In large concentrations (36 % NaCl and 34 % KCl by mass of water), NaCl and KCl have been shown to retard class G cement [7]. At the cement level replaced in this study (10 wt%), the concentration of Cl was too low (< 3 wt%) to retard the setting and would have been expected to accelerate hydration instead.

Therefore, the reduced degree of reaction after 1 day could have been caused by the MSWI residues' metal content. Raw Ama had a high concentration of Pb (12000 mg/kg) and Zn (55000 mg/kg), while Raw Nuu had a high concentration of Zn (33000 mg/kg). The potential accelerants in the two fly ashes may then have helped offset the hydration delay. The delayed early hydration is easily observed with TGA (Fig. 4), as the pastes with Raw Ama and Raw Nuu had between 5 and 10% bound water and 1% $Ca(OH)_2$ after 1 day of hydration, compared to 14% bound water and 12% $Ca(OH)_2$ in the Qua paste. During the 1-90 days of hydration, alite, belite, tricalcium aluminate, and brownmillerite's peak intensities were reduced. However, after 90 days of hydration, they remained visible, compared to the Qua paste, suggesting that the degree of reaction was reduced. This is corroborated by the TGA, as the amount of bound water and portlandite measured after 90 days were less than the paste with quartz. The paste with Raw Nuu did contain more portlandite than the paste with Raw Ama, suggesting a higher degree of reaction in the paste with Raw Nuu after 90 days, despite binding less water. This may be due to lower Zn concentration in Raw Nuu. Monocarbonate (M) was not detected with XRD in the pastes with Raw Ama or Raw Nuu. Only hemicarbonate (H) formed in the paste with Raw Ama (barely detectable), while Friedel's salt (F) formed in the paste Raw Nuu. The results of the thermodynamic modelling support this observed phase development. Monocarbonate would be below the XRD detection limit (2 %) if more than 30% of Raw Ama reacted, forming ettringite instead due to its high SO_3 and low Al_2O_3 content, while Friedel's salt would be the only detectable phase if more than 32 % of Raw Nuu had reacted, due to the high Cl content. The difference in bound water content

between the pastes with Raw Ama and Raw Nuu after 1 and 3 days of hydration could be due to a higher ettringite content in the paste with Raw Ama.

In contrast, the cement paste with Raw Rya had similar peak intensities for the initial clinker phases after one day of hydration as the 100 wt% CEM I and Qua pastes and had the highest amount of bound water after 1 and 3 days of hydration together with a similar portlandite content as the paste with quartz. Furthermore, after 90 days of hydration, the peak intensities remained similar to the CEM I, suggesting that Raw Rya does not inhibit hydration and contained more bound water than the paste with quartz. Raw Rya contains lower concentrations of heavy metals than Raw Ama and Raw Nuu and has a Zn concentration of 9100 mg/kg. Raw Rya does have a high concentration of Cu (10200 mg/kg). However, at 10 wt% cement substitution, the concentration of Cu in the paste may be low enough to have a beneficial effect instead of a detrimental effect on hydration. The paste with Raw Rya formed Friedel's salt instead of monocarbonate, similarly to Raw Nuu. The thermodynamic model results confirm this by favouring Friedel's salt formation instead of monocarbonate with an increasing percentage of reacted ash. Similarly to the paste with Raw Nuu, if more than 32% of the ash has reacted, monocarbonate can not be detected with XRD. As the portlandite content measured with TGA was similar to the paste with quartz after 1 and 3 days, the increased bound water is likely, not due to additional C-S-H but due to increased ettringite and the formation of Friedel's salt. The pastes with Raw Ama and Raw Rya both had a reduction in portlandite content between 3 and 28 days of hydration, which may indicate some form of portlandite consumption.

3.2.3 EDR treated MSWI residues

Fig. 6 shows the XRD diffractograms and thermodynamic modelling results of the cement pastes with EDR Ama, EDR Nuu and EDR Rya. The cement pastes showed peaks for alite (A), belite (Be), tricalcium aluminate (Ta) and brownmillerite (Br) after one day of hydration, suggesting a higher degree of hydration after one day compared to the paste with the raw MSWI residues. Gypsum (G) and anhydrite (An) peaks were identified after 1 day of hydration, which disappeared after 3 days of hydration, implying an excess of gypsum in the early hydration stages. After the EDR treatment, the MSWI residues contained gypsum and bassanite. The blended pastes may, therefore, contain more

gypsum than could react within 1 day. Excess gypsum was not predicted in the thermodynamic modelling, see Fig. 6.

Compared to the raw MSWI residues, the pastes with the treated MSWI residues consistently bound more water than the paste with quartz. Furthermore, the pastes with the treated MSWI residues had a similar portlandite development over time as the raw MSWI residues with some key differences. The pastes with EDR Ama and EDR Nuu had a higher portlandite content after 1 day of hydration than the pastes with raw Ama or raw Nuu. However, it remained lower than the paste with quartz, indicating that EDR Ama and EDR Nuu may still inhibit hydration to a degree. The EDR treatment also changed the phases developing in the pastes. Cement paste with EDR Nuu or EDR Rya developed hemicarbonate (H) after 3 days and monocarbonate (M) after 28 days, similar to the CEM I and Qua paste, instead of Friedel's salt (F), which was seen for the raw MSWI residues. Thermodynamic modelling corroborates this, as monocarbonate is now present with ettringite, regardless of the amount of reacted MSWI residue. Therefore, it is impossible to estimate the amount of reacted EDR Nuu or EDR Rya via the previously used method. The paste with EDR Ama developed similarly to paste with Raw Ama, except hemicarbonate were no longer detected, with ettringite (E) being the only AFt/AFm phase observed, attributed to EDR Ama's low Al_2O_3 concentration and high SO_3 concentration compared to the other MSWI residues. The thermodynamic modelling results show a similar development, and together the tests indicate that more than 35 % of EDR Ama has reacted as monocarbonate was not detected in the paste by XRD. The increased bound water observed in the paste with the treated MSWI residues could be due to an increased ettringite and monocarbonate content the more the MSWI residues react. In the pastes with treated MSWI residue, the thermodynamic modelling showed an increase in C-S-H and a decrease in portlandite due to the increased SiO_2 content in the ashes. However, as evidenced by the Frattini test, the treated MSWI residues reactivity appears to be slow, suggesting this may only be achievable after extended hydration.

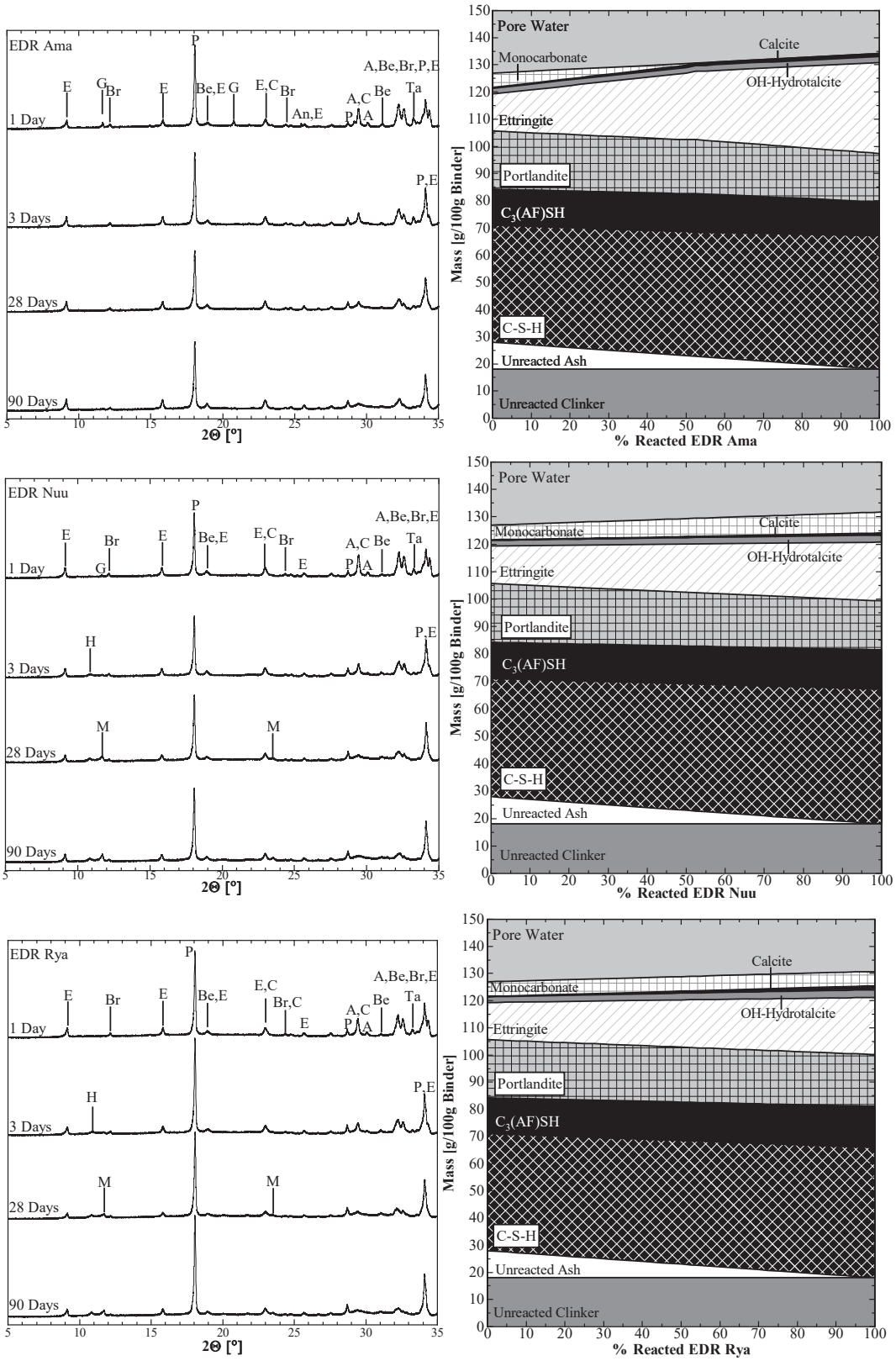

Fig. 6. XRD patterns and Thermodynamic modelling of paste with EDR Ama (top), EDR Nuu (middle) and EDR Rya (bottom). Alite (A), belite (Be), tricalcium aluminate (Ta), brownmillerite (Br), portlandite (P), ettringite (E), hemicarbonate (H), monocarbonate (M), anhydrite (An), gypsum (G) and calcite (C).

3.3 Setting time

The initial and final setting times measured for the various cement pastes are shown in Fig. 7. The setting time test results showed that the CEM I paste had an initial set (column bottom) after 5 h, while the final set (column top) occurred after 10 h. Substituting 10 wt% cement with quartz resulted in a slightly faster initial set (4.8 h), which may be due to the inert quartz having a filler effect [60]. However, the inert quartz has a larger particle size distribution than the cement, see Table 2, suggesting the acceleration may be due to a dilution effect [7].

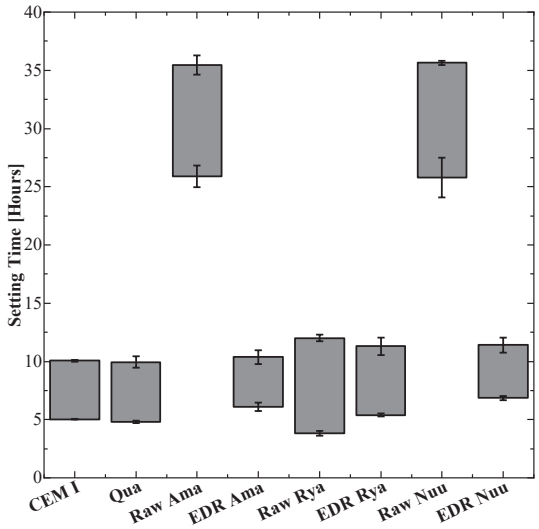

Fig. 7. Initial and final setting times. The error bars indicate standard variation.

The impact of the differences in hydration and phase development observed between the treated and raw MSWI residues were apparent for the setting time and compressive strength (section 3.4). Treating the MSWI residues reduced the initial and final setting time delay of Raw Ama by 20 and 25 h and Raw Nuu by 19 and 24 h, respectively, conforming with the CEM I and Qua paste setting. In contrast, the treatment did not improve the setting of the paste with Raw Rya. The cement paste with Raw Rya had an accelerated initial set, occurring after 4 h and an extended final set by 2 h, compared to the CEM I and Qua paste. EDR Rya delayed the initial setting to after 5 h and extended the final set by 1 h. As suggested by the initial clinker phases' peak intensities, bound water and portlandite content, cement pastes with Raw Ama or Raw Nuu do not hydrate and set within 24 hours. As previously discussed, this may be attributed to the concentration of heavy metals in the MSWI residues. Fig. 8a depicts the total concentration of Cd, Cr, Cu, Pb and Zn as mol/kg binder in the cement pastes, together with the

concentration of 0.18 mol/kg used in [8], at which a delayed setting was observed. The cement pastes with Raw Ama and Raw Nuu had the highest concentration of metals in the paste and the most extended delay in the initial and final setting. Raw Rya contained a lower concentration of heavy metals than the other MSWI residues. At low concentrations, Zn and Pb may improve setting [52,54], which, together with its other potentially accelerative components, could be why Raw Rya had a faster initial set and delayed final set. The treated MSWI residues still had a high concentration of heavy metals. The improved setting time could result from differences in metal leachability. As shown in Fig. 8b, the EDR treated MSWI residues have a lower leachable metal content than the raw MSWI residues. The treated MSWI residues also contained gypsum or bassanite, which may extend the induction period [45] and account for the treated MSWI residues delay in the initial setting time.

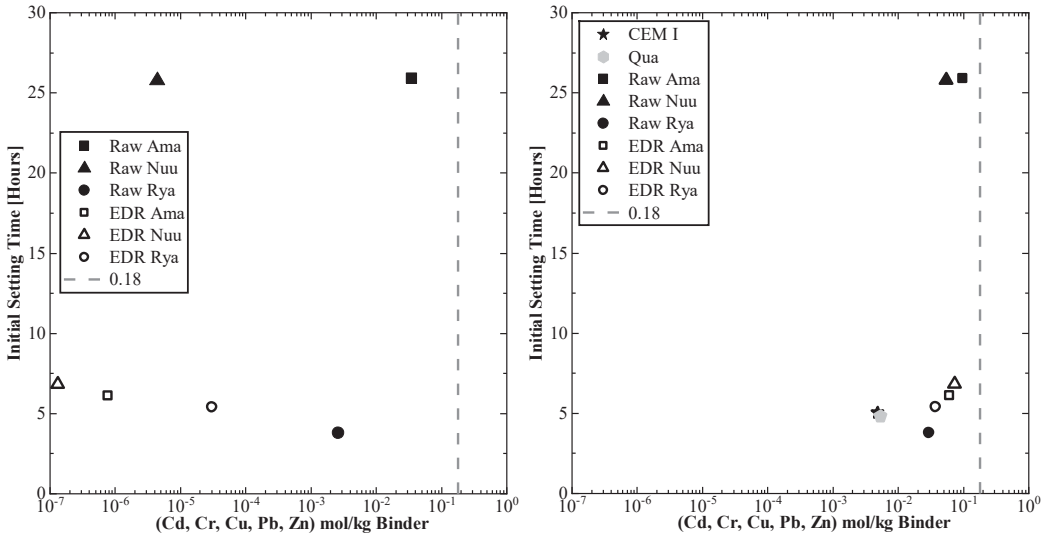

Fig. 8. Initial setting time versus (a) total metal content in the cement paste samples (b) and leachable metals in the cement paste samples. The dashed line is 0.18 mol/kg binder, as used in [7].

3.4 Assessment of mechanical properties

The calculated macroporosity of the tested mortar prisms is shown in Fig. 9. The EDR treatment improved the macroporosity of the mortars. EDR Ama and EDR Rya resulted in macroporosities of 0.7 and 0.3 % (similar to the Qua mortar), while Raw Ama and Raw Rya resulted in macroporosities of 1.2 and 1,1 %, respectively. The most significant improvement was for Raw Nuu, as mortar prisms with Raw Nuu had a macroporosity of 8.3%, while prisms with EDR Nuu had a macroporosity of 1.2 %. The substantially higher macroporosity increase in Raw Nuu mortar may be due to metallic aluminium. A high concentration of metallic aluminium is likely in Greenlandic MSWI fly ash, as metal from

household waste is not commonly separated [61]. At high pH, metallic aluminium dissolves according to the following reaction [9]:

$$2Al_{(s)} + 2OH^-_{(aq)} = 2Al_2O^-_{(aq)} + 2H_{2(g)}$$

Dihydrogen gas release leads to gaseous inclusions, expanding the volume of fresh pastes and potentially cracking the mortar. Such expansion was observed in the mortar prisms with Raw Nuu, with the mortar expanding out of the moulds. The metallic aluminium concentration in raw Nuuk-Fa was not measured, as XRF analysis measures the total metal content. The EDR treatment may have reduced the concentration of metallic aluminium by extracting the aluminium or causing the previously described reactions. Raw Ama and Raw Rya may contain traces of metallic aluminium, which could account for the increased macroporosity. Heavy metals such as Pb and Zn may also increase the pore structure and volume [54,62] of mortar and could be the reasons for the MSWI residue's effect on macroporosity.

The mortar prisms' compressive strength (normalised) is shown in Fig. 10a as a function of time and in Fig. 10b as a function of bound water. The compressive strength test of the mortar with quartz showed that a 10% substitution with an inert material reduced the mortar's compressive strength by 14% after 1 to 3 days of curing and 21-23% after 28 and 90 days of curing. The lower difference in strength between the CEM I and Qua mortar after 1 to 3 days of curing compared to 28 and 90 days may result from the accelerated setting time.

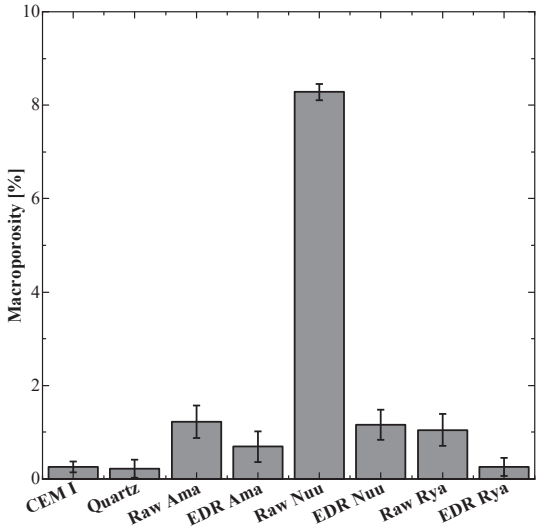

Fig. 9. Calculated average macroporosity of mortar samples.

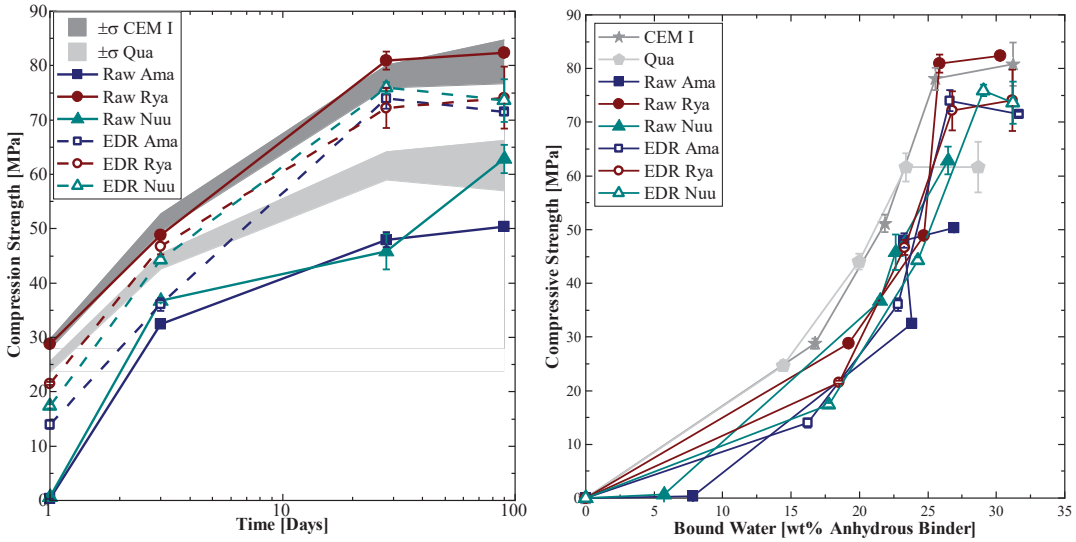

Fig. 10. Compressive strength (normalised to air free) as a function of time and bound water. Error bars and grey areas indicate +/- one

For the two investigated MSWI fly ashes (Ama and Nuu), the EDR treatment vastly improved the compressive strength of the mortar. This was, however, not the case for Rya. After 1 day of curing, the compressive strength of the mortars with the treated MSWI residues was lower than the mortar with quartz, and after three days, it was higher than or equal to the mortar with quartz, except for mortar with EDR Ama. The treated MSWI residues did result in a delayed set attributed to the MSWI residues gypsum or bassanite content, prolonging the induction period (see Section 3.2 and 3.3). EDR Ama had a higher sulphite content than the other MSWI residues, which may have inhibited the early age strength. Although the early age compressive strength of the mortar with the treated MSWI residues was less than mortar with quartz, it does represent an improvement. The delayed cement paste hydration (see Section 3.2 and 3.3) in samples with Raw Ama or Raw Nuu resulted in compressive strength of less than 1 Mpa. After three days of curing, the improvement from electrodialytically treating the MSWI residues was more discernable. The mortar with treated MSWI residues achieved compressive strengths between 70-75 Mpa after 90 days, 10 Mpa more than mortar with quartz, while mortar with Raw Ama had a compressive strength of 10 Mpa lower than the mortar with quartz. After 90 days, the mortar with Raw Nuu did achieve a similar compressive strength as the mortar with quartz. However, the actual measured compressive strength is less than the mortar with quartz. See supplementary material. Treating Raw Rya did not improve the compressive strength development, despite the composition and phase development changes. Mortar with Raw Rya had a compressive strength similar to the CEM I

mortar at all of the tested dates, which may be due to the accelerated initial set and high bound water content. The cement paste with EDR Rya had a higher bound water content than the paste with Raw Rya but lower compressive strength, the reason for this is not clear. The EDR treated MSWI residues had a higher bound water content than paste with quartz and CEM I paste but lower compressive strength than the 100 wt% CEM I mortar. The higher bound water content is attributed to a higher ettringite and monocarbonate content in the samples, resulting in a higher compressive strength than the mortar with quartz. While the other raw or treated MSWI residues may inhibit early C-S-H formation, Raw Rya may promote C-S-H formation, therefore, achieving a similar strength to the CEM I mortar.

4 Conclusions

The impact of electrodialytic remediation (EDR) of MSWI fly ash/air pollution control (APC) residue on cement hydration and the development of mechanical properties (setting and compressive strength) were investigated for two MSWI fly ash samples and one MSWI APC residue. The performance was investigated for 10% Portland cement replacement and compared to mixtures with an inert material (quartz).

EDR reduced the initial setting time of blended cement pastes with the two MSWI fly ashes from 25 to 6 hours and the final setting time from 35 to 12 hours; the improved performance was attributed to the removal of retarding components such as heavy metals. Furthermore, EDR reduced the macroporosity and volume expansion, which was high for especially blended mortars of one of the untreated MSWI fly ashes; this might be explained by a high amount of metallic aluminium resulting in gas evolution.

Combined XRD and thermodynamic modelling showed the relative increase of ettringite and monocarbonate in the phase assemblage. They indicated that approximately 35% of one of the EDR treated MSWI fly ashes reacted in the blended cement paste. Limited change of phase assemblage for the two other MSWI residues did not allow a similar assessment. The contribution seems to be hydraulic as the investigated samples showed no pozzolanic reactivity.

EDR increased the compressive strength of blended, Portland cement-based mortars compared to a mortar with quartz, indicating that all MSWI residues reacted to some extent. The untreated MSWI APC residue also contributed positively to strength development. The two untreated MSWI fly ashes resulted in lower strength development than the mortar with quartz; the reason for the positive behaviour of the untreated MSWI APC residue requires further investigation.

The results indicate that electrodialytic remediation improves the performance of MSWI fly ash in Portland cement-based materials, while MSWI APC residues might be used without pre-treatment.

5 Acknowledgements

This paper and the research behind it would not have been possible if not for the lab technicians Ebba Schnell, Natasja Due and Erasmus + scholarship recipient Nuria Bernárdez Rodas who helped to conduct and maintain the bench-scale electrodialytic remediation experiments, treating the MSWI fly ash used in this study. The lab technicians are further acknowledged for their assistance with several measurements used in this paper. The people working at Amager Resource Center, Borås Energi och Miljö and Kommuneqarfik Semersooq are also recognised for their interest in the study, their cooperation, and sampling and sending the MSWI fly ash to the Technical University of Denmark.

6 References

[1] Jos G.J. Olivier; Greet Janssens-Maenhout; Marilena Muntean; Jeroen A.H.W. Peters, Trends in global CO2 emissions 2016, (2016) 86.

[2] K.L. Scrivener, V.M. John, E.M. Gartner, Eco-efficient cements: Potential, economically viable solutions for a low-CO2, cement-based materials industry, (2016).

[3] C. Ferreira, A. Ribeiro, L. Ottosen, Possible applications for municipal solid waste fly ash, Journal of Hazardous Materials. 96 (2003) 201–216.

[4] O. Hjelmar, Disposal strategies for municipal solid waste incineration residues, Journal of Hazardous Materials. 47 (1996) 345–368. https://doi.org/10.1016/0304-3894(95)00111-5.

[5] F. Zunino, D.P. Bentz, J. Castro, Reducing setting time of blended cement paste containing high-SO3 fly ash (HSFA) using chemical/physical accelerators and by fly ash pre-washing, Cement and Concrete Composites. 90 (2018) 14–26. https://doi.org/10.1016/j.cemconcomp.2018.03.018.

[6] S. Kumar, C.V.S.K. Rao, Effect of sulfates on the setting time of cement and strength of concrete, Cement and Concrete Research. 26 (1996) 643. https://doi.org/Doi 10.1016/S0008-8846(96)90013-7.

[7] C.A.A. Rocha, G.C. Cordeiro, R.D. Toledo Filho, Use of thermal analysis to determine the hydration products of oil well cement pastes containing NaCl and KCl, Journal of Thermal Analysis and Calorimetry. 122 (2015) 1279–1288. https://doi.org/10.1007/s10973-015-4949-6.

[8] N. Gineys, G. Aouad, D. Damidot, Managing trace elements in Portland cement - Part I: Interactions between cement paste and heavy metals added during mixing as soluble salts, Cement and Concrete Composites. 32 (2010) 563–570. https://doi.org/10.1016/j.cemconcomp.2010.06.002.

[9] J.E. Aubert, B. Husson, A. Vaquier, Metallic aluminum in MSWI fly ash: Quantification and influence on the properties of cement-based products, Waste Management. 24 (2004) 589–596. https://doi.org/10.1016/j.wasman.2004.01.005.

[10] P. Piantone, F. Bodénan, R. Derie, G. Depelsenaire, Monitoring the stabilization of municipal solid waste incineration fly ash by phosphation: Mineralogical and balance approach, Waste Management. 23 (2003) 225–243. https://doi.org/10.1016/S0956-053X(01)00058-7.

[11] Z. Jing, X. Ran, F. Jin, E.H. Ishida, Hydrothermal solidification of municipal solid waste incineration bottom ash with slag addition, Waste Management. 30 (2010) 1521–1527. https://doi.org/10.1016/j.wasman.2010.03.024.

[12] M.G. Li, C.J. Sun, S.H. Gau, C.J. Chuang, Effects of wet ball milling on lead stabilization and particle size variation in municipal solid waste incinerator fly ash, Journal of Hazardous Materials. 174 (2010) 586–591. https://doi.org/10.1016/j.jhazmat.2009.09.092.

[13] Z. Yang, S. Tian, R. Ji, L. Liu, X. Wang, Z. Zhang, Effect of water-washing on the co-removal of chlorine and heavy metals in air pollution control residue from MSW incineration, Waste Management. 68 (2017) 221–231. https://doi.org/10.1016/j.wasman.2017.06.039.

[14] K. Huang, K. Inoue, H. Harada, H. Kawakita, K. Ohto, Leaching behavior of heavy metals with hydrochloric acid from fly ash generated in municipal waste incineration plants, Transactions of Nonferrous Metals Society of China (English Edition). 21 (2011) 1422–1427. https://doi.org/10.1016/S1003-6326(11)60876-5.

[15] K.S. Wang, K.Y. Chiang, J.K. Perng, C.J. Sun, The characteristics study on sintering of municipal solid waste incinerator ashes, Journal of Hazardous Materials. 59 (1998) 201–210. https://doi.org/10.1016/S0304-3894(97)00147-7.

[16] S. Chou, S. Lo, C. Hsieh, C. Chen, Sintering of MSWI fly ash by microwave energy, 163 (2009) 357–362. https://doi.org/10.1016/j.jhazmat.2008.06.100.

[17] J.E. Aubert, B. Husson, A. Vaquier, Use of municipal solid waste incineration fly ash in concrete, Cement and Concrete Research. 34 (2004) 957–963. https://doi.org/10.1016/j.cemconres.2003.11.002.

[18] K.L. Lin, K.S. Wang, B.Y. Tzeng, C.Y. Lin, The reuse of municipal solid waste incinerator fly ash slag as a cement substitute, Resources, Conservation and Recycling. 39 (2003) 315–324. https://doi.org/10.1016/S0921-3449(02)00172-6.

[19] T. Lenormand, E. Rozière, A. Loukili, S. Staquet, Incorporation of treated municipal solid waste incineration electrostatic precipitator fly ash as partial replacement of Portland cement: Effect on early age behaviour and mechanical properties, Construction and Building Materials. 96 (2015) 256–269. https://doi.org/10.1016/j.conbuildmat.2015.07.171.

[20] Z. Chen, S. Lu, M. Tang, J. Ding, A. Buekens, J. Yang, Q. Qiu, J. Yan, Mechanical activation of fly ash from MSWI for utilization in cementitious materials, Waste Management. 88 (2019) 182–190. https://doi.org/10.1016/j.wasman.2019.03.045.

[21] G.M. Kirkelund, P.E. Jensen, Electrodialytic treatment of Greenlandic municipal solid waste incineration fly ash, Waste Management. 80 (2018) 241–251. https://doi.org/10.1016/j.wasman.2018.09.019.

[22] W. Chen, G.M. Kirkelund, P.E. Jensen, L.M. Ottosen, Electrodialytic extraction of Cr from water-washed MSWI fly ash by changing pH and redox conditions, Waste Management. 71 (2018) 215–223. https://doi.org/10.1016/j.wasman.2017.09.035.

[23] C. Dias-Ferreira, G.M. Kirkelund, P.E. Jensen, The influence of electrodialytic remediation on dioxin (PCDD/PCDF) levels in fly ash and air pollution control residues, Chemosphere. 148 (2016) 380–387. https://doi.org/10.1016/j.chemosphere.2016.01.061.

[24] G.M. Kirkelund, M.R. Geiker, P.E. Jensen, Electrodialytically treated MSWI APC residue as substitute for cement in mortar, Nordic Concrete Research. (2014) 1–16.

[25] B.A.R. Ebert, B.-M. Steenari, M.R. Geiker, G.M. Kirkelund, Screening of untreated municipal solid waste incineration fly ash for use in cement-based materials: chemical and physical properties, SN Applied Sciences. 2 (2020). https://doi.org/10.1007/s42452-020-2613-7.

[26] B.A.R. Ebert, G.M. Kirkelund, "UNDER REVIEW" Effects of chlorides and sulphates on leaching from mortar with raw and electrodialytically treated MSWI fly ash, Journal of Hazardous Materials. (2021).

[27] Á. Fernández, B. Lothenbach, M.C. Alonso, J.L. García Calvo, Thermodynamic modelling of short and long term hydration of ternary binders. Influence of Portland cement composition and blast furnace slag content, Construction and Building Materials. 166 (2018) 510–521. https://doi.org/10.1016/j.conbuildmat.2018.02.007.

[28] S. Rémond, D.P. Bentz, P. Pimienta, Effects of the incorporation of Municipal Solid Waste Incineration fly ash in cement pastes and mortars - II: Modeling, Cement and Concrete Research. 32 (2002) 565–576. https://doi.org/10.1016/S0008-8846(01)00722-0.

[29] DS/EN 196-1 2005 Metoder til prøvning af cement – Del 1: Styrkebestemmelse Methods of testing cement – Part 1: Determination of strength, (2016).

[30] DS/EN 12457-1: Characterisation of waste - Leaching - Compliance test for leaching of granular waste materials and sludges - Part 1: One stage batch test at a liquid to solid ratio of 2 l/kg for materials with high solid content and with particle size bel, Dansk Standard, 2002.

[31] DS/EN 196-5: Methods of testing cement - Part 5: Pozzolanicity test for pozzolanic cement, Dansk Standard, 2011.

[32] DS/EN 196 3 + A1: Methods of testing cement - Part 3: Determination of setting times and soundness, Dansk Standard, 2009.

[33] B. Lothenbach, P. Durdzinski, K. de Weerdt, Thermogravimetric Analysis, in: K. Scrivener, R. Snellings, B. Lothenbach (Eds.), A Practical Guide to Microstructural Analysis of Cementitious Materials, CRC Press, 2016: pp. 177–213.

[34] D.A. Kulik, T. Wagner, S. v. Dmytrieva, G. Kosakowski, F.F. Hingerl, K. v. Chudnenko, U.R. Berner, GEM-Selektor geochemical modeling package: Revised algorithm and GEMS3K numerical kernel for coupled simulation codes, Computational Geosciences. 17 (2013) 1–24. https://doi.org/10.1007/s10596-012-9310-6.

[35] B. Lothenbach, D.A. Kulik, T. Matschei, M. Balonis, L. Baquerizo, B. Dilnesa, G.D. Miron, R.J. Myers, Cemdata18: A chemical thermodynamic database for hydrated Portland cements and alkali-activated materials, Cement and Concrete Research. 115 (2019) 472–506. https://doi.org/10.1016/j.cemconres.2018.04.018.

[36] D.A. Kulik, Improving the structural consistency of C-S-H solid solution thermodynamic models, Cement and Concrete Research. 41 (2011) 477–495. https://doi.org/10.1016/j.cemconres.2011.01.012.

[37] DS/EN 1015-3: Methods of test for mortar for masonry - Part 3: Determination of consistence of fresh mortar (by flow table), Dansk Standard, 1999.

[38] B. Osbæck, The influence of Air content by Assessing the pozzolanidc activity of fly ash by strength testing, Cement and Concrete Research. 15 (1985) 53–64.

[39] P.C. Hewlet, M. Liska, Lea's Chemistry of Cement and Concrete, Fifth Edit, Elsevier, 2019.

[40] DS/EN 450-1: Fly ash for concrete - Part 1: Definition, Specification and conformity criteria, Dansk Standard, 2012.

[41] H. Justnes, Influence of SCMs on hydration and durability of blended cements - Chemical and Physical Principles, Journal of the Chinese Ceramic Society. 13 (2554) 1359–1371.

[42] B. Lothenbach, K. Scrivener, R.D. Hooton, Supplementary cementitious materials, Cement and Concrete Research. 41 (2011) 1244–1256. https://doi.org/10.1016/j.cemconres.2010.12.001.

[43] M. Thomas, Supplementary Cementing Materials in Concrete, CRC Press, 2013.

[44] H. sheng Shi, L. li Kan, Characteristics of municipal solid wastes incineration (MSWI) fly ash-cement matrices and effect of mineral admixtures on composite system, Construction and Building Materials. 23 (2009) 2160–2166. https://doi.org/10.1016/j.conbuildmat.2008.12.016.

[45] B. Mota, T. Matschei, K. Scrivener, S. Kumar, C.V.S.K. Rao, The influence of sodium salts and gypsum on alite hydration, Cement and Concrete Research. 75 (2015) 53–65. https://doi.org/10.1016/j.cemconres.2015.04.015.

[46] I. Jawed, J. Skalny, Alkalis in cement: A review II. Effects of Alkalies on Hydration and Performance of Portland Cement, Cement and Concrete Research. 32 (1978) 147–156.

[47] D.P. Bentz, F. Zunino, D. Lootens, Chemical vs. Physical Acceleration of Cement Hydration., Concrete International : Design & Construction. 38 (2016) 37–44.

[48] T. Vehmas, A. Kronlöf, A. Cwirzen, Calcium chloride acceleration in ordinary Portland cement, Magazine of Concrete Research. 70 (2018) 856–863. https://doi.org/10.1680/jmacr.17.00079.

[49] V.S. Ramachandran, Calcium chloride in concrete- applications and ambiguities., Canadian Journal of Civil Engineering. 5(2) (1978) 213–221.

[50] F.R. Lago, J. Dweck, T. Analysis, Evaluation of Influence of Salt in the Cement Hydration to Oil Wells, 20 (2017) 743–747.

[51] M. Zajac, A. Rossberg, G. le Saout, B. Lothenbach, Influence of limestone and anhydrite on the hydration of Portland cements, Cement and Concrete Composites. 46 (2014) 99–108. https://doi.org/10.1016/j.cemconcomp.2013.11.007.

[52] S. Komarneni, E. Breval, D.M. Roy, R. Roy, Reactions of some calcium silicates with metalcations, Cement and Concrete Research. 18 (1988) 204–220.

[53] T. Mangialardi, A.E. Paolini, A. Polettini, P. Sirini, Optimization of the solidification/stabilization process of MSW fly ash in cementitious matrices, Journal of Hazardous Materials. 70 (1999) 53–70. https://doi.org/10.1016/S0304-3894(99)00132-6.

[54] B. COHEN, J. PETRIE, CONTAINMENT OF CHROMIUM AND ZINC IN FERROCHROMIUM FLU DUSTS BY CEMENT-BASED SOLIDIFICATION, Canadian Metallurgical Quarterly. 36 (1997) 251–260. https://doi.org/10.1081/E-EEE2-120046011.

[55] D.L. Cocke, The binding chemistry and leaching mechanisms of hazardous substances in cementitious solidification/stabilization systems, Journal of Hazardous Materials. 24 (1990) 231–253. https://doi.org/10.1016/0304-3894(90)87013-8.

[56] F.K. Cartledge, L.G. Butler, D. Chalasani, H.C. Eaton, F.P. Frey, E. Herrera, M.E. Tittlebaum, S.L. Yang, Immobilization Mechanisms in Solidification/Stabilization of Cd and Pb Salts Using Portland Cement Fixing Agents, Environmental Science and Technology. 24 (1990) 867–873. https://doi.org/10.1021/es00076a012.

[57] C.S. Poon, A.I. Clark, C.J. Peters, R. Perry, Mechanisms of metal Fixation and leaching by cement based fixation processes, Waste Management and Research. 3 (1985) 127–142. https://doi.org/10.1016/0048-9697(85)90161-5.

[58] B. Lothenbach, G. le Saout, E. Gallucci, K. Scrivener, Influence of limestone on the hydration of Portland cements, Cement and Concrete Research. 38 (2008) 848–860. https://doi.org/10.1016/j.cemconres.2008.01.002.

[59] T. Matschei, B. Lothenbach, F.P. Glasser, The role of calcium carbonate in cement hydration, Cement and Concrete Research. 37 (2007) 551–558. https://doi.org/10.1016/j.cemconres.2006.10.013.

[60] K.L. Scrivener, B. Lothenbach, N. de Belie, E. Gruyaert, R. Snellings, A. Vollpracht, TC 238-SCM : hydration and microstructure of concrete with SCMs State of the art on methods to determine degree of reaction of SCMs, (2015) 835–862. https://doi.org/10.1617/s11527-015-0527-4.

[61] R. Eisted, T.H. Christensen, Waste management in Greenland: Current situation and challenges, Waste Management and Research. 29 (2011) 1064–1070. https://doi.org/10.1177/0734242X10395421.

[62] F. Sanchez, R. Barna, A. Garrabrants, D.S. Kosson, P. Moszkowicz, Environmental assessment of a cement-based solidified soil contaminated with lead, Chemical Engineering Science. 55 (2000) 113–128. https://doi.org/10.1016/S0009-2509(99)00281-X.

Conference Paper I

The Effect of MSWI Fly Ash on Mortar Workability

Benjamin A. R. Ebert, Britt-Marie Steenari, Mette R. Geiker, Gunvor M. Kirkelund

International Conference on Sustainable Materials, Systems and Structures (SMSS 2019)
New Generation of Construction Materials
20-22 March 2019 – Rovinj, Croatia

THE EFFECT OF MSWI FLY ASH ON MORTAR WORKABILITY

Benjamin A. R. Ebert (1), Britt-Marie Steenari (2), Mette R. Geiker (3) and Gunvor M. Kirkelund (1)

(1) Department of Civil Engineering, Technical University of Denmark, Denmark

(2) Chemistry and Chemical Engineering, Chalmers University of Technology, Sweden.

(3) Department of Structural Engineering, Norwegian University of Science and Technology, Norway.

Abstract

Management of fly ash from municipal solid waste incineration (MSWI) is problematic, due to the fly ash toxicity and leaching. The ash could potentially serve as a partial cement substitute, similarly to fly ash from coal incineration. In this work, the potential of two different MSWI fly ashes as partial cement substitutes were analysed by testing the ashes effect on the workability. This was achieved by investigating the variations in consistency (ease of flow), caused by increasing fly ash substitution, immediately after mixing and after 30 minutes, on mortar mixes containing 5, 10 and 20% cement replacement. The first fly ash had little impact on the consistency, except at 10% substitution where the flow was reduced by 30% compared to a reference. The second reduced the flow by 16, 29 and 70% with increasing substitution. With the addition of superplasticizer, a consistency similar to the reference was achieved. Samples with high amounts of cement replaced by ash had a higher reduction in flow after 30 minutes compared to a reference. The addition of superplasticizer reduced the flow loss after 30 minutes except for a 20% substitution.

Keywords: Mortar, MSWI Fly Ash, Consistency, Superplasticizer

1. INTRODUCTION

In recent years, countries have undergone changes to their management of municipal solid waste. Instead of landfilling, waste is recycled or incinerated at combined heat and power plants. Municipal solid waste incineration (MSWI) is a frequently used procedure, utilizing the waste for energy gain, reducing the amount landfilled. However, it results in environmentally strenuous by-products in the form of fly ash that remains underused. The high content of heavy metals in fly ash indicate that fly ash pose a potential threat to the environment, due to leaching and toxicity [1]. The fly ash could potentially serve as a partial cement substitute, similarly to

coal fly ash, when producing concrete [2,3], immobilizing the heavy metals and decreasing the environmental load [4]. In addition, cement production accounts for around 8% of the global CO_2 emission each year [5]. Substitution of cement with MSWI fly ash, could make concrete more sustainable and remove the otherwise unused fly ash from circulation.

Previous research by Aubert et al. [2] and Bertolini et al. [3] determined that the replacement of cement with MSWI fly ash led to a reduction in workability of fresh mortar, requiring alteration to the mixture design. The alterations could be changes to the water/cement ratio or the inclusion of superplasticizers in the mixing process [2]. Aubert et al. and Bertolini et al. both washed their ashes to reduce chloride and heavy metal content. Aubert et al. also stabilized the heavy metals through phosphation and calcined the ash. Additionally, they washed an ash sample with Na_2CO_3 to reduce the metallic aluminium amount and remove $CaSO_4$. The previously mentioned two studies focused on the mechanical strength and overall concrete properties, instead of the workability. The aim of this study is to investigate the potential of using untreated MSWI fly ash as a partial cement substitute, based on the workability properties. Accomplished by determining the changes in consistency (ease of flow) with increasing fly ash substitution, as well as studying the loss of consistency over time, and the effect of including superplasticizer.

2. EXPERIMENTAL

2.1 Materials

Two MSWI ashes were collected. The first from Nuuk incineration, a small-scale grate-fired plant in Greenland, designated Nuuk-FA, and ash from Borås Energi och Miljö, a large-scale fluidized bed plant in Sweden designated Borås-FA. The two ashes were dried for 24 hours at 50°C prior to mixing.

The experiments were done using a CEM I 52.5 N (MS) (LA) cement. The chemical composition of the cement and the two MSWI fly ashes are given in Table 1, determined by X-ray fluorescence.

Table 1: Chemical composition of cement and ashes.

	CEM I	Nuuk-FA	Borås-FA
Al_2O_3	5.41	3.97	4.53
CaO	64.1	33.6	40.58
Cl	0.04	20.0	12.0
Cr_2O_3	0.01	0.04	0.06
Fe_2O_3	3.80	0.66	1.72
K_2O	0.44	10.72	2.41
MgO	1.03	0.91	1.66
Na_2O	0.30	21.57	6.20
P_2O_5	0.30	1.26	1.67
SiO_2	19.7	4.71	5.99
SO_3	3.23	7.74	8.74
TiO_2	0.22	1.13	2.34
LOI	1.56	31.16	21.36

The particle size distribution of the ashes and cement was measured by laser diffractometry using a Mastersizer 2000. Standard sand as specified in DS/EN 196-1 was used for the mortar. A modified acrylic polymer based superplasticizer was used as an additive. The plasticizer used was based on designed performance polymers and have a low viscosity of < 30 mPa·s, a pH of 6.5±1 and a density of $1.06\pm0.02\frac{g}{cm^3}$.

3.2 Sample Preparation

Mortar samples were prepared, based on the method described in DS/EN 196-1. 450g of cement was used, with a water-cement ratio of 0.5. For this series of testing 5, 10 and 20% of the cement was substituted with ash. Table 2 shows the series of mixes done. Superplasticizer was only used together with Borås-FA. Each mix was repeated 3 times.

Cement and fly ash blends were pre-mixed dry for 2 minutes at the mixers lowest setting, to achieve complete homogenisation. The mixer used has two settings, corresponding to the speeds described in DS/EN 196-1. At the onset of mixing, demineralised water was added to the blend and subsequently stirred as specified in DS/EN 196-1. For the samples including superplasticizer, the plasticizer was added to the mixing water before mixing.

Table 2: Series of samples prepared.

	CEM I [g]	Nuuk-FA [g]	Borås-FA [g]	Plasticizer
Ref	450.0			-
Nuuk5	427.5	22.5		-
Nuuk10	405.0	45.0		-
Nuuk20	360.0	90.0		-
Borås5	427.5		22.5	-
Borås10	405.0		45.0	-
Borås20	360.0		90.0	-
Borås5SP	427.5		22.5	+
Borås10SP	405.0		45.0	+
Borås20SP	360.0		90.0	+

3.3 Consistency Measurement

The consistency of the samples was measured with a flow table, using the technique specified in DS/EN 1015-3. The mould used had the dimensions specified in DS/EN 1015-3, except for the height, that was 50 mm instead of 60 mm. The mould was filled halfway with mortar and smoothed with at least 10 strokes of a tamper. The mould was then topped and smoothed again with at least 10 strokes of the tamper. The mould was then removed and the flow table was jolted with 1 jolt each second for 15 seconds. Finally, the diameter of the resulting circle was measured twice at 90-degree angles to each other. The mean of the two measurements was reported as the flow value. The 100 mm internal bottom diameter of the mould was subtracted from the final results. The initial consistency was measured 6 minutes after the water was added. To test the loss of consistency over time, the mortar was left to hydrate in the bowl with a plastic sheet cover. After 30 minutes of hydration, the consistency was measured again using the described procedure.

3. RESULTS & DISCUSSION

3.1 Particle Size Distribution

The particle size distribution of the ashes and cement are shown in Figure 1. The particle size distributions of the two ashes both have similar fractions between 1 and 10 µm, and curvature. However, Nuuk-FA contains a higher volume of larger particles compared to Borås-FA. The two ashes, however, deviate from CEM I. They are not as fine-grained, with the majority of their particles being larger than CEM I, and do not contain a small fraction of large particles around 100 µm.

Figure 1: Particle Size Distribution.

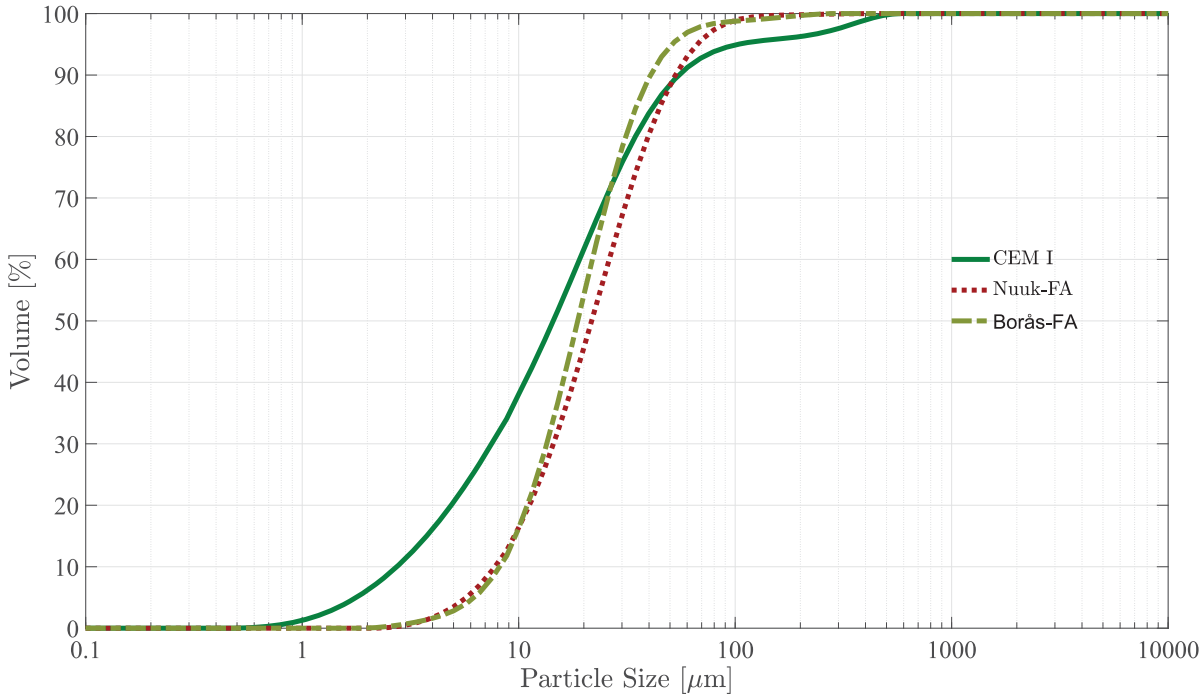

3.2 Initial consistency

The differences in initial consistency, and over time, with increasing cement substitution is displayed in Table 2, together with the mortar samples made with superplasticizer. The addition of MSWI fly ash is shown to have a detrimental effect on consistency. Although, the impact of the two ashes differs.

Replacement with 5% Nuuk-FA exhibited no significant changes in consistency, deviating approximately 3% from the reference. Replacement with 10% Nuuk-FA leads to a 30% reduction in flow. This indicates a loss in consistency with increasing substitution. Surprisingly, 20% substitution with Nuuk-FA resulted in a consistency similar to the 5% replacement. The decrease and increase in consistency suggest that substitution with Nuuk-FA has an initial adverse effect on the consistency; however, at higher substitution rates the ash does not affect

the consistency. With no marked effect on the consistency at 5 and 20% replacement, experiments with superplasticizer were deemed irrelevant.

Contrary to the results with Nuuk-FA, substitution with Borås-FA had a noticeable effect on the mortar consistency. Replacement with 5% Borås-FA resulted in a flow reduction of 16%, while a replacement with 10 and 20% reduced the flow by 29 and 70% respectively. Increasing substitution, therefore, results in decreased consistency. This decrease trends toward a linear interaction between the loss of consistency and replacement amount. This poses a significant challenge for concrete production, since a high replacement with Borås-FA, would be unsuited for jobs requiring a high fluidity.

The addition of superplasticizer in the mixing water negates this loss in consistency. By adding an increasing amount of plasticizer for each substitution percentile, similar flow values as the reference were achieved. An average of 0.92, 2.18 and 6.35 g superplasticizer was added to the 5, 10 and 20% mixes respectively, in order to compensate for the loss in consistency. The superplasticizer required, to achieve the desired consistency, greatly increases for higher substitutions.

It was expected, based on the results of Aubert et al. [2] and Bertolini et al. [3], that substitution with increasing amounts of MSWI fly ash would lower the consistency of the mortar, despite their ashes being treated. The results with Borås-FA corresponds to the results determined by Aubert et al. [2] and Bertolini et al. [3] using flow time testing from the French standard NF P 15-437 and Vebe respectively. Aubert et al. [2] found that the flow time was more than doubled when replacing 25% cement with fly ash, while Bertolini et al. [3] found that a 30% substitution resulted in no slump after 13 s Vebe time. Aubert et al. [2] concluded that substitution of cement with MSWI fly ash leads to a strong reduction in workability, requiring changes to the water-cement ratio or the addition of superplasticizer.

Aubert et al. [2] attribute the loss of workability to the porosity of the ashes or increase in water demand, due to the high surface area of ultrafine neoformed calcite in the ash. Although untreated, the two ashes tested in this article contain large amounts of calcium and therefore may contain calcite. The calcite is unlikely to be neoformed as in [2]. The particle size distribution showed relatively large particles, suggesting that the loss of consistency is not caused by ultrafine calcite. Although not measured during the tests in this article, differences in porosity between the Nuuk-FA and Borås-FA could be a likely cause for their different effect on the consistency as Aubert et al. [2] suggests.

Table 2: Measured flow value (mm) after 6 and 30 minutes.

	Nuuk-FA		Borås-FA		Borås-FA + Plasticizer	
	6 min	30 min	6 min	30 min	6 min	30 min
Ref	70.38±7.13	61.28±7.13	70.38±7.13	61.28±7.13	70.38±7.13	61.28±7.13
5%	68.39±4.86	59.94±5.11	58.85±6.26	53.15±0.61	67.45±1.41	59.03±2.29
10%	49.02±7.05	42.82±7.58	49.99±9.00	31.79±5.84	67.86±11.1	55.13±14.9
20%	67.43±3.70	38.99±1.29	20.87±10.4	1.79±1.43	66.81±9.11	12.92±7.70

3.3 Loss of consistency after 30 minutes

In addition to decreasing the initial consistency, substitution with MSWI fly ash is shown to further reduce the consistency after 30 minutes. For both Nuuk-FA and Borås-FA, a 5% substitution does not intensify the loss of consistency after 30 minutes, compared to the reference. In contrast, a 10 and 20% replacement with Borås-FA resulted in a loss of flow approximately twice as big as the reference loss. Although a 10% substitution with Nuuk-FA reduced the initial consistency, the loss over time remained similar to the reference. Oppositely, a 20% replacement with Nuuk-FA showed no effect on the initial consistency but greatly affected the consistency after 30 minutes, resulting in a flow loss 3 times greater than the reference.

The addition of superplasticiser had varying effects on the consistency loss over time. In the case of 5% substitution with Borås-FA, the loss of flow over time were similar to the reference, while for a 10% substitution, the superplasticizer improved the loss over time. However, it had no effect on the 20% substitution. Although the initial consistency was improved, the flow after 30 minutes was reduced by approximately 54 mm, 6 times greater than the flow loss of the reference.

The changes in consistency after 30 minutes could be caused by the chemical composition of the ashes. The two ashes both contain different elements in varying amounts that can affect the cement hydration differently. Chen et al. [6] determined that NaCl, KCl and $CaCl_2 \cdot 2H_2O$ were present in a tested MSWI fly ash, suggesting their presence in Nuuk-FA and Borås-FA. Different compounds have varying effects on hydration, such as NaCl and $CaCl_2$ accelerating the hydration [7] and [8], while sulphate is reported to both accelerate and retard the hydration [9] and [10]. However, further studies are required to better understand the effect of MSWI fly-ash on cement hydration.

The results show that depending on the ash, large cement replacements hampers the consistency. Superplasticizer improves the initial consistency. However, the increased loss of workability both initially and after 30 minutes would make early age concrete work increasingly difficult, when utilizing a high substitution rate.

4. CONCLUSIONS

- Depending on the type of MSWI fly ash used, the initial consistency of the mortar is either unaffected or greatly decreased with increasing ash substitution. Borås-FA reduced the consistency by 16, 29 and 70% for a 5, 10 and 20% substitution. A 5 and 20% substitution with Nuuk-FA did not affect the initial consistency, yet a 10% substitution reduced the consistency by 30%.
- High MSWI fly ash substitution results in an increased loss in consistency after 30 minutes. The two ashes showed no increase in flow loss after 30 minutes with a 5% substitution. Substitution with 10 and 20% Borås-FA increased the flow loss by a factor of two, while replacement with 20% Nuuk-FA increased the flow loss by a factor of three.
- Superplasticizer improves the initial loss in consistency. With superplasticizer, a consistency similar to the reference was achieved regardless of the substitution amount. Although increasing amounts of superplasticizer were needed for higher substitutions. The addition of superplasticizer decreased the flow loss after 30 minutes, except for a 20% substitution where the flow was reduced by a factor of 6 compared to the reference.

- To better understand the loss in initial consistency and over time, future studies will include investigations of the effect of the fly ash porosity, as well as the potential effect the chemical composition has on the consistency. Furthermore, supplementary flow and fluidity experiments with additional MSWI ashes could be made to get an overall better understanding of MSWI ashes influence on the consistency.

ACKNOWLEDGEMENTS

Nuuk Incineration and Borås Energi och Miljö are recognized for contributing the fly ash for this series of experiments.

REFERENCES

[1] H. Zhang, Y. Zhao, Toxicity Analysis of Municipal Solid Waste Incineration (MSWI) Fly Ash, 2009 3rd Int. Conf. Bioinforma. Biomed. Eng. (2009) 1–4. doi:10.1109/ICBBE.2009.5163694.

[2] J.E. Aubert, B. Husson, N. Sarramone, Utilization of municipal solid waste incineration (MSWI) fly ash in blended cement. Part 2. Mechanical strength of mortars and environmental impact, J. Hazard. Mater. 146 (2007) 12–19. doi:10.1016/j.jhazmat.2006.11.044.

[3] L. Bertolini, M. Carsana, D. Cassago, A.Q. Curzio, M. Collepardi, MSWI ashes as mineral additions in concrete, Cem. Concr. Res. 34 (2004) 1899–1906. doi:10.1016/j.cemconres.2004.02.001.

[4] L. Kozakova, T. Bakalar, M. Zelenak, M. Prascakova, Solidification of MSWI fly-ash with regard to hazardous metals leaching, Acta Montan. Slovaca. 18 (2013) 129–139.

[5] Jos G.J. Olivier; Greet Janssens-Maenhout; Marilena Muntean; Jeroen A.H.W. Peters, Trends in global co 2 emissions 2016, (2016) 86.

[6] W.S. Chen, F.C. Chang, Y.H. Shen, M.S. Tsai, C.H. Ko, Removal of chloride from MSWI fly ash, J. Hazard. Mater. 237–238 (2012) 116–120. doi:10.1016/j.jhazmat.2012.08.010.

[7] F.R. Lago, J. Dweck, T. Analysis, Evaluation of Influence of Salt in the Cement Hydration to Oil Wells, 20 (2017) 743–747.

[8] V.S. Ramachandran, Calcium chloride in concrete- applications and ambiguities., Can. J. Civ. Eng. 5(2) (1978) 213–221.

[9] P.K. Metha, P.J.M. Monteiro, Concrete microstructure, properties and materials, Fourth Edi, Mc Graw Hill Education, n.d.

[10] S. Kumar, C.V.S.K. Rao, Effect of sulphates on the setting time of cement and strength of concrete, Cem. Concr. Res. 26 (1996) 643. doi:Doi 10.1016/S0008-8846(96)90013-7.

Conference Abstract I

Valorization of MSWI Fly Ash for Use in Cement Based Materials

Benjamin A. R. Ebert, Britt-Marie Steenari, Mette R. Geiker, Gunvor M. Kirkelund

Valorization of MSWI Fly Ash for Use in Cement Based Materials

Benjamin Ebert*[1], Gunvor Kirkelund[1], Britt-marie Steenari[2], Mette R. Geiker[3]

1: Department of Civil Engineering, Technical University of Denmark

2: Chemistry and Chemical Engineering, Chalmers University of Technology

3: Department of Structural Engineering, Norwegian University of Science and Technology
*Corresponding author email: bareb@byg.dtu.dk

Abstract

The European Union trends in municipal solid waste management has changed in the last couple of decades, with recycling, recovery and incineration being the major waste management methods in several member states [1]. Municipal solid waste incineration (MSWI) is the common practise of burning waste for heat and energy recovery, at combined heat and power plants. This results in a waste volume reduction of up to 90% [2] and bi-products of bottom and fly ash. The fly ash contains heavy metals, salts and organic toxins and is regarded as a hazardous material, that remains underused and are dumped in secure landfills [2].

It could potentially be utilized as a resource for making cement based materials, similarly to fly ash from coal incineration. Pre-treating the fly ash could be required, in order to remove the salts and heavy metals, reducing the hazardousness. Possible methods of treatment could be the extraction of metals from the ash using electrodialytic remediation [3] or solvent extraction [4]. Minimal research in to the feasibility of utilizing the subsequent treated residue of these methods have been done. The purpose of this PhD project is to treat MSWI fly ash using remediation and extraction and analysing the viability of using the treated ash in cement based materials.

Keywords: MSWI fly ash, Pre-treatment, Cement, Electrodialytic remediation,Solvent extraction

References

[1] EC, Being wise with waste : the EU' s approach to waste management, Publ. Off. Eur. Union. (2010) 20. doi:10.2779/93543.

[2] K.L. Lin, K.S. Wang, C.Y. Lin, C.H. Lin, The hydration properties of pastes containing municipal solid waste incinerator fly ash slag, J. Hazard. Mater. 109 (2004) 173–181. doi:10.1016/j.jhazmat.2004.03.014.

[3] G.M. Kirkelund, C. Magro, P. Guedes, P.E. Jensen, A.B. Ribeiro, L.M. Ottosen, Electrodialytic removal of heavy metals and chloride from municipal solid waste incineration fly ash and air pollution control residue in suspension - Test of a new two compartment experimental cell, Electrochim. Acta. 181 (2015) 73–81. doi:10.1016/j.electacta.2015.03.192.

[4] J. Tang, Removal and Recovery of Metals from Municipal Solid Waste Incineration Ashes by a Hydrometallurgical Process Department of Chemistry and Chemical Engineering, 2017.

Valorization of MSWI Fly Ash for Use in Cement Based Materials

Benjamin A. R. Ebert*[1], Gunvor M. Kirkelund[1], Britt-marie Steenari[2] & Mette R. Geiker[3]

1. Department of Civil Engineering, Technical University of Denmark, Denmark
2. Chemistry and Chemical Engineering, Chalmers University of Technology, Sweden
3. Department of Structural Engineering, Norwegian University of Science and Technology, Norway

* Corresponding author email: bareb@byg.dtu.dk

Abstract

Fly ash from municipal solid waste incineration is regarded as a hazardous material and remains unutilized. If the fly ash is valorized it will represent a new potential resource. The purpose of this PhD project is therefore to investigate the value of using waste derived fly ash in cement based materials. This is accomplished by pre-treating the ash reducing the hazardous, and reusing it in cement based materials.

MSWI fly ash

Municipal solid waste incineration (MSWI) is the practise of burning waste for heat and energy. A bi-product of MSWI is a hazardous fly ash, containing heavy metals, salts and organic toxins, that remains unused. This project focuses on ashes from Amager Ressource Center (Denmark), Borås Energy och Miljö (Sweden) and Nuuk incineration (Greenland)

PhD project

Valorization of MSWI fly ash for use in cement based materials is a joint alliance research project between the Technical University of Denmark (DTU), Chalmers university of Technology (Chalmers) and the Norwegian University of Science and Technology (NTNU)

ARC Nuuk Borås

Pre-Treatment

To better utilize the fly ash, a pre-treatment step is implemented, separating the hazardous elements, and reducing the overall harmfulness of the ash.

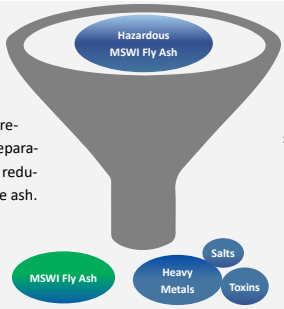

Treatment method

The pre-treatment consists of washing, removing the water soluble elements, and either electrodialytic remediation (EDR) or solvent extraction removing the heavy metals.

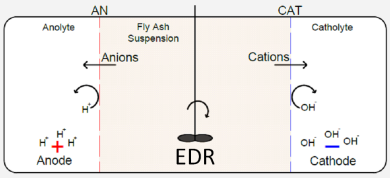

Scientific Goals

01 Assessing the efficiency of pretreating the MSWI fly ash with either electrodialytic remediation or solvent extraction.

02 Determining the mechanical and rheological properties of cement based materials containing raw and pre-treated MSWI fly ash.

03 Evaluating the environmental impact of cement based materials containing MSWI fly ash by investigating the heavy metal leaching at different stages of hydration.

04 Determine the effect of MSWI fly ash on cement hydration in terms of reactivity and phase development, as well as its effect on durability.

Samples

The effect MSWI fly ash has on cement based materials is tested by analysing mortar and cement paste samples in both a fresh and hardened state.

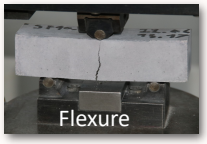

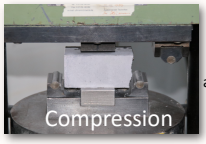

Mortar properties

Hardened mortar samples are used to test the fly ashes effect on compressive and flexural strength, as well as the elastic modulus. Fresh mortar are tested for consistency, air entrainment and setting time.

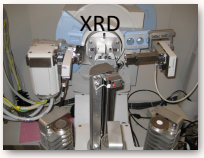

Paste properties

Paste samples are used to test the phase development as well as the hydration scheme, using thermogravimetry (TGA), X-ray diffraction (XRD) and calorimetry.

Additional Experiments

Further experimentation is planned in order to determine the leaching of heavy metals from mortar as well as the effect of MSWI fly ash on concrete durability.

Outcome

The outcome of this project clarify the potential for using MSWI fly ash as a cement replacement, as well as the effectiveness of pre-treating the ash.

Additional Note I

Alternative Strategies for Using MSWI Fly Ash in Cement-Based Materials

Benjamin A. R. Ebert, Gunvor M. Kirkelund

Additional Note I: Alternative strategies for using MSWI fly ash in cement-based materials

Introduction

Waste management represents a significant problem in today's society, with incineration being an attractive option for reducing the volume and weight of waste [1]. The problem with waste incineration is that it produces new waste, albeit in minor amounts [1]. The fly ash and air pollution control (APC) residues resulting from waste incineration are considered final residues and are landfilled [1]. Finding ways of utilising the residues instead is of interest, with concrete manufacturing being an appealing alternative. Previous studies have researched replacing cement, using MSWI fly ash as an SCM, or replacing sand, using MSWI fly ash as an aggregate, for concrete manufacturing [1–5]. However, investigating other potential strategies for using MSWI fly ash residues for concrete manufacturing is vital for determining the optimal use. Ebert et al. [6] found that one of their studied raw residues had an accelerating effect on cement hydration, while an electrodialytically treated residue had a high sulphate content. Therefore, the present study investigates the possibility of using the raw residue as a hydration accelerator like $CaCl_2$ [7,8] and using the treated residue to replace gypsum in ordinary Portland cement. This is achieved by investigating the two residues effect on setting time.

Materials and Method

Materials

Two MSWI fly ash residues were investigated in this study, one from Ryaverket, Borås, Sweden and one from Amager Bakke, Copenhagen, Denmark. The residue from Ryaverket (*Rya*) was extracted from the flue gas stream after the APC with a textile filter. The residue from Amager Bakke (*Ama*) was extracted before the APC with an electrostatic precipitator and subsequently treated with electrodialytic remediation (EDR). The chemical and mineralogical composition of the two residues was described in the study by Ebert and Kirkelund [6] in detail. The residues oxide compositions are reproduced here for reference. See Table 1. For the EDR treatment, the residue was first washed (L/S 5) three times with deionised water, after which 3 kg of the washed residue were mixed with 30 litres of deionised water in a stirred container to avoid sedimentation. For 28 days, a constant current (1 A) was maintained across the suspension to leach and separate heavy metals from the residue into electrolyte solutions. The suspension was filtered (45 µm) and dried at 50°C, after which the remaining dried residue was crushed manually with a mortar and pestle. The performed EDR treatment are explained in detail in [6]. The untreated residue from Ryaverket was also dried at 50°C before using it in the experiments.

Table 1: Oxide composition of tested residues, as given in [6].

	SiO_2	Al_2O_3	Fe_2O_3	CaO	MgO	SO_3	K_2O	Na_2O	P_2O_5	Cl
Rya	6.4	4.7	1.8	42	1.8	8.9	2.7	7.0	2.2	13
EDR Ama	14	2.3	2.4	28	0.4	30	1.0	0.7	2.1	0.1

An ordinary Portland cement, CEM I 52.5 N (MS/LA), consisting of 95-100% clinker and 3.7% limestone (thermogravimetric measurement) and a CEM I 52.5 N (MS/LA) without any added limestone or gypsum were also used as part of this study. Their respective oxide compositions are given in Table 2. Furthermore, laboratory-grade $CaCl_2$ was also used as part of this study

Table 2: Oxide composition of CEM I cement and CEM I with no limestone or gypsum.

	SiO	Al_2O_3	Fe_2O_3	CaO	MgO	SO_3	K_2O	Na_2O	P_2O_5	Cl
CEM I	20	5.4	3.8	61	1.0	3.2	0.4	0.3	0.3	0.04
CEM I NLG	23	6.7	6.1	>56	1.5	1.3	1.3	1.2	0.3	0.04

Setting Time Test

The cement paste's initial and final setting time were measured using the method specified in EN 196-3: 2009 [9] and an automatic Vicat apparatus Matest E044N Vicatronic. The test specifies that the mould used should be inverted after the initial setting time has been measured. However, the mould was not inverted as specified, and the final setting time was measured on the same surface as the initial.

The cement paste for the accelerated hydration test was prepared per EN 196-3: 2009 [9] with the following deviations. 500g of CEM I cement was mixed with a solution of 5, 10 or 15g of Rya or $CaCl_2$ and 250g deionised water, corresponding to 1, 2 and 3% of the cement weight. The mixing procedure was as follows: The cement was placed in a 5L stainless steel bowl, and one solution was added. Immediately after the cement and solution came into contact, the mixture was mixed at 140 rpm for 60 s, followed by 30 s at 285 rpm. The mixing was then halted for 90 s, and the paste adhering to the bowl's walls was scraped off towards the bowl's middle. The paste was then mixed for an additional 60 s at 285 rpm.

The cement paste for the gypsum replacement test was mixed in the same way as the paste for the accelerated hydration test. However, these tests used 467.2g CEM I NLG + 32.8g Ama and 250g deionised water. The ratio of 467.2g CEM I NLG + 32.8g Ama ensures that the blend contains 3.2 wt % SO_3, the same as CEM I.

A reference mixture (*Ref*) of just CEM I cement and deionised water was also prepared. The setting time test was repeated three times for each mix.

Results and Discussion

MSWI Fly Ash Residue as an Accelerator

The results of the accelerative setting time test are shown in Figure 1. The results show that with the performed test, the CEM I cement used had an initial setting time after 5 hours of hydration and a final setting time after 10 hours of hydration. Using increasing amounts of $CaCl_2$ decreased the initial and final setting time and decreased the time between the initial and final sets.

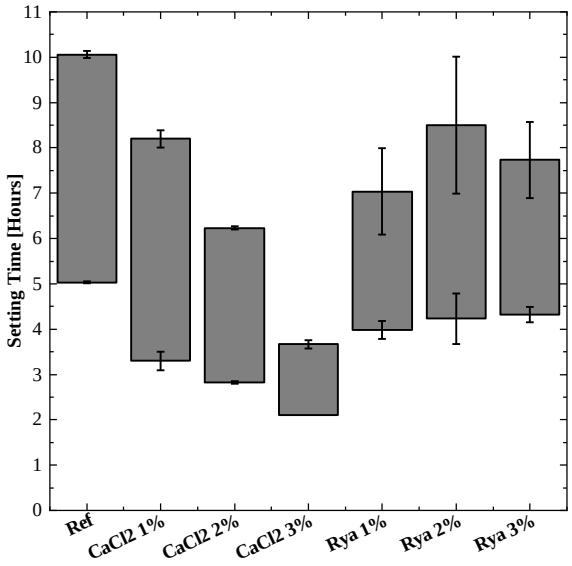

Figure 1: Setting time test results for reference, $CaCl_2$ and Rya.
Error bars represent the standard deviation of three tests.

With 1% $CaCl_2$ added to the mixing water, the initial set occurred after 3.3 hours, while the final set occurred 5 hours after that. Using 3% $CaCl_2$, the initial set occurred after 2.1 hours, while the final set occurred 1.6 hours after that. Combining the raw residue Rya with the mixing water in the same way as for the $CaCl_2$ did decrease the initial and final set. However, the results differed from $CaCl_2$ and had a higher standard deviation. Using 1% Rya the initial set occurred after 4 hours and the final set 3 hours after that. Using 2% or 3% Rya also accelerated the initial set to occur after 4 hours, while the final set occurred 4 and 3.5 hours later, respectively. The accelerative effect does not increase with an increasing amount of Rya, as $CaCl_2$ does. This may be due to the heterogeneous composition of the

MSWI residue, resulting in an inconsistent accelerative effect. However, using 1% Rya as a set accelerator seems feasible.

MSWI Fly Ash Residue as a Gypsum Replacement

The results of the gypsum replacement test are shown in Figure 2. Using sulphur-rich EDR treated MSWI fly ash is feasible as the CEM I NLG and AMA blend had its initial set after 5 hours of hydration, similarly to the reference cement. However, the final set occurred after 10.5 hours of hydration instead of 10 hours. It may be hypothesised that delay is because some of the sulphates in AMA is bound as $PbSO_4$ instead of $CaSO_4$. During the mixing process, small clumps were observed in the mixture that was not observed in the reference mixture, which may be hardened cement. Despite causing a delay in the final set, replacing the gypsum in ordinary Portland cement with EDR treated MSWI fly ash may still be feasible. Without the addition of EDR AMA, the CEMI NLG cement stiffened and had a consistency of wet clay before the mixing process had finished.

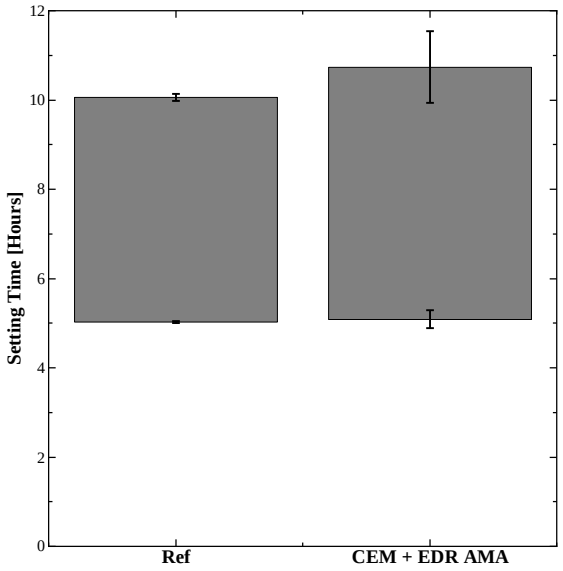

Figure 2: Setting time test result for the reference and CEM I NLG + EDR AMA.

Potential of MSWI Fly Ash Residue as an Accelerator or Gypsum Replacement

Although using Rya as a set accelerator and AMA as a gypsum replacement may be feasible alternative uses for MSWI fly ash residues, their heavy metal content remains a problem. The European standard EN 206 [10] states that bio ash may only be used if it does not increase the heavy metal content of a blended binder by more than 50%. Although MSWI fly ash is not bio ash, the criteria may be used here. Table 2 shows the increase in heavy metal content of the respective blended

binders with Rya and AMA. Using just 1 wt% Rya may increase the Zn content of the binder by 390 % while using 6.56 wt% AMA may increase the Zn content of the binder by 10030 %.

Table 2: Increase in metal content.

	1 wt% Rya	6.56 wt% EDR AMA
Cd	200 %	980 %
Cr	12 %	140 %
Cu	56 %	24 %
Pb	19 %	1100 %
Zn	390 %	10030 %

Conclusion

Using MSWI fly ash residue as an accelerator may be a feasible alternative for resuing MSWI fly ash. However, due to the residues heterogeneous chemical composition, using only 1 wt% of the residue may be the best alternative. Using high sulphur EDR treated MSWI fly ash as a gypsum replacement is also feasible but may result in a 1-hour delay of the final set. However, the heavy metal content of the ashes remains too high, both after the treatment and when used in small doses.

References

[1] J.E. Aubert, B. Husson, A. Vaquier, Use of municipal solid waste incineration fly ash in concrete, Cement and Concrete Research. 34 (2004) 957–963. https://doi.org/10.1016/j.cemconres.2003.11.002.

[2] J.E. Aubert, B. Husson, N. Sarramone, Utilisation of municipal solid waste incineration (MSWI) fly ash in blended cement. Part 2. Mechanical strength of mortars and environmental impact, Journal of Hazardous Materials. 146 (2007) 12–19. https://doi.org/10.1016/j.jhazmat.2006.11.044.

[3] S. Remond, P. Pimienta, D.P.P. Bentz, S. Rémond, D.P.P. Bentz, P. Pimienta, Effects of the incorporation of Municipal Solid Waste Incineration fly ash in cement pastes and mortars I. Experimental study, Cement and Concrete Research. 32 (2002) 303–311. https://doi.org/10.3130/jaabe.3.1.

[4] L. Bertolini, M. Carsana, D. Cassago, A.Q. Curzio, M. Collepardi, MSWI ashes as mineral additions in concrete, Cement and Concrete Research. 34 (2004) 1899–1906. https://doi.org/10.1016/j.cemconres.2004.02.001.

[5] T. Lenormand, E. Rozière, A. Loukili, S. Staquet, Incorporation of treated municipal solid waste incineration electrostatic precipitator fly ash as partial replacement of Portland cement: Effect on early age behaviour and mechanical properties, Construction and Building Materials. 96 (2015) 256–269. https://doi.org/10.1016/j.conbuildmat.2015.07.171.

[6] B.A.R. Ebert, G.M. Kirkelund, “UNDER REVIEW” Effects of chlorides and sulphates on leaching from mortar with raw and electrodialytically treated MSWI fly ash, Journal of Hazardous Materials. (2021).

[7] T. Vehmas, A. Kronlöf, A. Cwirzen, Calcium chloride acceleration in ordinary Portland cement, Magazine of Concrete Research. 70 (2018) 856–863. https://doi.org/10.1680/jmacr.17.00079.

[8] V.S. Ramachandran, Calcium chloride in concrete- applications and ambiguities., Canadian Journal of Civil Engineering. 5(2) (1978) 213–221.

[9] DS/EN 196 3 + A1: Methods of testing cement - Part 3: Determination of setting times and soundness, Dansk Standard, 2009.

[10] D. Standard, Dansk standard og overensstemmelse – Regler for anvendelse af EN 206 i Danmark Concrete – Specification , performance , production and conformity –, (2019) 1–58.

Appendix

Appendix A: Principal Component Analysis

How to interpret a Principal Component Analysis

Principal component analysis (PCA) may very well form the basis for multivariate data analysis by simplifying an extensive matrix of data in terms of its principal components, also known as latent variables. In general, almost any data set can be simplified by PCA and can be used to identify similarities and differences in a data set without altering the data's overall interpretation [143]. How and what a PCA model does is best explained with an example.

Consider an arbitrary data set consisting of several samples. See Table A1 for an example. For each sample, several variables have been measured. Each sample could represent a human and each variable a physical property such as blood pressure, cholesterol level, weight, blood sugar. In such an example, your health is a latent variable that is being measured [143].

Table A1: Dataset example.

	Sample 1	Sample 2	Sample 3	Sample 4	Sample 5	Sample 6
Variable 1	10	12	8	2	4	1
Variable 2	7	5	4	2	3	1
Variable 3	11	8	10	3	1	3
Variable 4	6	8	5	2	4	6

A problem occurs if you were to plot the samples in a graph when you have four or more variables, see Figure A1. When looking at the first three variables, two groups in the data can be observed, which could hypothetically be interpreted as healthy and unhealthy individuals. To make the same determination with four or more variables, a PCA model can be used. How to set up a PCA model is best explained geometrically, with a two-dimensional example.

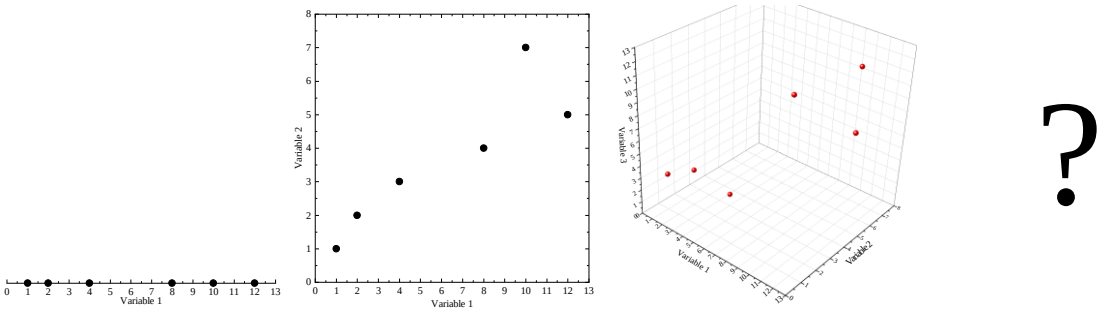

Figure A1: Plots of dataset for 1 variable (a), 2 variables (b), 3 variables (C) and 4 variables (d).

First, the data is pre-processed by mean-centring and scaling, shifting the data to the coordinate system centre, while each variable has equal scaling. See Figure Xa and Xb. Centring removes the arbitrary bias from the measurements that are unwanted in the model [143]. The data are scaled to unit variance, removing the different units from the measured variables. Shifting the data does not change how the data points are positioned relative to each other. The first principal component is then calculated by finding the best fit line going through origo that best explains the samples with minimum residual error [143]. See Figure Xc. Another way of expressing this is that the best fit line goes in the direction of maximum variance of the projections onto the line [143].

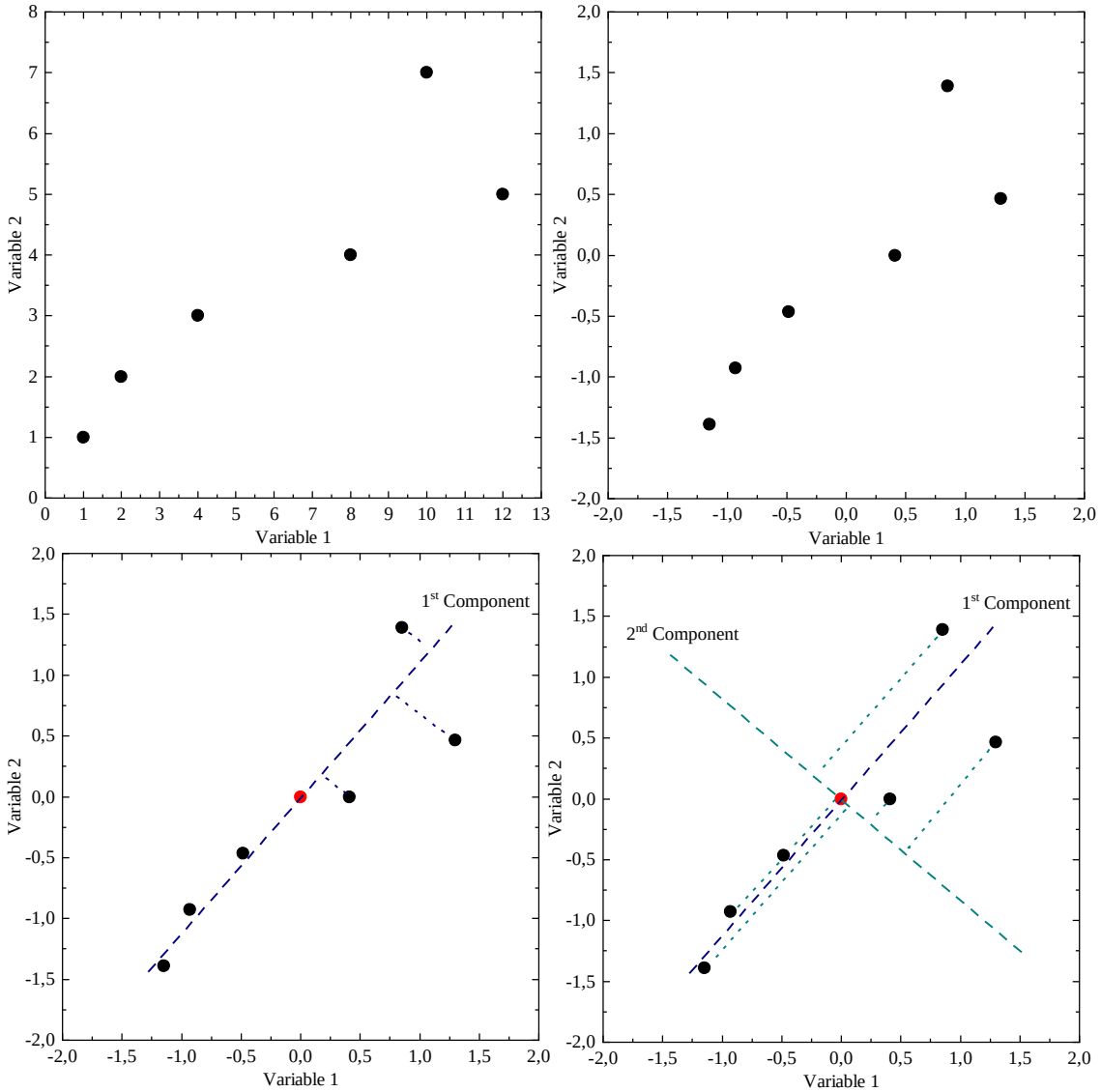

When the best fit line is found, the location of each sample onto the line is marked. This is done by finding the 90-degree projection of each observation onto the line [143]. The distance from the origin to the projected point along the line is called the score. Each sample has a score value for any given component. The score value is a linear combination of the sample's vector and the component's direction vector. When the first component is found, the second component can be determined. The second component also goes through origo and can point in any direction as long as it is perpendicular to the first component. The second component's direction vector is rotated until a direction is found, giving the greatest variance in the score values when projected on this new component. See Figure Xd. In the two-dimensional example, the different sample's vectors were 1 x 2 vectors, while the first and second components direction vectors were 2 x 1 vectors.

The same principles explained for the two-dimensional example are valid for any dataset consisting of *N* samples and *K* variables. The sample's vectors are then 1 x K vectors, while the components direction vectors are *K* x 1 vectors. Each samples score is then a linear combination of *K* terms, as each variable contributes to a samples score. The common terminology for the direction vectors is loadings because they show how the initial variables load, creating the component. There is, in theory, one principal component for each variable in a data set consisting of *N* samples and *K* variables. However, in practice, the number of principal components is equal to either the number of variables or the number of samples, whichever is the smaller number. It is unnecessary to calculate all principal components as each successive component accounts for less and less of the data set variation. When the scores and direction vectors (loading) have been calculated, a score plot and a loadings plot can be made. See Figure Xa and Xb for examples plots of the data in Table X. Samples with variables close to the average appear at the score plot's origin. If a samples score is far from the origin, it is either an outlier or a naturally extreme observation. It can, in general, be inferred why a sample is at the outer edge of a score plot in combination with the loadings. Samples that are initially similar to each other are similar in the score plot, while dissimilar samples are much further apart. Variables that have little contribution to a direction have almost zero weight in that loading. Strongly correlated variables in a loadings plot of one component vs another will appear near each other, while negatively correlated variables will appear diagonally opposite each other. Fig. A2 depicts the score plot and loadings plot from a PCA of the example data in table A1. From it, it can be seen that samples 1-3 are clustered together and that samples 4-6 are clustered, suggesting that these clusters of samples are similar. Furthermore, from the loadings plot, it appears that variable 1-3 are correlated and that variable 1-3 may be negatively correlated with variable 4.

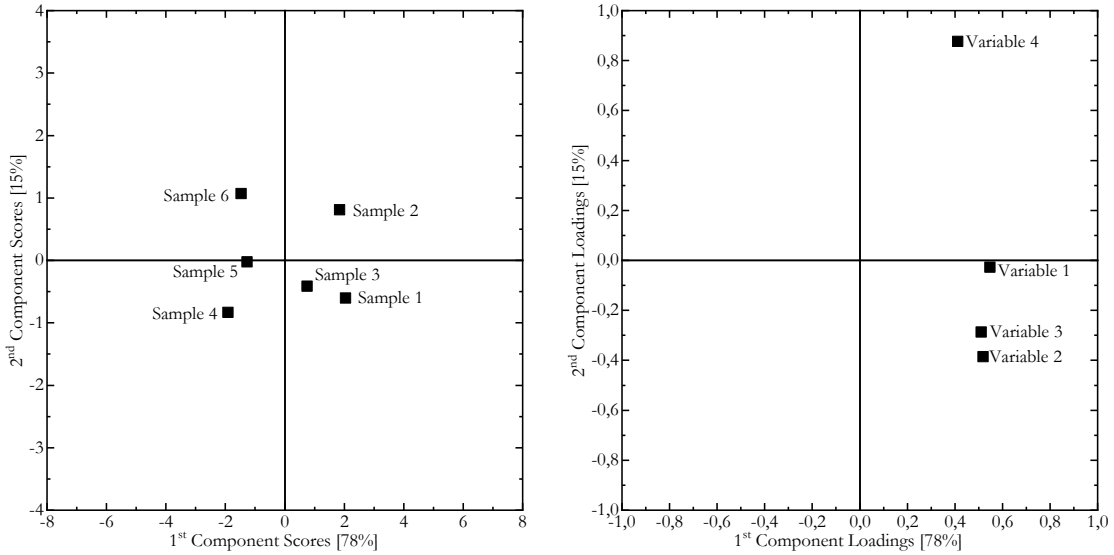

Figure A2: Example of a score plot and loadings plot from a PCA.

Program and Procedure used

The program used to perform the PCA's was the statistical program Simca (version 14.1) by Sartorius Stedim Biotech. The default settings of this version of the program were used for the calculations.

- Scaled and centred coefficients.
- Standardised residual with R^2 specified as the explained variance.
- Cross-validation was used for the fitting, with seven cross-validation groups.
- A maximum of 200 iterations was used.
- The missing data tolerance %(Var) was 5.
- The confidence level on parameters was set to 95%.

The experimental data used for PCA included the residues presented in the thesis and MSWI fly ash residues found in the literature. MSWI fly ash residues from the literature were only included if the study listed the type of furnace and flue gas filter used to extract the fly ash and if the country of origin was specified. The composition of the waste incinerated was not considered as part of the analysis due to inadequate reporting of the waste composition in the literature. The variables in the PCA's were Al_2O_3, Fe_2O_3, SiO_2, CaO, MgO, Na_2O, K_2O, SO_3, Cl, Cd, Cr, Cu, Pb, Zn. If a study used in the analysis did not report the oxide content but the element content, the corresponding oxide content was then calculated based on the element content. 51 MSWI fly ash residues were acquired from published literature [45,50,112–128].

Appendix B: Solvent Extraction

The solvent extraction experiments were performed using 3.5 ml glass vials sealed with plastic lids and an IKA Vibrax VXR Basic thermostat sample shaker. The vials were shaken at 500 rpm to ensure the organic phase consisting of kerosene (Solvent 70) was mixed with the acidic aqueous phase. The temperature was during all the experiments was 25°C. The aqueous phase volume was equal to the organic phase volume (phase ratio of 1). The chosen extractant was the aldoxime LIX860N-I, see Fig B1, which is designed to extract Cu.

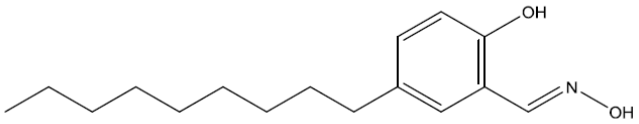

Figure B1: Chemical structure of LIX860N-I as depicted in [144].

LIX860N-I is a 5-nonylsalicylaldoxime containing OH groups and N. Aldoximes are well known for forming stable complexes with Cu(II). The extraction of a given metal (M) from an acidic aqueous phase can be written as [144]:

$$M^{z+}_{aq} + zHA_{org} \quad \leftrightarrow \quad MA_{z,org} + zH^{+}_{aq}$$

HA is the protonated organic extractant.

Two series of experiments were performed. The first consisted of varying the concentration of LIX860N-I in the organic phase, while the second consisted of varying the contact time between the organic and aqueous phases. Cu concentration in the organic phase was not measurable with ICP-OES. The concentration of Cu was instead determined based on the concentration in the aqueous phase before and after the experiments.

Appendix C: Electrodialytic Remediation

Lab-Scale Experiements

A two-compartment cell with the anode in the fly ash suspension and a three-compartment cell was used to perform the series of lab-scale experiments. The dimensions of the three-compartment cell are shown in Fig. C1. The compartments of the cells consist of open-ended polymethyl methacrylate cylinders with inner and outer diameters of 8 and 10 cm, respectively. The end of a compartment not connected to another compartment was sealed with polymethyl methacrylate plates. Sealant was used between each compartment and end plates to prevent leaking. The combined cell was fastened together using steel rods.

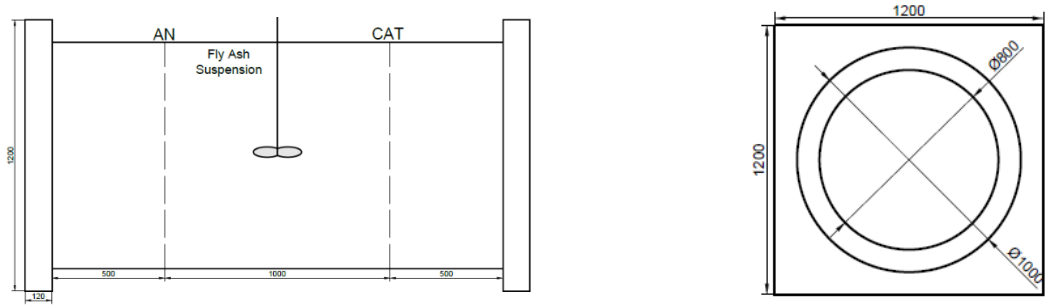

Figure C1: Dimensions of a three-compartment cell. Frontview (left) and sideview (right). All measurements are in mm.

The exchange membranes separating the anolyte and catholyte were from Ionics. The anion exchange membranes consisted of charged groups of quaternary ammonium (type 204 SZRA B02249C), while the cation exchange membranes were made with sulfonated copolymer groups (type CR67HUY N12116B). The stirrers were made from flexible plastic pieces fastened to glass rods with a rubber stopper. Heto motors or Vos 14 overhead stirrers were used to stir the suspension. The anode and cathode were made from platinum-coated titanium wire with a diameter of 3 mm. The electric current was maintained with a Hewlett Packard E3612A DC power supply. The electrolyte solutions were circulated in a closed circuit via pumps.

All lab-scale experiments were performed using 100g MSWI fly ash and 350ml deionized water for the suspension. 500ml 0.01M $NaNO_3$ adjusted pH 2 with 1:1 HNO_3 were used for the anolyte and catholyte. The experiments lasted for 28 days, where a constant electric current of 50 mA was applied to each cell—corresponding to 1 mA/cm^2 membrane. The pH and conductivity of the suspension were measured daily, together with the pH of the electrolytes. The pH of the electrolytes was adjusted to pH < 2 with 1:1 HNO_3 if required. The experiments were performed at ambient temperature. Fig. C2 shows the lab-scale experimental cells while used.

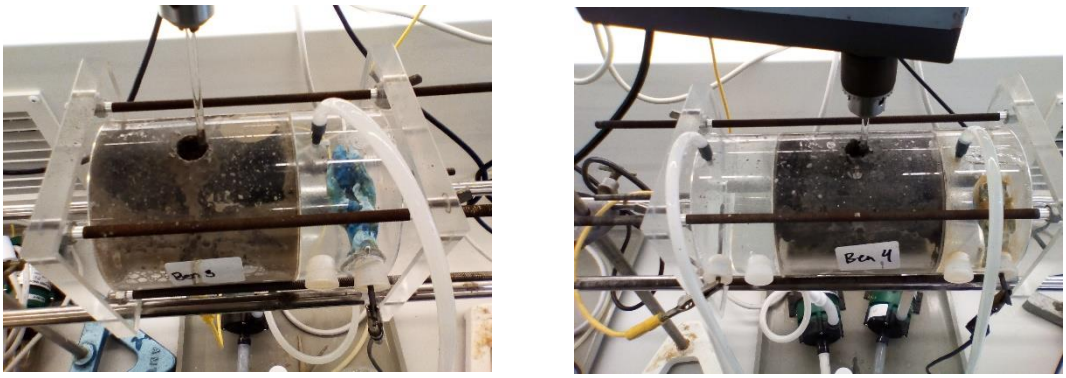

Figure C2: Lab-scale experimental setup of a two-compartment cell (left) and a three-compartment cell (right).

At the end of the experiments, the suspension was filtered through a 45 μm filter. The treated materials were dried at 50°C, and their content of primary elements and trace metals were measured with x-ray fluorescence analysis. The membranes and stirrer were submerged in 1M HNO_3, while the electrodes were submerged in 5M HNO_3. The trace metal content in the acidic liquids and the suspension liquids were then measured with ICP-OES.

The MSWI fly ash residues were washed with deionised water at L/S 5 three times as a pre-treatment. 100 g of ash was mixed with 500 ml deionised water in an Erlenmeyer flask and manually shaken. The liquid phase was then decanted through a Frisentte type 1125 filter after each wash. After the third wash, the entire sample was filtered and dried at 50°C.

Bench-Scale Experiements

The bench-scale experimental setup used is similar to the three-compartment lab-scale cell where the anode, anolyte, cathode and catholyte were separated from the suspension. Fig. C3 depicts a principal sketch of the bench-scale setup. However, it differs from the scale cylindrical cells in that the entire setup was built in a 60x40x32 cm^3 PVC plastic container.

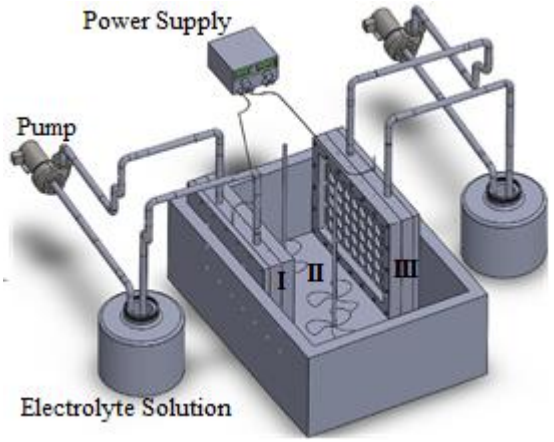

Figure C3: Principal sketch of the electrodialytic remediation bench-scale setup.
Anode compartment (I), suspension chamber (II) and cathode compartment (III). From journal paper III [110].

The anode and cathode were placed in separate electrode units (PVC plastic compartments) built into the container, where individual pumps circulated the electrolyte solutions. The entire container then functioned as the suspension chamber. The electrodes were platinum-coated titanium meshes (4x20 cm^2) from durAnode®. The electrode unit's side facing the suspension chamber contained either a 27x37 cm^2 anion exchange membrane (type 20 SZRA B02249) or a cation exchange membrane (type CR67 HUY B12116B). Both membranes were from Ionics. The suspension was stirred by three propellers connected to Vos 13 overhead stirrers from VWR. The power supply for the anode and cathode was a Blanko- model Q J-3003C III.

The bench-scale experiments were performed using 3 kg MSWI fly ash and 30-litres deionised water for the suspension. The anolyte and catholyte were each 5 litres of 0.01M $NaNO_3$ adjusted to pH 2 with 1:1 HNO_3. The experiments were maintained for 28 days at ambient temperatures, during which a constant electric current of 1 A was applied, corresponding to 1 mA/cm^2 membrane. The pH of the suspension and electrolytes were measured daily, together with the conductivity of the suspension. The pH of the electrolytes was adjusted to less than pH 2, with 1:1 HNO_3 if required. Figure X is a picture of the bench-scale setup.

At the end of the experiments, the treated material, membranes, stirrers and liquids were processed similarly to the lab-scale experiment post-processing. Furthermore, the bench-scale experiments' residue was washed three times at L/S 5, similarly to the lab-scale experiment procedure.

Removal Percentage Calculation

The total wt% of removed metals may be calculated based on the total metal content in the residue before the treatment or the total sum of metals removed and remaining in the sample after the treatment. For this series of lab-scale and bench-scale experiments, the wt% of removed metals was calculated based on the total content before EDR treatment. Calculating the removal % based on the total content of metals before the treatment may result in removal % >100%. In contrast, calculating the removal % based on the total sum after the treatment may overestimate the result.

The total content of metals in the residue may be calculated using ICP-OES or XRF analysis. Fig. C4 shows the total content of Cd, Cr, Cu, Pb and Zn in three MSWI fly ash residues before and after EDR treatment. Before the treatment, the two methods result in roughly similar metal concentrations, except for Cr, where XRF analysis is several 100 mg/kg higher than ICP-OES. Although, in general, XRF analysis gives a higher metal concentration than ICP-OES. After the treatment, the difference between the two measurements is higher, especially for Residue A. This

may be attributed to the precipitation of compounds that can be decomposed during the sample preparation for ICP-OES, such as microwave digestion at low pH. Using the ICP-OES measurements would, in that instance, lead to erroneous recovery percentage, as shown in Fig. C5. For this reason, measuring with XRF analysis was chosen.

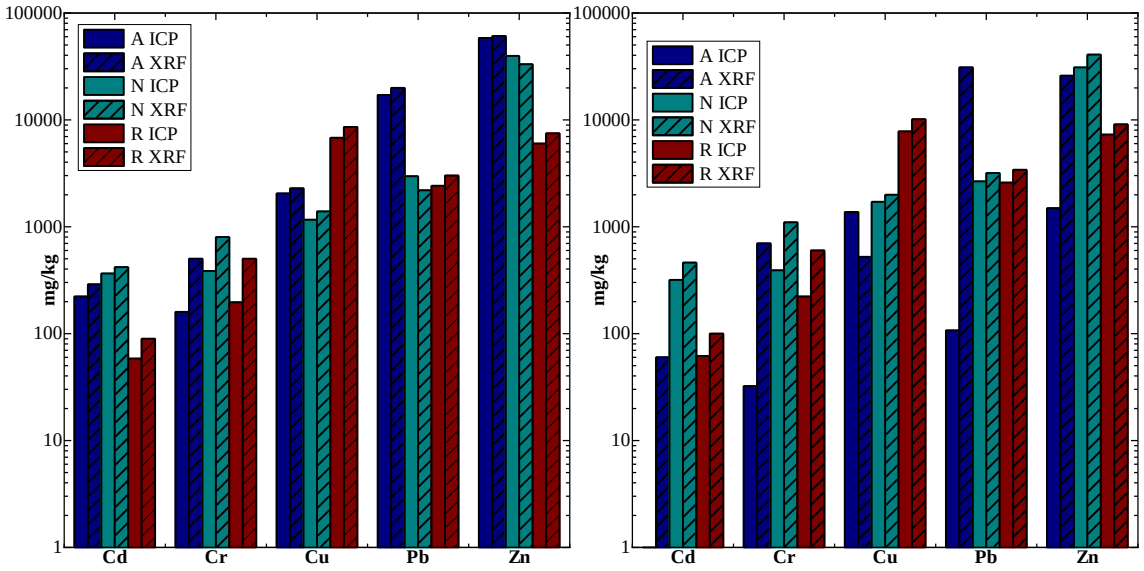

Figure 4: Total concentration of Cd, Cr, Cu, Pb and Zn in three residues
Before (left) and after (right) bench-scale EDR. As measured with ICP-OES and XRF analysis.

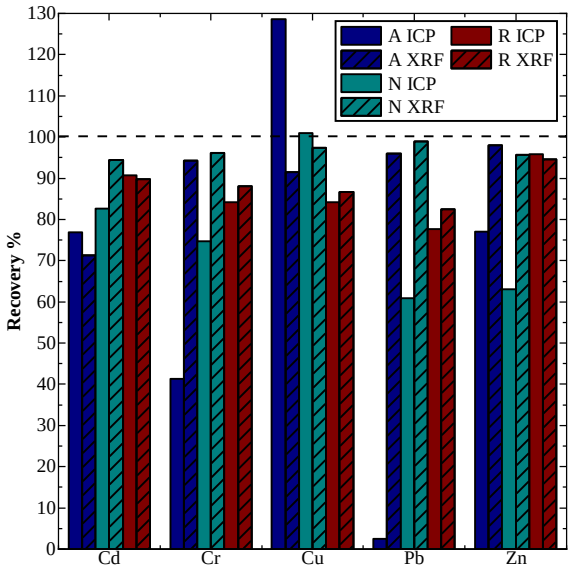

Figure 5: Recovery % calculated based on ICP measurement and XRF analysis.

Appendix C: Thermodynamic Modelling

The phase development of cement paste containing the various residues was modelled using the Gibbs free energy minimization program (GEMS). The program computes equilibrium phase assemblages and speciation in complex chemical systems. The software normally uses the PSI-GEMS database for its computations, but the CEMDATA 18 database [101] was also used for this series of modelling. The CSHQ model proposed by Kulik was used for modelling the C-S-H Q phase [145]. The two databases used does not account for the effect heavy metals has on the phase assemblage. The program input for the residues was the oxide compositions shown in Subsection 7.3.5, scaled so that the oxides shown were equal to 100 wt%. The modelled paste consisted of 50 g water, 90 g cement and 10 g residue. The percentage of reacted residue was incrementally changed, while the amount of reacted cement was assumed to be 80%. The process simulation mode used was the direct sequential change of bulk composition/ or constraints (S).

Input: System Definition

Phases/Species	**L**	**T:**	**On/OFF**	**UC**	**Add**	**UG**	**Go**	**Correc**
aq_gen	81	a	+	g	0	J	0	
gas_gen	6	g	+	g	0	J	0	
C3(AF)S0.84H	2	s	+	g	0	J	0	
CSHQ	6	s	+	g	0	J	0	
ettringite-AlFe	2	s	-	g	0	J	0	
ettringite-FeAl	2	s	-	g	0	J	0	
monosulph-AlFe	2	s	+	g	0	J	0	
monosulph-FeAl	2	s	+	g	0	J	0	
straetlingite	2	s	+	g	0	J	0	
ettringite	2	s	+	g	0	J	0	
SO4_OH_AFm	2	s	+	g	0	J	0	
OH_SO4_AFm	2	s	+	g	0	J	0	
SO4_CO3_AFt	2	s	+	g	0	J	0	
CO3_SO4_AFt	2	s	+	g	0	J	0	
hydrotalc-pyro	2	s	+	g	0	J	0	
MSH	2	s	-	g	0	J	0	
Al(OH)3am	1	s	-	g	0	J	0	
Al(OH)3mic	1	s	-	g	0	J	0	

Input: System Definition continued

Phases/Species	L	T:	On/OFF	UC	Add	UG	Go Correc
Gibbsite	1	s	-	g	0	J	0
Kaolinite	1	s	+	g	0	J	0
Graphite	1	s	-	g	0	J	0
Mayenite	1	s	+	g	0	J	0
Belite	1	s	+	g	0	J	0
Aluminate	1	s	+	g	0	J	0
Alite	1	s	+	g	0	J	0
Ferrite	1	s	+	g	0	J	0
CA	1	s	+	g	0	J	0
CA2	1	s	+	g	0	J	0
C2AH75	1	s	+	g	0	J	0
C3AH6	1	s	-	g	0	J	0
C4AH11	1	s	+	g	0	J	0
C4AH13	1	s	+	g	0	J	0
C4AH19	1	s	+	g	0	J	0
CAH10	1	s	+	g	0	J	0
C4AsH105	1	s	+	g	0	J	0
C4AsH12	1	s	+	g	0	J	0
C4AsH14	1	s	+	g	0	J	0
C4AsH16	1	s	+	g	0	J	0
C4AsH9	1	s	+	g	0	J	0
Chabazite	1	s	+	g	0	J	0
ZeoliteP	1	s	+	g	0	J	0
C2ASH55	1	s	+	g	0	J	0
C4AcH9	1	s	+	g	0	J	0
C4Ac0.5H105	1	s	+	g	0	J	0
C4Ac0.5H12	1	s	+	g	0	J	0
C4Ac0.5H9	1	s	+	g	0	J	0
C4AcH11	1	s	+	g	0	J	0
Friedels	1	s	+	g	0	J	0
Kuzels	1	s	+	g	0	J	0
C6AsH13	1	s	+	g	0	J	0
C6AsH9	1	s	+	g	0	J	0

Input: System Definition continued

Phases/Species	L	T:	On/OFF	UC	Add	UG	Go Correc
Aragonite	1	s	+	g	0	J	0
Calcite	1	s	+	g	0	J	0
C3FH6	1	s	+	g	0	J	0
C4FH13	1	s	+	g	0	J	0
C3FS0.84H4.32	1	s	+	g	0	J	0
C3FS1.34H3.32	1	s	+	g	0	J	0
C4Fc05H10	1	s	+	g	0	J	0
C4FcH12	1	s	+	g	0	J	0
Dolomite-dis	1	s	+	g	0	J	0
Dolomite-ord	1	s	+	g	0	J	0
lime	1	s	+	g	0	J	0
Portlandite	1	s	+	g	0	J	0
Anhydrite	1	s	+	g	0	J	0
Gypsum	1	s	+	g	0	J	0
hemihydrate	1	s	+	g	0	J	0
thaumasite	1	s	-	g	0	J	0
Iron	1	s	-	g	0	J	0
Fe-carbonate	1	s	+	g	0	J	0
Siderite	1	s	+	g	0	J	0
Hematite	1	s	-	g	0	J	0
Magnetite	1	s	-	g	0	J	0
Ferrihydrite-am	1	s	+	g	0	J	0
Ferrihydrite-mc	1	s	+	g	0	J	0
Goethite	1	s	-	g	0	J	0
Pyrite	1	s	+	g	0	J	0
Troilite	1	s	+	g	0	J	0
Melanterite	1	s	+	g	0	J	0
arcanite	1	s	+	g	0	J	0
syngenite	1	s	+	g	0	J	0
K-oxide	1	s	+	g	0	J	0
OH-hydrotalcite	1	s	+	g	0	J	0
Magnesite	1	s	+	g	0	J	0
Brucite	1	s	+	g	0	J	0

Input: System Definition continued

Phases/Species	L	T:	On/OFF	UC	Add	UG	Go	Correc
thenardite	1	s	+	g	0	J		0
Natrolite	1	s	+	g	0	J		0
ZeoliteX	1	s	+	g	0	J		0
ZeoliteY	1	s	+	g	0	J		0
Na-oxide	1	s	+	g	0	J		0
Sulphur	1	s	+	g	0	J		0
Quartz	1	s	-	g	0	J		0
Silica-amorph	1	s	-	g	0	J		0

The controls used for the process modelling was:

```
xa_[{O2}]          =: 0.1;          % Ensures oxidative conditions
xa_[{Aqua}]        =: 50;           % Water content in the paste
modC[J][1]         =: cNu;          % Incrementally increasing variable
xa_[{Residue}]     =: modC[J][1];   % Residue content in the paste
modC[J][0]         =: 90*0.8;       % Content of reacted cement
xa_[{AA_OPC}]      =: modC[J][0];   % Cement content
```

The sampling consisted of

```
xp[J]                   =: cNu;
yp[J][0]                =: phM[{aq_gen}];
yp[J][1]                =: phM[{gas_gen}];
yp[J][2]                =: phM[{C3(AF)S0.84H}];
yp[J][3]                =: phM[{CSHQ}];
yp[J][4]                =: phM[{ettringite}];
yp[J][5]                =: phM[{SO4_CO3_AFt}];
yp[J][6]                =: phM[{CO3_SO4_AFt}];
yp[J][7]                =: phM[{C4AcH11}];
yp[J][8]                =: phM[{Friedels}];
yp[J][9]                =: phM[{C3FS0.84H4.32}];
yp[J][10]               =: phM[{Portlandite}];
yp[J][11]               =: phM[{Gypsum}];
yp[J][12]               =: phM[{thenardite}];
yp[J][13]               =: phM[{arcanite}];
yp[J][14]               =: phM[{Brucite}];
yp[J][15]               =: phM[{OH-hydrotalcite}];
yp[J][16]               =: phM[{Calcite}];
yp[J][17]               =: 10-cNu;          % Amount of unreacted residue
yp[J][18]               =: 90*0.2;          % Amount of unreacted cement
```

Residues originating from the combustion of municipal solid waste were investigated to utilise MSWI fly ash residues as partial cement replacements. The chemical composition of several MSWI fly ash residues was evaluated with multivariate data analysis. Three residues were selected for further study, as they would provide a broad interpretation of MSWI fly ash residues performance in general. The chemical composition of the three residues was unsuited for use in cement-based materials, and the residues were subsequently treated with electrodialitic remediation to improve the residues' characteristics and recover the valuable metals in the residues. The treatment was not successful in recovering large amounts of the valuable but did improve the performance of the residues in cement-based materials. Two of the three treated residues resulted in improved hydration and phase development and increased compressive strength, while several issues caused by the residues were no longer occurred.

DTU Civil Engineering

Brovej 118
2800 Kongens Lyngby
Tel. 45251700

www.byg.dtu.dk

87-7877-567-1